Cooperative Control of Autonomous Multi-Vessel Systems for Floating Object Manipulation

Du, Z.

DOI
10.4233/uuid:87ade27f-bf2d-483c-af31-37176ebb7db9

Publication date
2022

Document Version
Final published version

Citation (APA)
Du, Z. (2022). *Cooperative Control of Autonomous Multi-Vessel Systems for Floating Object Manipulation*. [Dissertation (TU Delft), Delft University of Technology]. https://doi.org/10.4233/uuid:87ade27f-bf2d-483c-af31-37176ebb7db9

Important note
To cite this publication, please use the final published version (if applicable).
Please check the document version above.

Cooperative Control of Autonomous Multi-Vessel Systems for Floating Object Manipulation

Proefschrift

ter verkrijging van de graad van doctor
aan de Technische Universiteit Delft,
op gezag van de Rector Magnificus prof.dr.ir. T.H.J.J. van den Hagen,
voorzitter van het College voor Promoties,
in het openbaar te verdedigen op dinsdag 27 september 2022 om 12:30 uur

door

Zhe DU
Master of Science in Traffic Information Engineering and Control,
Wuhan University of Technology, Wuhan, China
geboren te Wuhan, China.

Dit proefschrift is goedgekeurd door de promotoren:
Prof.dr. R.R. Negenborn
Dr. V. Reppa

Samenstelling promotiecommissie:

Rector Magnificus	voorzitter
Prof.dr. R.R. Negenborn	Technische Universiteit Delft, promotor
Dr. V. Reppa	Technische Universiteit Delft, copromotor

Onafhankelijke leden:

Prof.dr.ir. P. H. A. J. M. van Gelder	TBM, Technische Universiteit Delft
Prof.dr.ir. M. van Koningsveld	CiTG, Technische Universiteit Delft
Dr.ir. J. Szłapczyńska	Gdynia Maritime University
Dr. L. Reinhardt	Roskilde University
Prof.dr.ir. T. A. Johansen	Norwegian University of Science and Technology

To my fiancée, Yunhui Liu
my parents, Jiazheng Du and Xiaomin Xiao

Preface

Recalling the first day I came to the TU Delft, excitement and curiosity feeling fill my mind, looking forward to a long and plentiful PhD study life. Now, four years have gone fleeting, it's time to complete my PhD research and say goodbye. At the end of this fantastic journey, I would like to acknowledge everyone that inspired, helped, encouraged, trusted, and accompanied me.

To begin with, I cannot be more thankful for my promoter, Prof. Dr. Rudy R. Negenborn. I still remember the online interviewing day, during the Chinese new year in Wuhan, Rudy provided me with the exciting opportunity of working as a PhD candidate at TU Delft, which changed the trajectory of my life. Although having a lot of responsibilities, Rudy is always approachable and kind. During every process meeting, he always encourages me to explore different ideas, stimulating me to think in an academic way and be an independent researcher. Many good ideas and inspirations are generated after our discussion.

Also, my great appreciation goes to Dr. Vasso Reppa, who is one of the best examples for supervisors. She understands the research works of her students in detail so that can provide concrete and constructive suggestions. Vasso not only gave me inspiration in my academic research but also helped me to improve my paper writing skills. The comments I get from her on each of my draft papers are always full of pages, which I have greatly benefited from. She also helped me build connections with engineers in KOTUG towage and maritime company since my project is related to towing operations. Vasso's supervision is patient and motivating. In every progress meeting, all my confusion and problems are answered and solved, and have clearer objectives for the next step.

Thanks to my colleagues and friends in Delft. It is delightful to work with Linying Chen, Qingsong Zeng, Wenjing Guo, Xiao Lin, Zongchen Li, Xiao Li, Yunpeng Yan, Mingxin Li, Pan Fang, Xiaohuan Lyu, Vittorio Garofano, Ali Haseltalab, Pablo Segovia Castillo, Breno Beirigo, Rie Larsen, Qianyi Chen, Marc Fransen, Nikolaos Kougiatsos, Adrien Nicolet, Sietske de Geus. I'm lucky to have the chance to meet friends with Jian Tan and his wife Xu Chen, Xiuhan Chen, Yapeng Li, Wei Tao, Rongxin Song, and Yimeng Zhang. I would also like to thank secretaries Patty and Pauline for always being kind and helpful.

Thanks to the China Scholarship Council that sponsors my research and supports my daily expenses in the Netherlands.

Thanks to the colleagues from Wuhan University of Technology, it is the origin of the journey of my research. Thanks to Prof. Yuanqiao Wen who supervised my master's research and enlightened me on how to do research. Thanks to Prof. Yamin Huang who is a good role model that I should always learn. Thanks to Lei Du and Yongqing Cai, they are friends and also big brothers that take care of me. Thanks to Man Zhu, Yi Liu, Yimeng Zhang, Wei Tao, and Rongxin Song, their passion for research has always inspired me.

Contents

Chapter 1

Introduction

Autonomous vessels have been under investigation for over 80 years since the 1940s [11]. The regulatory endorsement of the International Maritime Organization (IMO) and the support of some pivotal shipping market players in recent years motivate autonomous vessels to start playing a significant role in the shipping industry. Autonomous vessels utilized in civil and commercial applications however have not yet received much attention. In addition, as the complexity and scale of the applications increase, many scholars gradually transform their focus from single-vessel systems to multi-vessel systems. Thus, autonomous multi-vessel systems applied in the shipping industry will be a promising research direction in the near future.

This chapter provides an introduction to the research background, the research gaps (motivation), and the research questions. The contribution and outline of this thesis are presented as well.

1.1 Background

Autonomous vessels have over the last decades started to gain increasing attention [11] With the increasing maturity and popularity of the advancing technologies of information, communication, sensors, automatic control and computational intelligence, we have seen the application scenarios of the autonomous vessels being gradually extended from fundamental research to civil and commercial uses [33, 34].

To ensure that the regulatory framework for autonomous vessels keeps pace with technological developments, the Maritime Safety Committee (MSC) of the International Maritime Organization (IMO) has started to include the autonomous vessels issue in its 98th session in 2017 [79]. For a better regulatory scoping exercise in the future, the IMO put forward a formal generic concept,"Maritime Autonomous Surface Ship (MASS)", which is defined as a ship, to a varying degree, that can operate independently of human interaction [80]. Meanwhile, the degrees of autonomy are defined as shown in Fig 1.1. There are four degrees to judge the autonomy of a vessel: Degree 1 means only part of processes and operations are automated, while the main control of the vessel has to be seafarers; Degrees 2 and 3 refer to the remotely controlled vessel, the difference is that seafarers are on board in the case

Degree 1	Degree 2	Degree 3	Degree 4
Ships with automated processes and decision support	Remotely controlled ship with seafarers on board	Remotely controlled ship without seafarers on board	Fully autonomous ship
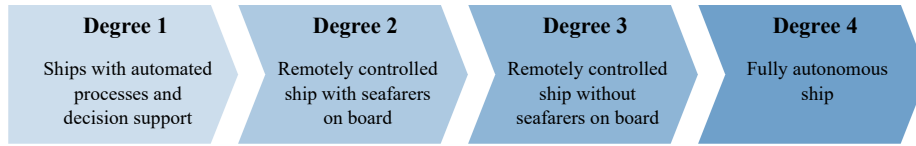
Figure 1.1: Four degrees of autonomy [80]

(a)	(b)

Figure 1.2: Application examples of multi-vessel systems: (a) formation cluster control in a vessel-train shape [82]; (b) floating object manipulation in a ship berthing scenario [94].

of Degree 2 while no seafarers are on board in the case of Degree 3; Degree 4 is the fully autonomous vessel, which is able to make decisions and determine actions by itself.

The endorsement of the IMO facilitates a large number of research works focusing on autonomous vessels, meanwhile, the involved applications become more complex and its scale is larger, such as coastal reconnaissance [184], marine assets protection [139], marine habitat mapping [1], oil spill response [152], ship towage [62], offshore platform transportation [76], and many more. However, the majority of works have been done on autonomy for a single vessel. There is a lack of research on considering explicit interactions between multiple autonomous vessels. Moreover, it is noticed that to realize the above-mentioned complex applications, more than one vessel is required to cooperate with each other for allocating the work. Thus, the focus on autonomous vessel-related research works is transferred from single vessel systems to multi-vessel systems in nearly decades.

The studies of autonomous multi-vessel systems are classified into two main directions according to the way of connections between vessels: formation cluster control and floating object manipulation [44]. Formation cluster control involves clustering multiple vessels as a formation while keeping a certain distance for collision avoidance. The connections between vessels are realized through digital networks. The formation can adopt various shapes and is flexible to be maintained, deconstructed and reconstructed based on the different specific applications (an example shown in Fig 1.2 (a)). Floating object manipulation refers to the situation in which multiple vessels cooperatively manipulate a floating object. The connections between the vessels and the floating object are through physical contact (an example shown in Fig 1.2 (b)). Because of the physical connection, the floating object manipulation system has less ability to maneuver and more constraints on its dynamics.
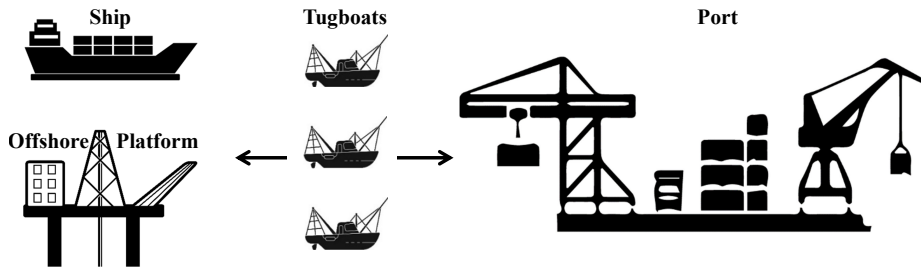
Figure 1.3: Tugboats build the connections between ships or platforms and the port

Since the beginning of the 21st century, the topic of formation cluster control has started to attract scholars attention [154], several matured formation control methods, like leader-follower [147], virtual structure [174], and behavior-based [7], are proposed to cope with different typical missions. However, the research of floating object manipulation has just started in recent years, the existing works are limited and in their infancy.

1.2   Motivation

The emerging technologies and the endorsement of the IMO motivate that several serious shipping market players have declared that they have seriously considered the development of "smart shipping" or "autonomous shipping", where the"intelligent ships" are the most important part [4]. However, due to the poor maneuverability and control performance of the large ship [101], meanwhile, to play the advantages of low cost, high mobility, and eco-friendly [129], the present "intelligent ships" are usually designed in small or medium sizes from 2 m long to 15 m long [11]. Thus, the main direction of "intelligent ships" is to develop small-size autonomous surface vessels (ASV). In the shipping industry, there is a kind of small-size vessel that plays an important role in building the connections between cargo ships or offshore platforms and the port, which is the tugboat. As shown in Fig 1.3, the transportation of large ships or offshore platforms from the open sea to ports requires multiple tugboats. Therefore, the tugboat is a good candidate for one of the first vessel classes to become autonomous [135].

In fact, there have been already many autonomous tugboat-related collaborated projects carried out between marine-related technology companies, research institutes and local governments [40]. Some well-known projects are listed in Table 1.1. It can be seen from Table 1.1 that these projects have started five years ago and the places of implementation are over Europe, Asia and America. Some of them are supported by local port authorities and maritime bureaus (e.g., maritime and port authority of Singapore and American bureau of shipping). Although the majority of projects focus on remotely controlled tugboats, which belong to autonomy degree 2 according to IMO definition (Fig 1.1), they took a big step to develop the full autonomous vessels for smart shipping.

Despite the advantages of low cost, high mobility, and eco-friendly characterizing the small size autonomous vessels, it is noticed that the limited power and capacity of these small size vessels restrain their capabilities to carry out more complex missions [103]. That is why the multi-vessel cooperative system is a significant and promising direction for the

next development of ASVs. The working process of tugboats is a typical example of multi-vessel cooperation, where the operation characteristics depend on the floating object manipulation.

Table 1.1: Projects of autonomous tugboat.

Start Year	Demonstration Place	Collaborators	Project
2016	TRANSAS Navi-Trainer Simulation System	Pacific Maritime Institute; Robert Allan Ltd; Transas Maritime Industry	Testing of control systems for the remotely operated "Ramora" tug [164]
2017	Denmark	Svitzer; Kongsberg Maritime; American Bureau of Shipping	RECOTUG: fully remotely controlled commercial tug [165]
2017	Denmark	Rolls-Royce; Svitzer; Lloyd's Register	Remotely operated tug "Svitzer Hermod" [109]
2018	Japan	NYK Group (Japan); Japan Marine Science; Japan's Ministry of Land, Infrastructure, Transportation and Tourism	Remotely controlled coastal ships and tugboats [134]
2018	Netherlands	KOTUG; Rotortug; Captain AI (in 2020)	Remotely controlled tugboat "RT Borkum" [166]
2019	Singapore	Wärtsilä; PSA Marine; Maritime and Port Authority of Singapore	IntelliTug project: Autonomous harbour tug [110]
2020	Singapore	ST Engineering; PACC offshore services holdings	Smart Maritime Autonomous Vessel (SMAV) project for autonomous tug [167]
2020	United Arab Emirates	Robert Allan Ltd; Abu Dhabi Ports	Develop Unmanned autonomous tugboats [111]
2020	Netherlands	Herman Senior; Sea Machines Robotics; Damen Shipyards	Upgrade a shoal tugboat "Teddy" for remote control [143]

Start Year	Demonstration Place	Collaborators	Project
2021	Singapore	Technology company ABB; Keppel Offshore & Marine; Maritime and Port Authority of Singapore	Remotely controlled tug "Maju 510" [168]
2021	Denmark	Damen Shipyards; Sea Machines Robotics	Remotely controlled tug "Nellie Bly" for the voyage around Denmark (Machine Odyssey) [169]
2021	Turkey	Vallianz Holdings Limited; SeaTech Solutions	All-electric tug "EVT-60" [170]
2021	China	Wärtsilä; China Classification Society; Tianjin Port Group	Semi-Autonomous Tugs [171]
2021	U.S.	Foss Maritime; Sea Machines Robotics	Autonomous tug "Rachael Allen" [172]
2021	U.S.	Technology company ABB; Crowley Maritime Corporation	Fully Electric Tug "eWolf" [112]

Among the limited research investigation of multi-vessel cooperative systems, this thesis focuses on finding cooperative control solutions for the physically connected autonomous multi-vessel system to safely and efficiently manipulate a large floating object in the environments of ports, inland waters, and offshore. The importance of investigating the autonomous physically connected multi-vessel systems becomes more and more clear, as illustrated by the regulatory endorsement of MASS from IMO, the development plan of "smart shipping" from the shipping industry, and the latest collaborative projects of autonomous tugboats.

Due to the limited number of research works, the main research gaps for autonomous physically connected multi-vessel systems can be identified with respect to the system modelling and the controller design. The above two aspects can be taken as a clue to reviewing the existing related literature, and the concrete research gaps will be illustrated in Chapter 2 after finishing the literature review.

1.3 Research questions

The main research question of this thesis is:

How to design a scalable and cooperative control scheme for multiple ASVs to manipulate a floating object through physical interconnections?

To answer the above question, several sub-questions have to be addressed as follows:

Q1: *What are the characteristics and concrete research gaps of the physically connected multi-vessel system?*

Although the research of the physical-connected multi-vessel system has recently started and the existing works are limited, it can still review and summarize this literature to find the characteristics of this system and make a classification. Comparing the various ways of physical connection allows for selecting the foundation of the system modelling in this thesis. Meanwhile, several significant control attributes should be deeply analyzed for identifying the concrete research gaps.

Q2: *How to establish the dynamics model of the physically connected multi-vessel system, and the control framework?*

System modelling is the foundation of this thesis. According to the different degrees of freedom (DOF), application scenarios, and usages, there are many methods for representing the motion of a vessel [56]. It is the key to choosing a proper way to model the vessel dynamics and find the connections between the floating object and vessels for establishing the kinematic model of the physically connected multi-vessel system. Then, a model-based control approach for such a complex system can be designed and a scalable control architecture can be established, where the criteria should include the characteristics of the controlled system, the control objectives, the constraints required to satisfy, etc.

Q3: *How to increase the robustness of the towing operation to handle the influence of environmental disturbances in port areas?*

Ship towing operation in port areas is a basic mission for tugboats. To manipulate a large ship from the anchorage to the pier, multiple tugboats are usually required to cooperate to allocate proper forces and moments to an unpowered large ship. During the manipulation process, the influence of environmental disturbances in port areas should be considered to increase the robustness of the towing operation.

Q4: *In what way can the multi-vessel system avoid collisions with static and dynamic obstacles to improve the safety of towage operations in inland waterways?*

Collision avoidance is always the most important mission for a vessel sailing on the water. Since the physical-connected multi-vessel system has less ability of maneuvering, resolving collisions with static and dynamic obstacles in the congested inland waterways becomes significant for improving the safety of towage operations.

Q5: *How to improve the quality of the manipulation process and achieve multiple control objectives as much as possible for a ship-towing system?*

Improving the quality of the manipulation process can increase the efficiency of the operations and smooth the motion of the vessels and the floating object in the physical-connected multi-vessel system, which can be achieved by speed regulation. So the position, heading, distance (to the obstacles), and speed of the floating object are all required to control, creating a multi-objective control problem.

Q6: *In what way can we increase the flexibility and efficiency of the cooperation of multiple vessels for an offshore platform transportation system of the open sea?*

Usually, the functional role of each tugboat is unchangeable in a towing system. However, for some cases, like transportation of an offshore platform from inland water to the open sea, the power that tugboats provided is in excess. Such cases then provide a chance to increase the flexibility and efficiency of the towing system that adjust the functional role of each tugboat in real-time according to the different situations.

1.4 Contributions

The contributions of this thesis are summarized below:

(1) Thorough review the research of floating object manipulation. Several categories of manipulation ways, their characteristics, and corresponding control methods are summarized to provide a better and clear understanding of this topic for research peers. Meanwhile, research gaps are identified to improve the safety and efficiency of the manipulation process [47].

(2) Establishing the model of the multi-vessel floating object towing system. The relations of kinematics and kinetics between the floating object and each vessel are derived to describe the states of the whole system motion, which lays the foundation of the model-based controller design [40].

(3) Designing the cooperative control approaches for the multi-vessel floating object towing system to improve system safety, process efficiency, and scenario adaptability. Based on different control architectures (centralized and distributed) and vessel functional roles (fixed and adaptive), a set of control schemes are proposed to cope with different environment disturbances (winds, waves, and currents) for achieving different control objectives (position, heading, distance to the obstacle and velocity) [41][42][45][46].

1.5 Thesis outline

The outline of this thesis is shown in Figure 1.4, where this chapter introduces the main research subject of this thesis; Chapter 2 identifies the concrete research gaps of the problem this thesis focuses on; Chapter 3 lays the research foundation of this thesis; Chapters 4 to 7 conduct case studies in different application scenarios; Chapter 8 is the conclusion. More specifically:

Chapter 2 (addresses research question **Q1**) reviews literature about floating object manipulation. Four kinds of manipulation ways, namely "attaching", "caging", "pushing", and "towing" are summarized in this chapter. The advantages and disadvantages of each manipulation way are discussed in detail, meanwhile, the attributes of control objective, control architecture, collision avoidance, environmental disturbances, and role of each vessel are analyzed to identify the research gaps in the floating object manipulation problem.

Chapter 3 (addresses research question **Q2**) mainly builds the system model and introduces the principles of the research approaches used in this thesis. Besides, the assumptions made and the model parameters used are explained. Thus, this chapter is the research foundation for the following chapters in this thesis.
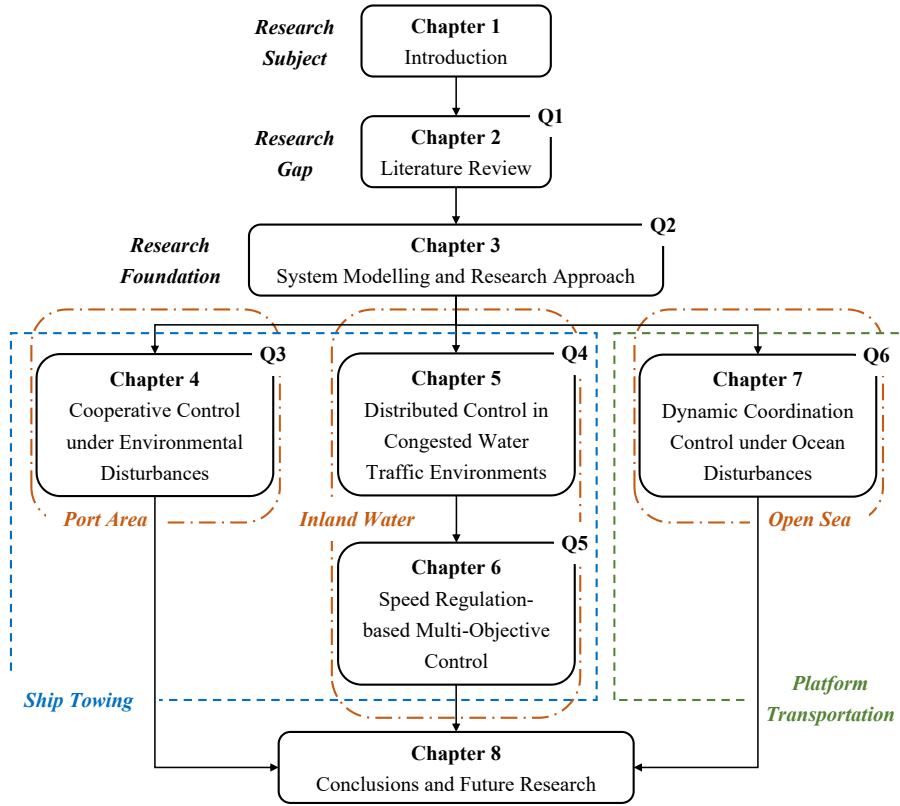
Figure 1.4: The outline of this thesis.

Chapter 4 (addresses research question **Q3**) focuses on ship towing in port areas. The control architecture is centralized and the control objective is to manipulate a large ship to a desired position with a desired heading. The environmental disturbances in port areas are mainly the wind effects. So a robust control scheme are proposed to make the ship towing system against wind influences.

Chapter 5 (addresses research question **Q4**) and Chapter 6 (addresses research question **Q5**) present the research on the ship towing on inland waters. Due to the limited navigation space and the larger number of vessels in inland waters, collision avoidance becomes an important objective for the ship towing system. Chapter 5 proposes a distributed control scheme to manipulate the ship to the destination with no collisions. With the same application scenario, Chapter 6 focuses more on the towing process. Besides control objectives of the position, heading, and collision avoidance, the speed of the manipulated ship is also controlled to make the system trajectories smooth and the towing process efficient. So a speed regulation-based multi-objective control scheme is proposed in this chapter.

Chapter 7 (addresses research question **Q6**) addresses the offshore platform transportation problem at open sea. The tugboats in the ship towing system of Chapter 4 to Chapter 6 have fixed roles that, the leader tugboat accelerates the ship's speed and steers its heading, the follower tugboat reduces the ship's speed and steadies its heading. While in the

offshore platform transportation system, to make sure the safety of the platform the number of tugboats is usually increased. Thus, this chapter proposes a dynamic coordination control scheme for the offshore platform transportation system to increase the flexibility of tugboats and the efficiency of the towing process, and cope with the ocean disturbances (winds, waves, and currents).

Chapter 8 concludes the thesis and provides directions for future research.

Chapter 2

Literature Review of Floating Object Manipulation

The research topic of this thesis is the floating object manipulation with a physically connected multi-vessel system. To have a better understanding of this topic and find research gaps from the existing related research, a literature review is conducted in this chapter to comprehensively summarize the characteristics of several typical maritime object manipulation ways and discuss their advantages and disadvantages. With that, this chapter addresses the first research question (**Q1**): "What are the characteristics and concrete research gaps of the physically connected multi-vessel system?"

This chapter is organized as follows. Section 2.1 briefly introduces the problem of object manipulation from the field of multi-robot systems to multi-vessel systems. Section 2.2 summarizes four typical maritime object manipulation ways from the existing research works, including the characteristics of the manipulated objects and the application scenarios. Section 2.3 analyses the control objectives of the manipulated floating objects and the control architecture of the different manipulation ways. Section 2.4 investigates collision avoidance and disturbances handling of the manipulation system in different manipulation ways. Section 2.5 discusses the role of each vessel in the floating object manipulation system. Section 2.6 concludes the chapter and identifies the research gaps.

Parts of this chapter have been published in [47][1].

2.1 The Problem of Object Manipulation

Object manipulation or object transportation is a typical research problem in the field of cooperative mobile robotics. When an object is required to move to a specific place but its size or weight is so large or heavy that it can not be manipulated by a single robot, multiple robotics cluster together to cooperatively transport the object [177]. Research works on object manipulation by multi-robot systems (MRS) can be categorized into three types (as shown in Fig 2.1): **grasping**, **pushing**, and **caging** [181].

---

[1]Z. Du, R. R. Negenborn, and V. Reppa. Review of floating object manipulation by autonomous multi-vessel systems. Submitted to a journal, 2022.
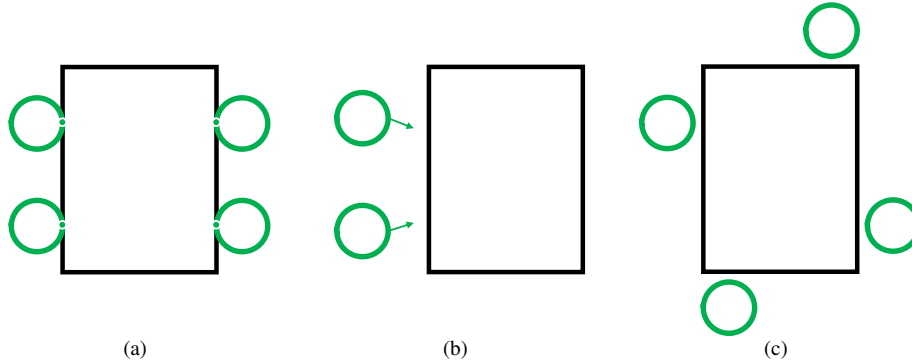
Figure 2.1: Three types of object manipulation by multi-robot systems (the black box stands for the manipulated object, the green circle is the robot): (a) grasping; (b) pushing; (c) caging.

Grasping manipulation (Fig 2.1 (a)) is the way that all robots are physically attached to the object, and the configuration of the manipulation system is unchangeable during transportation. The advantage of this manipulation is that the connections between the object and robots are tight and the object can be fully controlled by the robots so that the motion of the object is easy to predict [49]. Thus, the condition of form closure (the object has no way out from the surrounding robots) or force closure (the object is in a state of force equilibrium) is usually satisfied in this case. However, the disadvantage is that grasping requires additional tools such as a gripper or a manipulator. Besides, the effective positioning of the robots around the object to form an optimal configuration is an issue that has to be solved to avoid the case of the unbalanced distribution for the grasping manipulation system [177].

Pushing (Fig 2.1 (b)) is a manipulation way that multiple robots exert pushing forces on the object. Because there is no strict requirement of physical contact with the object all the time, this type is also called conditional closure manipulation [181]. It is also for this reason, pushing manipulation does not guarantee form closure or force closure and results in the manipulated object "escaping" from the control of robots or moving on an inefficient trajectory, which is the main disadvantage [177]. On the other hand, pushing is a simple strategy that is easy to implement, and it can manipulate a large object which is hard to be grasped [49]. Thus, this type of manipulation is tackled as a "box-pushing" problem [60].

Caging manipulation (Fig 2.1 (c)) is also called object closure, which means multiple robots are distributed forming a bounded movable area to entrap the object toward the destination. In some scholars' opinion, because the contact between the object and robotics in this manipulation type does not need to be maintained all the time, caging is seen as a special case of pushing manipulation [177]. On the other hand, the object is restrained in the bounded area, which ensures robots will not lose control of the object, the object closure is analogous to form closure with less strict conditions [49]. Caging requires less degree of precision in relative positions and orientations between the object and robots, so the advantage lines in more freedom and robustness compared to the manipulations relying on force closure [132]. However, the shape and size of the object should be carefully investigated because these features are related to the minimum number of robots required to surround
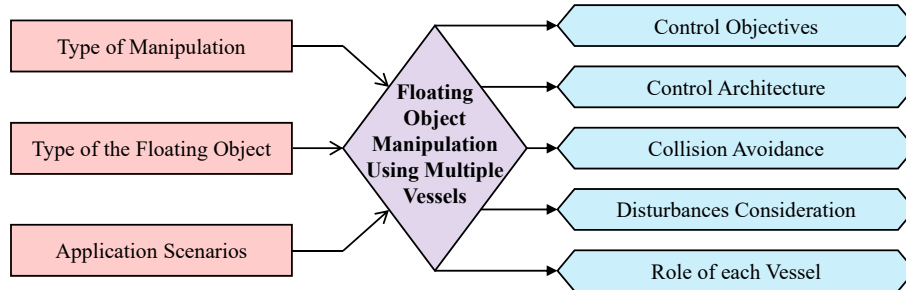
Figure 2.2: Classification of the floating object manipulation problem.

the object [177].

The above three typical manipulations briefly summarize the solutions to the problem of object manipulation by multi-robot systems, and the definition, characteristics, advantages, and disadvantages of each manipulation category are introduced. However, the operation space of multi-robot systems is usually ground, which is characterized by flat and stable with fewer disturbances. When the operation space switches to the waters, whose working conditions are characterized by undulating, dynamic, and more disturbing, the solutions to the problem of floating object manipulation by multi-vessel systems have to be reframed.

Fig 2.2 shows the framework of the floating object manipulation problem by multi-vessel systems used in this section to review the existing related research works. Where the type of manipulation, type of the floating object, and application scenarios are the elements to determine the modelling of the system and the problem; the control objectives, control architecture, collision avoidance, disturbances consideration, and the role of each vessel are the elements to decide the approach used to solve the problem.

The next section will use the type of manipulation as a key clue to summarize four typical solutions for the problem of floating object manipulation by multi-vessel systems in the maritime field.

2.2 Floating Object Manipulation in the Maritime Field

The three elements of determining the system modelling and the problem are discussed in this part. As shown in Fig 2.3, there are four types of manipulation for the solution of the floating object manipulation problem: **attaching**, **caging**, **pushing**, and **towing**. The floating object is categorized into two types, diffused liquid (e.g., spilled oil or hazardous chemicals, shown in Fig 2.4 (a)) and large structure (e.g., large ship or offshore platform, shown in Fig 2.4 (b)); while the application scenarios can be classified into three categories: port areas, inland waterways, and offshore waters. Different manipulation ways will reflect their own advantages of dealing with a certain type of floating object in the specific application scenarios. Thus, the type of manipulation is the key factor to summarize the research of floating object manipulation.
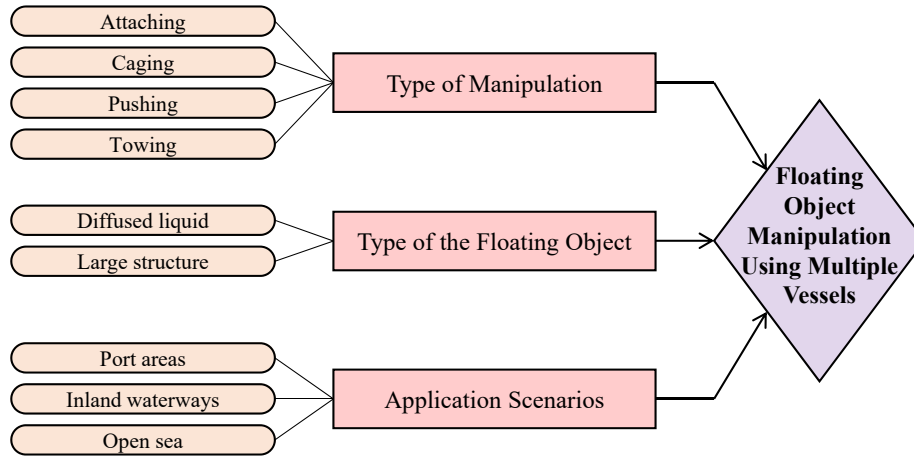
Figure 2.3: Classification of the type of manipulation, type of the floating object, and application scenario from the existing literature of floating object manipulation.
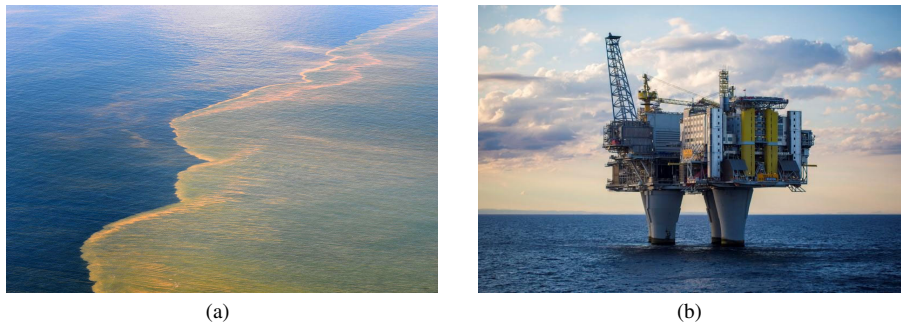
Figure 2.4: Two types of the floating object: (a) Diffused liquids (spilled oil) [178]; (b) Maritime structures (offshore platform) [38].

2.2.1 Manipulation of Attaching

Attaching is the manipulation that multiple vessels cluster together attached to the floating object in a fixed manner, as shown in Fig 2.5. In this manipulation way, multiple vessels approach the manipulated object and form a proper configuration to prevent the object from escaping. After all the vessels are physically attached to the object, the configuration of the manipulation system is not changed, which is similar to the way of grasping in object manipulation by multi-robot systems. The attached vessels are regarded as thrusters to provide power for the object, so the combined body is usually an over-actuated system and the main research question is how to allocate the multiple control inputs to the manipulated object [86].

The difference between the grasping manipulation by multi-robot system and the object

(a)   (b)

Figure 2.5: Manipulation of attaching: (a) Schematic diagram (the black box stands for the manipulated object, the blue shape is the vessel); (b) Application example of a tugboat attaching to a large ship [36].

attaching manipulation by multi-vessel system is that the latter is more strict to the number and distribution of vessels, which should be an even number and evenly distributed. The reason lies in that the water surface is dynamic with fluctuations, and the attached vessels have to make the object force equilibrium in the vertical direction to ensure the motion of the system is stable in the plane.

The related research works of object attaching are listed in Table 2.1. It can be seen that the number of vessels in the manipulation of object attaching is usually four [14, 15, 17, 50, 54, 55, 158] and six [16, 21–23, 83, 99], which is the number to satisfy force closure and form closure, respectively. While in some cases, the floating object is too large that requires more than ten vessels to manipulate [51–53]. The research work [27] adopts a special object attaching manipulation by using three vessels: two vessels are symmetrically and closely located on the two sides of the object connected by short cables, and one vessel attaches at the back of the object laying on its central axis. The type of floating objects in research of object attaching are large structures, and the application scenarios are mainly the port areas and offshore waters.

There is a special case in the attaching manipulation called self-attaching. As shown in Fig 2.6, multiple vessels gather together and are physically attached to each other to become a floating platform, and the object can be loaded on such a combined platform. Although the manipulated object in this way is not floating on the water, the connection process between the vessels can be a reference for the realization of the manipulation way of object attaching. The main research questions in this manipulation are how to design the connection device and how to cooperatively plan the trajectories of multiple vessels. These issues are usually ignored in the research of object attaching manipulation.

The connection device should be designed to make sure that the connection between vessels is tight and docked precisely.The connection device usually consists of two parts: "male" and "female" located on the two sides of the vessel. Some examples can be seen in Fig 2.7. The cooperative trajectory planning of multiple vessels is solved by using the graph theory and optimization methods, for example, the Dijkstra algorithm combining with

Table 2.1: Classification of existing literature on the manipulation of object-attaching.

Paper	Number of vessels	Type of the floating object		Application Scenarios		
		Diffused liquid[*]	Large Structure	Port Areas	Inland Waterways	Offshore Waters
[54]	6		✓	✓		
[158]	6		✓			✓
[50]	6		✓			✓
[51]	≥ 10		✓			✓
[55]	6		✓	✓		
[52]	≥ 10		✓			✓
[53]	≥ 10		✓			✓
[14]	6		✓			✓
[15]	6		✓			✓
[22]	4		✓	✓		
[83]	4		✓			✓
[23]	4		✓			✓
[21]	4		✓	✓		
[99]	4		✓	✓		
[16]	4		✓			✓
[27]	3		✓		✓	
[17]	6		✓			✓

[*] The reason for this column being empty is that the manipulation of object-attaching can only carry out on a solid floating object.

                                    (a)   (b)
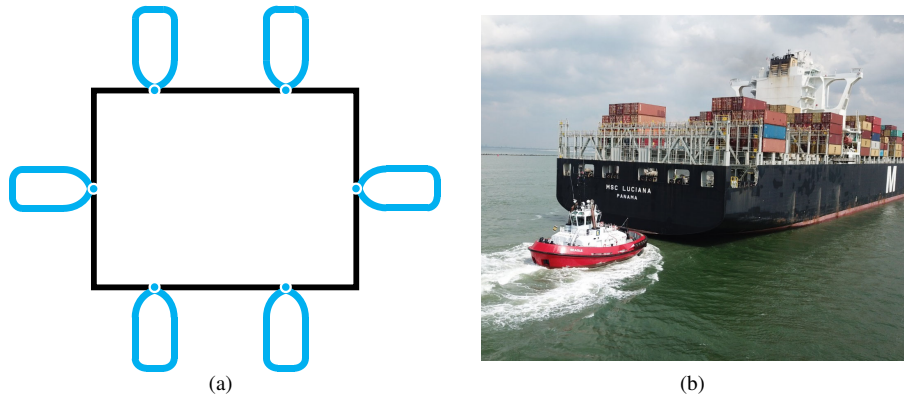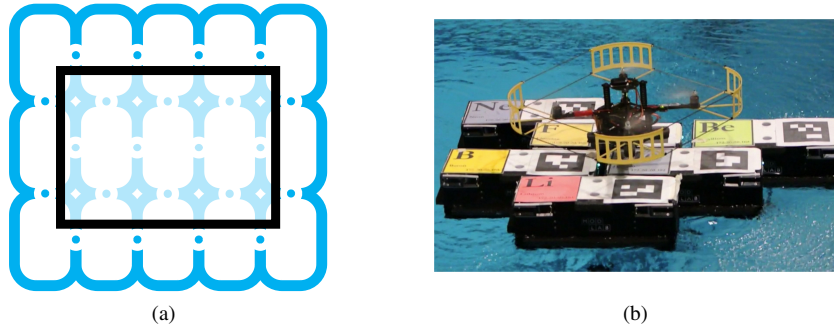
Figure 2.6: Manipulation of self-attaching: (a) Schematic diagram (the black box stands for the manipulated object, the blue shape is the vessel); (b) Application example of a drone landing on a platform formed of multiple ASVs [126].

the Hungarian algorithm [126] and the B-spline curve combining with the mixed integer quadratic programming [58], so that each vessel can reach its goal point for docking without collisions.

                          (a)   (b)
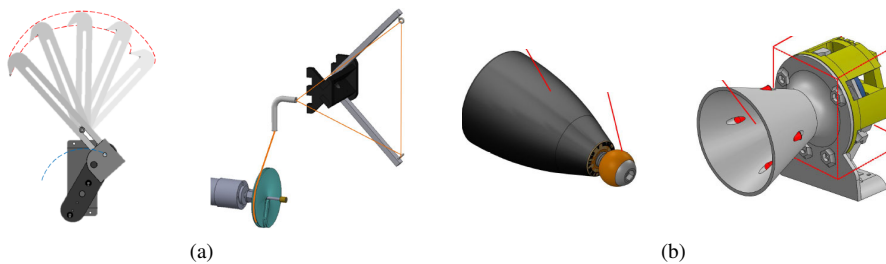
Figure 2.7: Two examples of the designed connection device: (a) the left hook is "male", the right loop is "female" [66]; (b) the left bearing stud is "male", the right funnel is "female" [117].

The related research works of object attaching are listed in Table 2.2, the number of vessels is greatly varying according to their applications and the loaded objects. If the application is to make vessels self-assembling as a floating platform or a bridge connecting the banks for transport of other vehicles (autonomous cars, drones) or people, the number of vessels is usually more than ten [66, 126, 180]. While if the load is a small object, like domestic waste, the numbers can be just two or three [58, 89, 117, 124]. Different from the manipulation of object attaching, the application scenarios in self-attaching are only the inland waterways. The self-assembled system is sensitive to disturbances, while there are fewer environmental disturbances in the inland waters. To ensure the safety of the self-assembled system, inland waterways are the best option.

Table 2.2: Classification of existing literature on the manipulation of self-attaching.

Paper	Number of vessels	Object to be transported	Application Scenarios		
			Port Areas	Inland Waterways	Offshore Waters
[126]	> 10	Autonomous cars, drones		✓	
[66]	> 10	Autonomous cars, drones		✓	
[124]	3	Wastes, goods		✓	
[89]	3	Wastes		✓	
[180]	> 10	People, goods		✓	
[117]	2	Goods		✓	
[58]	3	Small object		✓	

(a)   (b)
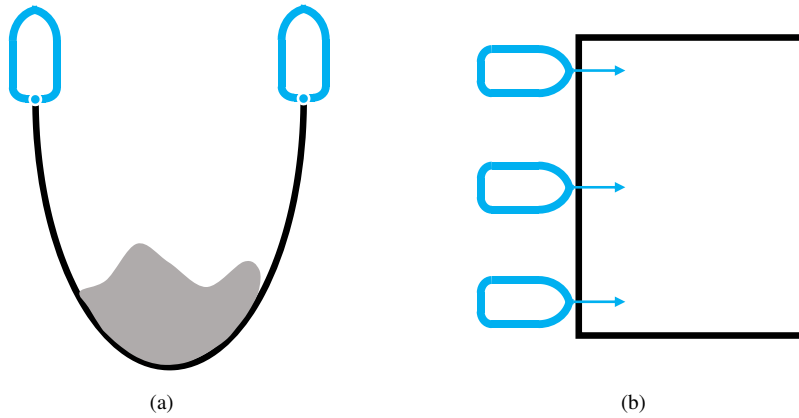
Figure 2.8: Two manipulation ways that the floating object has more degrees of freedom (the black box and the grey shadow stand for the manipulated object, the blue shape is the vessel, and the black curve stands for the towing boom or floating rope): (a) caging; (b) pushing.

2.2.2 Manipulation of Caging and Pushing

Compared to the way of attaching, the manipulated floating object in manipulations of caging and pushing has more degrees of freedom but has fewer degrees of control.

Caging manipulation (as shown in Fig 2.8 (a)) in the maritime field means the object is manipulated by a long enough floating rope connected to one or more vessels. It is noticed that the definition of caging here is different from the definition used in research of multi-robot object manipulation. In the multi-robot systems, the caging manipulation happens on the ground environments which are usually three degrees of freedom (DOF) (surge, sway, and yaw), so the object can be safely and stably restrained by the multiple robots with

<div align="center">(a)   (b)</div>
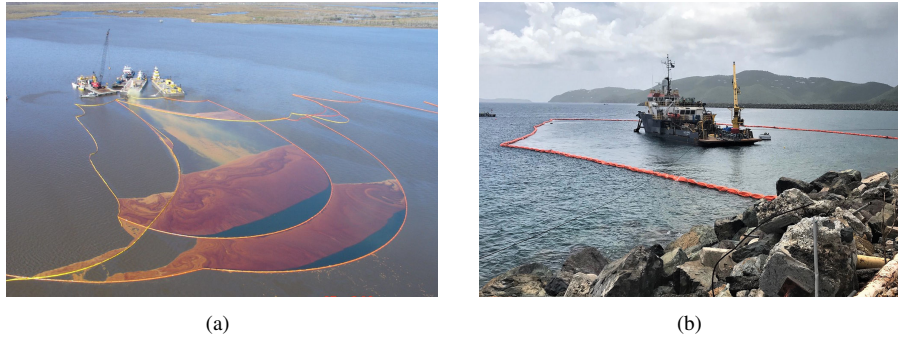
Figure 2.9: Applications of the caging manipulation: (a) oil spill skimming and cleaning [113]; (b) quayside ship mooring [163].

proper configurations. However, there are six DOF (surge, sway, heave, roll, pitch, and yaw) in waters. It is difficult to prevent collisions between the object and the vessels in such a fluctuated, dynamic, and more harsh environment. Thus, the caging manipulation in the maritime field has to be implemented with the help of a media, the floating rope.

Pushing manipulation (as shown in Fig 2.8 (b)) in the maritime field has the same meaning as that of in the research of multi-robot object manipulation, implying that multiple vessels exert only pushing forces on the floating object. Despite the same definition, the manipulation details are different. For the multi-robot systems, because of the static operation space of the ground, the contact between the object and robots doesn't have to maintain all the time [114, 115]. Consequently, the motion of the object is more flexible. While for the multi-vessel systems, restrained by the dynamic operation space of the waters, a part of the research work aims to make the vessels keep in touch with the floating object through the whole process for the sake of safety [31, 144].

The related research works of caging and pushing manipulation are listed in Table 2.3 and Table 2.4, respectively. It is observed from Table 2.3 that the number of vessels in the manipulation of caging is usually two [9, 12, 13, 84, 130, 150–152], and the type of floating object is only the spilled oil [12, 13, 57, 84, 130, 150–152, 193]. The mission of oil spill skimming and cleaning is a typical operation in maritime accident emergency response (as shown in Fig 2.9 (a)). The whole procedure can be summarized in four steps: first, two vessels drag a boom (the device that can prevent oil from floating around) towards the accident location; then, the two vessels adjust their states to adopt a proper angle of attack of the boom to capture the oil spill; next, the vessels converge to a closer mutual distance to confine the oil spill; finally, the vessels drag the oil spill to a suitable place [152]. Thus, the application area of the caging manipulation is mainly the offshore waters. Besides the floating object of spilled oil, the small object [9] and large ship [85, 149] can be also manipulated by caging. The process of a small object caging is similar to that of the oil spill recovery, cooperated by two vessels. The operations of a large ship caging are implemented by only one vessel which tows a boom around the ship to moor it along the quayside (as shown in Fig 2.9 (b)).

For the research of pushing manipulation from Table 2.4, there is no specific value of

Table 2.3: Classification of existing literature on the manipulation of caging.

Paper	Number of vessels	Type of the floating object		Application Scenarios		
		Diffused liquid	Large Structure	Port Areas	Inland Waterways	Offshore Waters
[9]	2	small solid object				✓
[130]	2	✓				✓
[152]	2	✓				✓
[150]	2	✓				✓
[151]	2	✓				✓
[84]	2	✓				✓
[12]	2	✓				✓
[13]	2	✓				✓
[57]	6	✓				✓
[149]	1		✓	✓		
[85]	1		✓	✓		
[193]	5	✓				✓

Table 2.4: Classification of existing literature on the manipulation of pushing.

Paper	Number of vessels	Type of the floating object		Application Scenarios		
		Diffused liquid*	Large Structure	Port Areas	Inland Waterways	Offshore Waters
[146]	4		✓	✓		
[188]	3		✓	✓		
[72]	2		✓	✓		
[73]	2		✓	✓		
[122]	3		✓	✓		
[31]	3		✓	✓		
[144]	1		✓	✓		

* The reason for this column being empty is that the manipulation of pushing can only carry out on a solid floating object.

the number of vessels. The type of the object belongs to the large structure, as in the research of object attaching manipulation. Usually two or three vessels are deployed to manipulate a large box object [31, 72, 73, 122, 188]. If the vessel has enough power, the number can be one [144], otherwise, there requires more than three vessels for manipulation [146]. However, the application scenarios are restrained in port areas. Because the vessels in this manipulation can only provide pushing forces, the floating object is difficult to be controlled. In addition, compared to the open sea, the port areas are characterized by fewer environmental disturbances; compared to the inland waterways, the port areas have more operational space. So the typical application is to push a large ship approaching the berth by tugboats in port areas [125].

2.2.3   Manipulation of Towing

Towing is the manipulation that the object is controlled by tied ropes (or cables) which are connected to vessels, as shown in Fig 2.10 (a). This is the type that the research of multi-robot object manipulation does not consider but it is very often applied in the maritime field, such as ship towing for port berthing, as shown in Fig 2.10 (b). Besides the maritime field, the application of towing manipulation actually can be found in road (track-trailer in Fig 2.11 (a)) and air transport (drone delivery in Fig 2.11 (b)).

However, the majority of research works still focus on maritime transport, because the ropes between the object and vessels are the distance from each other to ensure safety in the manipulation process, especially in some dangerous cases, like harsh sea conditions and restricted waters (passing congested canals and narrow bridges) [68]. Thus, towing is a proper way for multiple vessels to manipulate a floating object in the dynamic water environments.

(a)   (b)
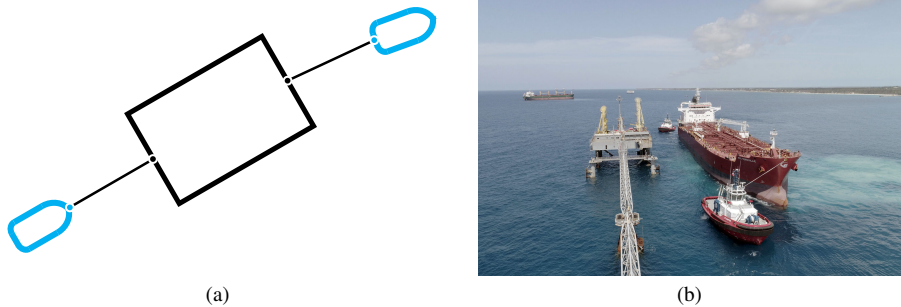
Figure 2.10: Manipulation of towing: (a) schematic diagram; (b) application example of ship towing for port berthing [95].

The related research works of towing manipulation are listed in Table 2.5. Except for literature [10], whose focus is on moored interconnected structures of self-manipulation, the number of vessels can be classified into three cases: one, two, and four. In the manipulation of one vessel towing case [5, 19, 20, 81, 98, 116, 138, 161, 190, 192], the floating object can be transported from the initial area to the goal area with the desired heading but is difficult to the specific location. Because the vessel in front of the object provides a pulling

(a)   (b)

Figure 2.11: Application of towing manipulation in other field: (a) Track trailer [90]; (b) Drone delivery [39].

force that can only move the object and slowly adjust its heading, while the braking is realized by the damping of the waters. For the two-vessel towing manipulation, there are other two situations. The first one is when deploying both vessels in front of the object to increase the efficiency of the heading adjusting, but the braking operation is still passive [62, 63, 182, 186]. In the second situation, the object is located between the two vessels so that the front vessel can increase and the behind vessel can decrease the speed of the object [40–45, 71]. The last case is to use four vessels towing a large floating platform [48, 76, 183]. In this case, the manipulated object and vessels combine an over-actuated system, so the object is fully controlled. The type of floating object in this manipulation is a large marine structure, and their application scenarios vary from port areas to inland waterways to offshore waters.

2.2.4 Summary

The research share of existing literature of the four floating object manipulations are summarised and compared in Table 2.6. From the existing related literature, the research of attaching and towing manipulation are dominant, because they have wild application scenarios.

Attaching is an effective manipulation. The advantage lies in that the connection between the object and the vessels is tight and secure, and the manipulated object is fully controlled by multiple vessels. So the object has good maneuverability. While the disadvantage is that it puts extra demand on the design of the connection device, and the trajectory of each vessel is required to plan for preventing collisions with each other. The type of the floating object is a large structure and the application scenarios are mainly port areas and the open sea.

Caging is a gentle manipulation. The connection between the object and the vessels is not strong but gives more freedom to the floating object. This manipulation is usually applied for coping with a specific problem of oil spill skimming and cleaning. There is no need to direct contact between the object and vessels, so there is no need to take measures to avoid collisions. But the model of the floating boom is required to be derived. The type of the floating object is diffused liquids and the application scenarios are the open sea.

Table 2.5: Classification of existing literature on the manipulation of towing.

Paper	Number of vessels	Type of the floating object		Application Scenarios		
		Diffused liquid	Large Structure	Port Areas	Inland Waterways	Offshore Waters
[62]	2		✓			✓
[63]	2		✓			✓
[186]	2		✓			✓
[81]	1		✓			✓
[76]	4		✓			✓
[183]	4		✓			✓
[192]	1		✓			✓
[5]	1		✓			✓
[190]	1		✓			✓
[161]	1		✓			✓
[182]	2		✓	✓		
[138]	1		✓			✓
[98]	1		✓			✓
[71]	2		✓	✓		
[20]	1		✓	✓		
[19]	1		✓	✓		
[10]	5		✓			✓
[116]	1		✓			✓
[40]	2		✓	✓		
[41]	2		✓	✓		
[44]	2		✓		✓	
[43]	2		✓		✓	
[42]	2		✓		✓	
[45]	2		✓		✓	
[48]	4		✓			✓

Table 2.6: Comparison of different manipulations.

Manipulation	Advantage	Disadvantage	Share
Attaching	1. Tight Connection; 2. Good maneuverability of the object.	1. Design of additional device; 2. Planning of vessel trajectory.	36%
Caging	1. Without collisions between the object and vessels; 2. More freedom of the object.	1. Limitation of the object; 2. Modelling of the boom.	18%
Pushing	1. Easy implementation; 2. More freedom of the object.	1. Limitation of the scenarios; 2. Unsafe in case of disturbances.	10%
Towing	1. Safe distances between the object and vessels; 2. Balanced freedom and maneuverability of the object.	Complex towing system model	36%

Pushing is a simple manipulation. It is easy to implement and the floating object in this manipulation has more freedom. However, the incomplete control of the object restrains its application and increases the manipulation risk under the disturbance environments. So the research works on this manipulation are not many. In real cases, pushing is used as an auxiliary operation to collaborate other manipulations for assisting ship berthing. The type of the floating object is a large structure and the application scenarios are port areas.

Towing is a practical manipulation. The connection between the object and vessel requires a media of rope or cable, which reserves certain distances between the object and vessels to ensure manipulation safety. So it can manipulate a floating object in the environment of dynamic waters with harsh weather conditions. The manipulated object has more freedom than attaching and better maneuverability than caging and pushing. Thus, towing operation is a common practice in maritime transport. But the model of the towing manipulation system is difficult to derive. The type of the floating object is a large structure and the application scenarios can be port areas, inland waterways, and the open sea.

Thus, considering the maneuverability of the floating object, the safety of the manipulation system, and the flexibility of the application scenarios, the towing manipulation can be a proper choice to manipulate a large marine structure for improving the automatic of the shipping industry and the efficiency of the global logistics.

2.3   Analysis of Control Objectives & Control Architecture

This section analyzes the control objectives concerned and the control architecture used in the existing research works on floating object manipulation. As shown in Fig 2.12, the control objective here means the states that the manipulated object is expected to achieve, which consist of three aspects: position, heading, and velocity. The control architecture is another important property for floating object manipulation. For a multi-vessel system, the control architecture can be centralized, decentralized, and distributed. In a centralized
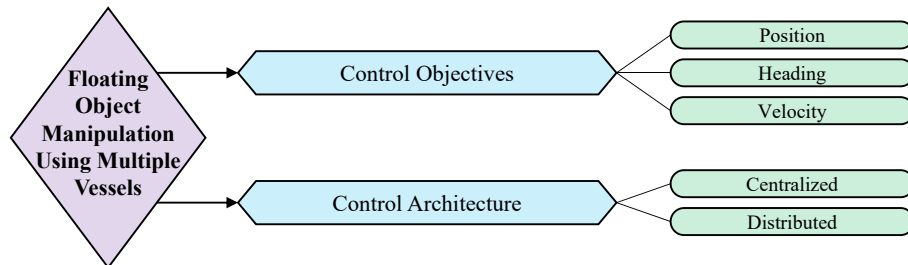
Figure 2.12: Summary of the control objectives and control architecture in the research of floating object manipulation.

architecture, all vessels are independent and directly interact only with a center; for decentralized control, each vessel is controlled by itself with no information exchange for each other; in distributed control architecture, all agents are allowed to communicate with neighbors to share their information [136]. For a floating object manipulation system, to transport an object in the undulating and dynamic water environments, the vessels have to collaborate either following commands by a center that processes information, or communicating with each other by sharing its local information. Thus, the control architecture of centralized and distributed are usually applied in this field.

In the existing research works, the only path or trajectory planning-related and self-attaching-related articles are not included in the summary of this section. The reason for excluding the second article kind is that the control objective of the self-attaching manipulation is not for the manipulated object. Thus, the control objective and control architecture of the rest literature are summarized in Table 2.7.

In the way of attaching, the main control objective is to simultaneously control the position and heading of the object, where the specific control tasks are manipulation of a large marine structure to (1) track a predefined trajectory [23, 27]; (2) move to the desired position with desired heading [14–17, 21, 22, 50, 54, 55, 83, 99, 158]. A few papers work on velocity control to make the manipulation system maintain an expected speed [52, 53]. For the control architecture, because of the large number of vessels (usually more than 4 according to Table 2.1) working on this type of manipulation, the majority of works propose a distributed architecture, which has the advantage of lower computation time, scalable application scenarios, and tolerance to failures [121].

In the way of caging, the control objective is only the position of the floating object, because this manipulation cannot fully control the object. Therefore, the specific control tasks are (1) transportation of the spilled oil or a small object to a safe place [9, 12, 13, 57, 84, 130, 150–152]; (2) restriction of a large ship within a safe place [85, 149]. For the control architecture, 50% of the research works use distributed architecture for better implementation of real vessel tests [9, 84, 130, 150–152]. The remainder works choose the centralized one to control one vessel [85, 149] or to do simulation experiments and simple field tests [12, 13, 57].

In the way of pushing, the control objective focuses on the object's position and heading, where scholars in [72, 73, 122, 188] use 2 to 3 vessels pushing a large box object to a

Table 2.7: Classification of the control objectives and control architecture for the floating object manipulation literature*.

Research works	Control Objective			Control Architecture	
	Position	Heading	Velocity	Centralized	Distributed
Attaching [54] [158] [50] [55] [14] [15] [22] [83] [23] [21] [27]	✓	✓			✓
[99] [16] [17]	✓	✓		✓	
[52] [53]			✓		✓
Caging [9] [130] [152] [150] [151] [84]	✓				✓
[12] [13] [57] [149] [85]	✓			✓	
Pushing [188] [72] [73]	✓			✓	
[122]	✓				✓
[31] [144]	✓	✓		✓	
[146]	✓	✓			✓
Towing [161] [20] [19] [116]	✓			✓	
[192]		✓		✓	
[81] [182] [138] [98] **[41] [44] [48] [46]**	✓	✓		✓	
[62] [63] [186] [76] [183] **[40] [42]**	✓	✓			✓
[43] [45]	✓	✓	✓		✓

* The boldly marked papers are the academic achievements belonging to the author of this thesis.

goal position, and researchers in [31, 144, 146] control the vessels direction to adjust the heading of the object in the pushing process. For the control architecture, the majority of works use centralized architecture to find global optimal control inputs for the pushing vessels [31, 72, 73, 144, 188]. While a few papers consider distributed control architecture to increase the robustness of the pushing manipulation system.

In the way of towing, the control objective is similar to the way of attaching that involves all the three states of the manipulated object. Papers [19, 20, 116, 161] focus on position control to tow the object following the path. The research work [192] focuses on heading control to tow the object keeping its course. In the research works of simultaneously controlling the position and heading of the object, the research papers [62, 63, 81, 98, 138, 183, 186] focus on trajectory tracking, while the research papers [40–42, 44, 48, 76, 182] focus on the desired position and heading reaching. A few works study the control of all the states (position, heading and velocity) of the object to make the manipulation system follow the waypoints, adjust its heading, and track the speed profile [43, 45]. For the control architecture, more than half of the research works use centralized architecture, but the majority of these works consider a one-vessel manipulation system.

2.4   Consideration of Collision Avoidance & Disturbances

This section analyzes the safety and robustness of the floating object manipulation system when dealing with collisions and environmental disturbances. As shown in Fig 2.13, there are three aspects of collision avoidance (CA) for the floating object manipulation system: self CA, static obstacle CA, and dynamic obstacle CA. Self CA means to prevent collisions inside the floating object manipulation system, i.e. between the object and vessels. It is a basic safety measure to ensure that the towing manipulation works properly. Static and dynamic obstacle CA is to keep the manipulation system away from the external potential dangerous targets, such as no-navigation zone, anchorage, and other moving vessels.

Considering disturbances is an important issue to increase the robustness of the manipulation system. In the maritime environment, disturbances usually refer to winds, waves, and currents. Wind effects can be formulated by wind speed and direction [2, 119, 131, 148], and can also be represented by simplifying as external bounded forces to the system [8, 59, 100, 189]. Wave effects are relatively complex because the wave model is built based on the wave spectra and the theory of response amplitude operators (RAOs) [56]. Thus, scholars usually use trigonometric functions to simulate the wave influence [102, 123, 127, 162]. As to currents, their effects reflect on the relative velocities of the vessels to the waters [56].

Existing research works that tackle the problem of the collision avoidance and handling disturbances for the floating object manipulation system are summarized in Table 2.8.

In the way of attaching, a large number of research works do not consider the collision avoidance problem [14–17, 21–23, 50, 52, 54, 55, 83, 99, 158]. They ignore the approaching process of the vessels to the floating object and assume that all the vessels have already attached to the object. On the contrary, scholars of [53] use the artificial potential field for regulating the motion of the vessels to avoid collisions with each other while establishing contact with the object. Authors in [27] use distributed model predictive control to ensure safe distances from vessels to the floating object and from the manipulation system to the static and dynamic obstacles. For the disturbances consideration, research works [14, 15,
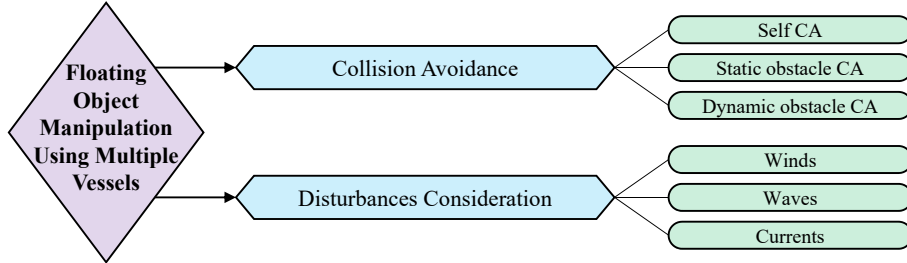
Figure 2.13: Summary of the collision avoidance and disturbances consideration in the research of floating object manipulation.

Table 2.8: Classification of the collision avoidance and disturbances consideration for the floating object manipulation literature.

Research works		Collision Avoidance			Disturbances		
		Self	Static	Dynamic	Winds	Waves	Currents
Attaching	[54] [158] [50] [55] [52] [22] [23] [16] [17]			–			
	[53]	✓					
	[27]	✓	✓	✓			
	[14] [15] [83] [21]					✓	
	[99]				✓		✓
Caging	[151] [84] [12] [13] [57]			–			
	[9] [130]	✓					
	[152] [150]				✓		
	[149] [85]				✓	✓	
Pushing	[122] [31] [144]			–			
	[146] [188] [72] [73]	✓					
Towing	[62] [63] [138] [98] **[40] [43] [48]**	✓					
	[182]	✓			✓		
	[183] [116]	✓				✓	
	[186] [192] **[41]**	✓			✓	✓	
	[161]	✓			✓		✓
	[81] [76] **[46]**	✓			✓	✓	✓
	[20] [19]	✓		✓			
	[44] [42] [45]	✓	✓	✓			

21, 83] take into account wave influence on a large floating object manipulation system in the offshore environment; [99] focuses on wind and current effects in port areas. While the rest of the papers have no investigation of environmental disturbances.

In the way of caging, only a few papers address the collision avoidance problem, where the focus is just on the collisions between vessel each other [9, 130]. The reason can be analyzed as follows. First, the manipulated object is captured and transported by a long floating rope or boom, which highly reduces the risk of colliding with vessels. Second, the manipulation scenarios are usually offshore waters, which is considered a working space without static obstacles. Third, the manipulated floating object is usually flammable and explosive dangerous goods (spilled oil), so no vessels or other moving targets are close to the caging manipulation system. More than half of the works do not concern the problem of disturbance effects. Research works [150, 152] consider wind influence causing motion errors of the boom-towing system for oil spill recovery, and they use distributed PID controller to compensate for such errors. Papers [85, 149] consider wind and wave effects in the deployment of booms along with quayside mooring ships. Such effects in the authors' opinion are positive, because it helps to get a suitable shape for the boom being towed.

In the way of pushing, none of the papers concern collision avoidance of the external static and dynamic obstacles, because the motion of the floating object in this manipulation is not fully controlled by vessels, the pushing manipulation system has no ability to cope with external obstacles. Despite this, half of the works focus on collision avoidance between the object and vessels. In works [72, 73, 146], researchers control and plan the approaching speeds and trajectories of the vessels respectively to prevent collisions between the object and vessels and among the vessel themselves. In [188], a limit cycle approach is used to control the vessels' posture and prevent collisions, which is to control the vessels' velocity and orientation to avoid the elliptical cycle around an obstacle. No works consider disturbances, probably due to the limited control of the floating object.

In the way of towing, due to the safe distance enabled by the towline, it is observed that all the research works have addressed the problem of self CA by establishing the desired kinematics towing system model. Scholars in [19, 20] define line-following and circle-following guidance paths to make the towing vessel have no collisions with another moving vessel. Scholars in [42, 44, 45] combine model predictive control strategy and the designed ship reference guidance system to make the towing system avoid static and dynamic obstacles in complex water traffic environments, and the collision avoidance operations comply with the COLREGS rules. For the disturbances consideration, the number of papers in this type of manipulation is larger than the other three ones. Some research works consider one type of disturbance, like winds [182] and waves [116, 183]; while some scholars focus on two types of disturbance effects, such as both winds and waves [41, 186, 192] and both winds and currents [161]. Especially, there are papers that consider all the environmental disturbances (wind, wave and current) to a towing system in the scenario of offshore waters [48, 76, 81].

2.5 Assignment of Vessel Role

This section focuses on the role of each vessel in the floating object manipulation system. As shown in Fig 2.14, there are four roles for the vessels in the manipulation system sum-

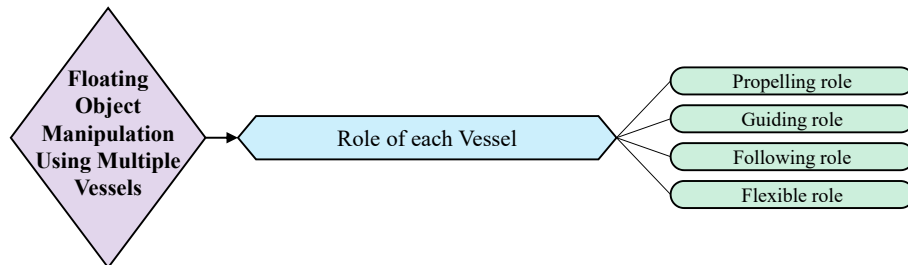*Figure 2.14: Summary of the role of each vessel in the research of floating object manipu-
lation.*

marized from the existing research works: propelling, guiding, following, and flexible role.

A vessel has the role of propelling means that it is directly in contact with the floating
object and provides pushing force to move this object. The direction of the provided pushing
force is the heading of the vessel. Because it is required to be contacted directly, the floating
object cannot be a liquid. Guiding and following roles need media (usually ropes, cables
or booms) to make a physical connection between the object and vessels. A vessel plays
the role of guiding means that it is located in front of the object along the direction of
motion and provides pulling force to lead this object moving; while a vessel plays the role
of following means that it is located behind the object along the direction of motion and
provides dragging force to brake this object. The schematic diagram of these three roles are
shown in Fig 2.15. The flexible role means that a vessel can switch roles between guiding
and following. The reason for such a mutual conversion is that the vessels in the guiding
and the following roles have the same way of manipulation, towing. These two roles can be
switched by adjusting the position and heading of the vessel.

The role of each vessel in the floating object manipulation system in the existing research
works is summarized in Table 2.9.

In the way of attaching, only one paper [27] uses three vessels where one vessel plays
propelling role attached behind the object and two vessels play guiding roles located at the
two sides of the obstacle. The rest of the works consider all the vessels in their manipulation
system as the propelling role. Because one vessel can provide the propelling force in only
one direction, to fully control the object, the number of vessels is usually more than four.
In the way of caging, due to the floating object being manipulated by a rope or boom towed
by one or two vessels, the vessels in the research works of this manipulation type have the
guiding role. In the way of pushing, the role of vessels is the same as in the majority of
works in attaching manipulation, the propelling role. The difference is since the vessels do
not have to contact the object all the time, the force direction to move the object is not fixed,
the number of vessels does not require to be large (usually 1 to 4).

The vessels of the floating object manipulation system in the above three ways of manip-
ulation have their specific fixed roles. However, the vessel roles in the towing manipulation
can be more flexible and complex.

As shown in Fig 2.16, there are five situations of the vessel role in the existing research
works. In literature [5, 19, 20, 81, 98, 116, 138, 161, 190, 192], authors use one guiding
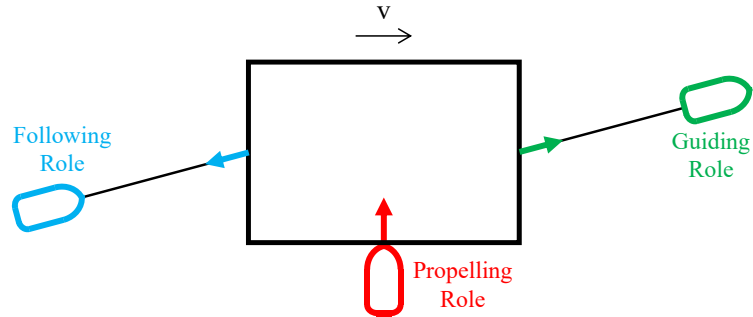
Figure 2.15: Schematic diagram of the vessel roles in the floating object manipulation system.

Table 2.9: Statistics of the role of each vessel for the floating object manipulation literature.

Research works	Number of vessels	Role of the vessel			
		Propelling	Guiding	Following	Flexible
Attaching [54] [158] [50] [51] [55] [52] [53] [14] [15] [22] [83] [23] [21] [99] [16] [17]	≥ 4	all			
[27]	3	1	2		
Caging [9] [130] [152] [150] [151] [84] [12] [13] [57] [149] [85]	$1 \sim 2$		all		
Pushing [146] [188] [72] [73] [122] [31] [144]	$1 \sim 4$	all			
Towing [81] [192] [5] [190] [161] [138] [98] [20] [19] [116]	1		1		
[62] [63] [186] [182]	2		2		
[71] **[40] [41] [44] [43] [42] [45]**	2		1	1	
[76] [183]	4		4		
[48] [46]	4				4
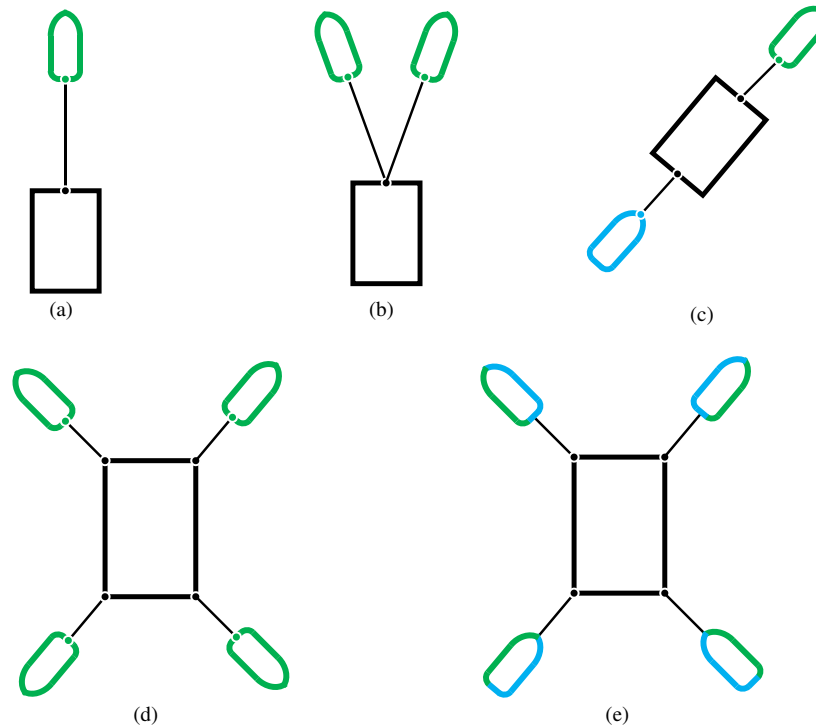
Figure 2.16: Situations of the vessel role in the existing research works (the black box represents the manipulated object, the green shape is the guiding vessel, the blue shape is the following vessel, the green and blue combined shape stands for the vessels can switch roles between guiding and following): (a) one guiding vessel; (b) two guiding vessels; (c) one guiding and one following vessel; (d) four guiding vessels; (e) four flexible vessels.

tugboat to control the position and heading of the object (Fig 2.16 (a)). To improve the efficiency of the heading control, some scholars use two guiding vessels towing the object [62, 63, 182, 186] (Fig 2.16 (b)). There is another configuration of the two-vessel towing system, taking one vessel as the guiding role and another vessel as the following role [40–45, 71] (Fig 2.16 (c)). The advantages of this configuration are that the velocity and trajectory of the object are fully controlled and well maintained, respectively, since the role of the following vessel can reduce the speed and stabilize the heading of the object. When the number of vessels increases to four, some researchers assign the guiding role to all the vessels to cooperatively manipulate the floating object [76, 183] (Fig 2.16 (d)). The object in this configuration has good maneuverability, however, the fact is that the hydrodynamic parameters of the vessel model are calculated based on the forward motion (the heading is toward the goal). If the configuration of Fig 2.16 (d) is applied, at least two vessels' heading is opposite to the goal in the process of manipulation, and the hydrodynamic parameters of these vessels are changed. This will result in the problem of model uncertainties. To solve this problem, some scholars adopt the flexible role to all the vessels [46, 48] (Fig 2.16 (e)).

In this way, the manipulation system can always keep two vessels with guiding and two vessels with following role in the towing process. Without reducing maneuverability, the manipulation system can effectively transport the floating object and the motions of all the vessels are satisfied with their hydrodynamic models.

2.6 Conclusions

This chapter reviews the existing research works on the floating object manipulation problem. It addresses the first research question **Q1**: What are the characteristics and concrete research gaps of the physically connected multi-vessel system?

Inspired by the object manipulation research in the field of multi-robot systems, four typical maritime object manipulation ways are summarized from the existing research works: attaching, caging, pushing, and towing. For each manipulation way, its definition and characteristics, the common type of the floating object, and the application scenarios are discussed in detail. For finding the research gaps, we analyze the control objectives concerned, the control architecture used, the collision avoidance involved, the environmental disturbances considered, and the role of each vessel in the floating object manipulation system. The complete and detailed framework and review outline of the floating object manipulation problem are shown in Fig 2.17.

For the control objective, the majority of research works emphasize the position and heading control of the floating object, while the velocity is a lack of concern. For the control architecture, except for the attaching manipulation, more than half of the works in the other three manipulation ways propose centralized control. For the problem of collision avoidance, few papers focus on collision avoidance of external static and dynamic obstacles for the floating object manipulation system. For handling disturbances, except for the towing manipulation, the majority of the works in the other three manipulation ways do not address this issue. For the assignment of vessel role, the vessels applying manipulation of attaching, caging, and pushing have their specific fixed roles. For the manipulation of towing, the vessels in the manipulation system have more flexible roles, and the role of the vessel can be switched.

Overall, it can be concluded that towing manipulation has the advantage of manipulation system safety, floating object controllability, and application scenarios flexibility, which can be a proper choice to manipulate a large marine structure. The research gaps of this manipulation lie in that: (1) complex towing system model; (2) implementation of the distributed control architecture; (3) collision avoidance of the external static and dynamic obstacles; (4) velocity control of the floating object; (5) flexible vessel role strategy of the swarm-vessel towing.

Based on the above findings, in the next chapter (Chapter 3), the research foundation of this work is presented, including research assumptions, basic vessel model, generic towing system model, control method, and control architecture. Cooperative control schemes in different operational scenarios, control objectives, environmental disturbances, collision avoidance, and vessel roles are investigated in the subsequence chapters (Chapter 4 – 7).
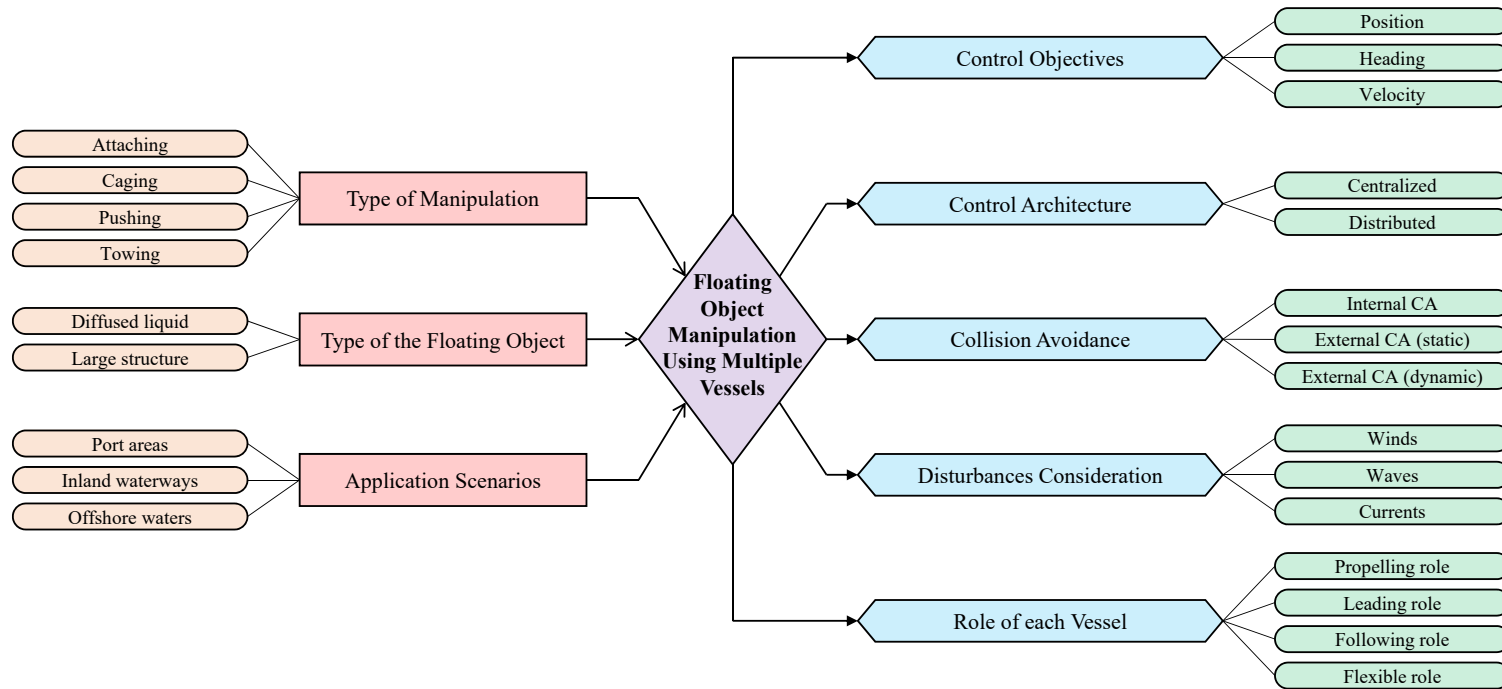
Figure 2.17: A detailed framework and review outline of the floating object manipulation problem.

Chapter 3

System Modelling and Control Framework

As concluded in Chapter 2, the way of towing is selected in this work to manipulate a large marine structure. This chapter addresses the second research question (**Q2**): "How to establish the dynamics model of the physically connected multi-vessel system, and the control framework?".

The organization of this chapter is as follows. Section 3.1 introduces the assumptions made in this research; Section 3.2 presents the model of the vessels, whose kinematics and kinetics models can precisely represent the characteristics of the vessel's motion; Section 3.3 proposes the generic model of the towing system based on Section 3.2; Section 3.4 and 3.5 focus on the control framework of this research, where Section 3.4 elaborates the control methods and Section 3.5 is for the control architectures; Section 3.6 concludes this chapter.

Parts of this chapter have been published in [40][1].

3.1   Research Assumptions

For this research, several assumptions are made, which are related to system modelling, control design, and application scenarios; and all of them are supported by the corresponding justifications [153].

A1: *In the towing system model, the towline is treated as a massless and non-elastic rope.*

The towing system consists of the floating object, the tugboats, and the towlines. The first two components can be represented by the vessel models, while the model of towline is usually ignored by the majority of related research. In a few works, the catenary model is used to represent the tension, resistance, and elasticity of the towline [27] [161], expressed as:

$$T = \left(H_D - 2\frac{T}{\omega}\sinh^{-1}\left(\frac{\omega L_R/2}{T}\right) \right) \frac{EA}{L_R}$$

---

[1]Z. Du, V. Reppa, and R. R. Negenborn. Cooperative control of autonomous tugs for ship towing. IFAC-PapersOnLine, 53(2):14470-14475, 2020.
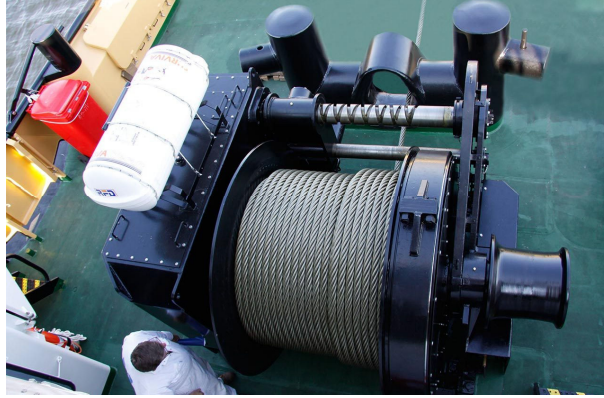
Figure 3.1: Towing winch [37].

where T is the component of the towline tension in the horizontal plane; H_D is the horizontal distance between the two ends of the towline; ω is the weight of the towline per unit length; L_R is the length of the towline; E is the Young's modulus of the towline; A is the cross-sectional area of the stream.

It is noticed that this model applies to the towline that is sizable, elastic, and can not ignore its mass, which usually appears in the situation of real maritime towing operations. However, in this thesis, the models of the small-scale lab vessels are used to validate the towing process via simulations. Thus, the towline can be simply treated as a massless and non-elastic rope. Another notable point is although the cables are not elastic, their length might be varying by controlling the winch, which means the winch can elongate and shorten the towline.

A2: *In the control system, the calculated towing forces (control inputs) can be achieved by the winch, and the towline can be always tight through the winch.*

In this thesis, the control system is designed to calculate the towing forces to manipulate the floating object. The towing force on the towline is controlled by the winch located on the tugboats (as shown in Fig 3.1). In practice, the winch controller can not exactly provide the expected towing force through the towline to the floating object. However, since the scope of this research focuses on high-layer control, which is the computation of the forces on the towline, the low-layer winch control [157] (including the detailed winch system model [156]) is not considered.

In the towing control-related literature the majority of papers [63, 71, 76, 81, 98, 161, 182, 183, 186, 192] simplify the part of winch control. Since usually the control order is generated frequently, every short period there will be new towing forces on the towlines. From a micro perspective, during this short period, the towline goes through the process of first tight and then slack; from a macro perspective, the towline can be seen as always tight in such a quick time instant.

Thus, the calculated towing forces (control inputs) by the proposed controllers are assumed to be perfectly achieved. Moreover, the winch can guarantee the action of

the restoring force to the tugboat and ensure the towline be always tight.

A3: *In the application scenarios of port areas, the dominant source of environmental disturbances is the wind, the unknown effects (waves and currents) are considered bounded random disturbances.*

Marine environmental disturbances are usually the effects mixed with winds, waves, and currents. In different application scenarios, the effects will be biased. In the scenarios of port areas, the wind influence is dominant [91]. Although in some cases waves may indeed be significant, they are considered unexpected events. Most of the research related to ship-berthing control in port areas [2, 119, 131, 148] take wind as the main environmental influence to the vessels.

After comprehensive consideration, the environmental disturbances, in this case, are divided into two parts: the wind effects and the unknown effects (mainly refer to waves and currents). Since the second part has limited influence, it can be seen as bounded random disturbances.

A4: *In the application scenarios of inland waterways, the speed of the towing system is slower than other moving vessels; if there is a close-quarters situation, it only happens between the towing system and one vessel.*

The operation of towing is a hazardous and challenging task, especially in inland waterways. According to the International Regulations for preventing Collisions at Sea (COLREGS), a vessel engaged in a towing operation can be seen the vessel restricted in her ability to maneuver [78]. Thus, the speed of the towing system is usually slower than other moving vessels and the overtaking situations do not happen for safety reasons. Conversely, other vessels will also stay away from the towing system as much as possible. If there is a close-quarters situation, the towing system only needs to deal with one vessel.

A5: *In the application scenarios of offshore waters, the waves are the long-crested and the currents are irrotational.*

In the application scenarios of offshore waters, all the three ocean effects (wind, waves, and currents) should be considered, where wave force contributes the majority of the total environment load. Waves are classified into two categories. Long-crested waves are the waves propagated from one direction, while the short-crested waves are the combination of different long-crested waves propagated from different directions [97]. Although the short-crested waves are closer to the real sea condition, since the offshore scenarios in this research are not far from the shore and the focus is on the control strategy, the long-crested waves are considered. Similarly, the ocean currents are simplified to irrotational constant currents, which only concern its speed and direction [56].

3.2 Modelling of Vessels

The motion of a vessel can be represented in 6 degrees of freedom (DOF): surge, sway, heave, roll, pitch, and yaw. Fig 3.2 shows the six motions in the body-fixed reference frame.
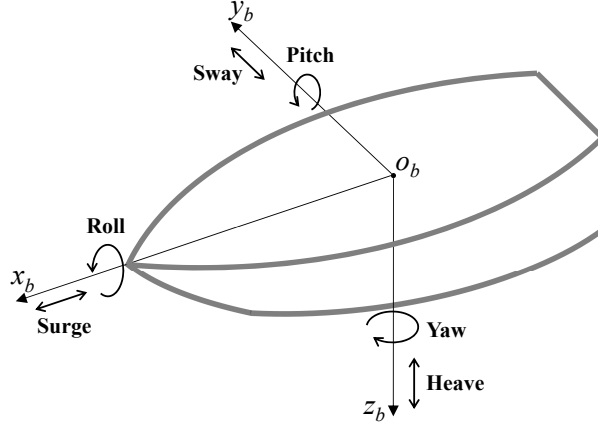
Figure 3.2: The 6 DOF motion of a vessel in the body-fixed reference frame.

To describe these motions mathematically, the vessel model is developed and established. There are two main ways of modelling the vessel motion: component form and vectorial representation. The component form is a classical way with the Taylor-series expansions to describe the hydrodynamic forces, but it often results in complicated forms with hundreds of elements. The vectorial representation uses matrices and vectors to simplify the equations of motion. It exploits physical system properties to reduce the number of coefficients needed for control [56]. Thus, the vectorial representation is adopted to establish the vessel model in this thesis for marine control systems design.

Considering the motion of vessels in the horizontal plane (surge, sway, and yaw) is the focus of this thesis, the 3 DOF model is used to formulate the kinematics (3.1) and kinetics (3.2) model of a vessel:

$$\dot{\boldsymbol{\eta}}(t) = \boldsymbol{R}\big(\psi(t)\big)\mathbf{v}(t) \tag{3.1}$$

$$\dot{\mathbf{v}}(t) = \boldsymbol{M}^{-1}\Big(-\boldsymbol{C}\big(\mathbf{v}(t)\big)\mathbf{v}(t) - \boldsymbol{D}\big(\mathbf{v}(t)\big)\mathbf{v}(t) + \boldsymbol{\tau}(t) + \boldsymbol{\tau}_E(t)\Big), \tag{3.2}$$

where $\boldsymbol{\eta}(t) = [x(t)\ y(t)\ \psi(t)]^{\mathrm{T}} \in \mathbb{R}^3$ is the position vector in the world frame (North-East-Down) including position coordinates $\big(x(t),\ y(t)\big)$ and heading $\psi(t)$ (as shown in Fig 3.3); $\mathbf{v}(t) = [u(t)\ v(t)\ r(t)]^{\mathrm{T}} \in \mathbb{R}^3$ is the velocity vector in the body-fixed frame containing the velocity of surge $u(t)$, sway $v(t)$ and yaw $r(t)$; $\boldsymbol{R} \in \mathbb{R}^{3\times3}$ is the rotation matrix from the body frame to the world frame, which is a function of heading:

$$\boldsymbol{R}\big(\psi(t)\big) = \begin{bmatrix} \cos\big(\psi(t)\big) & -\sin\big(\psi(t)\big) & 0 \\ \sin\big(\psi(t)\big) & \cos\big(\psi(t)\big) & 0 \\ 0 & 0 & 1 \end{bmatrix}.$$

The terms $\boldsymbol{M} \in \mathbb{R}^{3\times3}$ and $\boldsymbol{C} \in \mathbb{R}^{3\times3}$ are the mass (inertia) and Coriolis-Centripetal matrices, both of them consist of rigid-body and added-mass parts: $\boldsymbol{M} = \boldsymbol{M}_{RB} + \boldsymbol{M}_A$, $\boldsymbol{C} = \boldsymbol{C}_{RB} + \boldsymbol{C}_A$, where
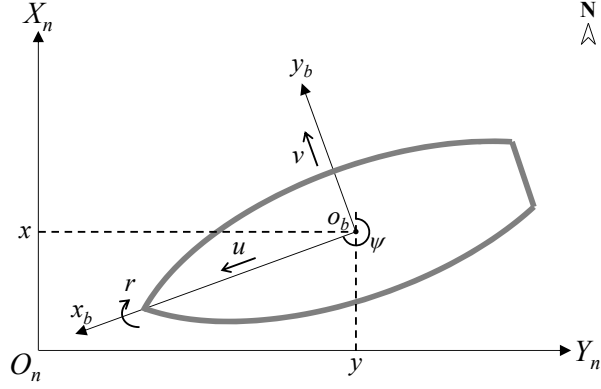
Figure 3.3: The 3 DOF motion of a vessel in the body-fixed and NED reference frame.

$$\boldsymbol{M}_{RB} = \begin{bmatrix} m & 0 & 0 \\ 0 & m & mx_g \\ 0 & mx_g & I_z \end{bmatrix}, \quad \boldsymbol{M}_A = \begin{bmatrix} -X_{\dot{u}} & 0 & 0 \\ 0 & -Y_{\dot{v}} & -Y_{\dot{r}} \\ 0 & -Y_{\dot{r}} & -N_{\dot{r}} \end{bmatrix},$$

$$\boldsymbol{C}_{RB} = \begin{bmatrix} 0 & 0 & -m(x_g r(t) + v(t)) \\ 0 & 0 & mu(t) \\ m(x_g r(t) + v(t)) & -mu(t) & 0 \end{bmatrix},$$

$$\boldsymbol{C}_A = \begin{bmatrix} 0 & 0 & Y_{\dot{v}}v(t) + 0.5(Y_{\dot{r}} + N_{\dot{v}})r(t) \\ 0 & 0 & -X_{\dot{u}}u(t) \\ -Y_{\dot{v}}v(t) - 0.5(Y_{\dot{r}} + N_{\dot{v}})r(t) & X_{\dot{u}}u(t) & 0 \end{bmatrix}.$$

The term $\boldsymbol{D} \in \mathbb{R}^{3 \times 3}$ is the damping matrix, including linear and non-linear parts: $\boldsymbol{D} = \boldsymbol{D}_l + \boldsymbol{D}_n$, where

$$\boldsymbol{D}_l = \begin{bmatrix} -X_u & 0 & 0 \\ 0 & -Y_v & -Y_r \\ 0 & -N_v & -N_r \end{bmatrix},$$

$$\boldsymbol{D}_n = \begin{bmatrix} -X_{|u|u}|u(t)| & 0 & 0 \\ 0 & -Y_{|v|v}|v(t)| - Y_{|r|v}|r(t)| & -Y_{|v|r}|v(t)| - Y_{|r|r}|r(t)| \\ 0 & -N_{|v|v}|v(t)| - N_{|r|v}|r(t)| & -N_{|v|r}|v(t)| - N_{|r|r}|r(t)| \end{bmatrix}.$$

The terms $\boldsymbol{\tau}(t) \in \mathbb{R}^3$ and $\boldsymbol{\tau}_E(t) \in \mathbb{R}^3$ are the controllable input vector and environmental disturbances vector in the body-fixed frame, respectively:

$$\boldsymbol{\tau}(t) = \begin{bmatrix} \tau_u(t) \\ \tau_v(t) \\ \tau_r(t) \end{bmatrix}, \quad \boldsymbol{\tau}_E(t) = \begin{bmatrix} \tau_{Eu}(t) \\ \tau_{Ev}(t) \\ \tau_{Er}(t) \end{bmatrix}.$$

Table 3.1: Information on the small-scale vessels used in this thesis.
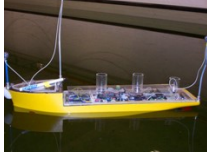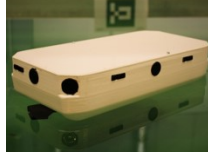
Vessel	*CyberShip II* [155]	*TitoNeri* [67]	*Delfia* [28]
Physical Picture			
Length	1.255 m	0.97 m	0.38 m
Width	0.29 m	0.30 m	0.185 m
Actuators	1) Two stern propellers with two rudders; 2) One bow thruster.	1) Two stern azimuth thrusters; 2) One bow thruster.	Two azimuth thrusters located at the sides of the bow and the stern.

Table 3.2: Parameters of the used vessels in this thesis.

		CyberShip II [155]		
m	23.800		N_v	0.03130
x_g	0.046		N_r	-1.900
I_z	1.760		$X_{\|u\|u}$	-1.32742
$X_{\dot{u}}$	-2.0		$Y_{\|v\|v}$	-36.47287
$Y_{\dot{v}}$	-10.0		$Y_{\|r\|v}$	-0.805
$Y_{\dot{r}}$	- 0.0		$Y_{\|v\|r}$	-0.845
$N_{\dot{r}}$	- 1.0		$Y_{\|r\|r}$	-3.450
$N_{\dot{v}}$	- 0.0		$N_{\|v\|v}$	3.95645
X_u	-0.72253		$N_{\|r\|v}$	0.130
Y_v	-0.88965		$N_{\|v\|r}$	0.080
Y_r	-7.250		$N_{\|r\|r}$	-0.750
		TitoNeri [67]		
m	16.9		$Y_{\dot{v}}$	-49.2
x_g	0.0		$Y_{\dot{r}}$	0.0
I_z	0.51		$N_{\dot{v}}$	0.0
$X_{\dot{u}}$	-1.2		$N_{\dot{r}}$	-1.8
		Delfia [28]		
m	3.345		$N_{\dot{r}}$	-0.110
x_g	0.0		X_u	-2.734
I_z	0.031		Y_v	-4.60250
$X_{\dot{u}}$	-0.2310		Y_r	0.79546
$Y_{\dot{v}}$	-1.334		N_v	0.50439
$Y_{\dot{r}}$	0.0		N_r	-0.22243

Table 3.1 shows the information on the small-scale vessels used in this thesis. The vessel *CyberShip II* is developed by Norwegian University of Science and Technology (NTNU). It is a 1:70 scale replica of a supply ship. The vessel *TitoNeri* and vessel *Delfia* are developed by Delft University of Technology (TU Delft). *TitoNeri* is a small model tugboat (1:30) of roughly a meter long and width of 30 centimeters, *Delfia* is a box-shaped ASV prototype with two 360° steering propellers (one at the bow and the other at the stern), whose design is to make maneuvering in crowded environments easier than actual solutions.

The parameters of the three vessels are shown in Table 3.2. It can be observed that the parameters in the mass ($\boldsymbol{M}$) and Coriolis-Centripetal ($\boldsymbol{C}$) matrices of the three models are identified, but the damping part ($\boldsymbol{D}$) has different considerations. The model of *CyberShip II* provides all the parameters of the linear and non-linear parts in the damping matrix, while the model of *Delfia* only provides the parameters of the linear part ($\boldsymbol{D}_l$). The model of *TitoNeri* replace the whole damping part $\boldsymbol{D}\big(\mathbf{v}(t)\big)\mathbf{v}(t)$ to the drag forces vector $\boldsymbol{\tau}_{\mathrm{drag}}(t)$:

$$
\boldsymbol{\tau}_{\mathrm{drag}}(t) = \left[\begin{array}{c} \tau_{\mathrm{dragu}}\big(\psi(t),u(t)\big) \\ \tau_{\mathrm{dragv}}\big(\psi(t),v(t)\big) \\ \tau_{\mathrm{dragr}}\big(r(t)\big) \end{array}\right],
$$

where the elements of τ_{dragu} and τ_{dragv} are the drag forces in x and y direction, which are calculated through the polynomial fitting. The polynomial function is determined by the velocity in the corresponding direction and the heading angles. The element of τ_{dragr} is the drag moment, calculated by the polynomial function of yaw velocity. The process of polynomial fitting and the detailed parameters of the polynomial function can refer to [18].

3.3 Modelling of the Towing System

This section details the kinematic and kinetic model of the towing system.

3.3.1 Kinetics of the Towing System

For a towing system with a non-powered floating object and n tug boats, the forces on the floating object and tugboat i are shown in Fig 3.4 and Fig 3.5. As to the floating object, the controllable inputs $\boldsymbol{\tau}_{\mathrm{FO}}(t)$ (in (3.2), $\boldsymbol{\tau}(t) \triangleq \boldsymbol{\tau}_{\mathrm{FO}}(t)$) come from the towline, which can be formulated as:

$$
\boldsymbol{\tau}_{\mathrm{FO}}(t) = \sum_{i=1}^{n} \boldsymbol{\tau}_{\mathrm{fo}i}(t)
$$

$$
\boldsymbol{\tau}_{\mathrm{fo}i}(t) = \boldsymbol{B}_{\mathrm{fo}i}(t)F_i(t),
$$

(3.3)

where n is the number of tugs; $\boldsymbol{\tau}_{\mathrm{fo}i}(t)$ represents the towing forces and moment by Tug i; $F_i(t)$ is the towing force from the tug i through the towline; $\boldsymbol{B}_{\mathrm{fo}i}(t) \in \mathbb{R}^3$ is the configuration matrix with respect to the object-body frame, it is a function of the towing angle $\alpha_i(t)$ expressed as:

$$
\boldsymbol{B}_{\mathrm{fo}i}(t) = \left[\begin{array}{c} \cos\big(\alpha_i(t)\big) \\ \sin\big(\alpha_i(t)\big) \\ l_i\big[\sin\big(\alpha_i(t)\big)\cos(\gamma_i) - \cos\big(\alpha_i(t)\big)\sin(\gamma_i)\big] \end{array}\right],
$$

(3.4)
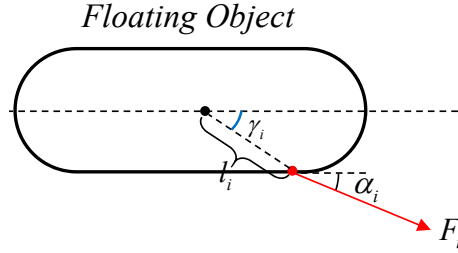
Figure 3.4: Forces on the object of a towing system.
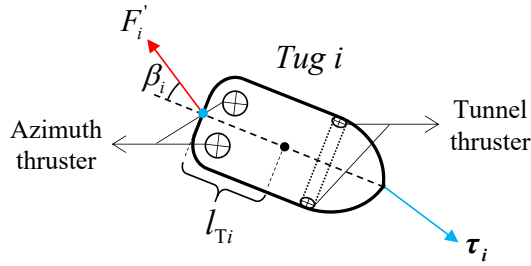
Figure 3.5: Forces on tug i of a towing system.

where l_i is the distance from the center of gravity of the object to the object towing point; γ_i is the angle between the heading of the object and the direction from the center of gravity of the object to the towing point (shown in Fig 3.4).

In order to validate the manipulation of the floating object flexibly, the model of *TitoNeri* is chosen as the tugboat in this thesis, whose actuator system contains two stern azimuth thrusters and one bow tunnel thruster (as shown in Fig 3.5), known as the *ASD tug* [68]. With the help of three thrusters, the tugboat can obtain omnidirectional forces and moments. Thus, the controllable input $\boldsymbol{\tau}_i(t)$ (in (3.2), $\boldsymbol{\tau}(t) \triangleq \boldsymbol{\tau}_i(t)$) of the tugboat i can be formulated as:

$$\boldsymbol{\tau}_i(t) = \boldsymbol{\tau}_{Ti}(t) + \boldsymbol{\tau}_{Fi}(t), \tag{3.5}$$

where $\boldsymbol{\tau}_{Ti}(t) \in \mathbb{R}^3$ denotes the forces and moment provided by the tug actuator system; $\boldsymbol{\tau}_{Fi}(t) \in \mathbb{R}^3$ represents the forces and moment to compensate for the reaction of towing force, which can be expressed as:

$$\boldsymbol{\tau}_{Fi}(t) = \boldsymbol{B}_{Ti}(t)F_i^{'}(t), \tag{3.6}$$

where $\boldsymbol{B}_{Ti}(t) \in \mathbb{R}^3$ is the configuration matrix with respect to the tug-body frame. This term is a function of the tug angle $\beta_i(t)$ (this angle will be defined and calculated in the next sub-section), expressed as:

$$\boldsymbol{B}_{Ti}(t) = \begin{bmatrix} \cos\left(\beta_i(t)\right) \\ \sin\left(\beta_i(t)\right) \\ l_{Ti}\sin\left(\beta_i(t)\right) \end{bmatrix}, \tag{3.7}$$

where l_{Ti} is the distance from the center of gravity of the tugboat to the tug towing point (shown in Fig 3.5).

The term $F_i^{'}(t)$ is the force applied through a controlled winch onboard the tugboat to the towline. According to the first and second assumptions (**A1** and **A2**), we have

$$F_i^{'}(t) \equiv F_i(t). \tag{3.8}$$

Overall, combining (3.2) – (3.8), the kinetics of the floating object and the tugboat i in a towing system can be formulated as:

$$\dot{\mathbf{v}}_{\text{FO}}(t) = \mathbf{M}_{\text{FO}}^{-1}\Big(-\mathbf{C}_{\text{FO}}\big(\mathbf{v}_{\text{FO}}(t)\big)\mathbf{v}_{\text{FO}}(t) - \mathbf{D}_{\text{FO}}\big(\mathbf{v}_{\text{FO}}(t)\big)\mathbf{v}_{\text{FO}}(t) +$$
$$\sum_{i=1}^{n}\big\{\mathbf{B}_{\text{fo}i}\big(\alpha_i(t)\big)F_i(t)\big\} + \boldsymbol{\tau}_{E_{\text{FO}}}(t)\Big), \tag{3.9}$$

$$\dot{\mathbf{v}}_i(t) = \mathbf{M}_i^{-1}\Big(-\mathbf{C}_i\big(\mathbf{v}_i(t)\big)\mathbf{v}_i - \mathbf{D}_i\big(\mathbf{v}_i(t)\big)\mathbf{v}_i(t) + \boldsymbol{\tau}_{Ti}(t) +$$
$$\mathbf{B}_{Ti}\big(\beta_i(t)\big)F_i(t) + \boldsymbol{\tau}_{E_i}(t)\Big). \tag{3.10}$$

Overall, (3.9) and (3.10) show that the kinetic interconnection between the system of a floating object and tugboats is the towing force $F_i(t)$. For the floating object, the towing force is the power that makes it move; while for tugboats, the towing force is the resistance that needs to be compensated.

3.3.2   Kinematics of the Towing System

The kinematics modelling of the towing system is to find the geometric motion relations between the floating object and the tugboats. Due to the position and heading of the floating object being the control objectives that we want to achieve, the desired position and heading of the tugboats can be calculated based on these data of the floating object.

As shown in Fig 3.6, the desired position (x_{id}, y_{id}) and heading (ψ_{id}) of the tug i are expressed as:

$$x_{id}(t) = x_{\text{FO}}(t) + l_i \sin\big(\psi_{\text{FO}}(t) + \gamma_i\big) + l_{\text{tow}i}\sin\big(\psi_{id}(t)\big) + l_{Ti}\sin\big(\psi_{id}(t)\big)$$
$$y_{id}(t) = y_{\text{FO}}(t) + l_i \cos\big(\psi_{\text{FO}}(t) + \gamma_i\big) + l_{\text{tow}i}\cos\big(\psi_{id}(t)\big) + l_{Ti}\cos(\psi_{id}(t))$$
$$\psi_{id}(t) = \psi_{\text{FO}}(t) + \alpha_i(t),$$

where $l_{\text{tow}i}$ is the desired length of the towline that guarantees the collision avoidance between the object and tugboat i. It can be noticed that the desired states of the tug i are determined by the states of the floating object and the towing angle. Thus, the above equations can be transformed to the vectorial representation with variables the position vector of the object $\boldsymbol{\eta}_{\text{FO}}(t)$ and the towing angle $\alpha_i(t)$:

$$\boldsymbol{\eta}_{id}(t) = \boldsymbol{\eta}_{\text{FO}}(t) + (l_{\text{tow}i} + l_{Ti})\mathbf{E}_i(t) + l_i\mathbf{F}_i(t) + \alpha_i(t)[0\ \ 0\ \ 1]^{\text{T}}, \tag{3.11}$$

where $\mathbf{E}_i(t) \in \mathbb{R}^3$ and $\mathbf{F}_i(t) \in \mathbb{R}^3$ are the vectors related to the object's heading $\psi_{\text{FO}}(t)$ and
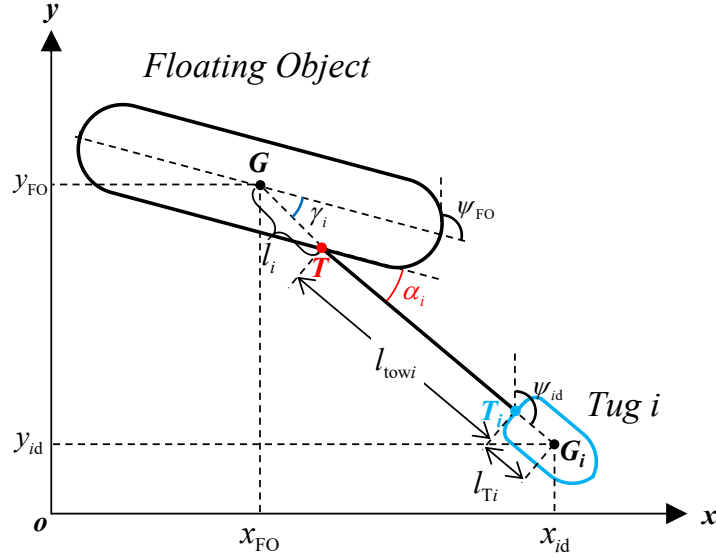
Figure 3.6: Kinematics of the towing system.

the towing angle $\alpha_i(t)$, expressed as:

$$\boldsymbol{E}_i(t) = \text{sgn}(i) \left[\begin{array}{c} \sin\left(\psi_{\text{FO}}(t) + \alpha_i(t)\right) \\ \cos\left(\psi_{\text{FO}}(t) + \alpha_i(t)\right) \\ 0 \end{array} \right], \tag{3.12}$$

$$\boldsymbol{F}_i(t) = \text{sgn}(i) \left[\begin{array}{c} \sin\left(\psi_{\text{FO}}(t) + \gamma_i\right) \\ \cos\left(\psi_{\text{FO}}(t) + \gamma_i\right) \\ 0 \end{array} \right], \tag{3.13}$$

where $\text{sgn}(i)$ is the sign function related to the relative position between the floating object and the tugboat i:

$$\text{sgn}(i) = \left\{ \begin{array}{ll} -1 & \text{if the tugboat } i \text{ is behind the floating object;} \\ 1 & \text{if the tugboat } i \text{ is in front of the floating object.} \end{array} \right. \tag{3.14}$$

Fig 3.7 shows the relations between the desired and actual heading of the Tug i. The tug angle $\beta_i(t)$ in (3.7) and (3.10) then can be calculated by combining the angle relations in Fig 3.6 and Fig 3.7):

$$\beta_i(t) = \psi_{\text{FO}}(t) + \alpha_i(t) - \psi_i(t), \tag{3.15}$$

where ψ_i is the actual heading of the tugboat i.

Overall, (3.11) shows that the kinematic interconnection between the system of a floating object and tugboats is the towing angles $\alpha_i(t)$. For the floating object, the towing angle is the control input determining the direction of the towing force; while for tugboats, the towing angle is the configuration variable determining the reference position and heading.
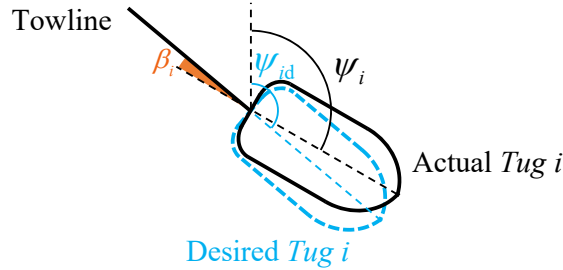
Figure 3.7: Relations between the desired and actual Tug i.
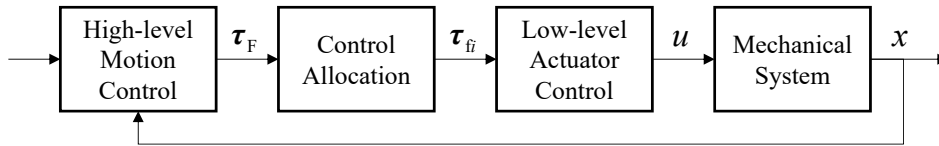
Figure 3.8: Control system structure with control allocation module.

3.4 Control Methods

According to (3.9), the control inputs of the floating object are the towing forces $F_i(t)$ and towing angles $\alpha_i(t)$. When the number of tugboats is equal or more than two, the number of control inputs of the floating object will be more than its DOF. In such a case, the towing system becomes an over-actuated mechanical system. The over-actuated systems are often applied in practice because of the need for actuator redundancy to meet fault tolerance and control reconfiguration or the requirements of certain actuators for being shared among several control systems with different objectives [87].

A control system containing the module of control allocation can be illustrated in Fig 3.8. First, the motion controller in the high-level control computes virtual control inputs $\boldsymbol{\tau}_F$ for the system, which are usually the forces and moments. Then, the control allocation module divides the $\boldsymbol{\tau}_F$ to several small control inputs $\boldsymbol{\tau}_{fi}$ according to the number of actuators. Finally, each actuator controller in the low-level control calculates the actual control inputs u to the mechanical system.

In our cases, the virtual forces and moment $\boldsymbol{\tau}_{FO}$ is computed for manipulating the object in the floating object motion control. Through the control allocation, $\boldsymbol{\tau}_{FO}$ is divided into n number of forces and moments $\boldsymbol{\tau}_{foi}$. These forces and moments are finally transformed to towing forces F_i and angles α_i to directly affect on the floating object. The actuators for the floating object are the tugboats.

In summary, the control allocation problem is required to compute multiple control inputs and involves multiple kinds of control constraints, such as control input saturation, system dynamics, actuator rate constraints, physical configuration restraints, etc. Thus, optimization-based control strategies are usually adopted to solve such a multi-control input multi-control constraint problem.

For a floating object manipulation system with n number of tugboats, the control allo-

cation problem solved by optimization-based control method is formulated as:

$$\text{minimize} \quad J_{\text{FO}}\big(\boldsymbol{X}_{\text{FO}}(t), \boldsymbol{U}_{\text{FO}}(t)\big) \tag{3.16}$$

$$\text{subject to} \quad \forall\, i \in n: $$

$$\boldsymbol{X}_{\text{FO}}(t) \in \mathbb{X}_{\text{FO}} \tag{3.17}$$

$$\boldsymbol{U}_{\text{FO}}(t) \in \mathbb{U}_{\text{FO}} \tag{3.18}$$

$$g_i\big(\boldsymbol{X}_{\text{FO}}(t), \boldsymbol{U}_{\text{FO}}(t)\big) = f_i\big(\boldsymbol{X}_i(t), \boldsymbol{U}_i(t), \boldsymbol{U}_{\text{FO}}(t)\big), \tag{3.19}$$

where $\boldsymbol{X}_{\text{FO}}(t) = [\boldsymbol{\eta}_{\text{FO}}(t)\ \ \mathbf{v}_{\text{FO}}(t)]^{\text{T}}$ and $\boldsymbol{U}_{\text{FO}}(t) = [F_1(t)\ \ \alpha_1(t)\ \ ...\ \ F_n(t)\ \ \alpha_n(t)]^{\text{T}}$ are the states and control inputs of the floating object, respectively; $\mathbb{X}_{\text{FO}}$ represents constraints of the floating object dynamics; $\mathbb{U}_{\text{FO}}$ stands for constraints due to the control input saturation. The term $g_i\big(\boldsymbol{X}_{\text{FO}}(t), \boldsymbol{U}_{\text{FO}}(t)\big)$ stands for the function of the towing system kinematics, referring to (3.11); $f_i\big(\boldsymbol{X}_i(t), \boldsymbol{U}_i(t), \boldsymbol{U}_{\text{FO}}(t)\big)$ represents the dynamics of the tugboat i, referring to (3.1) and (3.10). Equation (3.19) means that the towing system should satisfy the desired configuration, which is an interconnecting constraint between the floating object and the tugboat i.

Correspondingly, for the tugboat i, the optimization-based control problem is then formulated as:

$$\text{minimize} \quad J_i\big(\boldsymbol{X}_i(t), \boldsymbol{U}_i(t)\big) \tag{3.20}$$

$$\text{subject to} \quad \boldsymbol{X}_i(t) \in \mathbb{X}_i \tag{3.21}$$

$$\boldsymbol{U}_i(t) \in \mathbb{U}_i \tag{3.22}$$

$$f_i\big(\boldsymbol{X}_i(t), \boldsymbol{U}_i(t), \boldsymbol{U}_{\text{FO}}(t)\big) = g_i\big(\boldsymbol{X}_{\text{FO}}(t), \boldsymbol{U}_{\text{FO}}(t)\big), \tag{3.23}$$

where $\boldsymbol{X}_i(t) = [\boldsymbol{\eta}_i(t)\ \ \mathbf{v}_i(t)]^{\text{T}}$ and $\boldsymbol{U}_i(t) = \boldsymbol{\tau}_{Ti}(t)$ are states and control inputs of the tugboat i; $\mathbb{X}_i$ represents constraints of the tugboat i dynamics; $\mathbb{U}_i$ stands for constraints due to the control input saturation.

However, since the maneuverability of the towing system is quite limited, in some scenarios like congested waterways just calculating the current control inputs is not enough for ensuring the safety of the towing system (collision avoidance). Thus, the predictive optimization-based control strategy is developed and applied to compute a set of control inputs within a certain horizon. The representative approach is model predictive control (MPC).

The predicted control inputs are achieved based on the system model inside the MPC controller [140] [6]. As shown in Fig 3.9, the measured states from the system are used by the model to calculate the predicted states, the optimizer then uses these states as the initial condition to compute future control inputs in the premises of the control objective and constraints, and sends them back to the model. After finishing the predictive horizon, the first step of the calculated control inputs is sent to the real system.

Because control problems are often solved by digital computers, the continuous-time system model has to be discretized [118] [179]. For the floating object and tugboat i, the
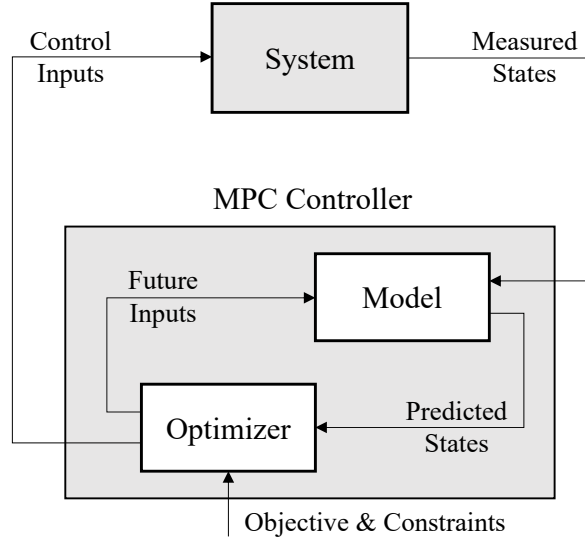
Figure 3.9: Structure of model predictive control.

discretized system model can be formulated as:

$$\boldsymbol{X}_{\text{FO}}(k+1) = \boldsymbol{X}_{\text{FO}}(k) + \int_{kT_s}^{(k+1)T_s} f_{\text{FO}}\big(\boldsymbol{X}_{\text{FO}}(t), \boldsymbol{U}_{\text{FO}}(t)\big)dt, \tag{3.24}$$

$$\boldsymbol{X}_i(k+1) = \boldsymbol{X}_i(k) + \int_{kT_s}^{(k+1)T_s} f_i\big(\boldsymbol{X}_i(t), \boldsymbol{U}_i(t)\big)dt, \tag{3.25}$$

where k is the discrete time step; T_s is the sampling time; f_{FO} and f_i is the dynamics of the floating object and tugboat i, respectively.

Thus, the MPC-based control problem for the floating object and tugboat i can be expressed as:

$$\text{minimize} \quad \sum_{h=1}^{H_{\text{P}}} J_{\text{FO}}\big(\boldsymbol{X}_{\text{FO}}(k+h|k), \boldsymbol{U}_{\text{FO}}(k+h|k)\big) \tag{3.26}$$

$$\text{subject to} \quad \forall\, i \in n,\ \forall\, h \in H_{\text{P}}:$$

$$\boldsymbol{X}_{\text{FO}}(k+h|k) \in \mathbb{X}_{\text{FO}} \tag{3.27}$$

$$\boldsymbol{U}_{\text{FO}}(k+h|k) \in \mathbb{U}_{\text{FO}} \tag{3.28}$$

$$g_i\big(\boldsymbol{X}_{\text{FO}}(k+h|k), \boldsymbol{U}_{\text{FO}}(k+h|k)\big) =$$
$$f_i\big(\boldsymbol{X}_i(k+h|k), \boldsymbol{U}_i(k+h|k), \boldsymbol{U}_{\text{FO}}(k+h|k)\big), \tag{3.29}$$

$$\text{minimize} \quad \sum_{h=1}^{H_{\text{P}}} J_i\big(\boldsymbol{X}_i(k+h|k), \boldsymbol{U}_i(k+h|k)\big) \tag{3.30}$$

subject to $\forall\, h \in H_\mathrm{P}$:

$$\boldsymbol{X}_i(k+h|k) \in \mathbb{X}_i \tag{3.31}$$

$$\boldsymbol{U}_i(k+h|k) \in \mathbb{U}_i \tag{3.32}$$

$$f_i\big(\boldsymbol{X}_i(k+h|k),\boldsymbol{U}_i(k+h|k),\boldsymbol{U}_\mathrm{FO}(k+h|k)\big) = $$
$$g_i\big(\boldsymbol{X}_\mathrm{FO}(k+h|k),\boldsymbol{U}_\mathrm{FO}(k+h|k)\big), \tag{3.33}$$

where H_P is the length of the prediction horizon; h is the hth time prediction step; $k+h|k$ is the prediction at time step $k+h$ based on the instant time step k.

3.5   Control Architectures

According to Section 2.3, most of the methods for floating object manipulation focus on centralized and distributed architectures.

In the centralized control architecture (shown in Fig 3.10), there is only a central control agent calculating the control inputs for n number of systems, so the optimizer solves a large global optimization problem. For the floating object towing system, the cost function in the centralized control architecture is formulated as:

$$J_\mathrm{Central} = J_\mathrm{FO} + \sum_{i=1}^{n} J_i. \tag{3.34}$$

In the distributed control architecture (shown in Fig 3.11), multiple control agents are deployed in different control layers to collaboratively achieve the control objectives. Usually, a supervisor control agent is located in the high layer to divide a global control objective and assign control tasks. The local control agents calculate the specific control input aiming for each system. For the floating object towing system, the cost function in the distributed control architecture is separated into multiple small functions corresponding to the object and each tugboat.

However, since the optimizer in each control agent calculates its optimization problem individually, the interconnecting constraints between each control agent can not be guaranteed. To satisfy the interconnecting constraints between the floating object and each tugboat in our case (equations (3.29) and (3.33)), the alternating direction method of multipliers (ADMM) is used.

The ADMM is a widely used algorithm well suited to solve distributed convex optimization problems, especially for consensus problems [141]. It coordinates the solutions of small local sub-problems to find a solution of a large global problem. The idea of the ADMM is to blend the dual ascent optimization approach with the augmented Lagrangians method of multipliers, which is characterized by superior decomposability and convergence properties [160].

For our case, the augmented Lagrangian form of the floating object manipulation problem at time instant k can be formulated as:
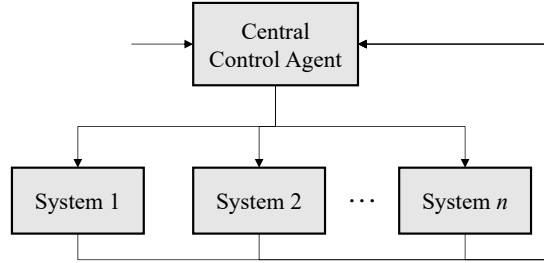
Figure 3.10: Centralized control architecture.
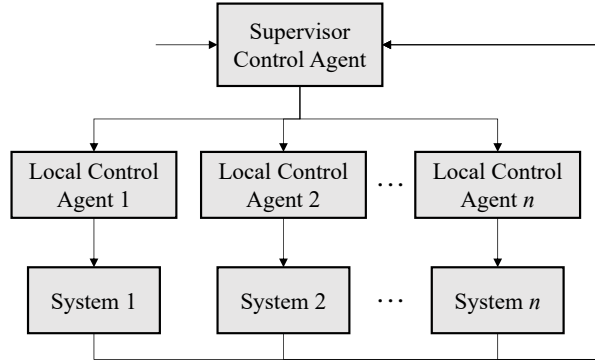
Figure 3.11: Distributed control architecture.

$$
\begin{aligned}
L_p\big(\boldsymbol{U}_{\mathrm{FO}}(k),\boldsymbol{U}_i(k),\lambda_i(k)\big) = {} & J_{\mathrm{FO}}\big(\boldsymbol{U}_{\mathrm{FO}}(k)\big) \;+\; \sum_{i=1}^{n}\Big\{J_i\big(\boldsymbol{U}_i(k)\big)\Big\} \;+\; \\
& \sum_{i=1}^{n}\Big\{\lambda_i^{\mathrm{T}}(k)\big[f_i\big(\boldsymbol{U}_i(k),\boldsymbol{U}_{\mathrm{FO}}(k)\big)-g_i\big(\boldsymbol{U}_{\mathrm{FO}}(k)\big)\big]+ \\
& \quad (\rho_i/2)\big\|f_i\big(\boldsymbol{U}_i(k),\boldsymbol{U}_{\mathrm{FO}}(k)\big)-g_i\big(\boldsymbol{U}_{\mathrm{FO}}(k)\big)\big\|_2^2\Big\},
\end{aligned}
\tag{3.35}
$$

where $\lambda_i(k)$ is the Lagrange multiplier or also called dual variable; $\rho_i > 0$ is the penalty parameter.

It can be seen that the right-hand side of (3.35) consists of three parts. The first and second parts are the cost functions of the floating object and tugboats. The third part is the interconnecting constraint between the floating object and each tugboat. Thus, the optimization of L_p is not only to minimize the cost functions J_{FO} and J_i, but also to satisfy the interconnecting constraint (make f_i equals to g_i).

Then, the iteration procedure of the ADMM at time instant k is formulated as follows:

$$\boldsymbol{U}_i^s(k) := \underset{\boldsymbol{U}_i(k)}{\arg\min} \left(J_i(\boldsymbol{U}_i(k)) + \lambda_i^{s-1}(k)^{\mathrm{T}} \left[f_i(\boldsymbol{U}_i(k), \boldsymbol{U}_{\mathrm{FO}}^{s-1}(k)) - g_i(\boldsymbol{U}_{\mathrm{FO}}^{s-1}(k)) \right] \right.$$
$$\left. + (\rho_i/2) \left\| f_i(\boldsymbol{U}_i(k), \boldsymbol{U}_{\mathrm{FO}}^{s-1}(k)) - g_i(\boldsymbol{U}_{\mathrm{FO}}^{s-1}(k)) \right\|_2^2 \right), \tag{3.36}$$

$$\boldsymbol{U}_{\mathrm{FO}}^s(k) := \underset{\boldsymbol{U}_{\mathrm{FO}}(k)}{\arg\min} \left(J_{\mathrm{FO}}(\boldsymbol{U}_{\mathrm{FO}}(k)) + \sum_{i=1}^n \left\{ \lambda_i^{s-1}(k)^{\mathrm{T}} \left[f_i(\boldsymbol{U}_i^s(k), \boldsymbol{U}_{\mathrm{FO}}(k)) - g_i(\boldsymbol{U}_{\mathrm{FO}}(k)) \right] \right.\right.$$
$$\left.\left. + (\rho_i/2) \left\| f_i(\boldsymbol{U}_i^s(k), \boldsymbol{U}_{\mathrm{FO}}(k)) - g_i(\boldsymbol{U}_{\mathrm{FO}}(k)) \right\|_2^2 \right), \tag{3.37}$$

$$\lambda_i^s(k) := \lambda_i^{s-1}(k) + \rho_i \left(f_i(\boldsymbol{U}_i^s(k), \boldsymbol{U}_{\mathrm{FO}}^s(k)) - g_i(\boldsymbol{U}_{\mathrm{FO}}^s(k)) \right), \tag{3.38}$$

where s is the iteration, $\cdot^s$ stands for the corresponding variable at the sth iteration.

The termination criterion is provided based on the following residuals [160]:

$$\left\| R_{\mathrm{pri},i}^s(k) \right\|_2 = \left\| f_i(\boldsymbol{U}_i^s(k), \boldsymbol{U}_{\mathrm{FO}}^s(k)) - g_i(U_{\mathrm{FO}}^s(k)) \right\|_2 \le \varepsilon_{\mathrm{pri},i}^s(k),$$
$$\left\| R_{\mathrm{dual},i}^s(k) \right\|_2 = \left\| g_i(\boldsymbol{U}_{\mathrm{FO}}^s(k)) - g_i(\boldsymbol{U}_{\mathrm{FO}}^{s-1}(k)) \right\|_2 \le \varepsilon_{\mathrm{dual},i}^s(k), \tag{3.39}$$

where $R_{\mathrm{pri},i}^s$ and $R_{\mathrm{dual},i}^s$ are the primal and dual residual of the control agent i at iteration s; $\varepsilon_{\mathrm{pri},i}^s > 0$ and $\varepsilon_{\mathrm{dual},i}^s > 0$ are the corresponding feasibility tolerances, determined by

$$\varepsilon_{\mathrm{pri},i}^s(k) = \sqrt{n_s}\varepsilon^{\mathrm{abs}} + \varepsilon^{\mathrm{rel}} \max \left\{ \left\| f_i(\boldsymbol{U}_i^s(k), \boldsymbol{U}_{\mathrm{FO}}^s(k)) \right\|_2, \left\| g_i(\boldsymbol{U}_{\mathrm{FO}}^s(k)) \right\|_2 \right\},$$
$$\varepsilon_{\mathrm{dual},i}^s(k) = \sqrt{n_s}\varepsilon^{\mathrm{abs}} + \varepsilon^{\mathrm{rel}} \left\| \lambda_i^s(k) \right\|_2, \tag{3.40}$$

where n_s is the size of the variable $\boldsymbol{U}_i$; $\varepsilon^{\mathrm{abs}} > 0$ and $\varepsilon^{\mathrm{rel}} > 0$ are the absolute and relative tolerance, respectively.

The penalty parameter ρ_i^s of the control agent i at iteration s is usually designed to be variable according to the comparison of the primal and dual residuals to increase the speed of convergence. A typical scheme is expressed as follows [160]:

$$\rho_i^s := \begin{cases} a^{\mathrm{incr}}\rho_i^{s-1} & \text{if } \left\| R_{\mathrm{pri},i}^s(k) \right\|_2 > \mu \left\| R_{\mathrm{dual},i}^s(k) \right\|_2 \\ \rho_i^{s-1}/a^{\mathrm{decr}} & \text{if } \left\| R_{\mathrm{dual},i}^s(k) \right\|_2 > \mu \left\| R_{\mathrm{pri},i}^s(k) \right\|_2 \\ \rho_i^{s-1} & \text{otherwise,} \end{cases} \tag{3.41}$$

where $a^{\mathrm{incr}} > 1$ and $a^{\mathrm{decr}} > 1$ are the parameters to increase and decrease the penalty; $\mu > 1$ is the parameter to determine whether the penalty is updated. The idea behind this is to keep the primal and dual residual norms within the factor of μ of one another as they both converge to zero [160].

From the perspective of the distributed architecture implementation, the communication happens between the floating object and tugboats for exchanging their position, heading, velocity, force, environment, etc. information. This information is measured from the sensors of GPS, Gyro-Compass, IMU, Camera, Force measurement sensors, Anemometer, Wind Vane, etc.

3.6   Conclusions

This chapter introduces the research foundations of this thesis. It addresses the second research question **Q2**: How to establish the dynamics model of the physically connected multi-vessel system, and the control framework?

Section 3.1 describes five assumptions used in this research related to system modelling, control design, and application scenarios. Section 3.2 presents the motion model of a vessel, where the 3 DOF vectorial representation model is used in this thesis to represent the kinematics and kinetics of a vessel. Besides, the modelling information of three small-scale lab vessels used in our research is introduced, including size and hydrodynamic parameters. Section 3.3 proposes the generic model of the towing system, where the towing forces and towing angles are the kinetic and kinematic interconnections between the floating object and tugboats, respectively. Section 3.4 and 3.5 analyze the control method and control architecture used in our research. The generic framework of the relevant control methods and architectures are established aiming at the floating object towing problem.

It can be concluded that the towing forces and towing angles make connections between the floating object system and the tugboat system. On the one hand, these two variables are the key control inputs of the floating object; on the other hand, the towing forces are related to the control inputs of the tugboats, and the towing angles are involved in the reference trajectories of the tugboats. According to the characteristics of the towing system model, the predictive optimization-based control strategy is the proposed approach for our research, specifically, the approach of model predictive control (MPC). In addition, in the case of distributed control architecture, the alternating direction method of multipliers (ADMM) is used to achieve the consensus between the floating object and the multiple tugboats.

Based on the above research foundations, several specific cooperative control schemes are proposed for physically connected multi-vessel towing systems in the following chapters (Chapter 4 – 7). In the next chapter (Chapter 4), the research focus is the towing scenario in port areas with dominated wind disturbances.

Chapter 4

Cooperative Control of A Ship-Towing System under Environmental Disturbances in Port Area

Chapter 3 proposes the system model and control framework, which lays the foundations of this thesis. Starting from this chapter, the focus is the control design of a towing system considering specific scenarios. This chapter addresses the third research question (**Q3**): "How to increase the robustness of the towing operation to handle the influence of environmental disturbances in port areas?"

The organization of this chapter is as follows. Section 4.1 states the specific problem in this chapter, including the system model and control objectives. Section 4.2 models the environmental disturbances in port areas. Section 4.3 describes the design of the controller for the towing system according to the system model, control objectives, and control constraints. Section 4.4 presents the simulation results showing the performance of the proposed control scheme applied to small-scale lab vessels. Section 4.5 concludes this chapter.

Parts of this chapter have been published in [41][1].

4.1 Problem Statement

4.1.1 Towing System and Control Objective

Without loss of generality, we consider a towing system that consists of one manipulated ship and two tugboats as shown in Fig 4.1, where the two tugboats have enough power to perform the towing process. The ship is set as no power, so the power sources (control inputs) of the towing system are offered by the two tugs. The front tug (Tug 2) is to increase

---

[1]Z. Du, R. R. Negenborn, and V. Reppa. Cooperative multi-agent control for autonomous ship towing under environmental disturbances. *IEEE/CAA Journal of Automatica Sinica*, 8(8):1365-1379, 2021.
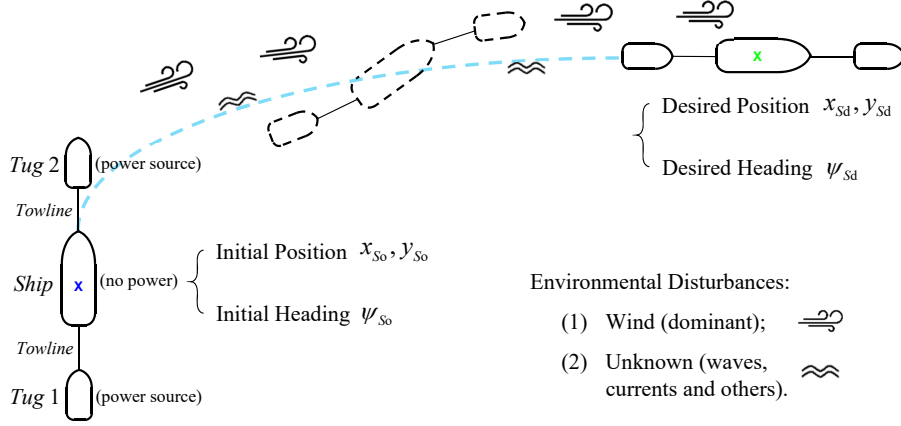
Figure 4.1: Ship-towing system, control objective, and application scenario.

the speed and adjust the heading of the ship, while the aft tug (Tug 1) is to decrease the speed and stabilize the heading of the ship.

The control objective is to move the ship from the initial position x_{So}, y_{So} and heading ψ_{So} to the desired position x_{Sd}, y_{Sd} and heading ψ_{Sd}. In the whole manipulation process, the towing system is influenced by the environmental disturbances, including the dominant effect of wind and the other unknown effects (waves and currents).

4.1.2 Dynamics Model of the Ship and Two Tugboats

The forces on the manipulated ship are shown in Fig 4.2, the dynamics model of the manipulated ship is expressed as:

$$
\begin{aligned}
\dot{\boldsymbol{\eta}}_S(t) &= \boldsymbol{R}\big(\psi_S(t)\big)\mathbf{v}_S(t) \\
\dot{\mathbf{v}}_S(t) &= \boldsymbol{M}_S^{-1}\Big(-\boldsymbol{C}_S\big(\mathbf{v}_S(t)\big)\mathbf{v}_S(t) - \boldsymbol{D}_S\big(\mathbf{v}_S(t)\big)\mathbf{v}_S(t) - \\
&\quad \boldsymbol{B}_{S1}(t)F_1(t) + \boldsymbol{B}_{S2}(t)F_2(t) + \boldsymbol{\tau}_{E_S}(t)\Big),
\end{aligned}
\tag{4.1}
$$

where $\boldsymbol{B}_{S1}(t)$ and $\boldsymbol{B}_{S2}(t)$ can be formulated according to (3.4). It is noticed from Fig 4.2 that the angle between the heading of the ship and the direction from the center of gravity of the object to the towing point (γ_i) equals to 0, so the two configuration matrices are expressed as:

$$
\boldsymbol{B}_{S1}(t) = \begin{bmatrix} \cos\big(\alpha_1(t)\big) \\ \sin\big(\alpha_1(t)\big) \\ l_1\sin\big(\alpha_1(t)\big) \end{bmatrix} \qquad \boldsymbol{B}_{S2}(t) = \begin{bmatrix} \cos\big(\alpha_2(t)\big) \\ \sin\big(\alpha_2(t)\big) \\ l_2\sin\big(\alpha_2(t)\big) \end{bmatrix},
\tag{4.2}
$$

where l_1 and l_2 are the distance from the center of gravity of the ship to its stern and bow, respectively.
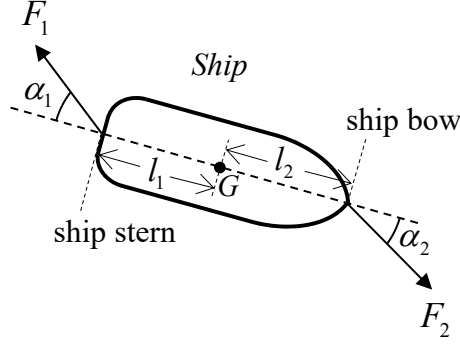
Figure 4.2: Forces on the manipulated ship.
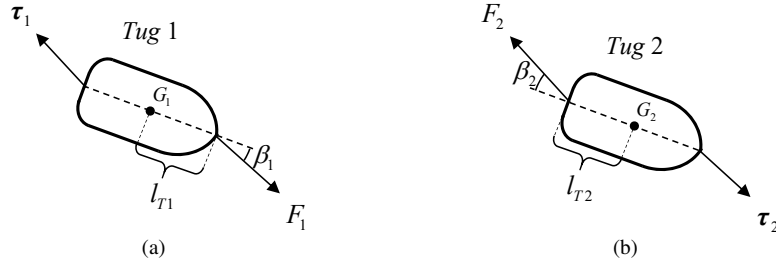
Figure 4.3: Forces on the tugboats: (a) Tug 1; (b) Tug 2.

The forces on the two tugboats are shown in Fig 4.3. It can be seen that the towing force to the Tug 1 is propulsion, the towing force to the Tug 2 is resistance. Thus, the dynamics models of the two tugboats are expressed as:

$$
\begin{aligned}
\dot{\boldsymbol{\eta}}_i(t) &= \boldsymbol{R}\big(\psi_i(t)\big)\mathbf{v}_i(t) \qquad (i = 1,2)\\
\dot{\mathbf{v}}_1(t) &= \boldsymbol{M}_1^{-1}\Big(-\boldsymbol{C}_1\big(\mathbf{v}_1(t)\big)\mathbf{v}_1(t) - \boldsymbol{D}_1\big(\mathbf{v}_1(t)\big)\mathbf{v}_1(t)+\\
&\qquad \boldsymbol{\tau}_{T1}(t) + \boldsymbol{B}_{T1}(t)F_1(t) + \boldsymbol{\tau}_{E1}(t)\Big)\\
\dot{\mathbf{v}}_2(t) &= \boldsymbol{M}_2^{-1}\Big(-\boldsymbol{C}_2\big(\mathbf{v}_2(t)\big)\mathbf{v}_2(t) - \boldsymbol{D}_2\big(\mathbf{v}_2(t)\big)\mathbf{v}_2(t)+\\
&\qquad \boldsymbol{\tau}_{T2}(t) - \boldsymbol{B}_{T2}(t)F_2(t) + \boldsymbol{\tau}_{E2}(t)\Big),
\end{aligned}
\tag{4.3}
$$

where $\boldsymbol{B}_{T1}(t)$ and $\boldsymbol{B}_{T2}(t)$ are given in (3.7).

4.1.3   Kinematics Model of the Towing System

Fig 4.4 shows the desired geometry configuration of the towing system. The desired position and heading of the two tugboats are given in (3.11). It can be seen from Fig 4.4 that $\gamma_1 = 0$, $\gamma_2 = 0$, and $\mathrm{sgn}(1) = -1$, $\mathrm{sgn}(2) = 1$; so the corresponding $\boldsymbol{E}_1(t)$, $\boldsymbol{F}_1(t)$ and $\boldsymbol{E}_2(t)$, $\boldsymbol{F}_2(t)$ are expressed as:
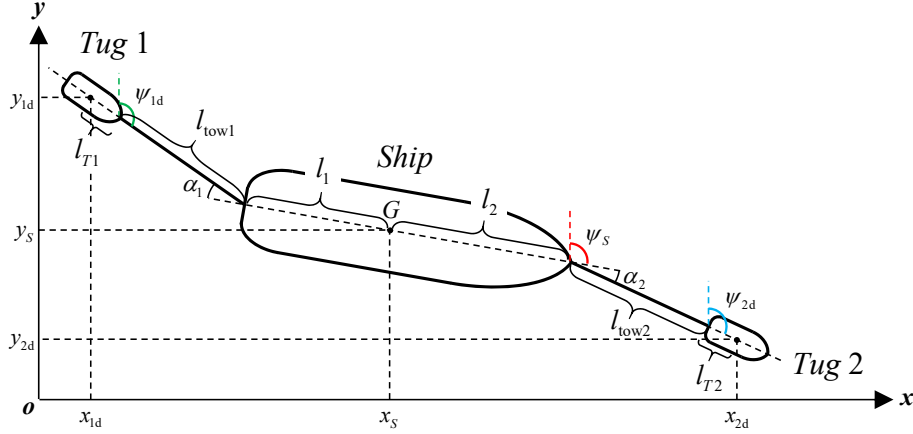
Figure 4.4: Desired geometry configuration of the towing system.

$$\boldsymbol{E}_1(t) = - \begin{bmatrix} \sin(\psi_S(t) + \alpha_1(t)) \\ \cos(\psi_S(t) + \alpha_1(t)) \\ 0 \end{bmatrix} \quad \boldsymbol{F}_1(t) = - \begin{bmatrix} \sin(\psi_S(t)) \\ \cos(\psi_S(t)) \\ 0 \end{bmatrix}, \qquad (4.4)$$

$$\boldsymbol{E}_2(t) = \begin{bmatrix} \sin(\psi_S(t) + \alpha_2(t)) \\ \cos(\psi_S(t) + \alpha_2(t)) \\ 0 \end{bmatrix} \quad \boldsymbol{F}_2(t) = \begin{bmatrix} \sin(\psi_S(t)) \\ \cos(\psi_S(t)) \\ 0 \end{bmatrix}. \qquad (4.5)$$

4.2 Environmental Disturbances Modelling

According to the third assumption (**A3**), the environmental disturbances $\boldsymbol{\tau}_E(t)$ consist of the dominant wind effects $\boldsymbol{\tau}_{\text{wind}}(t)$ and the low-impact unknown effects $\boldsymbol{\tau}_{\text{unknown}}(t)$ (mainly refer to waves and currents):

$$\boldsymbol{\tau}_E(t) = \boldsymbol{\tau}_{\text{wind}}(t) + \boldsymbol{\tau}_{\text{unknown}}(t). \qquad (4.6)$$

The wind effects can be modelled based on the wind speed denoted by $V_w(t)$ and wind direction denoted by $\beta_w(t)$. These two variables can be measured by an anemometer and a weather vane in real-time, respectively. In the case of vessel symmetry with respect to the *xz* and *yz* planes, the model of wind disturbances can be expressed as [56]:

$$\boldsymbol{\tau}_{\text{wind}}(t) = \frac{1}{2}\rho_a V_{rw}^2(t) \begin{bmatrix} -c_x \cos(\gamma_{rw}(t)) A_{\text{Fw}} \\ c_y \sin(\gamma_{rw}(t)) A_{\text{Lw}} \\ c_n \sin(2\gamma_{rw}(t)) A_{\text{Lw}} L_{oa} \end{bmatrix}, \qquad (4.7)$$

where ρ_a is the air density; c_x, c_y and c_n are the wind coefficients for horizontal plane motions; A_{Fw} and A_{Lw} are the transverse and lateral projected area of vessel above the water, respectively; L_{oa} is the overall length of vessel; $V_{rw}(t)$ and $\gamma_{rw}(t)$ are the relative wind speed

and the wind angle of attack relative to the vessel bow, respectively, calculated by:

$$V_{rw}(t) = \sqrt{u_{rw}^2(t) + v_{rw}^2(t)}$$
$$\gamma_{rw}(t) = \text{atan2}(v_{rw}(t), u_{rw}(t)),$$
(4.8)

$$u_{rw}(t) = u(t) - u_w(t)$$
$$v_{rw}(t) = v(t) - v_w(t),$$
(4.9)

$$u_w(t) = V_w(t)\cos(\beta_w(t) - \psi(t))$$
$$v_w(t) = V_w(t)\sin(\beta_w(t) - \psi(t)),$$
(4.10)

where $u_{rw}(t)$ and $v_{rw}(t)$ are the relative wind speed in the x and y directions (vessel body frame), respectively; $u_w(t)$ and $v_w(t)$ are the components of wind speed $V_w(t)$ in the x and y directions (world NED frame); $u(t)$, $v(t)$, and $\psi(t)$ stand for surge, sway, and yaw velocity of the vessel.

Since the trigonometric function can be used to approximate the spectrum of the waves, many ship motion control-related research works describe the unknown environmental disturbances using a sinusoidal function adding constant [102] [35] [123] [185] or random [77] [104] parts ($A\sin(\omega_1 t) + B \cdot \text{rand}(t)$). Then, the unknown disturbances are depicted in Fig 4.5 (a). However, for the environment near ports (windy but sheltered areas), the wave period is short ($A\sin(\omega_2 t) + B \cdot \text{rand}(t)$, $\omega_2 > \omega_1$) [68]. The short period wave is illustrated in Fig 4.5 (b). Compared to Fig 4.5 (c), which is depicted by a random function and a constant ($C \cdot \text{rand}(t) + D$), the two approximated ways are similar. According to the above analysis, the simpler way can reflect both the short period wave character and randomness. Thus, the unknown disturbances can be described by a random function plus a bias.

From the meteorological point of view, wind generates waves. Wave breaking affects exchanges between sea and atmosphere, and the (wind-driven) currents are induced by wave breaking and the Stokes drift [25]. For simplification, in this chapter waves and currents are considered generated by wind, which means their effects are related to the wind speed $V_w(t)$ and direction $\beta_w(t)$. Therefore, the unknown disturbances are expressed as:

$$\boldsymbol{\tau}_{\text{unknown}}(t) = \begin{bmatrix} k_X V_w(t)\big(\text{rand}(t) + a_X\big)\cos\big(\beta_w(t) - \psi\big)A_{FD} \\ k_Y V_w(t)\big(\text{rand}(t) + a_Y\big)\sin\big(\beta_w(t) - \psi\big)A_{LD} \\ k_N V_w(t)\big(\text{rand}(t) + a_N\big)\sin\big(\beta_w(t) - \psi\big)A_{LD}L_{oa} \end{bmatrix},$$
(4.11)

where k_X, k_Y and k_N are the unknown disturbance gain, whose values are less than 0.1; $\text{rand}(t)$ is the random function from 0 to 1; a_X, a_Y and a_N are the disturbance constant, whose values are less than 1; A_{FD} and A_{FD} are the transverse and lateral projected area of vessel under the water, respectively.

4.3 Design of Control Scheme

According to the towing system characterized by multiple control inputs and constraints, an optimization-based multi-layer control strategy is used. It has the advantage of performing different control tasks to coordinate multiple agents [26].

As shown in Fig 4.6, the physical layer at the bottom contains all the physical system
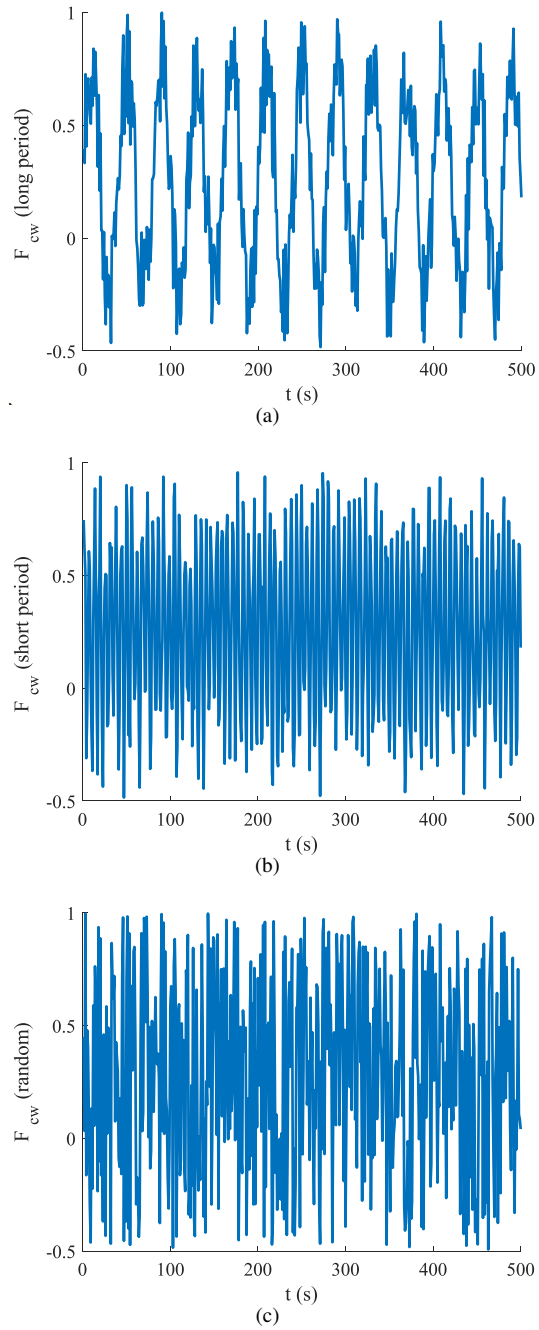
Figure 4.5: *Unknown disturbances description: (a) Sinusoidal function with a long period*
and random function; (b) Sinusoidal function with a short period and random
function; (c) Random function and constant.

$$\boldsymbol{\eta}_{Sd} \quad \mathbf{v}_{Sd} \quad V_w(t) \quad \beta_w(t)$$

Multi-vessel
Supervisory Controller

Control layer

Higher layer control

$F_1(t)$ $\boldsymbol{\eta}_{1d}(t)$ $\boldsymbol{\eta}_{2d}(t)$ $F_2(t)$

Lower layer control

Tug 1 Controller

Tug 2 Controller

$\boldsymbol{\eta}_1(t)$ $\mathbf{v}_1(t)$ $\boldsymbol{\eta}_S(t)$ $\mathbf{v}_S(t)$ $\boldsymbol{\eta}_2(t)$ $\mathbf{v}_2(t)$

$\boldsymbol{\tau}_{T1}(t)$ $\boldsymbol{\tau}_{T2}(t)$

Physical layer

Tug 1 System $\boldsymbol{\tau}_{S1}(t)$ Ship System $\boldsymbol{\tau}_{S2}(t)$ Tug 2 System

$\boldsymbol{\tau}_{E1}(t)$ $\boldsymbol{\tau}_{ES}(t)$ $\boldsymbol{\tau}_{E2}(t)$
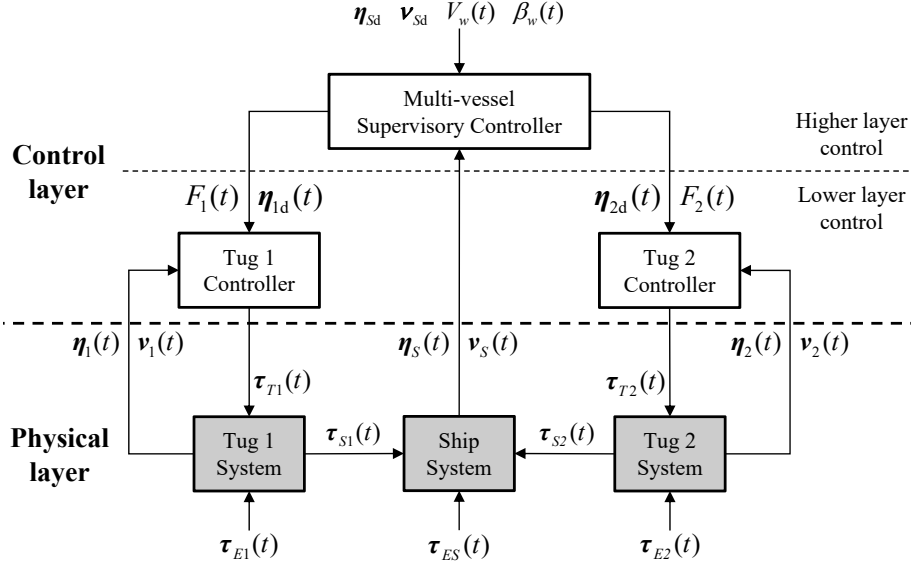
Figure 4.6: Control diagram for the multi-vessel towing system.

components, including hulls, actuators (thrusters), towlines, sensors, etc. The ship is manipulated by two tugs through towline which transfer towing forces and moment ($\boldsymbol{\tau}_{S1}(t)$, $\boldsymbol{\tau}_{S2}(t)$). All the physical systems are affected by the environmental disturbances ($\boldsymbol{\tau}_{E1}(t)$, $\boldsymbol{\tau}_{E2}(t)$ and $\boldsymbol{\tau}_{ES}(t)$).

The control layer is distributed in two sublayers: higher-layer control and lower-layer control. The higher-layer control objective is to coordinate the two tugs by allocating the tasks. Comparing the desired states ($\boldsymbol{\eta}_{Sd}, \mathbf{v}_{Sd}$) and actual states ($\boldsymbol{\eta}_S(t), \mathbf{v}_S(t)$) of the ship and acquiring the wind information ($V_w(t)$, $\beta_w(t)$), the supervisory controller generates the online desired trajectories ($\boldsymbol{\eta}_{1d}(t)$, $\boldsymbol{\eta}_{2d}(t)$) for two tugs. The lower-layer control objective is to execute the tasks allocated by the higher-layer control that makes each tugboat track its trajectory reference. Based on the tug reference trajectories ($\boldsymbol{\eta}_{1d}(t)$, $\boldsymbol{\eta}_{2d}(t)$) and current tug states ($\boldsymbol{\eta}_1(t)$, $\boldsymbol{\eta}_2(t)$, $\mathbf{v}_1(t)$, $\mathbf{v}_2(t)$), the tug controllers calculate the forces and moment that the thrusters should provide ($\boldsymbol{\tau}_{T1}(t)$, $\boldsymbol{\tau}_{T2}(t)$).

4.3.1 Supervisory Controller

The inner structure of the supervisory controller is shown in Fig 4.7. There are three core components: Optimizer, Adaptive Weight Calculator and Reference Computation Unit.

(1) Optimizer

The objective of the optimizer is to compute the towing forces and angles. Thus, the problem is to find a rational combination solution of $\alpha_1(t)$, $\alpha_2(t)$, $F_1(t)$, and $F_2(t)$ to minimize the cost function:

$$\boldsymbol{\eta}_S(t) \quad \boldsymbol{v}_S(t) \quad V_w(t) \quad \beta_w(t)$$
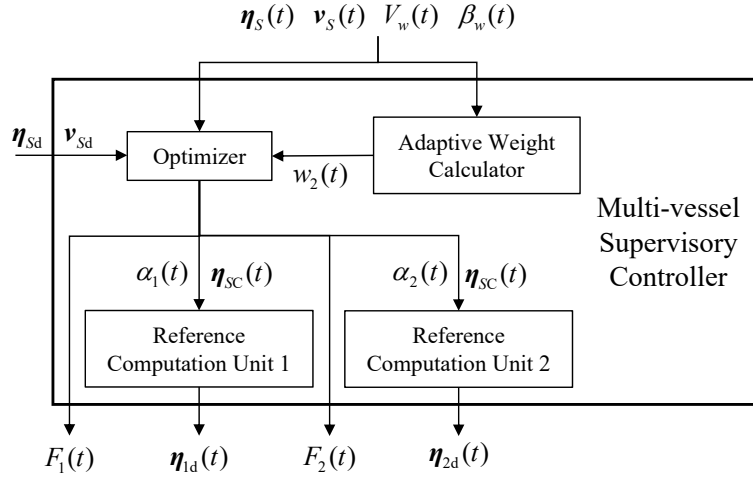
Figure 4.7: Inner structure of the multi-vessel supervisory controller.

$$
\begin{aligned}
J_S(t) &= \boldsymbol{e}_{\eta S}^{\mathrm{T}}(t) w_{S1}(t) \boldsymbol{e}_{\eta S}(t) + \boldsymbol{e}_{vS}^{\mathrm{T}}(t) w_{S2}(t) \boldsymbol{e}_{vS}(t) \\
\boldsymbol{e}_{\eta S}(t) &= \boldsymbol{\eta}_{SC}(t) - \boldsymbol{\eta}_{Sd} \\
\boldsymbol{e}_{vS}(t) &= \boldsymbol{v}_{SC}(t) - \boldsymbol{v}_{Sd},
\end{aligned}
\tag{4.12}
$$

where $\boldsymbol{e}_{\eta S}(t) \in \mathbb{R}^3$ and $\boldsymbol{e}_{vS}(t) \in \mathbb{R}^3$ are the position and velocity error, respectively; $w_{S1}(t)$ and $w_{S2}(t)$ are the adaptive weights defined in the next subsection, whose values are related to the current measured wind data and ship states; $\boldsymbol{\eta}_{SC}(t) \in \mathbb{R}^3$ and $\boldsymbol{v}_{SC}(t) \in \mathbb{R}^3$ are the calculated predicted ship position and velocity, which subject to the ship dynamics constraint (4.1) and (4.2).

According to the physical law and tug practical operation [68], the towing forces and angles have to satisfy the following saturation constraints:

$$
\begin{aligned}
-\alpha_{i\max} &\le \alpha_i(k) < \alpha_{i\max} \\
0 &\le F_i(t) \le F_{i\max} \qquad (i = 1, 2),
\end{aligned}
\tag{4.13}
$$

where $\alpha_{i\max}$ and $F_{i\max}$ are the maximum value of towing angle and towing force that the two towlines can reach and withstand, respectively.

Furthermore, the performance of the trajectory tracking in the lower-layer is related to the quality of the tug reference trajectory, which is affected by the change rate of the towing angles and forces. Thus, a saturation constraint of the change rate for the two towing angles and forces is set to make the reference trajectory smooth:

$$
\begin{aligned}
|\dot{\alpha}_i(t)| &\le \bar{\alpha}_i \\
|\dot{F}_i(t)| &\le \bar{F}_i \qquad (i = 1, 2),
\end{aligned}
\tag{4.14}
$$

where $\bar{\alpha}_i$ and $\bar{F}_i$ are the maximum change rate value of towing angle and force, respectively.

(2) Adaptive Weight Calculator

The two weight coefficients $(w_1(t), w_2(t))$ in the cost function (4.12) determine which part (position or velocity) the controller puts more efforts to regulate. If $w_1(t) >> w_2(t)$, the controller puts more effort into the ship position and the towing process is fast, but the towing trajectory is not smooth because of the large fluctuated velocity. In contrast, if $w_1(t) << w_2(t)$, the controller concentrates on regulating the ship velocity leading to a smoother trajectory, but the time of the whole process is much longer delaying other ship operations. Thus, the appropriate selection of the weight proportion plays an important role in the supervisory controller. To design adaptive weights, the following requirements should be taken into consideration.

- **Requirement 1**: Stable at the beginning

  At the beginning of the towing, the task for the two autonomous tugs is to adjust themselves to a proper configuration to manipulate the ship. To stabilize the towing system, the velocity in this phase should be low with minimum fluctuation. Thus, the controller should focus on regulating the ship velocity.

- **Requirement 2**: Reach the goal at the end

  At the end phase of the towing, as the towing system is approaching the goal, the velocity asymptotically goes to zero. The task at this moment is to make sure the ship reaches the desired position with the desired heading. Thus, the controller should decrease the ship velocity and accelerate the regulation of ship position.

- **Requirement 3**: Robust to the wind

  Due to the influence of the wind disturbances, it is difficult to stabilize the motion of the towing system at the beginning and the goal of the ship, especially the heading, is more difficult to achieve at the end phase. Thus, the controller should put more effort into satisfying the **Requirements 1** and **Requirements 2** according to the wind strength (V_w), and should prioritize the heading control.

- **Requirement 4**: Reduce control input oscillation

  Control input oscillation determines the practicality of the proposed approach. A practical control approach should have less oscillation of the control input. Thus, at the end phase of the towing, the value of the weight should be designed as constant; in other phases, the changes in the weight should be smooth and not too much.

Based on the above requirements, the position weight is set as $w_1(t) = \text{diag}(1, 1, 1)$, while the adaptive velocity weight $w_2(t) = \text{diag}(w_u(t), w_v(t), w_r(t))$ is designed as:

$$w_u(t) = w_v(t) = w_r(t) = k_0 \left(1 + V_w(t)\right)\left(d(t)/d_0\right)$$

$$d_0 = \sqrt{\left(x_{S_\text{d}} - x_{S_0}\right)^2 + \left(y_{S_\text{d}} - y_{S_0}\right)^2} \tag{4.15}$$

$$d(t) = \sqrt{\left(x_{S_\text{d}} - x_S(t)\right)^2 + \left(y_{S_\text{d}} - y_S(t)\right)^2},$$

whose terminal values $w_{2t}(t) = \text{diag}(w_{ut}(t), w_{vt}(t), w_{rt}(t))$ are set as:

$$
\begin{aligned}
w_{ut}(t) &= w_{vt}(t) = k_t \left[1 - V_w(t) / \left(V_w(t) + k_1 \right) \right] \\
w_{rt}(t) &= k_t \left[1 - V_w(t) / \left(V_w(t) + k_2 \right) \right],
\end{aligned}
\tag{4.16}
$$

where d_0 is the distance from the origin (x_{S0}, y_{S0}) to the destination (x_{Sd}, y_{Sd}); $d(t)$ is the distance from the current ship position $(x_S(t), y_S(t))$ to the destination, which is the position error. k_0, k_t, k_1, and k_2 are the positive coefficients: k_0 and k_t determine the initial and final value of the weight, so $k_0 > k_t > 1$; k_1 and k_2 define the final values of the linear and angular velocity weight, they are set to be $0 < k_2 < k_1 < 1$ to emphasize the heading control at the end phase.

As the value of $d(t)$ decreases over the process of towing, the adaptive weight $w_2(t)$ is decreasing according to (4.15). When the ship is so close to the destination that the adaptive weight value is smaller than the terminal setting in (4.16), the adaptive weight will be fixed on the terminal value.

(3) Reference Computation Unit

The Reference Computation Unit aims to calculate the desired position and heading of the tugboats in order to tow the ship. Once the towing forces and angles for the ship are provided by the higher layer control, the position and heading of the ship can be determined. Then, the desired position and heading of the tugboats can be calculated based on (3.11), (4.4) and (4.5).

Thus, the algorithm flow in the higher layer control is summarized in Algorithm 4.1.

Algorithm 4.1 - Higher layer control

Input: Desired ship position and velocity $\boldsymbol{\eta}_{Sd}$, $\mathbf{v}_{Sd}$;
          Current ship position and velocity $\boldsymbol{\eta}_S(t)$, $\mathbf{v}_S(t)$;
          Wind speed and angle $V_w(t)$, $\beta_w(t)$.

Step 1: Calculate current adaptive velocity weight $w_2(t)$ according to (4.15) and the corresponding terminal value according to (4.16).
          If $w_2(t) > w_t(t)$, then take $w_2(t)$ as the current adaptive weight; otherwise, take $w_t(t)$ as the current adaptive weight.

Step 2: Compute towing forces F_i and angles α_i according to the cost function (4.12), restricted by the ship dynamics (4.1) – (4.2), the wind disturbances (4.7) – (4.10), and the control constraints (4.13) – (4.14).

Step 3: Calculate the tug reference trajectory $\boldsymbol{\eta}_{id}(t)$ according to (3.11), (4.4) and (4.5).

Output: Towing forces $F_i(t)$ and Tug reference trajectory $\boldsymbol{\eta}_{id}(t)$.

4.3.2   Tug Controller

The objective of the Tug Controller is to determine the thruster forces and moment to track the reference trajectories ($\boldsymbol{\eta}_{id}(t)$). The problem can be expressed as finding $\boldsymbol{\tau}_i(t)$ for Tug i to minimize the cost function:

$$
\begin{aligned}
J_i(t) &= \boldsymbol{e}_{\eta i}^T(t)\boldsymbol{e}_{\eta i}(t) \\
\boldsymbol{e}_{\eta i}(t+1) &= \boldsymbol{\eta}_{iC}(t) - \boldsymbol{\eta}_{id}(t),
\end{aligned}
\tag{4.17}
$$

where $\boldsymbol{e}_{\eta i}(t) \in \mathbb{R}^3$ is the position error; $\boldsymbol{\eta}_{iC}(t) \in \mathbb{R}^3$ is the calculated predicted tug position vector, which is subject to the tug dynamics constraint (4.3).

The forces and moment of the thrusters satisfy the saturation constraints:

$$
-\boldsymbol{\tau}_{i\max} \le \boldsymbol{\tau}_i \le \boldsymbol{\tau}_{i\max} \qquad (i = 1, 2),
\tag{4.18}
$$

where $\boldsymbol{\tau}_{i\max}$ is the maximum value of the thruster forces and moment.

Thus, the algorithm flow in the lower layer control are summarized in Algorithm 4.2.

Algorithm 4.2 - Lower Layer Control

Input: Tug reference trajectory $\boldsymbol{\eta}_{id}(t)$ and Towing forces F_i;
   Current tug position and velocity $\boldsymbol{\eta}_i(t)$, $\mathbf{v}_i(t)$;
   Wind speed and angle $V_w(t)$, $\beta_w(t)$.

Step 1: Compute tug thruster forces and moment $\boldsymbol{\tau}_i(t)$ according to the cost function (4.17), restricted by the tug dynamics (4.3), the wind disturbances (4.7) – (4.10), and the control constraints (4.18).

Output: Tug thruster forces and moment $\boldsymbol{\tau}_i(t)$.

4.4   Simulations and Results Discussion

Computer simulation results are presented in this part to show the performance of the proposed control algorithm applied to scaled vessel models, followed by the discussion and analysis of the results.

The model of"*TitoNeri*" is used for the two tugboats, the model of "*CyberShip II*" is used for the manipulated ship. The parameters and the physical constraints of the towing system are shown in Table 4.1.

The environmental disturbances are simulated based on information provided by the port of Rotterdam [145]. According to its latest meteorological information, 98% of the wind effects are not greater than 7 Beaufort (the wind speed is between 13.9 m/s and 17.1 m/s). According to Froude's scaling law (shown in Table 4.2) [120], the scaled velocity is determined by the square root of the scaling factor. Since the scaling factor of the "*CyberShip II*" is 70 [155], the scaled wind speed can be expressed as:

Table 4.1: Parameters of the towing system.

Desired elongation of towline	$l_{\text{tow}_1} = 1$ m	$l_{\text{tow}_2} = 1$ m
Distance from the ship centers of gravity	$l_{S_1} = 0.67$ m	$l_{S_2} = 0.585$ m
Distance from the tug centers of gravity	$l_{T_1} = 0.5$ m	$l_{T_2} = 0.5$ m
Maximum values of the towing angles	$\alpha_{1\max} = 45°$	$\alpha_{2\max} = 45°$
Maximum values of the towing forces	$F_{1\max} = 3$ N	$F_{2\max} = 3$ N
Maximum values of the thruster forces	$\tau_{1\max} = 10$ N	$\tau_{2\max} = 10$ N
Maximum rate of change of towing angles	$\bar{\alpha}_1 = 5°/\text{s}$	$\bar{\alpha}_2 = 5°/\text{s}$
Maximum rate of change of towing forces	$\bar{F}_1 = 0.1$ N/s	$\bar{F}_2 = 0.1$ N/s

Table 4.2: Froude scaling of physical quantities[*].

Quantity	Units	Scaling Ratio	Quantity	Units	Scaling Ratio
Length	m	k_F	Acceleration	m/s	$k_F^{1/2}$
Time	s	$k_F^{1/2}$	Mass	kg	k_F^3
Frequency	1/s	$k_F^{-1/2}$	Force	N	k_F^3
Velocity	m/s	$k_F^{1/2}$	Moment	Nm	k_F^4

[*] k_F is the scaling factor of length.

$$V'_w = V_w/\sqrt{70}, \tag{4.19}$$

and the maximum value of the scaled wind speed is 17.1 m/s $\div \sqrt{70}$ = 2 m/s. For the unknown disturbances, the corresponding gains and constants are chosen as $k_X = 0.008$, $k_Y = 0.01$, $k_N = 0.0016$; $a_X = a_Y = a_N = 0.75$.

The initial position of the ship is located at the origin with zero degree of heading and no speed. The coordinates of the desired position are $(x_{S_d}, y_{S_d}) = (40, 25)$, and the desired heading is $\psi_{S_d} = 90°$ with no speed. We perform two simulation scenarios, with and without environmental disturbances, to compare the performance of the proposed multi-layer, multi-agent control architecture using constant and adaptive weights. Thus, two control schemes are designed: in the (A)-scheme, the supervisory controller uses constant weights with $w_2(t) = \text{diag}(150, 150, 150)$; in the (B)-scheme, the supervisory controller uses $w_2(t)$ defined through (4.15) and (4.16), the corresponding coefficients are set as $k_0 = 150$, $k_t = 50$, $k_1 = 0.15$, $k_2 = 0.01$.

4.4.1 Simulation without Disturbances

When there are no disturbances, the ship towing process using the (A) and (B) control schemes are shown in Fig 4.8. The two tugs cooperate to transport the ship to the goal position with the desired heading, but the time cost is different. In the first two sample times, the two control schemes have the same pace. At time $t_3 = 50$ s, the Tug 2 (blue) in
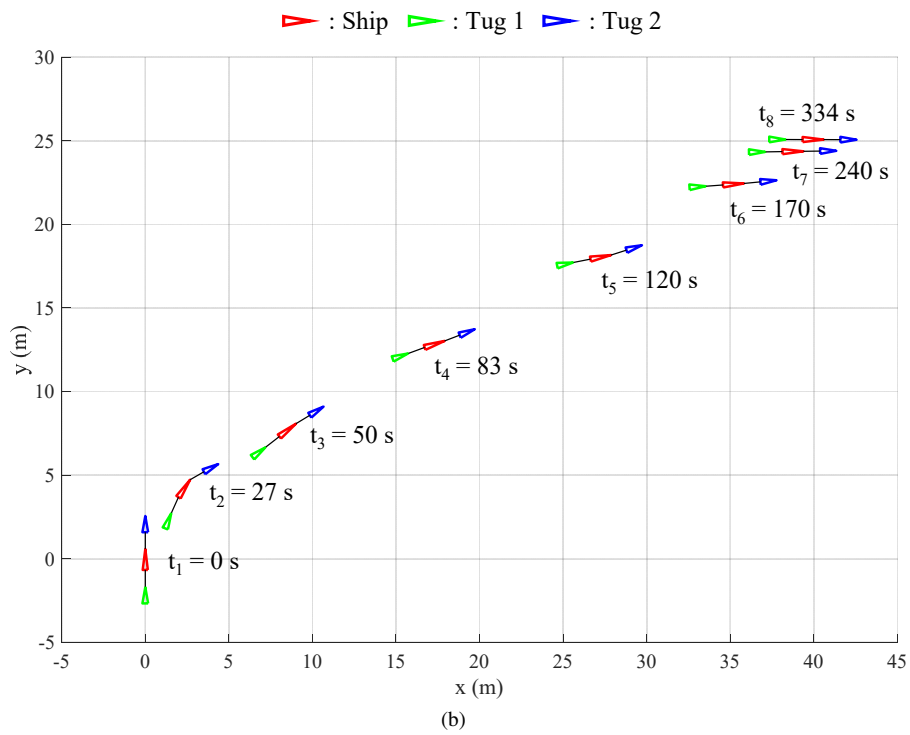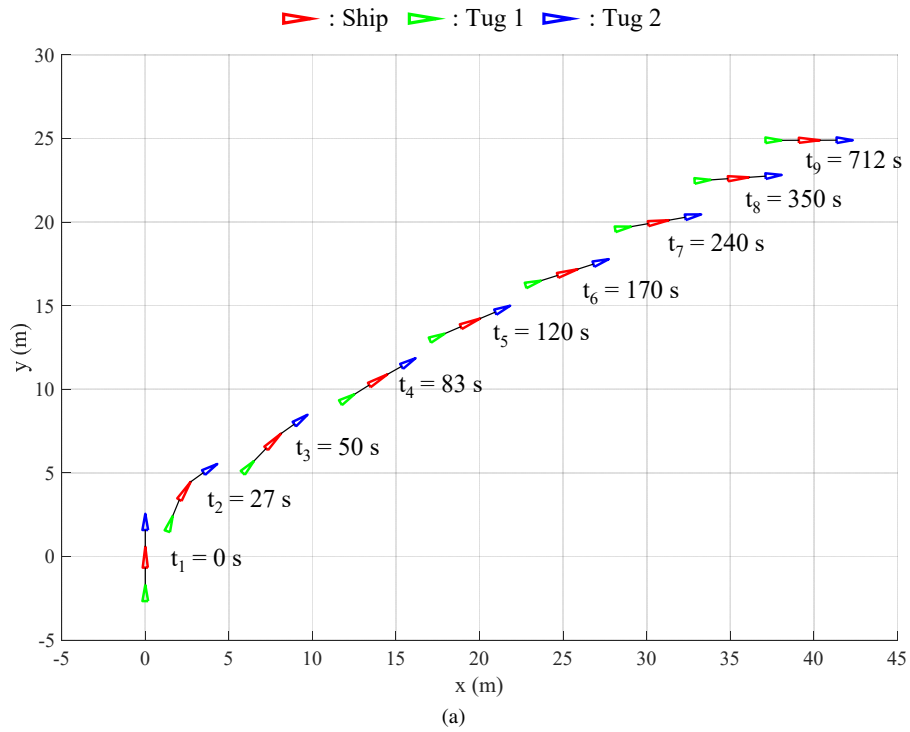
Figure 4.8: Ship towing process without disturbances: (a) (A)-control scheme; (b) (B)-control scheme.

Figure 4.9: Position, heading and velocities of the ship without disturbances using (A)-control scheme (solid, blue line) and (B)-control scheme (dotted, green line) algorithm; the dashed, red line represents the desired value.
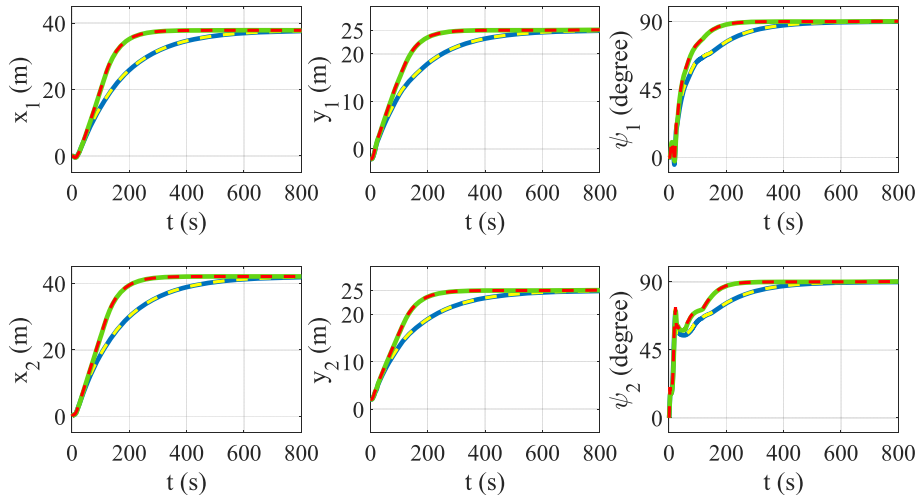
Figure 4.10: Position and heading of Tug 1 (the first row) and Tug 2 (the second row) without disturbances: the solid blue line and dashed yellow line are the actual and desired values by using (A)-control scheme; the solid green line and dashed red line are the actual and desired values by using (B)-control scheme.

Fig 4.8 (b) has already a horizontal displacement of 10 m, while it doesn't reach in Fig 4.8 (a). After t_3, the average speed of the towing system controlled by scheme B is higher than scheme A, so the time cost by scheme B is less than scheme A. From the character of the

Table 4.3: Performance without disturbances.

Performance	Position error (e_p)	Heading error (e_ψ)	Time cost (t)
(A)-control scheme	0.53%	0.10%	712 s
(B)-control scheme	0.14%	0.20%	334 s

system position under the nine sampled times, Fig 4.8 (a) shows the average distribution due to the constant velocity weight, while Fig 4.8 (b) is charactered dense in the beginning and end, sparse in the middle phase. This results from that the adaptive velocity weights (4.15) decrease as the towing system approaches the destination, the speed of the system increases. When the weights reach their terminal value they are constant, and the speed of the system decrease.

The states of the ship and two tugs are illustrated in Fig 4.9 and 4.10, respectively. From Fig 4.9, the velocities of the ship controlled by the two algorithms both converge to 0. The difference is that the peak value of the velocities using (B)-control scheme last a longer time, which makes the adaptive weights have a better time efficiency. From Fig 4.10, the actual position and heading (solid line) of the two tugs match well with their online desired values (dashed line), which reveals that the tug controllers also accomplish their tasks well.

Fig 4.11 shows the control input of the ship. Fig 4.11 (a) illustrates the two towing angles and two towing forces, which can be seen that the four values in both schemes are within the limitation ($\pm 45°$ for towing angles and 3 N for towing forces). The change in towing forces using the (B)-control scheme is earlier than (A). Fig 4.11 (b) shows the change rate of the four control inputs, they are all within the maximum values (between the two red dashed line) as we set. Fig 4.11 (c) is the resultant forces and moment, whose values in both schemes converge to zero eventually.

The performance of the two algorithms can be seen in Table 4.3, using the following indicators:

(1) Position error $e_p = |d_0 - d(t)|/d_0$;
(2) Heading error $e_\psi = |(\psi_S(t) - \psi_{S_d})/(\psi_{S_0} - \psi_{S_d})|$;
(3) Time cost t.

The time cost is defined such that the states of the ship should satisfy all the following conditions: *i*) The distance from the current position to the desired position is less than half length of the ship; *ii*) The difference between the actual and desired heading is less than 5 degrees; *iii*) The surge and sway velocities are less than 0.01 m/s, the yaw velocity is less then 0.01 rad/s. It can be seen that under the similar performance of the position and heading control, the (B)-control scheme outperforms much better for the time cost.

4.4.2   Simulation with Disturbances

The wind speed in this simulation is $V_w = 1$ m/s, the direction is $\beta_w = 45$ degrees coming from southwest. The towing process of the two algorithms are shown in Fig 4.12. Compared to the (A)-control scheme, the (B)-control scheme shows better robustness. Due to the disturbances, the (A)-control scheme makes the towing system steer toward the direction
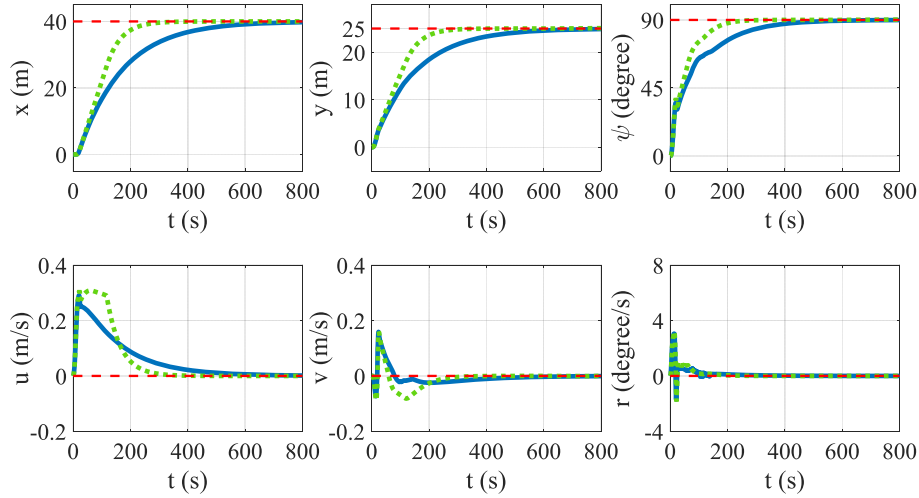
Figure 4.11: Control input of the ship without disturbances using (A)-control scheme (solid, blue line) and (B)-control scheme (dotted, green line) algorithm: (a) Towing angles and forces (red dashed line is the boundary); (b) Change rate of the angles and forces (red dashed line is the boundary); (c) Resultant forces and moment.

Figure 4.12: Towing process of the two algorithms with disturbances: (a) (A)-control scheme; (b) (B)-control scheme.

Figure 4.13: *Position, heading and velocities of the ship with disturbances using (A)-control scheme (solid, blue line) and (B)-control scheme (dotted, green line) algorithm; the dashed, red line represents the desired value.*
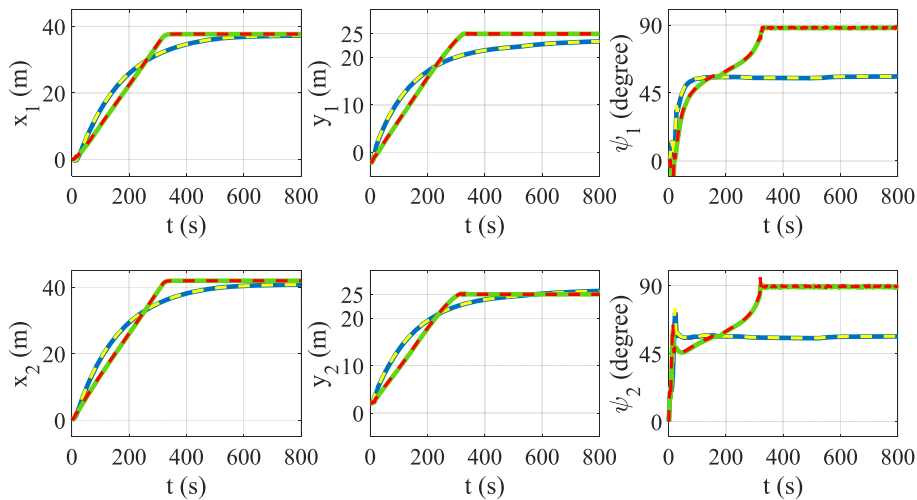
Figure 4.14: *Position and heading of Tug 1 (the first row) and Tug 2 (the second row) with disturbances: the solid blue line and dashed yellow line are the actual and desired values by using (A)-control scheme; the dotted green line and dashed red line are the actual and desired values by using (B)-control scheme.*

of environmental effects (the combined direction of the wind and unknown effects). In this configuration, the environmental forces affecting three vessels are the minimum (the force areas above and under the waters are minimum). So the system keeps this configuration

Table 4.4: Performance with disturbances.

Performance	Position error (e_p)	Heading error (e_ψ)	Time cost (t)
(A)-control scheme	2.14%	37.4%	800 s[*]
(B)-control scheme	0.21%	0.62%	406 s

[*] In the whole process, the difference between the current and the desired heading of the ship is more than 5 degrees, so the time cost is the maximum computation time (800 s).

to the end. The heading of the ship is finally around 55 degrees (see the evolution of ψ in Fig 4.13 blue line).

Using the (B)-control scheme, the speed of the towing system is slower at the beginning to stabilize the ship against the wind effect. It can be observed that until $t_7 = 240$ s, the ship in Fig 4.12 (a) keeps ahead of that in Fig 4.12 (b). After that, as the adaptive weights keep reducing, the system speed is increasing. At $t_8 = 406$ s, the ship in Fig 4.12 (b) achieved the goal. Under the disturbances, Fig 4.12 (a) still shows the average position distribution, while Fig 4.12 (b) is characterized as dense in the beginning and sparse in the end phase. In the simulation without disturbance (Fig 4.8 (b)), the values of the adaptive weights are changed from $[150\ 150\ 150]^T$ to $[50\ 50\ 50]^T$, which makes the velocity control focus on the beginning and end phase. In the simulation with disturbance (Fig 4.12 (b)), the values of the adaptive weights are changed from $[300\ 300\ 300]^T$ to $[6.5\ 6.5\ 0.5]^T$, which means that the velocity control is more concerned in the beginning phase, while the position and heading (especially the heading) control is emphasized in the end phase.

Fig 4.13 shows that by using the (B)-control scheme, the position and heading of the ship can reach their desired values and the linear velocities (u and v) converge to 0. The value of angular velocity (r) has a jump at about 320 seconds and then starts to fluctuate. The reason for such a change is that around 320 s, the position of the ship had already reached the desired value but not for its heading. At this moment, the controller put more effort into the heading control to make the ship have a large angular velocity. After achieving the desired heading, the wind and other disturbances still exist. In this condition, however, the desired heading is not a balanced state (the balanced state should be the heading in the end phase of the (A)-control scheme, around 55 degrees). Thus, the towing system has to continuously adjust to make the ship maintain its desired heading. Fig 4.14 shows that the actual position and heading of the two tugs match well with their online desired values.

The figure of control inputs (Fig 4.15 (a)) shows that the changes of towing angle are similar in both control schemes, the values of towing forces in the (B)-control scheme is greater than the (A)-control scheme, which reflects that the (B)-control scheme makes more effort to cope with the environmental disturbances. Despite this, the four control inputs in the (B)-control scheme are within the limitation (the green dotted line in Fig 4.15 (a) and (b) are all within the red dashed line). The value of the resultant forces and moment in Fig 4.15 (c), especially the yaw moment, are not exactly zero in the end. The reason is the same as mentioned to the ship angular velocity that the ship has to compensate for the environmental effects to maintain the desired states, especially for the heading.

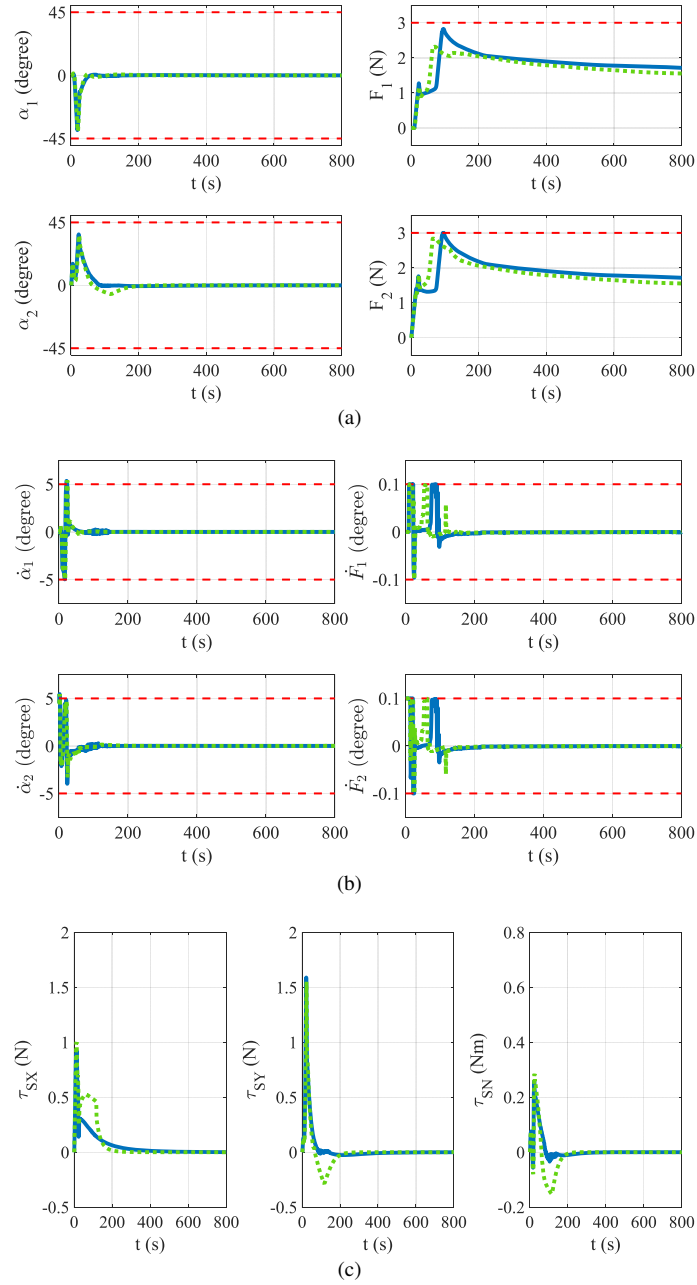The performance of the two control schemes in the case of simulated disturbances is
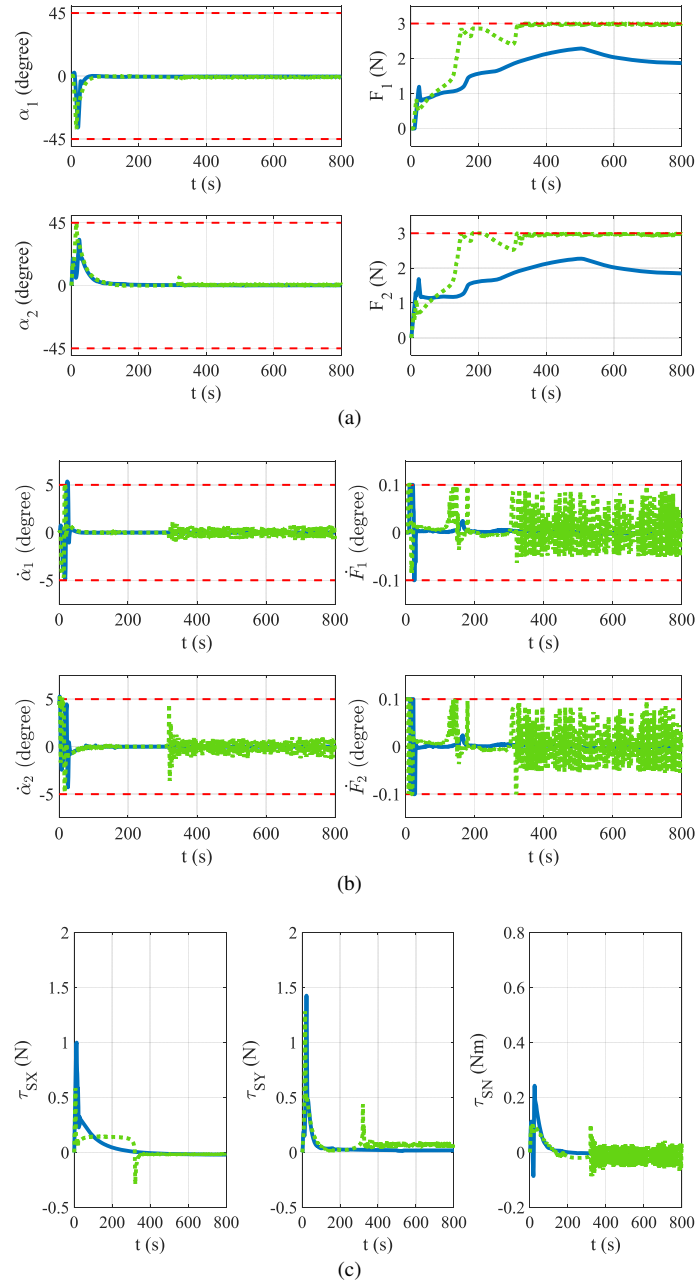
Figure 4.15: Control input of the ship with disturbances using (A)-control scheme (solid, blue line) and (B)-control scheme (dotted, green line) algorithm: (a) Towing angles and forces (red dashed line is the boundary); (b) Change rate of the angles and forces (red dashed line is the boundary); (c) Resultant forces and moment.
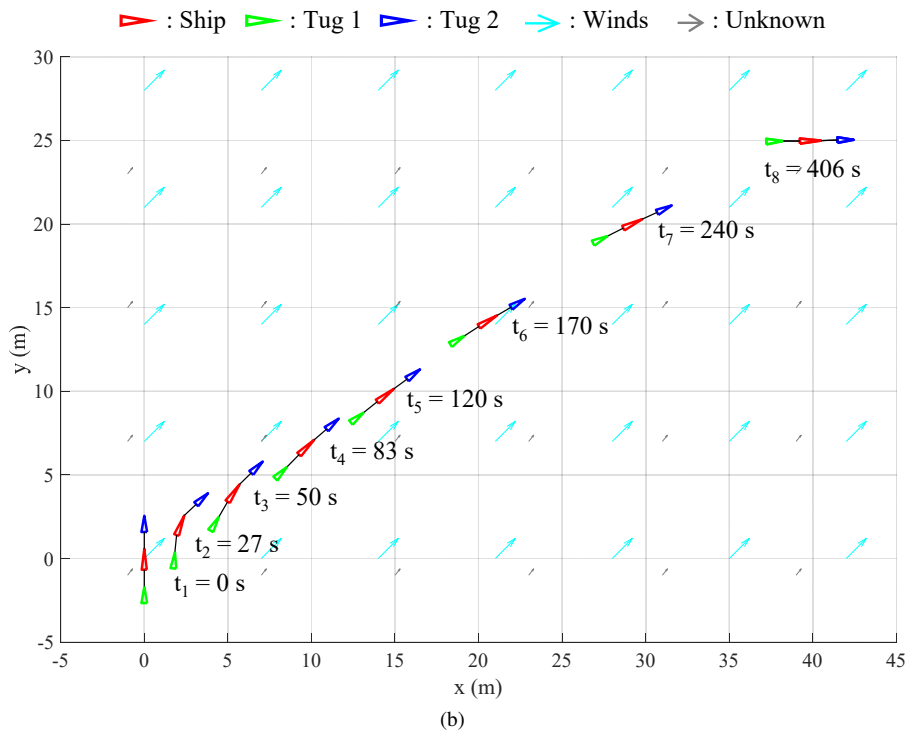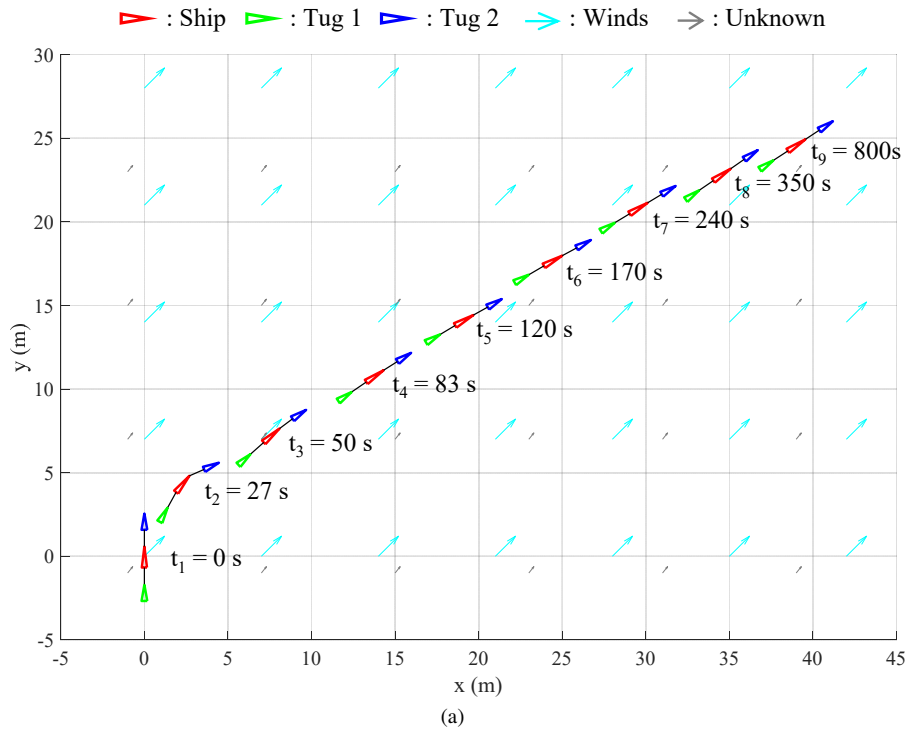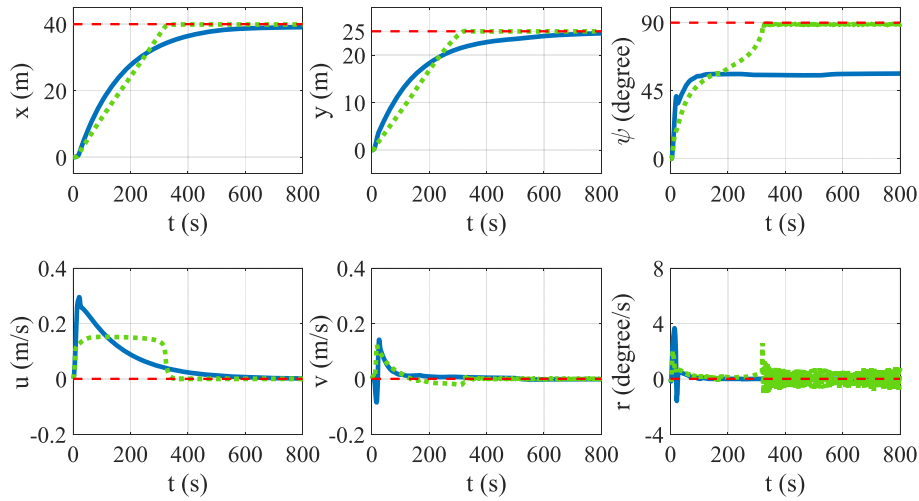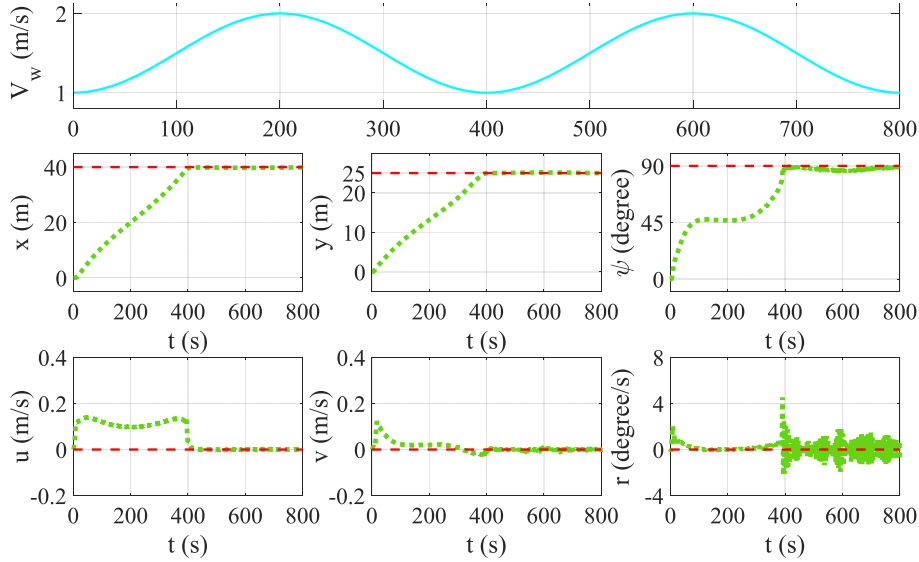
*Figure 4.16: Position, heading, and velocities of the ship (the second and third-row) under
the varying wind speed (the first row) disturbances using (B)-control scheme
algorithm.*

shown in Table 4.4. In this case, all the performance indexes in the (B)-control scheme
outperform the (A)-control scheme, especially for the heading control and time cost.

4.4.3   Simulations in Harsh Conditions

In this part, two sets of simulations are carried out to show the performance of the proposed
control scheme (B) under harsh conditions.

   In the first simulation, wind speed is set to be varying. As shown in Fig 4.16, the first
row is the wind speed varying from 1m/s to 2m/s. The second and third-row shows the
real-time ship states, which indicates that under the condition of varying wind speed, the
control scheme (B) can make sure that the ship achieves its desired position and heading.
The performance indexes: position error $e_p = 0.21\%$, heading error $e_\psi = 1.65\%$, time cost
$t = 472$ s.
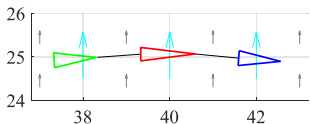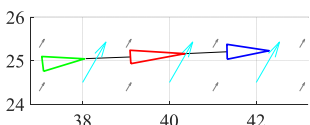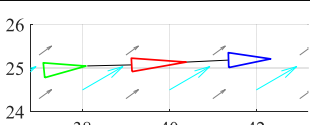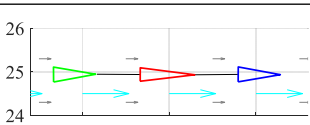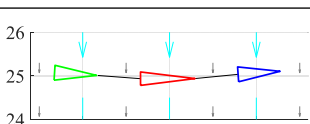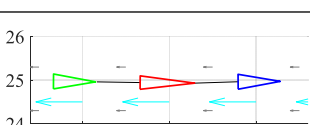
   In the second simulation, wind speed is set to be the maximum value (2 m/s) at all
time. The performance of the (B)-control scheme with different wind directions is shown in
Table 4.5.

   When the wind direction is $0°$ or $180°$, the position and heading control shows the best
performance. Since the goal heading is vertical to the wind direction, the two tugs form the
arching ($0°$) or sagging ($180°$) configuration to make the ship against the lateral forces, and
this manipulation costs more time.

   When the wind direction is $90°$ or $270°$, the values of position and heading error are
slightly higher, but the time cost is the minimum. This is because the goal heading is

parallel to the wind direction, and the force area is minimum. The two tugs only have to maintain the ship velocity being zero at the goal position.

Table 4.5: Performance of the (B)-control scheme with simulator wind speed 2 m/s.

Wind Direction	e_p	e_ψ	t	Final States of the Towing System [**]
0°	0.14%	0.26%	670 s	
30°	0.56%	4.55%	618 s	
45°	0.62%	4.65%	558 s	
60°	0.48%	3.28%	513 s	
90°	0.14%	0.30%	493 s	
180°	0.13%	0.13%	666 s	
270°	0.13%	0.68%	497 s	

[**] Blue arrows show the wind disturbances, grey arrows show the unknown disturbances.

When the wind direction is 30° or 45° or 60°, it is more difficult to achieve the desired position and heading (especially the heading). The disturbance effects, on one hand, force the ship to move; on the other hand, they make the ship difficult to achieve the goal heading. So it is hard to keep the ship steady (velocity zero) and turn the ship heading to the goal direction. Despite the above difficulties, the results show that both position and heading goals are achieved within tolerance.

Based on the above simulation results, the proposed control method shows the following abilities. First, it can coordinate the two autonomous tugs to cooperatively manipulate a ship to the desired position with the desired heading. Second, it can deal with the environmental disturbances (mainly wind) even in harsh conditions. Third, it properly adjusts the ship speed according to the current ship states making the towing process time-efficient. In a real situation, once we obtain the information of the real-scaled vessel model, the proposed control method can be used to coordinate the autonomous tugs to manipulate a ship to the desired position with the desired heading under the environmental disturbances.

4.5   Conclusions

This chapter focuses on the application of the object manipulation system for ship towing in port areas. It addresses the third research question **Q3**: How to increase the robustness of the towing operation to handle the influence of environmental disturbances in port areas?

A multi-layer multi-agent control scheme is proposed to manipulate a ship to reach a desired position with desired heading. The control scheme consists of a supervisory controller in the higher layer and two tug controllers in the lower layer. The supervisory controller computes the desired towing forces and angles by minimizing the cost function of position and velocity errors. The weight coefficients of the position and velocity in the cost function determine the performance of control. To guarantee that the towing system functions well under environmental disturbances, an adaptive weight function is designed. By applying this weight, the controller shows disturbance robustness, time efficiency and tracking performance. The calculated towing angles by the supervisory controller are used to compute the online reference trajectories for the autonomous tugs based on the kinematics of the ship towing system. The tug controller, on one hand, provides the towing forces to move the ship; on the other hand, it tracks the reference trajectory to reach the configuration determined by the towing angle.

Simulation experiments illustrate the performance of the proposed control scheme. When there are no disturbances, the proposed method shows more efficiency. When the motion of the towing system is affected by the wind (mainly) and unknown disturbances, the proposed method shows robustness guaranteeing that the ship is manipulated to a desired position with desired heading and velocity, even in harsh conditions.

In the next chapter, the towing scenario changes to inland waterways and the research focus becomes collision avoidance. Thus, how to adjust the cooperative control scheme to fit a new operational scenario and research problem will be investigated in Chapter 5.

Chapter 5

COLREGS-compliant Collision Avoidance of A Towing System in Congested Water Traffic Environments

This chapter addresses the fourth research question (**Q4**): "In what way can the multi-vessel system avoid collisions with static and dynamic obstacles to improve the safety of towage operations in inland waterways?".

The organization of this chapter is as follows. Section 5.1 introduces the research background, defines the research scope, and presents the control objective in this chapter. Section 5.2 proposes a COLREGS-compliant waypoint altering mechanism for the towing system to make the collision resolution comply with maritime regulations. Section 5.3 designs a distributed model predictive control scheme to cooperate multiple tugboats manipulating a large ship meanwhile avoiding obstacles. Section 5.4 shows the results of simulation experiments of the proposed control scheme for dealing with obstacle situations, meanwhile analyzing and explaining the results. Section 5.5 concludes the chapter.

Parts of this chapter have been published in [42][1].

5.1   Problem Statement

5.1.1   Research Background

As an essential requirement for autonomy, collision avoidance plays an important role in autonomous vehicle systems, like Unmanned Aerial Vehicles (UAVs), Unmanned Ground Vehicles (UGVs), and Autonomous Surface Vessels (ASVs), to ensure the safety of carrying out missions [191]. In the water traffic environment, all the vessels that take actions of

---

[1]Z. Du, R. R. Negenborn, and V. Reppa. COLREGS-compliant collision avoidance for physically coupled multi-vessel systems with distributed MPC. *Ocean Engineering*, 260:111917, 2022.

avoidance should comply with standards of global regulations called "The International Regulations for Preventing Collisions at Sea", shortly COLREGS [32].

Although COLREGS have been designed to be followed by humans, they must be obeyed during the operations of autonomous vessels in order to guarantee their lawfulness at sea [24]. For a single ASV system, research works usually combine rules 13-17 (the specific actions that the give-way vessel should take) with classical guidance or control methods to make the ASV avoid obstacles. In [61, 88, 176], scholars propose a COLREG-compliant model predictive control method for ship collision avoidance. Research works [187] and [30] focus on path planning of ASVs and propose COLREG-compliant Rapidly-exploring Random Tree (RRT) optimal planning strategy. In [3], a Fuzzy-logic based conflict detection and resolution algorithm is proposed for situations of multiple ships, where the fuzzy rules are defined in accordance with the COLREGs. Other research works use the methods of Velocity Obstacle (VO) [74] and Artificial Potential Fields (APF) [108] combined with COLREG rules to address collision avoidance problems for ASVs.

For a multi-ASV system, collision avoidance research focuses on the type of cyber-connected system. Researchers usually arrange a specific formation to coordinate multiple ASVs. The typical one is the triangle formation composed of three vessels [70, 75]. The triangle formation can easily adopt the leader-follower cooperative control strategy that maintains the vessel formation in premises of avoiding collision with islands and coast. For more than three vessels, the reconfigurable formation can be applied [8, 137]. This type of formation is often combined with a task-based (or behavior-based) cooperative control strategy in which a collision-avoidance task is carried out by changing the formation. Alternatively, a line formation (or a vessel-train formation) is proposed to deal with the collisions in a narrow waterway of port areas [26].

However, there is seldom research focusing on collision avoidance for a multi-vessel towing system. Therefore, the goal of this chapter is the design of a distributed control scheme capable of avoiding collisions for a physically interconnected multi-ASV system performing a towing process, and the avoidance operation adheres to COLREGS.

5.1.2 Research Scope

For an ASV, the most vital components are the Guidance, Navigation, Control (GNC) systems, which are generally constituted by onboard computers and software, responsible for managing the entire ASV system [105]. On the other hand, the collision avoidance problem consists of three components: motion prediction, conflict detection, and collision resolution [75]. Combining the above two frameworks, the collision avoidance problem in the ASV GNC systems can be expressed as shown in Fig 5.1.

It can be seen that the motion prediction module, which is to estimate the future trajectories of the own ship and the obstacles, involves the navigation and guidance systems; the conflict detection module, which is to check collision risk, belongs to the guidance system; the collision resolution module, which is to determine the evasive solutions, involves the control and guidance systems. Thus, considering the research subject of this thesis is the control of a multi-vessel towing system, collision resolution is the focus of this chapter while motion prediction and conflict detection are out of the research scope.
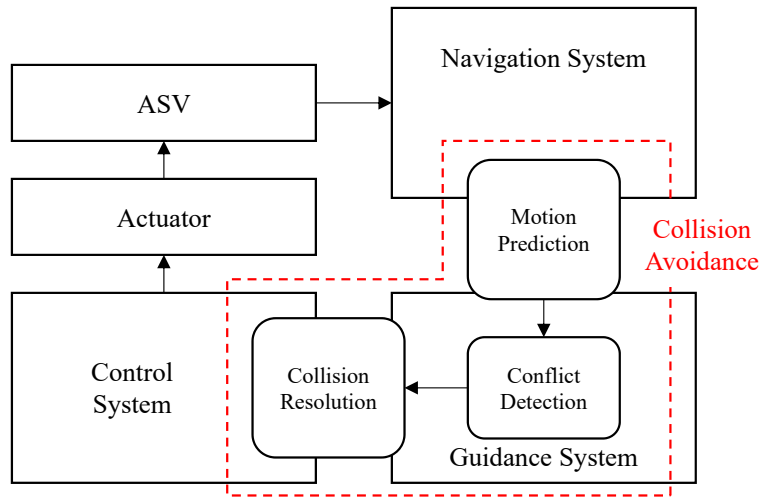
Figure 5.1: collision avoidance problem in the ASV GNC systems.
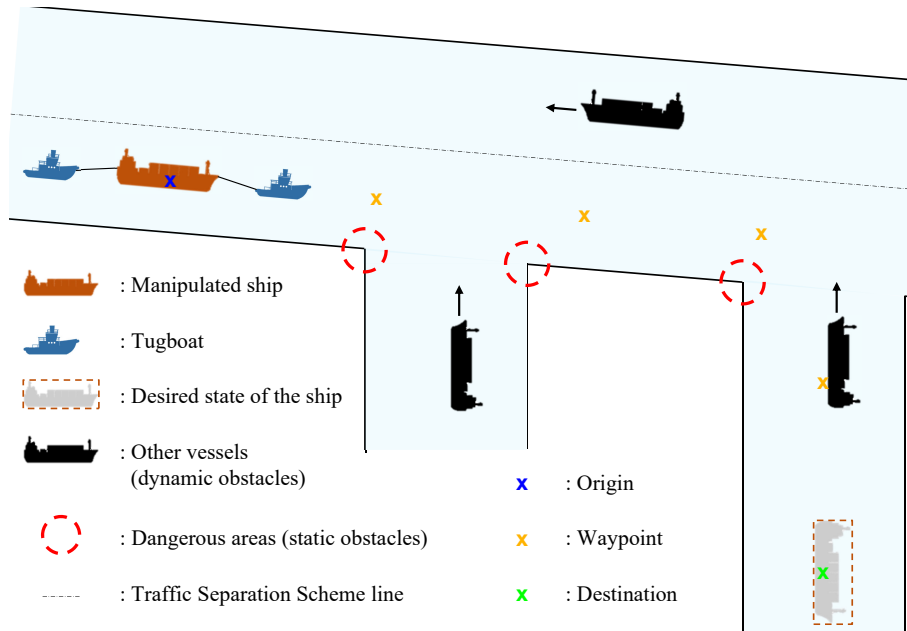
Figure 5.2: Control objectives of a multi-vessel towing system .
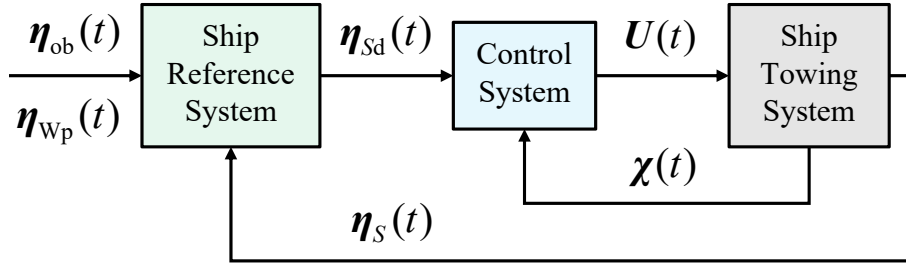
Figure 5.3: Main systems for performing the towing process.

5.1.3   Control Objective

As shown in Fig 5.2, the towing system in this chapter is still composed of one manipulated ship and two tugboats, where the ship is no power. The two autonomous tugs should cooperatively transport the ship following the predefined waypoints from the origin to the destination with the desired heading. In the process of waypoint following, the towing system will come across dangerous areas (static obstacles) and other vessels (dynamic obstacles). Thus, the distances from the towing system to the static and dynamic obstacles should also be controlled to ensure the safety of the towing process.

5.2   COLREGS-Compliant Waypoint Altering Mechanism

As shown in Fig 5.3, there are three main systems in performing the towing process. According to the information of obstacles ($\boldsymbol{\eta}_{\mathrm{ob}}(t)$), the predefined waypoints ($\boldsymbol{\eta}_{\mathrm{Wp}}(t)$), and the current position of the ship ($\boldsymbol{\eta}_{S}(t)$), the ship reference system provides the desired ship position and heading ($\boldsymbol{\eta}_{\mathrm{Sd}}(t)$) to the control system. The control system uses the above data and current states of the ship and two tugs ($\boldsymbol{\chi}(t)$) to calculate the control orders ($\boldsymbol{U}(t)$) that coordinates the two tugs to manipulate the ship and avoid obstacles. The function of the ship reference system, on one hand, is to provide the reference for the controller; on the other hand, it is to make the towing system adhere to the COLREGS. Thus, a COLREGS-compliant waypoint altering mechanism should be designed.

The COLREGS, which is made for a single vessel, include 41 rules divided into six parts, where rules 13 – 17 in Part B (Steering and Sailing Rules) explicitly prescribe actions that a vessel should take when encountering collision risk. Rules 13 to 15 provide definitions and operations of the three situations that a vessel may encounter: Overtaking, head-on, and crossing (as shown in Fig 5.4). Rule 16 describes the generic actions that the give-way vessels should take, and Rule 17 indicates the actions that the stand-on vessels should take.

Considering the characteristics of the physically-connected multi-vessel system with restricted maneuverability and relatively low speed, to make sure the towing system safe we assume that the operations taken by the autonomous tugboat will not make the own ship overtaking other target vessels (as a result, by default, Rule 13 is satisfied). So the collision avoidance focuses on the head-on (Rule 14) and crossing (Rule 15) situations. Meanwhile, we define a detection distance to the obstacle (explained next) to adjust the role of the

Overtaking   Head-on   Crossing
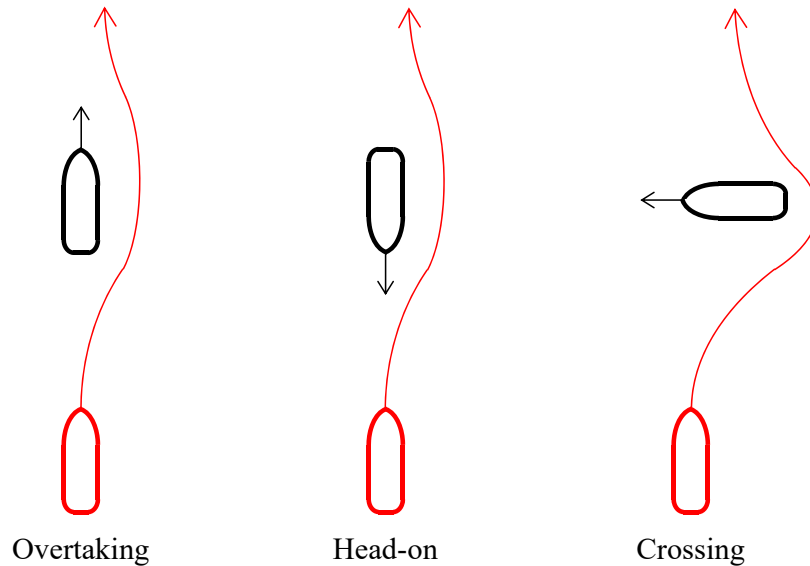
Figure 5.4: Collision avoidance actions vessel should take according to the COLREGS rules in three situations: the red one is the own-vessel (give-way vessel), the black one is the target vessel (stand-on vessel).

towing system: when the obstacle further away than such a distance, the towing system will have the role of "stand-on vessel" (Rule 17); otherwise, the risk is considered to be unrelieved and the towing system as having the role of a "give-way vessel", which has to take avoidance action (Rule 16). The prescribed actions in Rules 14 and 15 indicate that the give-way vessel should steer to the starboard side (right) so that each vessel passes on the port side (left) of each other. However, for the ship in the towing system, its movements are controlled by the two connected tugs. So the prescribed operations should be formulated in a different way.

In maritime practice, a set of fixed waypoints are usually applied in the towing process to guide it to its goal. If there are no dynamic obstacles, the system should follow this predefined path to get to the destination; otherwise, the potential collisions will happen on this path (as shown in Fig 5.5 (a)). In the presence of dynamic obstacles, these waypoints can be used as an alternative way for the COLREGS-based prescribed operations. As shown in Fig 5.5 (b) and (c), when encountering obstacles, the operation of starboard steering can be equivalently converted to a clockwise waypoint altering (the current goal waypoint W_p is altered by a new waypoint W_{pN}). The criteria for such a deviation from the nominal path is determined by comparing the detection distance d_D and obstacle distance $d_{ob}(t)$, expressed as:
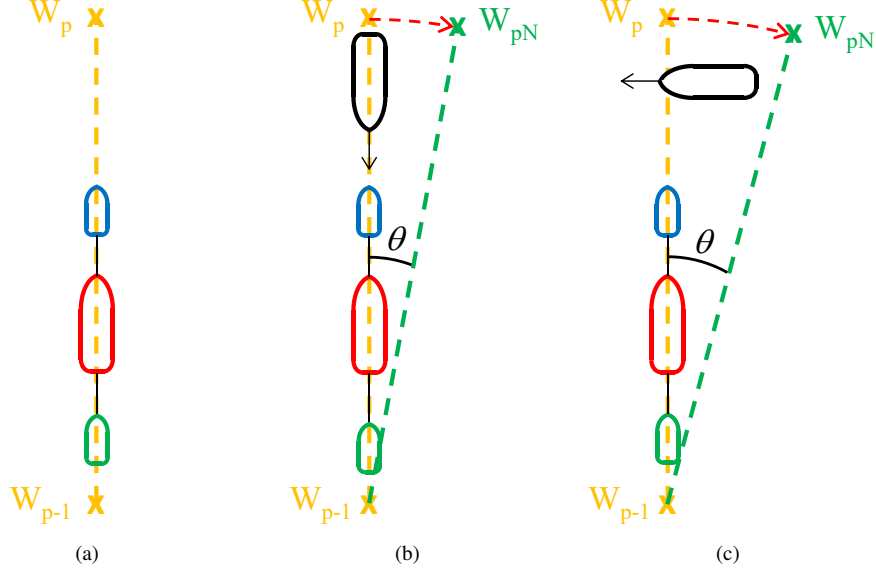
Figure 5.5: Ship reference scheme: (a) under normal condition; (b) under the head-on situation; (c) under the crossing situation.

$$
\begin{cases}
\boldsymbol{\eta}_{Sd}(t) = \boldsymbol{\eta}_{Sp}, & \text{if } d_{\text{ob}}(t) > d_{\text{D}} \\
\boldsymbol{\eta}_{Sd}(t) = \boldsymbol{\eta}_{Sn}, & \text{if } d_{\text{ob}}(t) \leq d_{\text{D}}
\end{cases}
$$
$$
d_{\text{ob}}(t) = \min\Big\{ d_{Sj}(t), d_{1j}(t), d_{2j}(t) \Big\},
\tag{5.1}
$$

where $\boldsymbol{\eta}_{Sp}$ and $\boldsymbol{\eta}_{Sn}$ are the predefined and the new (updated) position references of waypoint p, respectively. The parameter detection distance d_{D} is determined by the range of sensors. The terms $d_{Sj}(t)$, $d_{1j}(t)$, and $d_{2j}(t)$ are the distance from the obstacle j to the manipulated ship, to the tug 1, and to the tug 2, respectively. Their values are calculated according to the attributes of the obstacle: the static obstacle is treated as a circle, and the dynamic obstacle is treated as an ellipse. As seen in Fig 5.6, for $*$ represents the own vessel, the obstacle distance is then expressed as:

$$
d_{*j}(k) =
\begin{cases}
\overline{P_* O_j} & \text{for } j \text{ is circle obstacle} \\
\overline{P_* F_{j1}} + \overline{P_* F_{j2}} & \text{for } j \text{ is ellipse obstacle}
\end{cases}
$$
$$
\overline{P_* O_j} = \sqrt{(x_* - x_{Oj})^2 + (y_* - y_{Oj})^2}
\tag{5.2}
$$
$$
\overline{P_* F_{j1}} = \sqrt{(x_* - x_{Fj1})^2 + (y_* - y_{Fj1})^2}
$$
$$
\overline{P_* F_{j2}} = \sqrt{(x_* - x_{Fj2})^2 + (y_* - y_{Fj2})^2}
$$

where (x_*, y_*) is the coordinates of the own vessel, (x_{Oj}, y_{Oj}) is the coordinates of the static obstacle, (x_{Fj1}, y_{Fj1}) and (x_{Fj2}, y_{Fj2}) are the coordinates of the two focuses for dynamic
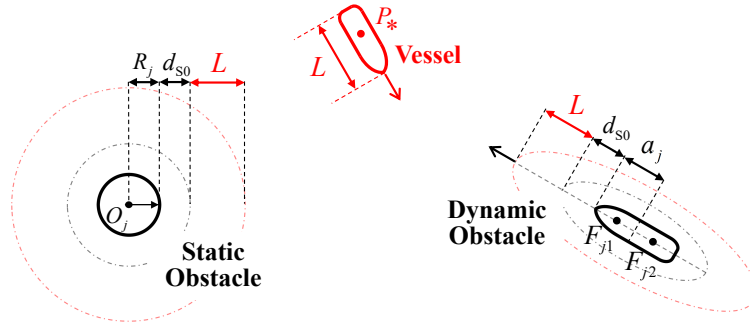
Figure 5.6: Distance of different obstacles

obstacle. Condition (5.1) implies that the risk of collision is defined considering all three vessels as an interconnected system and the collision avoidance should be guaranteed by all vessels.

The new waypoint is determined by an arc of the circle with center the last predefined waypoint $(p-1)$ and radius the distance between $p-1$ and p. The direction is clockwise for the operations of starboard steering. The planar coordinates (x_n, y_n) of the new waypoint can be computed as:

$$
\begin{bmatrix} x_n \\ y_n \end{bmatrix} = \begin{bmatrix} x_{p-1} \\ y_{p-1} \end{bmatrix} + r_{wp} \cdot \begin{bmatrix} \sin(\theta) \\ \cos(\theta) \end{bmatrix}
$$
$$
r_{wp} = \left\| \begin{bmatrix} x_{p-1} \\ y_{p-1} \end{bmatrix} - \begin{bmatrix} x_p \\ y_p \end{bmatrix} \right\|_2 ,
$$

(5.3)

where (x_{p-1}, y_{p-1}) is the coordinates of the last predefined waypoint; (x_p, y_p) are the co-ordinates of the current predefined waypoint; r_{wp} is the distance between the above two waypoints; θ is the altering angle ($\theta > 0°$ for clockwise rotation). The reference heading angle of the new waypoint can be expressed as

$$
\psi_n = \psi_p + \theta,
$$
(5.4)

where ψ_p is the current predefined course along the waterway direction.

The parameter θ should be chosen within a certain range to ensure the collision-free motion of the ship towing system considering spatial limitation like the bank of waterway during maneuvering. As shown in Fig 5.7, there is a maximum value for θ, which is calculated by [69]:

$$
\theta_{max} = \arctan \frac{d_2(t)}{d_1(t)}
$$

where $d_1(t)$ is the distance between two waypoints; $d_2(t)$ is the distance from the predefined path to the edge of the spatial boundaries. It can be seen that $d_1(t)$ and $d_2(t)$ are time-varying variables, because for different two waypoints, $d_1(t)$ will be different; for different
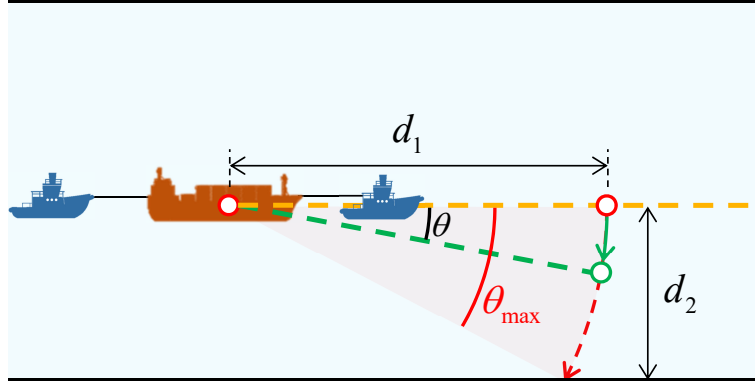
Figure 5.7: The maximum value of θ considering spatial limitation.
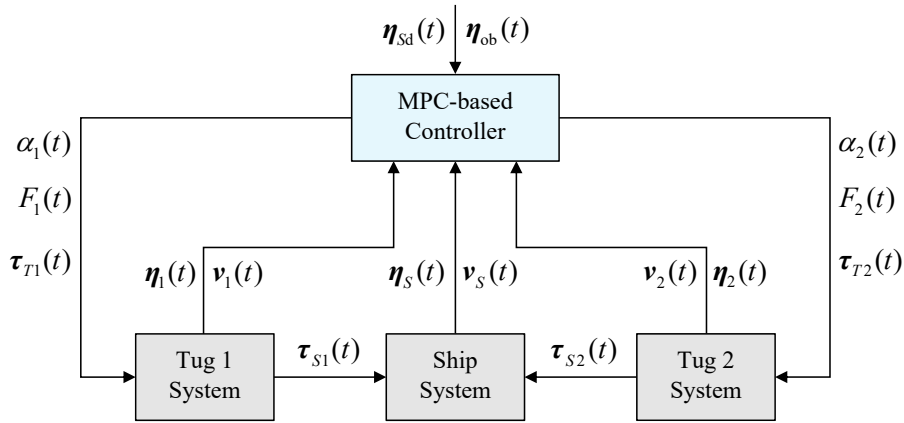
Figure 5.8: Centralized control diagram.

waterways, $d_2(t)$ will be different. Thus, the value of θ should satisfy: $0° < θ < θ_{max}$.

5.3 Design of Distributed Model Predictive Control

5.3.1 MPC-based Centralized Control Problem

The ship reference system is the first stage of collision resolution that focuses on complying with COLREGS. Considering the physical-connection constraints reducing the effectiveness of the steering operation and the low-speed conditions increasing the response time of the action, the second stage of collision resolution is performed in the control system.

As shown in Fig 5.8, at each time instant k, the MPC-based controller solves the following optimization problems to get the control inputs of the ship ($\tau_S = \{F_1, F_2, \alpha_1, \alpha_2\}$) and

the two tugs ($\boldsymbol{\tau}_{T_1} = \{\tau_{T_1 u}, \tau_{T_1 v}, \tau_{T_1 r}\}$, $\boldsymbol{\tau}_{T_2} = \{\tau_{T_2 u}, \tau_{T_2 v}, \tau_{T_2 r}\}$):

$$\min_{\boldsymbol{\tau}_S, \boldsymbol{\tau}_{T_1}, \boldsymbol{\tau}_{T_2}} \quad \sum_{h=1}^{H_P} J_S(k+h|k) + J_1(k+h|k) + J_2(k+h|k), \tag{5.5}$$

subject to i) Ship and tugs dynamics;

ii) Ship and tugs actuator saturation;

iii) System configuration restriction;

where H_P is the length of the prediction horizon; h is the hth time prediction step; $J_S(k+h|k)$, $J_1(k+h|k)$ and $J_2(k+h|k)$ are the prediction made at k about the cost function of the ship and two tugs at $k+h$, respectively. The cost function of the three vessels is designed as:

$$J_*(k) = w_{*1} \boldsymbol{e}_{\eta *}^{\mathrm{T}}(k) \boldsymbol{e}_{\eta *}(k) + w_{*2} \mathbf{v}_{*P}^{\mathrm{T}}(k) \mathbf{v}_{*P}(k) + w_{*3} \sum_{j=1}^{n} \left(d_{*j}(k) - d_{*j_d} \right)^{-2}$$
$$\boldsymbol{e}_{\eta *}(k) = \boldsymbol{\eta}_{*P}(k) - \boldsymbol{\eta}_{*d}(k), \tag{5.6}$$

where $*$ can be S or i ($i = 1, 2$), w_{*1}, w_{*2} and w_{*3} are the weight coefficients (positive scalar); $\boldsymbol{e}_{\eta *}(k) \in \mathbb{R}^3$ is the position error; $\boldsymbol{\eta}_{*d}(k) \in \mathbb{R}^3$ is the desired position vector. The term $\boldsymbol{\eta}_{*P}(k) \in \mathbb{R}^3$ and $\mathbf{v}_{*P}(k) \in \mathbb{R}^3$ are the predicted position and velocity; n is the number of obstacles. The term d_{*j_d} is the safe distance between the vessel and obstacle j, whose values are also calculated according to the attributes of the obstacle (see in Fig 5.6):

$$d_{*j_d} = \begin{cases} L_{oa} + R_j + d_{S0} & \text{for } j \text{ is circle obstacle} \\ 2(L + a_j + d_{S0}) & \text{for } j \text{ is ellipse obstacle} \end{cases}, \tag{5.7}$$

where L_{oa} is the length of the own-vessel; R_j is the radius of the circle obstacle j; a_j is the length of the long axis of the ellipse obstacle j; d_{S0} is the surplus distance (buffer) of the obstacles. Note that the safe distance d_{*j_d} is smaller than the detection distance d_D: $d_{*j_d} < d_D$.

It can be seen from (5.6) that the cost contains three parts. The first part is the position error, which is minimized to achieve path following. The second part is the velocity, whose role is to reduce the speed of the three vessels to make the motion of the system smooth. The third part is the distance error between the ship and the obstacles. It is a reciprocal quadratic term meaning that the further the ship from the safety distance of the obstacle, the less value of this term. This is the second stage of collision resolution ensuring that the ship keeps away from the obstacles.

The ship and tugs dynamics (the first constraint) are represented by the prediction model, calculated by discretizing the dynamic model with sampling time T_s (the subscript S stands for the ship, i ($i = 1, 2$) stands for the tugboat):

$$\boldsymbol{\eta}_{SP}(k+1) = \boldsymbol{\eta}_{SP}(k) + \int_{kT_s}^{(k+1)T_s} \boldsymbol{R}\big(\psi_S(t)\big)\boldsymbol{v}_S(t)dt$$

$$\boldsymbol{v}_{SP}(k+1) = \boldsymbol{v}_{SP}(k) + \int_{kT_s}^{(k+1)T_s} \boldsymbol{M}_S^{-1}\big[-\boldsymbol{C}_S\big(\boldsymbol{v}_S(t)\big)\boldsymbol{v}_S(t) - \boldsymbol{D}_S\boldsymbol{v}_S(t)$$
$$-\boldsymbol{B}\big(\alpha_1(t)\big)F_1(t) + \boldsymbol{B}\big(\alpha_2(t)\big)F_2(t)\big]dt, \tag{5.8}$$

$$\boldsymbol{\eta}_{iP}(k+1) = \boldsymbol{\eta}_{iP}(k) + \int_{kT_s}^{(k+1)T_s} \boldsymbol{R}\big(\psi_i(t)\big)\boldsymbol{v}_i(t)dt$$

$$\boldsymbol{v}_{iP}(k+1) = \boldsymbol{v}_{iP}(k) + \int_{kT_s}^{(k+1)T_s} \boldsymbol{M}_i^{-1}\big[-\boldsymbol{C}_i\big(\boldsymbol{v}_i(t)\big)\boldsymbol{v}_i(t) - \boldsymbol{D}_i\boldsymbol{v}_i(t)$$
$$+\boldsymbol{B}_i\big(\beta_i(t)\big)F_i(t) + \boldsymbol{\tau}_{Ti}(t)\big]dt. \tag{5.9}$$

The actuator saturation (the second constraint) is given in (4.13), (4.14), and (4.18). The configuration restriction (the third constraint) is to satisfy the configuration of the towing system to keep the desired geometrical relationship between the ship and tugs, which can be referred to Section 4.1.3.

5.3.2 ADMM-based distributed MPC Scheme

Although the centralized control scheme in Section 5.3.1 can solve the optimization problem, if the number of tugboats increases, the number of control inputs and constraints will increase, and the structure inside the controller will also change. To improve the proposed method applicably, it is necessary to divide such a large global optimization problem into several small local optimization problems. Thus, a distributed control scheme is designed by using the Alternating Direction Method of Multipliers (ADMM).

For our case, the MPC-based controller in Fig 5.8 can be divided into three sub-controllers according to their functions: Coordination controller, Tug 1 local controller, and Tug 2 local controller. As seen in Fig 5.9, the coordination controller, located on the ship, uses the information of ship desired position and heading $\boldsymbol{\eta}_{Sd}(t)$, obstacle position and heading $\boldsymbol{\eta}_{ob}(t)$, and the current states of the ship $\boldsymbol{\eta}_S(t)$, $\boldsymbol{v}_S(t)$ to compute the towing forces $F_i(t)$ and the desired tug trajectory reference $\boldsymbol{\eta}_{id}(t)$ which is a function of towing angles $\alpha_i(t)$. The tug local controller, located on the tug, uses the calculated towing force, tug trajectory reference, and the current states of tugs $\boldsymbol{\eta}_i(t)$, $\boldsymbol{v}_i(t)$ to first calculate the predicted position $\boldsymbol{\eta}_{iP}(t)$, and share this information with the coordination controller to reach a consensus between the predicted position and the tug reference trajectory ($\boldsymbol{\eta}_{iP}(t) = \boldsymbol{\eta}_{id}(t)$). Then, the coordination controller updates the towing forces and angles. When the consensus is achieved, the tug local controller outputs the thruster forces and moment $\boldsymbol{\tau}_{Ti}(t)$ to the tug system.

Based on the above analysis, the augmented lagrangian form for our problem at time instant k can be formulated as:

$$L_p\big(\boldsymbol{\tau}_S(k), \boldsymbol{\tau}_{Ti}(k), \lambda_i(k)\big) = J_S\big(\boldsymbol{\tau}_S(k)\big) + \sum_{i=1}^{2}\Big(J_i\big(\boldsymbol{\tau}_{Ti}(k)\big) + \lambda_i^{\mathrm{T}}(k)[\boldsymbol{\eta}_{iP}(k) - \boldsymbol{\eta}_{id}(k)]$$
$$+(\rho/2)\,\|\boldsymbol{\eta}_{iP}(k) - \boldsymbol{\eta}_{id}(k)\|_2^2\Big), \tag{5.10}$$

where $\lambda_i(k)$ is the Lagrange multiplier or dual variable, and ρ is the penalty parameter. Variable $\boldsymbol{\eta}_{id}(k)$ is a function of the towing angle ($\alpha_i(k)$) and the ship predicted heading
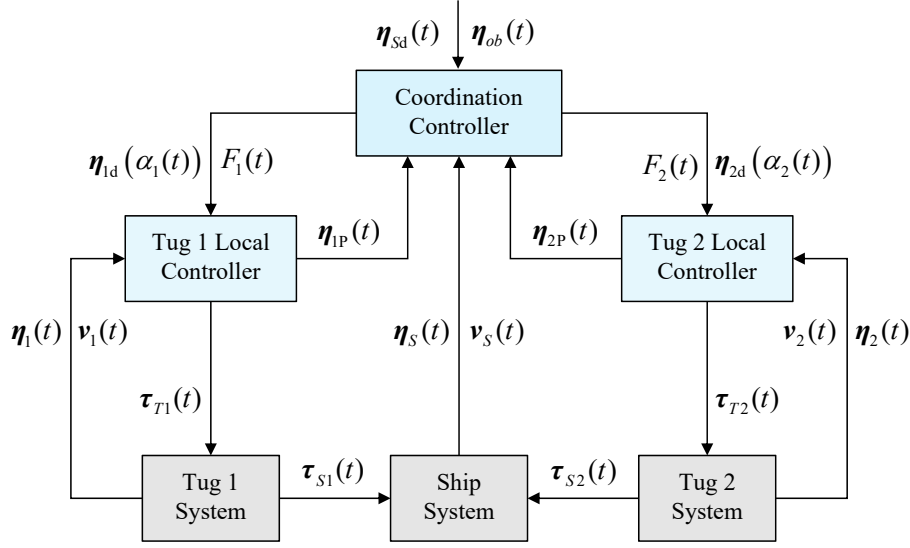
Figure 5.9: System control diagram.

$(\psi_{SP}(k))$. The variable $\alpha_i(k)$ is a part of the $\boldsymbol{\tau}_S(k)$, and $\psi_{SP}(k)$ can be calculated by ship dynamics (5.8). Thus, $\boldsymbol{\eta}_{id}(k)$ can be expressed as a function of $\boldsymbol{\tau}_S(k)$:

$$\boldsymbol{\eta}_{id}(k) = f_i\big(\boldsymbol{\tau}_S(k)\big). \tag{5.11}$$

Similarly, $\boldsymbol{\eta}_{i\mathrm{P}}(k)$ can be calculated by tug dynamics (5.9), so it is a function of $\boldsymbol{\tau}_{T_i}(k)$:

$$\boldsymbol{\eta}_{i\mathrm{P}}(k) = g_i\big(\boldsymbol{\tau}_{Ti}(k)\big). \tag{5.12}$$

Based on (5.10), (5.11), and (5.12), the ADMM form of the iterations are formulated as:

$$\boldsymbol{\tau}_{Ti}^s(k) := \underset{\boldsymbol{\tau}_{Ti}(k)}{\arg\min} \left(J_i\big(\boldsymbol{\tau}_{Ti}(k)\big) + \lambda_i^{s-1}(k)^{\mathrm{T}}\Big[g_i\big(\boldsymbol{\tau}_{Ti}(k)\big) - f_i\big(\boldsymbol{\tau}_S^{s-1}(k)\big)\Big] \right.$$
$$\left. + (\rho/2)\Big\| g_i\big(\boldsymbol{\tau}_{Ti}(k)\big) - f_i\big(\boldsymbol{\tau}_S^{s-1}(k)\big)\Big\|_2^2 \right), \tag{5.13}$$

$$\boldsymbol{\tau}_S^s(k) := \underset{\boldsymbol{\tau}_S(k)}{\arg\min} \left(J_S\big(\boldsymbol{\tau}_S(k)\big) + \sum_{i=1}^{2}\left(-\lambda_i^{s-1}(k)^{\mathrm{T}} f_i\big(\boldsymbol{\tau}_S(k)\big) \right. \right.$$
$$\left. \left. + (\rho/2)\Big\| g_i\big(\boldsymbol{\tau}_{Ti}^s(k)\big) - f_i\big(\boldsymbol{\tau}_S(k)\big)\Big\|_2^2 \right) \right), \tag{5.14}$$

$$\lambda_i^s(k) := \lambda_i^{s-1}(k) + \rho_i\Big(g_i\big(\boldsymbol{\tau}_{Ti}^s(k)\big) - f_i\big(\boldsymbol{\tau}_S^s(k)\big)\Big), \tag{5.15}$$

where s is the iteration with $s \in \{1, 2, \cdots S\}$, S is the maximum iteration; $\cdot^s$ stands for the corresponding variable at the sth iteration.

Algorithm 5.1 - ADMM-based Distributed Control

Input: Obstacle position $\boldsymbol{\eta}_{\mathrm{ob}}(t)$;

Desired ship position $\boldsymbol{\eta}_{Sd}(t)$;

Current ship position and velocity $\boldsymbol{\eta}_S(t)$, $\mathbf{v}_S(t)$;

Current tug position and velocity $\boldsymbol{\eta}_i(t)$, $\mathbf{v}_i(t)$.

For $s = 1 : S$

Step 1: At the lower level, each tug local controller calculates the thruster forces and moment of the tug $\boldsymbol{\tau}_{Ti}^s(k)$ according to (5.13), and sends the results to the coordination controller;

Step 2: At the higher level, the coordination controller computes the manipulation forces and moment for the ship $\boldsymbol{\tau}_S^s(k)$ according to (5.14);

Step 3: In both tug and coordination controllers, update the Lagrange multiplier $\lambda_i^s(k)$ according to (5.15);

Step 4: In coordination controller, update the primal $\varepsilon_{\mathrm{pri},i}^s(k)$ and dual $\varepsilon_{\mathrm{dual},i}^s(k)$ tolerances according to (5.17), and checks the primal $\boldsymbol{R}_{\mathrm{pri},i}^s(k)$ and dual $\boldsymbol{R}_{\mathrm{dual},i}^s(k)$ residuals whether they meet the termination criteria according to (5.16);

Step 5: If (5.16) is not satisfied, then repeat the above steps; otherwise, jump out of the iteration.

End

Output: Thruster forces and moment of the tug $\boldsymbol{\tau}_{Ti}^s(k)$;

Manipulation forces and moment for the ship $\boldsymbol{\tau}_S^s(k)$.

The termination criterion for the iterations is provided according to the following conditions:

$$
\begin{aligned}
\left\| \boldsymbol{R}_{\mathrm{pri},i}^s(k) \right\|_2 &= \left\| g_i\big(\boldsymbol{\tau}_{Ti}^s(k)\big) - f_i\big(\boldsymbol{\tau}_S^s(k)\big) \right\|_2 \leq \varepsilon_{\mathrm{pri},i}^s(k), \\
\left\| \boldsymbol{R}_{\mathrm{dual},i}^s(k) \right\|_2 &= \left\| f_i\big(\boldsymbol{\tau}_S^s(k)\big) - f_i\big(\boldsymbol{\tau}_S^{s-1}(k)\big) \right\|_2 \leq \varepsilon_{\mathrm{dual},i}^s(k),
\end{aligned}
\tag{5.16}
$$

where $\boldsymbol{R}_{\mathrm{pri},i}^s$ and $\boldsymbol{R}_{\mathrm{dual},i}^s$ are the primal and dual residual at iteration s; $\varepsilon_{\mathrm{pri},i}^s > 0$ and $\varepsilon_{\mathrm{dual},i}^s > 0$ are feasibility tolerances, determined by

$$
\begin{aligned}
\varepsilon_{\mathrm{pri},i}^s(k) &= \sqrt{n_s}\varepsilon^{\mathrm{abs}} + \varepsilon^{\mathrm{rel}} \max \Big\{ \left\| g_i\big(\boldsymbol{\tau}_{Ti}^s(k)\big) \right\|_2, \\
&\qquad\qquad \left\| f_i\big(\boldsymbol{\tau}_S^s(k)\big) \right\|_2 \Big\}, \\
\varepsilon_{\mathrm{dual},i}^s(k) &= \sqrt{n_s}\varepsilon^{\mathrm{abs}} + \varepsilon^{\mathrm{rel}} \left\| \lambda_i^s(k) \right\|_2,
\end{aligned}
\tag{5.17}
$$

where n_s is the size of the variable $\boldsymbol{\tau}_{Ti}$; $\varepsilon^{\mathrm{abs}} > 0$ and $\varepsilon^{\mathrm{rel}} > 0$ are the absolute and relative tolerance, respectively.

Overall, the ADMM-based distributed control scheme for a physically interconnected multi-ASV system performing a ship towing process is summarized in the **Algorithm 5.1**.

Table 5.1: Parameters of the control system.

Altering angle	$\theta = 15°$
Sampling time	$T_s = 1$ s
Prediction horizon	$H_P = 3$
Weight coefficient in cost function J_S	$w_{S1} = 1, w_{S2} = 75, w_{S3} = 1$
Weight coefficient in cost function J_i	$w_{i1} = 1, w_{i2} = 6, w_{i3} = 1, (i = 1, 2)$
Absolute and relative tolerance in ADMM	$\varepsilon^{abs} = 0.001, \varepsilon^{rel} = 0.001$
Maximum value of towing angles	$\alpha_{1\max} = 30°, \quad \alpha_{2\max} = 30°$
Maximum value of towing forces	$F_{1\max} = 3\text{N}, \quad F_{2\max} = 3\text{N}$
Maximum rate of the change of towing angles	$\bar{\alpha}_1 = 5°/\text{s}, \quad \bar{\alpha}_2 = 5°/\text{s}$
Maximum rate of the change of towing forces	$\bar{F}_1 = 0.3\text{N/s}, \quad \bar{F}_2 = 0.3\text{N/s}$

Table 5.2: Position[1] and heading[2] of the predefined waypoint.

$\boldsymbol{\eta}_{W_{P1}} = [-6.3 \ \ 14 \ \ 101.3]^T$	$\boldsymbol{\eta}_{W_{P2}} = [-7.7 \ \ 21 \ \ 101.3]^T$
$\boldsymbol{\eta}_{W_{P3}} = [-9.1 \ \ 28 \ \ 101.3]^T$	$\boldsymbol{\eta}_{W_{P4}} = [-10.7 \ \ 36 \ \ 101.3]^T$
$\boldsymbol{\eta}_{W_{P5}} = [-15 \ \ 40 \ \ 180]^T$	$\boldsymbol{\eta}_{W_{P6}} = [-22 \ \ 40 \ \ 180]^T$
$\boldsymbol{\eta}_{W_{P7}} = [-29 \ \ 40 \ \ 180]^T$	$\boldsymbol{\eta}_{W_{P8}} = [-36 \ \ 40 \ \ 180]^T$

[1] The unit is the meter.
[2] The heading of the waypoint is defined along the direction of the waterway, and the unit is
    the degree.

5.4   Simulations and Results Discussion

5.4.1   Simulation Setup

The models of "*CyberShip II*" and "*TitoNeri*" are still used as the manipulated ship and two tugboats, respectively (parameters are shown in Table 3.2). The parameters of the control system are given in Table 5.1.

   The objective is to cooperatively control two autonomous tugboats that safely manipulate the ship from the origin ($\boldsymbol{\eta}_{W_{PO}} = [-4.9 \ \ 7 \ \ 101.3°]^T$) to the destination ($\boldsymbol{\eta}_{W_{PD}} = [-43 \ \ 40 \ \ 180°]^T$). Between the origin and destination, there are eight predefined waypoints (the values are shown in Table 5.2), which should be followed when there are no obstacles. There are three static obstacles (a, b, c) and three dynamic obstacles (A, B, C) during the towing process, whose information is shown in Table 5.3.

Table 5.3: Information of the obstacles.

Obstacle	Length (m)	Width (m)	Course (degree)	Speed (m/s)	Position (initial)
Static a	1	1	-	0	(-10,15)
Static b	1	1	-	0	(-12,25)
Static c	1	1	-	0	(-14,35)
Dynamic A	1.48	0.48	0	0.07	(-19,21)
Dynamic B	1.48	0.48	0	0.07	(-22,40.75)
Dynamic C	1.48	0.48	0	0.07	(-38,40.5)

5.4.2   Results and Discussion

(1) Ship Towing Process

The towing process is shown in Fig 5.10, which is represented by ten sampled states of the towing system. From $t_1 = 0$ s to $t_2 = 100$ s, the control objective is path following. The two tugs manipulate the ship from the origin (W_{PO}) to the first waypoint (W_{P1}). From $t_2 = 100$ s to $t_3 = 190$ s, the system encounters the first avoidance scenario, crossing. In this case, the towing system has to avoid the first moving vessel and stay away from the dangerous area a. The trajectories indicate that the system executes starboard (right) side steering operation to bypass the moving vessel (satisfy the COLREGS), and all the trajectories did not cross over the dangerous area a. After avoiding the moving vessel, the system returns to the predefined path to continue to follow the rest of the waypoints, whose process is from $t_3 = 190$ s to $t_4 = 300$ s. From the trajectories, it is clear that the three vessels stay away from the dangerous area b and return to the third waypoint (W_{P3}).

From $t_4 = 300$ s to $t_5 = 405$ s, the towing system follows the predefined path to the forth waypoint (W_{P4}). From $t_5 = 405$ s to $t_6 = 495$ s, the towing system performs a starboard steering operation and comes across two obstacles, facing the avoidance scenario that contains both crossing and head-on. The trajectories show that the towing system carries out a heavy starboard steering to make the three vessels avoid the second moving obstacle, which makes the trajectory of the ship biases to the right-hand side of the fifth waypoint (W_{P5}), satisfying the COLREGS. Besides, all three vessels stay away from the dangerous areas c in the steering process, reflecting that the control scheme can make sure the towing system navigate in such a narrow waterway condition.

From $t_6 = 485$ s to $t_7 = 590$ s, the towing system again returns to the planned path to follow the sixth waypoint W_{P6}. From $t_7 = 590$ s to $t_8 = 690$ s, the system encounters the third avoidance scenario. The course of the third moving obstacle is right toward the seventh waypoint (W_{P7}), so this is the head-on scenario. The steering trajectories are illustrated that the towing system takes actions of starboard steering to pass on the port side of the third moving obstacle (satisfy the COLREGS). The period from $t_8 = 690$ s to $t_9 = 785$ s is the third returning process, aiming at the eighth waypoint (W_{P8}). The last period from $t_9 = 785$ s to $t_{10} = 969$ s is the stabilizing process that the two tugs stop the ship at the
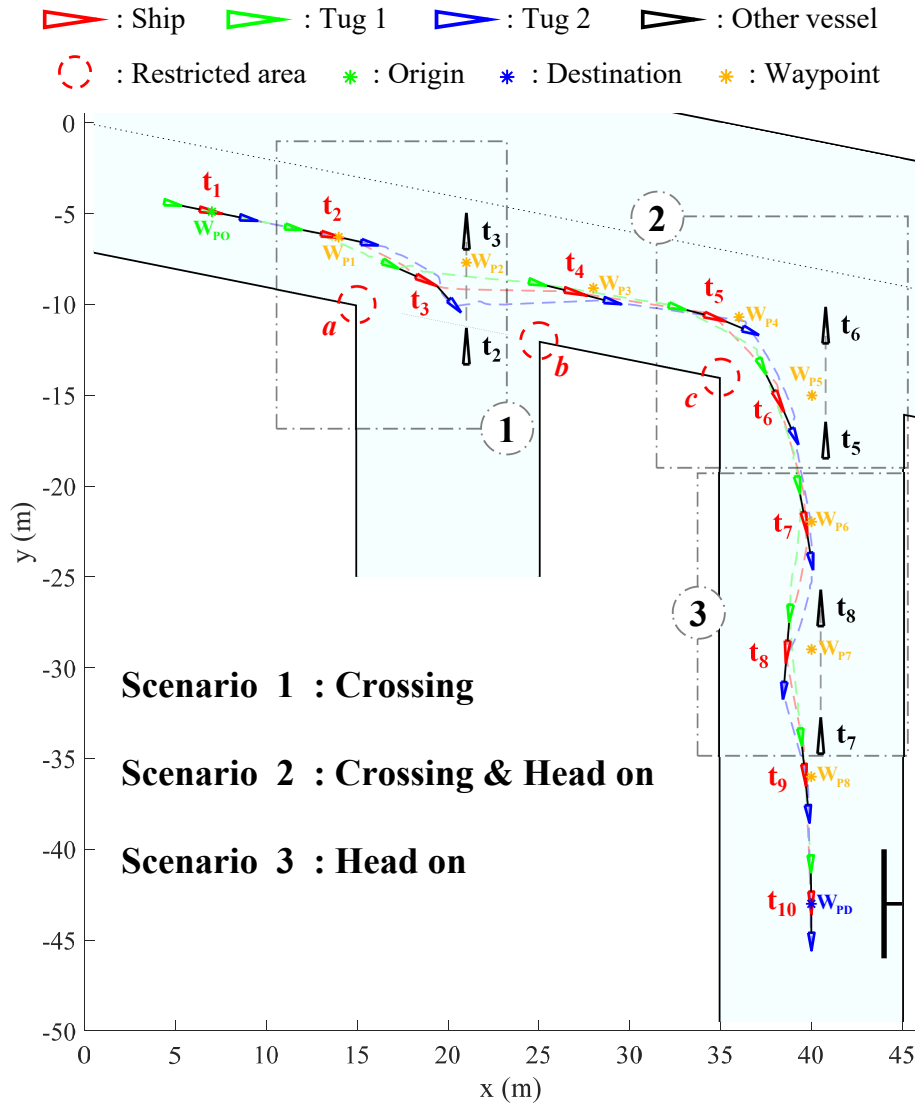
Figure 5.10: Towing process in congested water traffic environment: The black "T" shape stands for a pier, the tip of the marker representing a ship corresponds to the bow.

destination (W_{PD}) with desired heading.

Fig 5.10 shows that the proposed cooperative control algorithm can make the two autonomous tugs manipulate a ship to the destination with the desired heading without colliding the static and dynamic obstacles.

(2) Avoidance Scheme Comparison
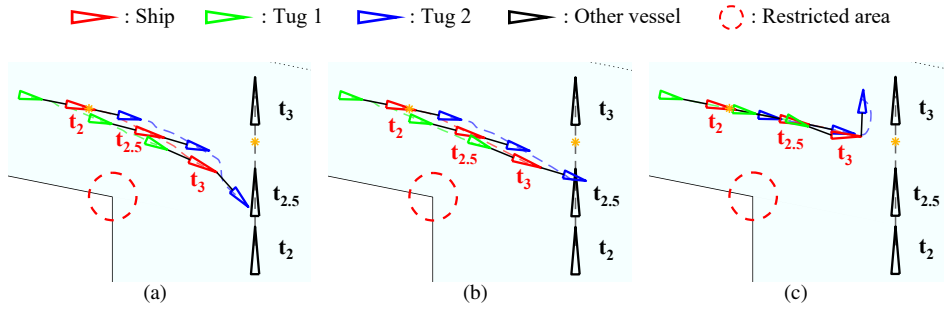
Figure 5.11: *Three collision resolution schemes are applied to deal with avoidance scenario 1 (crossing) during* $t_2 = 100$ s *to* $t_3 = 190$ s *($t_{2.5} = 135$ s): (a) Scheme I; (b) Scheme II; (c) Scheme III.*
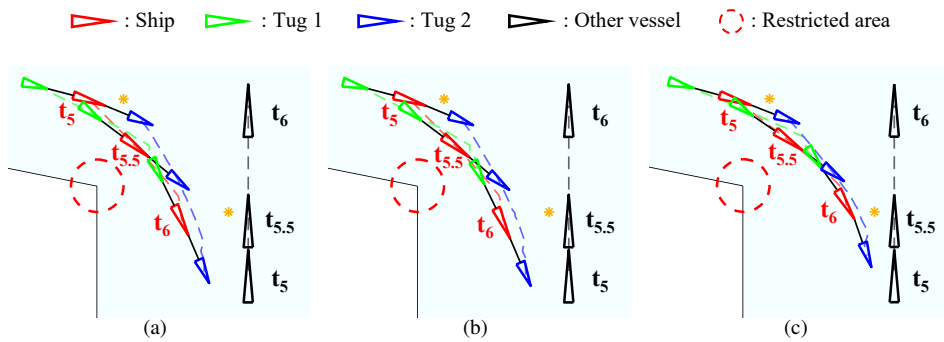
Figure 5.12: *Three collision resolution schemes are applied to deal with avoidance scenario 2 (crossing & heading) during* $t_5 = 405$ s *to* $t_6 = 495$ s *($t_{5.5} = 435$ s): (a) Scheme I; (b) Scheme II; (c) Scheme III.*

In order to show the necessity of the two stages of obstacle avoidance, three different collision resolution schemes are compared: Scheme I is the proposed scheme, combing the waypoint altering system (stage 1) and the distance cost function (stage 2); Scheme II is the one that only uses the waypoint altering system (stage 1); Scheme III is the one that only uses the distance cost function (stage 2). The collision resolution process of the three schemes applied to deal with the three different scenarios in Fig 5.10 is shown in Fig 5.11 - Fig 5.13.

For scenario 1 (Fig 5.11),scheme III makes the towing system steer the port side to avoid the obstacle, this operation violates the COLREGS rules. Scheme I and II comply
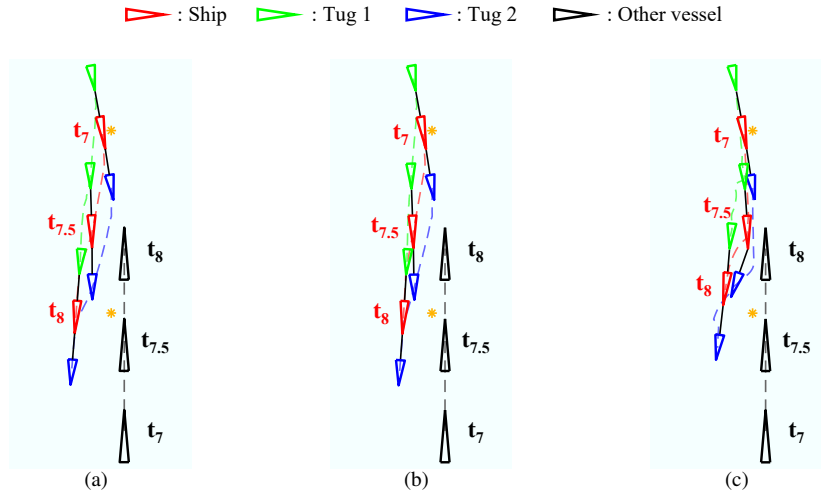
Figure 5.13: Three collision resolution schemes are applied to deal with avoidance scenario 3 (heading) during $t_7 = 590$ s *to* $t_8 = 690$ s ($t_{7.5} = 640$ s*): (a) Scheme I; (b) Scheme II; (c) Scheme III.*

with the rules making the towing system take action of starboard steering, while the scheme I has greater steering during $t_{2.5} = 135$ s and $t_3 = 190$ s to make sure the towing system stays away from the obstacle. For scenario 2 (Fig 5.12) and scenario 3 (Fig 5.13), the three schemes have similar collision resolutions that successfully bypass the obstacle and comply with the COLREGS rules. Compared to the other two schemes, the response time of the collision resolution in scheme III is longer, which makes the distance between the vessels in the towing system and the obstacles smaller at the beginning. To verify this, the performance indicator about the minimum distance between the three vessels in the towing system and the obstacles are proposed and calculated as follows:

$$D_{*j} = \min d_{*j}/L_{oa*} \qquad (5.18)$$

where d_{*j} is calculated by (5.2); L_{oa*} is the length of the vessel. Note that *i*) (5.18) normalizes the minimum distance by eliminating the effect of the length of the vessel; *ii*) the larger the D_{*j}, the safer the vessel.

The normalized minimum distance between the vessels in the towing system and the obstacles by using three avoidance schemes in three scenarios are shown in Table 5.4. In scenario 1, as the greater steering observed in Fig 5.11 (a), the values for three vessels by using scheme I are larger than scheme II. The COLREGS-violated steering in scheme III makes the value of tug 1 ($D_{\mathrm{ob}_1 1}$) a little larger than that in the scheme I, but the other two values are smaller (even than scheme II). In scenario 2, the results in schemes I and II are similar, larger than scheme III. In scenario 3, the superiority in scheme I is more obvious, and the result in scheme III is still the worst because of the longer response time.

Overall, the collision resolution scheme II has the largest normalized minimum distance between the vessels and obstacles in all three scenarios, revealing that the proposed control scheme is the safest in dealing with obstacles, and combining two collision resolution

Table 5.4: Normalized minimum distance between the vessels in the towing system
and the obstacles.

Scheme	Scenario 1 (Crossing)	Scenario 2 (Crossing & Head-on)	Scenario 3 (Head-on)	COLREGS Compliance	
	$D_{S1} = 2.45$	$D_{S2} = 2.65$	$D_{S3} = 1.43$	Scenario 1	✓
I	$D_{11} = 4.31$	$D_{12} = 3.97$	$D_{13} = 1.70$	Scenario 2	✓
	$D_{21} = 1.53$	$D_{22} = 2.41$	$D_{23} = 1.73$	Scenario 3	✓
	$D_{S1} = 2.30$	$D_{S2} = 2.62$	$D_{S3} = 1.23$	Scenario 1	✓
II	$D_{11} = 4.17$	$D_{12} = 3.95$	$D_{13} = 1.50$	Scenario 2	✓
	$D_{21} = 1.36$	$D_{22} = 2.34$	$D_{23} = 1.45$	Scenario 3	✓
	$D_{S1} = 1.93$	$D_{S2} = 2.19$	$D_{S3} = 1.13$	Scenario 1	×
III	$D_{11} = 4.40$	$D_{12} = 3.54$	$D_{13} = 1.30$	Scenario 2	✓
	$D_{21} = 1.44$	$D_{22} = 1.78$	$D_{23} = 1.67$	Scenario 3	✓

stages (the waypoint altering system and the distance cost function) is rational. The total computation time of the proposed method is 2147 s (the whole simulation time is 1000 s). For each collision avoidance scenario, the average computation time is the same. Thus, for every one-second simulation process, the proposed method spends 2 seconds to calculate the desired control inputs. The reason for this computation time is that the model of the towing system is nonlinear, while the iterations of the ADMM in this paper are ten to thirty. So the repeating nonlinear computation requires a lot of time.

(3) Control Architecture Comparison

In this subsection, we compare the results of the centralized and distributed control architecture applied under the above simulation conditions. The time-varying states of the ship and two tugs using the two control architectures are shown in Fig 5.14. It can be seen from the first row of the figure that in both architectures the ship achieves its desired position and heading eventually, and the varying of the values in each state are similar.

The differences are shown in the velocity of the second row. For the ship surge velocity (in red bold line in *u*), the changes in two architectures show similar results: Saw-shape undulations. The nine "sawtooths" indicate the process of waypoint following (eight way-points and a destination point). The reason for forming the "sawtooth" is the changes of position error. In each waypoint following process, the value of ship position error is maximum at the beginning, dominating in (5.6). The coordination controller at the moment focuses on reducing this error and then increases the ship surge speed to a large value. As the ship approaches the waypoint, the position error becomes small, the proportion of velocity part increases. The objective of the coordination controller gradually switches to velocities, the ship surge speed starts decreasing.

However, the changes in the two tugs' surge velocity (green and blue dashed line) in the two architectures are much different. In Fig 5.14 (a), these results show much more fluctuation compared to the ship; but in Fig 5.14 (b), these results are similar to the ship. This can be explained by the fact that the centralized control method is to solve a large global optimization problem concerning all the vessels, so the change of surge velocity of
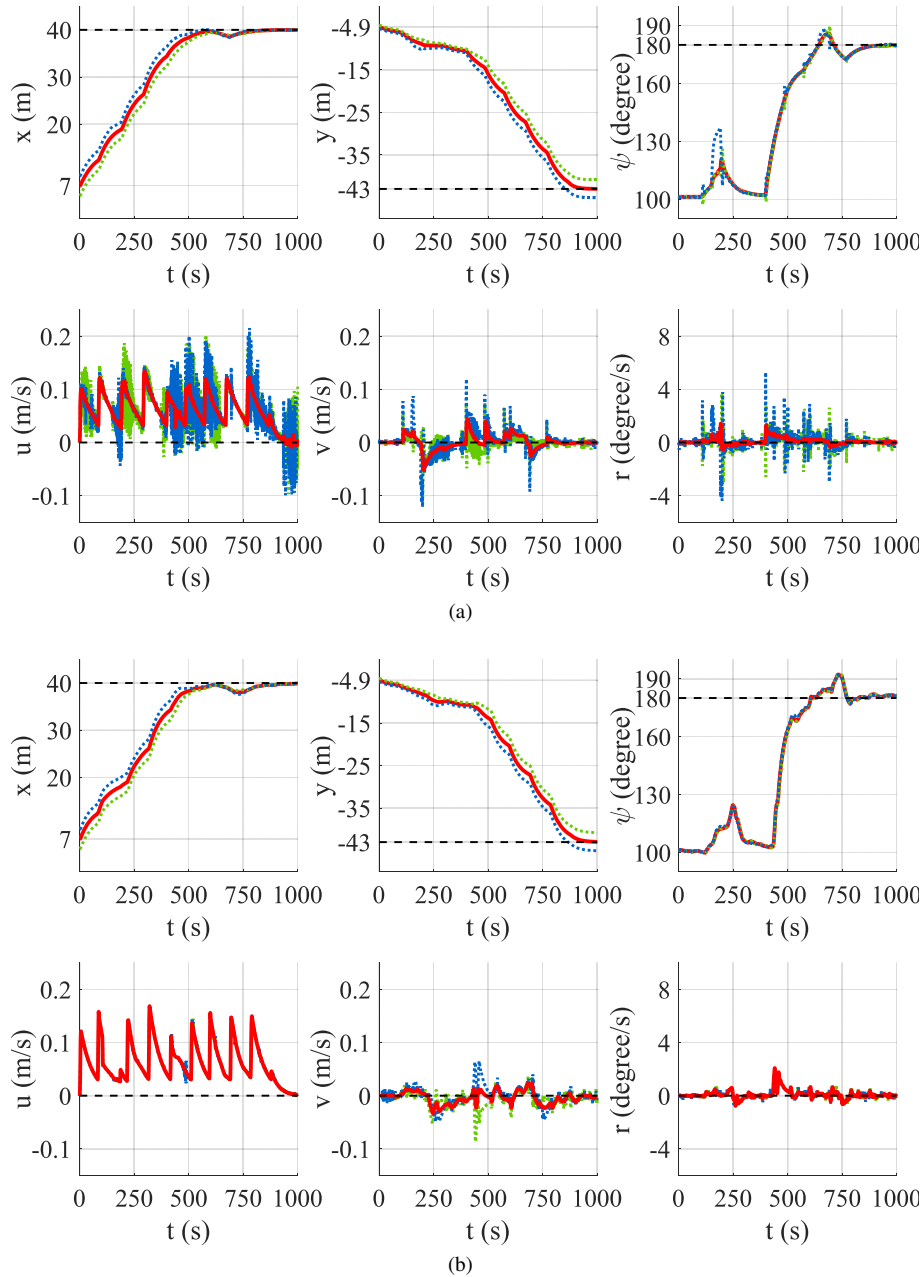
Figure 5.14: Six states (position (x,y), heading ψ and velocities u, v, r) of the ship (red bold line) and two tugs (green dashed line stands for Tug 1 and blue dotted line for Tug 2): (a) The distributed control architecture; (b) The centralized control architecture.
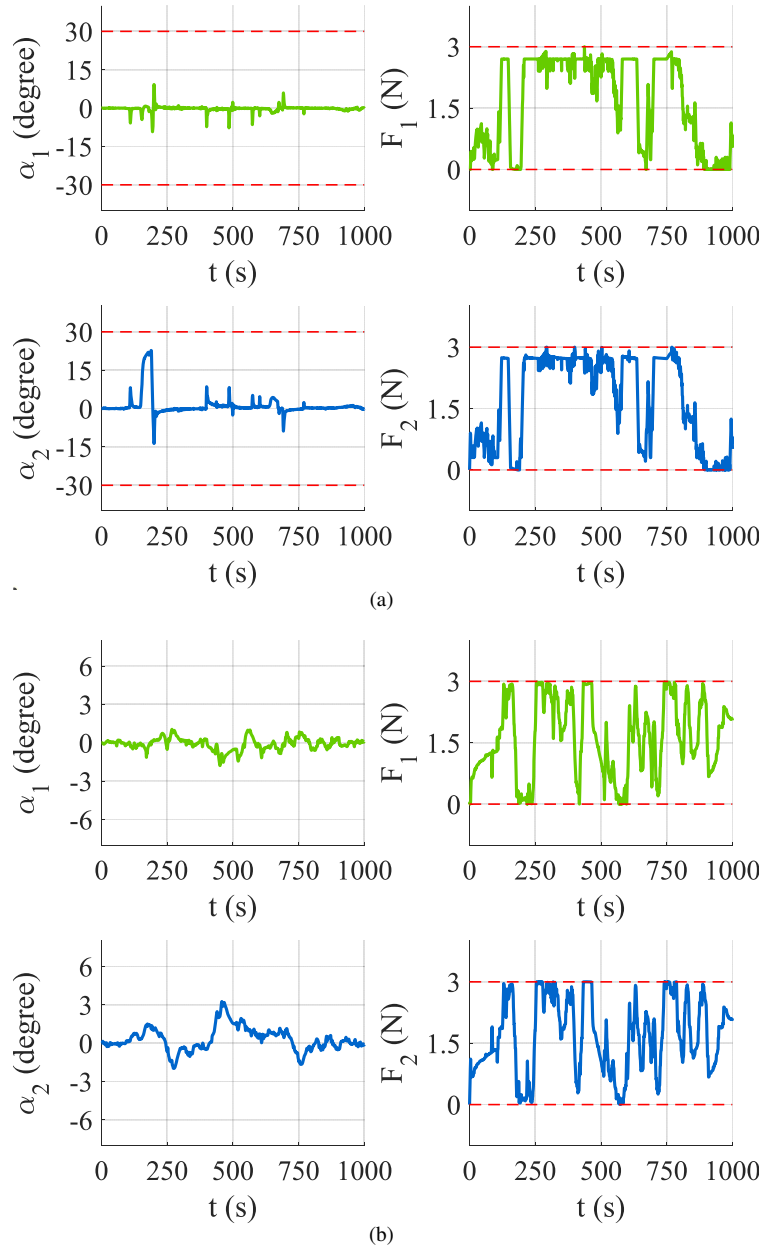
Figure 5.15: Towing angles and forces: (a) The distributed control architecture; (b) The centralized control architecture.

the tugs will be consistent with the ship as much as possible; while the distributed control method is to separately solve the local optimization problems for each vessel, leading to different surge of the tugs and ship. As the power of the ship is provided by the tugs, the
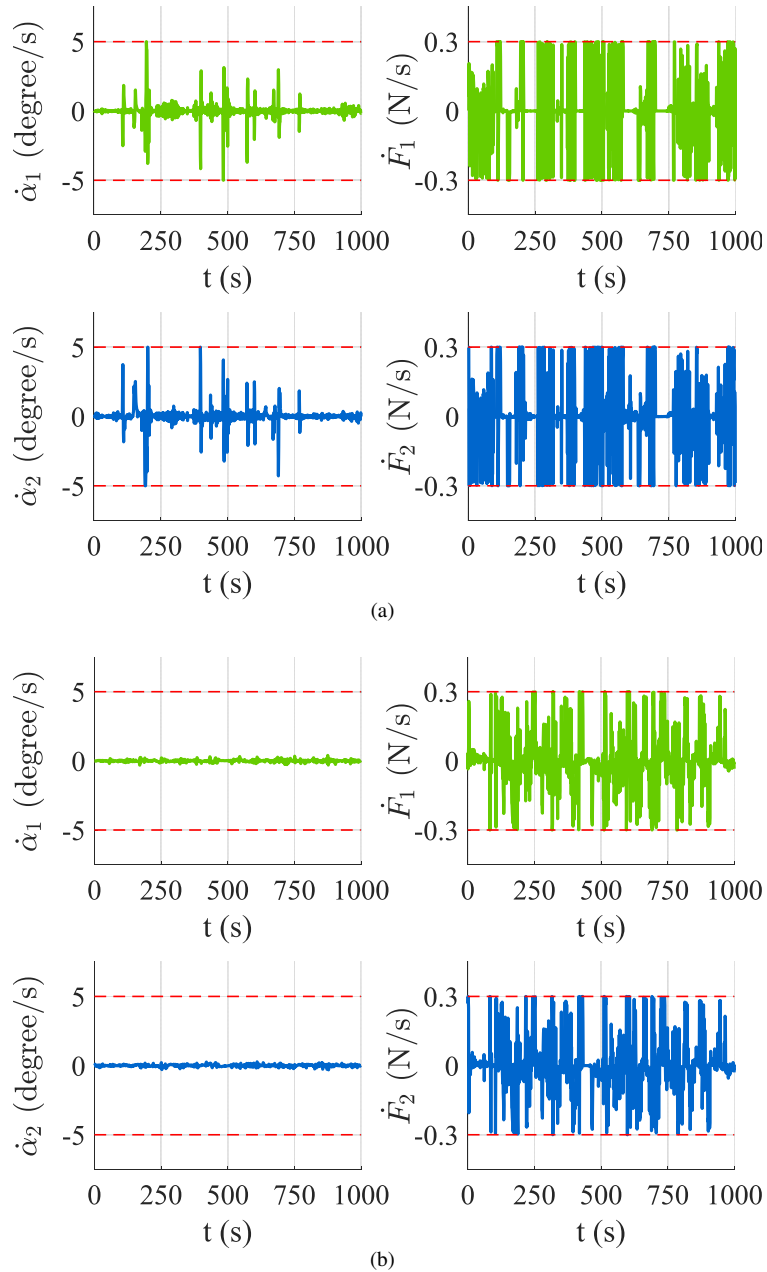
Figure 5.16: Change rate of the towing angles and forces: (a) The distributed control architecture; (b) The centralized control architecture.

surge velocity of the tugs have more frequent changes in the distributed control. The values of the sway (*v*) and yaw (*r*) velocity show large changes during the collision resolution

operations in both control architectures, but the magnitude and frequency of the changes in the distributed control are larger than that of the centralized.

Table 5.5: Avoidance performance of the distributed and centralized control.

Control Architecture	Normalized minimum distance to the obstacles		
	Scenario 1 (Crossing)	Scenario 2 (Crossing & Head-on)	Scenario 3 (Head-on)
Distributed	$D_{S1} = 2.45$	$D_{S2} = 2.65$	$D_{S3} = 1.43$
	$D_{11} = 4.31$	$D_{12} = 3.97$	$D_{13} = 1.70$
	$D_{21} = 1.53$	$D_{22} = 2.41$	$D_{23} = 1.73$
Centralized	$D_{ob_1 S} = 2.79$	$D_{ob_2 S} = 2.20$	$D_{ob_3 S} = 1.59$
	$D_{ob_1 1} = 5.25$	$D_{ob_2 1} = 3.08$	$D_{ob_3 1} = 2.12$
	$D_{ob_1 2} = 1.74$	$D_{ob_2 2} = 1.92$	$D_{ob_3 2} = 1.73$

Table 5.6: Control performance of the distributed and centralized control.

Control Architecture	Settling Time	Maximum Towline Elongation Error	
		Towline 1	Towline 2
Distributed	$T = 968$ s	$e_{l_{tow1}} = 5.79\%$	$e_{l_{tow2}} = 6.33\%$
Centralized	$T = 985$ s	$e_{l_{tow1}} = 5.15\%$	$e_{l_{tow2}} = 5.32\%$

The towing angles and forces are shown in Fig 5.15, and their change rate are shown in Fig 5.16. It is observed that the values of all the variables are within the boundary in both architectures, which satisfies the saturation constraints. For the two towing angles, *i)* their magnitude and change rate in distributed control is larger than that in centralized control; *ii)* the values of the forward angle (α_2) is larger than the after angle (α_1). The reason for the first observation is that the motion of tugs is consistent with the ship as much as possible in centralized control making the magnitude and change of the towing angle small. The second observation results from the different functions of the two tugs. The forward tug is to change the ship heading and increase the speed, the after tug is to stabilize the ship and reduce the speed. So the forward towing angle has larger change. For the two towing forces, the duration of maximum value and the frequency of change in distributed control is larger than that in centralized control, because compared to global optimization problem each separated local optimization problem makes each controller focus more on its own control objective, which results in the continuous high value of the control inputs.

The avoidance performance of the two control architectures is quantified and compared in Table 5.5. The normalized minimum distance between the vessels in the towing system and the obstacles using the centralized control method is larger than those using distributed control in scenarios 1 (crossing) and 3 (head-on). While in the more complex scenario 2 (crossing & head-on), the corresponding values using centralized control are smaller than those using distributed control. This indicates that the distributed control is better to deal with complex collision resolution problems.

The control performance is characterized by settling time and maximum towline elon-
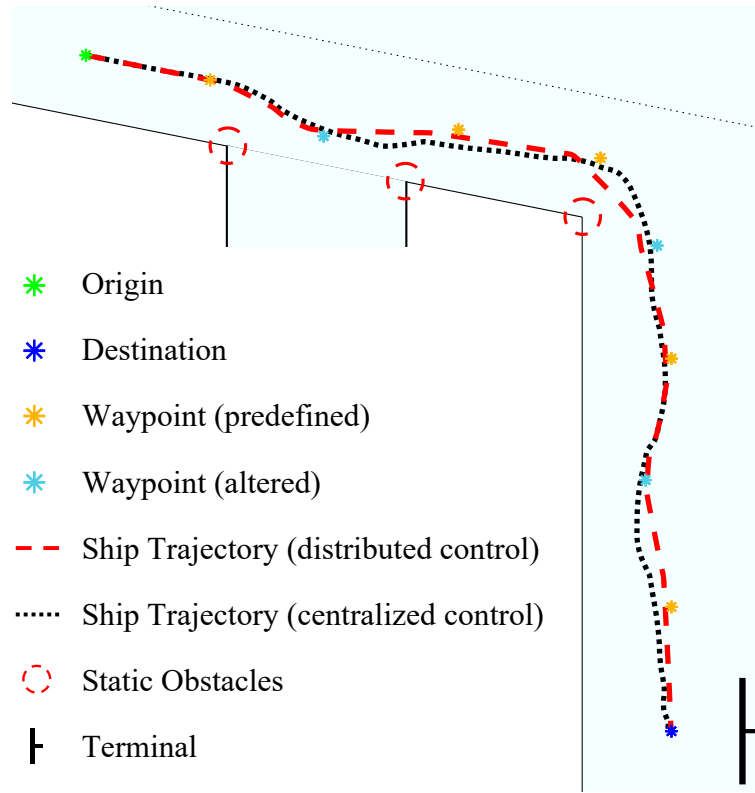
Figure 5.17: Trajectory of the manipulated ship by two control architectures.

gation error. The settling time is defined that the states of the ship satisfy the following conditions:

(i) The distance from the current position to the desired position is less than half length of the ship;

(ii) The difference between the actual and desired heading is less than 3 degrees;

(iii) The surge and sway velocities are less than 0.01 m/s, the yaw velocity is less then 0.01 rad/s.

The towline elongation error is calculated by:

$$e_{l_{\text{tow}i}} = \left| \frac{\max\left\{l_{\text{el}i}(k)\right\} - l_{\text{tow}i}}{l_{\text{tow}i}} \right|,$$

where $l_{\text{el}i}$ is the distance from the towing point of the tug i to the towing point of the ship; $l_{\text{tow}i}$ are the desired elongation of the towline i.

As seen in Table 5.6, the settling time applying the centralized control is a bit larger than the settling time of distributed control, but the maximum towline elongation error by

centralized control is smaller than distributed one. The difference in settling time may come from the different total travelling distance of the manipulated ship: 63.57 m for the centralized, 62.69 m for the distributed. The ship trajectory of the two control architectures are shown in Fig 5.17. It can be seen that the extra travelling parts happen in the avoidance process. Because of the lower tug maneuverability in centralized control, the collision resolution and waypoint returning operations are time-consuming. On the other hand, the better maneuverability of the tugs by distributed control makes the towing angles and forces more frequently changing, resulting in the larger value of the maximum towline elongation error. This indicator revels the smoothness of the towing process, but it can be seen that the difference of this indicator between the two control architectures is not much.

Overall, although there are some detailed differences (the tugs states, towing angles and forces) between the distributed and centralized control, the control objective achievements, the control constraints satisfaction, and the collision resolution and control performance are similar. For the settling time and total travelling distance, the distributed control outperforms. This reveals that in our application, the results of the distributed local optimization problem are quite close to the results of the centralized global optimization problem.

5.5   Conclusions

This chapter addresses the fourth research question **Q4**: In what way can the multi-vessel system avoid collisions with static and dynamic obstacles to improve the safety of towage operations in inland waterways?

A COLREGS compliant ADMM-based MPC approach is proposed to coordinate multiple autonomous vessels, dealing with obstacle avoidance in the towing process in restricted waters. A distributed model predictive control strategy was designed to decouple a large global optimization problem into three sub-optimization problems. The coordination MPC controller uses ship reference determined by the COLREGS compliant waypoint altering system to optimize the towing forces and angles for the ship waypoint following and obstacle avoidance. The tug local MPC controller on the tugboat utilizes the computed towing force and the tug reference calculated by the tug-ship configuration system to optimize the thruster forces and moment for the tug online trajectory tracking and obstacle avoidance. The consensus problem between the ship and tugs is solved by using the ADMM algorithm to find the optimal Lagrange multipliers (dual variables) to achieve the distributed control architecture.

Simulation experiments indicate that the proposed distributed control approach can avoid static and dynamic obstacles in restricted waterways for a physically interconnected multi-vessel system in the towing process, making the collision avoidance COLREGS compliant.

In the next chapter, the towing scenario remains the inland waterways but the control objective grows. To improve the quality of towing process and increase the safety of inland water transportation, the speed of the towing system is taken into account. Thus, how to handle the multiple control objectives will be investigated in Chapter 6.

Chapter 6

Speed Regulation-based Multi-Objective Control for A Ship-Towing System

Chapters 4 and 5 focus on designing a control scheme for a ship-towing system to achieve a specific goal, such as robustness against environmental disturbances and collision avoidance. However, the speed of the towing process was not considered in the control. In fact, speed is important for the towing system because it affects the quality of the towing process such as the smoothness of the trajectory and the efficiency of towing operation. The regulation of speed makes the number of control objectives increase, thus, this chapter addresses the fifth research question (**Q5**): "How to improve the quality of the manipulation process and achieve multiple control objectives as much as possible for a ship-towing system?".

This chapter is organized in five sections. Section 6.1 introduces the background, controlled towing system, and control objectives of the problem. Section 6.2 focuses on designing the multi-objective control scheme to regulate the position, heading, and speed of the manipulated ship and the distance from the towing system to the obstacles. Section 6.3 defines a set of key performance indicators for evaluating to what extent each control objective is achieved. Section 6.4 illustrates the results of simulation experiments to show the performance of the proposed control scheme for achieving the multiple control objectives. Section 6.5 concludes the chapter.

Parts of this chapter have been published in [45][1].

6.1 Problem Statement

6.1.1 Research Background

Maritime transportation applications always involve many control objectives, like waypoint (position) following, heading adjusting, and speed tracking. In some cases, the distance

---

[1]Z. Du, R. R. Negenborn, and V. Reppa. Multi-objective cooperative control for a ship-towing system in congested water traffic environments. Submitted to a journal, 2022.

is also controlled to resolve collisions. Different from the other three objectives which are directly related to specific missions, speed control focuses on improving the motion by smoothing the trajectory. There is limited research working on this control objective, mostly focusing on the single vessel system.

For the speed control of a single vessel system, the main research goal is to regulate the surge speed to a constant value. In [96], scholars propose a backstepping-based adaptive speed controller to maintain a reference speed; in [128], an adaptive and predictive controller is designed to regulate the autonomous vessel's surge speed as a fixed value under the unknown model parameters of surge dynamics. Some research works have investigated both the speed and heading control of the ASV to regulate surge speed and heading angle to make these two state variables reach the corresponding reference values [93, 106, 107, 159].

For the cyber-connected multi-vessel systems, the research goal is usually to coordinate the multiple ASVs for maintaining a specific formation, namely formation control. The control objectives of the ASVs in the formation system are mainly the position and heading. Authors in [29, 147, 175] use the leader-follower strategy to make a swarm of ASVs follow the trajectory of a (virtual) leader vessel. The desired relative position and heading between the leader and followers are the control objectives of each vessel. For the physically-connected multi-vessel system, the control objectives of dealing with the floating object manipulation problem are also focus on position and heading according to the literature review in Section 2.3.

As a typical application of the physically-connected multi-vessel systems, ship-towing transportation is an important but also hazardous and challenging task. In practice, before carrying out the towing operations, speed recommendations (by Shipowner [173] and DNV classification society [65]) are given to deal with emergencies, like bad weather and sudden changes in water depth. From the viewpoint of collision avoidance, all the vessels that take actions of avoidance should comply with the COLREGS. In this regulation, rules 13-17 are usually considered by scholars, but rule 6, which requests a safe speed for every vessel to take proper and effective action for avoiding collisions, is often ignored. Thus, it is necessary to take into consideration the speed control for a ship-towing system.

6.1.2   Towing system and Control Objective

The towing system concerned in this chapter still consists of three vessels: two ASVs are the tugboats located at the fore and aft of the manipulated ship, and the ship is connected with the two tugboats by towing line (as shown in Fig 6.1). Thus, the kinematics and kinetics model of the towing system is the same as in Chapters 4 and 5 and they are not illustrated in detail here.

What should be noticed is that because the model of vessels adopted in this thesis is the vectorial representation, it is easy to see from the mass and damping matrices that the 3 DoF model decomposes the motion of a vessel into forwarding and steering parts. The forwarding part refers to the surge motion, which means the motion along the x-axis in the vessel body-fixed reference frame; the steering part is the combination of the sway and yaw motion, which means the motion along the y-axis and the rotation along the z-axis in the vessel body-fixed reference frame. So the speed regulation (control) in this chapter refers to regulating the magnitude of the surge velocity.

Therefore, the problem in this chapter can be described in Fig 6.2. The two autonomous
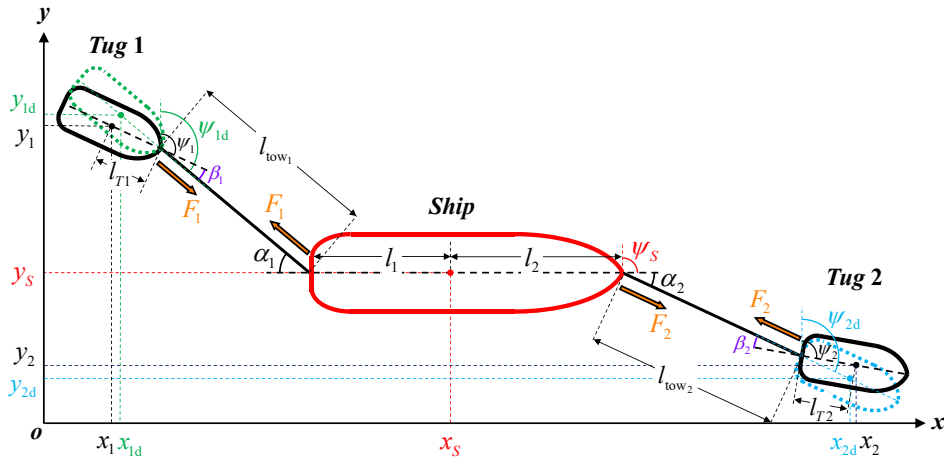
Figure 6.1: Configurations of the ship-towing system.
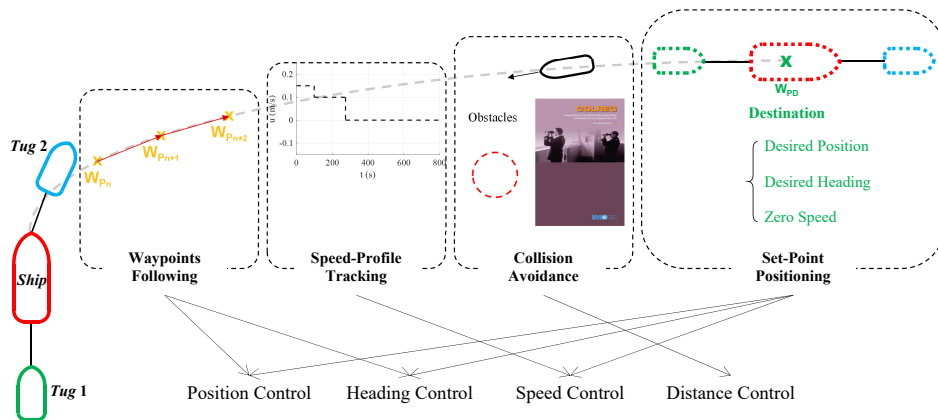
Figure 6.2: Problem statement and control objectives.

tugboats (the green vessel Tug 1 and the blue vessel Tug 2) should manipulate the unpowered ship (the red vessel) to the destination (W_{PD}). In the whole manipulation process, the ship-towing system has to accomplish four tasks: waypoints following, speed-profile tracking, collision avoidance, and set-point positioning. The task of waypoints following requires position and heading control, the speed-profile tracking is speed control, and the collision avoidance can be transformed to distance control. The above three tasks may be performed simultaneously. The task of set-point positioning needs to fix the ship to a desired position and heading with zero speed, so it involves position, heading, and speed control.

6.2   Multi-Objective Control Scheme

The basic idea of the multi-objective cooperative control scheme is to design controllers with different objectives distributed in two control layers.
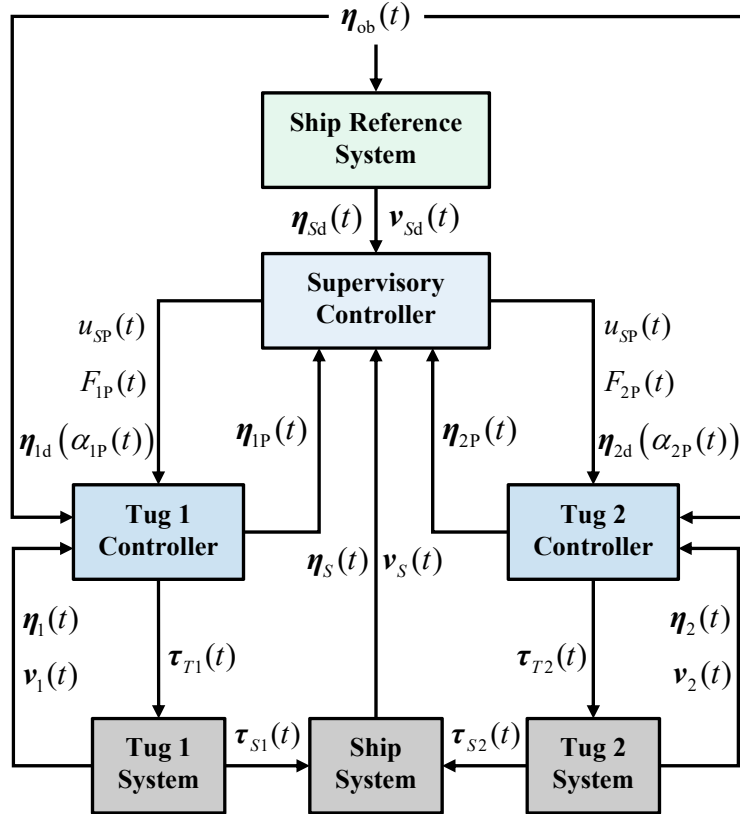
Figure 6.3: System control diagram.

As shown in Fig 6.3, in the higher-layer, according to the desired position, heading $\boldsymbol{\eta}_{Sd}(t)$ and speed $\mathbf{v}_{Sd}(t)$ of the ship output from the ship reference system, the obstacle information $\boldsymbol{\eta}_{ob}(t)$, and the current states of the ship $\boldsymbol{\eta}_S(t)$, $\mathbf{v}_S(t)$, the supervisory controller (located on the ship) carries out the tasks of waypoints following, speed profile tracking, and collision resolution for the transported ship. Meanwhile, it outputs the predicted ship surge speed $u_{SP}(t)$, the predicted towing forces $F_{iP}(t)$, and the desired tug trajectory $\boldsymbol{\eta}_{id}(t)$ (which is a function of the predicted towing angles $\alpha_{iP}(t)$).

The tug controller (located on the tugs) uses this data, the obstacle information, and the current states of tugs $\boldsymbol{\eta}_i(t)$, $\mathbf{v}_i(t)$ to perform the tasks of trajectory and surge speed tracking, and collision resolution. In order to reach a consensus between the lower-layer and higher-layer control, the tug controller first outputs the predicted tug position and heading $\boldsymbol{\eta}_{iP}(t)$ and shares them with the supervisory controller. Then, both higher and lower layer
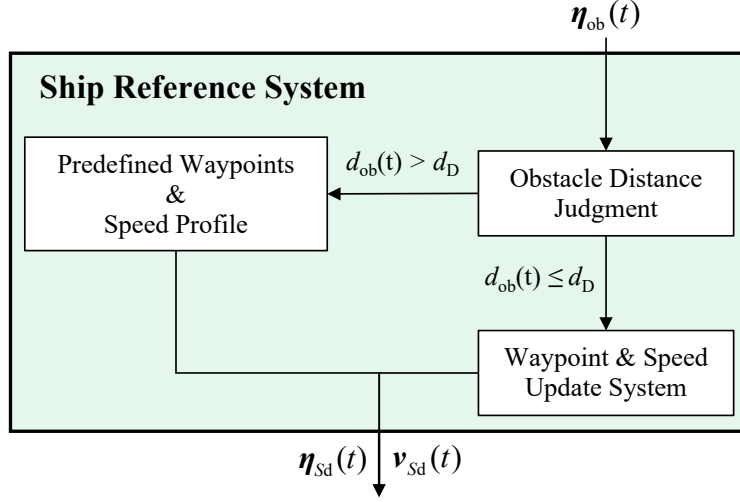
Figure 6.4: Structure of the ship reference system.

controllers update the corresponding data to make the predicted tug position and heading approach to the desired tug trajectory as much as possible ($\boldsymbol{\eta}_{iP}(t) \to \boldsymbol{\eta}_{id}(t)$). When the consensus is achieved, the tug controller outputs the thruster forces and moment $\boldsymbol{\tau}_{Ti}(t)$ to the tug system. Based on the calculated thruster propulsion, the two autonomous tugs cooperatively provide manipulating forces and moment ($\boldsymbol{\tau}_{S1}(t)$, $\boldsymbol{\tau}_{S2}(t)$) to make the ship achieve its multiple objectives.

6.2.1 Ship Reference System

The ship reference system is to provide the reference position, heading, and speed of the manipulated ship. The inside structure is shown in Fig 6.4. It can be seen that the references are determined by comparing between the detection distance d_D and obstacle distance $d_{ob}(t)$, expressed as:

$$\begin{cases} \boldsymbol{\eta}_{Sd}(t) = \boldsymbol{\eta}_p, \ \mathbf{v}_{Sd}(t) = \mathbf{v}_p & \text{if } d_{ob}(t) > d_D \\ \boldsymbol{\eta}_{Sd}(t) = \boldsymbol{\eta}_n, \ \mathbf{v}_{Sd}(t) = \mathbf{v}_n & \text{if } d_{ob}(t) \leq d_D \\ d_{ob}(t) = \min\left\{ d_{Sj}(t), d_{1j}(t), d_{2j}(t) \right\}, \end{cases} \tag{6.1}$$

where $\boldsymbol{\eta}_p$ and $\mathbf{v}_p$ are the predefined position and velocity references of waypoint p; $\boldsymbol{\eta}_n$ and $\mathbf{v}_n$ are the new (updated) position and velocity references; $d_{Sj}(t)$, $d_{1j}(t)$, and $d_{2j}(t)$ are the distances from the obstacle j to the manipulated ship, to the tug 1, and to the tug 2, respectively. Such a definition of the obstacle distance $d_{ob}(t)$ in (6.1) is the reason that the three vessels in the towing system are indivisible systems, the risk from the obstacles should be alert by the closest vessel.

The new reference $\boldsymbol{\eta}_n$ is calculated based on the COLREGS rules 13-17. The rules

explicitly prescribe the single vessel operation of starboard steering for dealing with the potential collisions. While for the multiple vessels in the towing system, the above operations can be equivalently converted to taking advantage of the waypoint clockwise altering to calculate the new position and heading, expressed as:

$$
\boldsymbol{\eta}_{\mathrm{n}} = \begin{bmatrix} x_{\mathrm{n}} \\ y_{\mathrm{n}} \\ \psi_{\mathrm{n}} \end{bmatrix} = \begin{bmatrix} x_{p-1} \\ y_{p-1} \\ \psi_p \end{bmatrix} + r_{wp} \begin{bmatrix} \sin(\theta) \\ \sin(\theta) \\ \theta/r_{wp} \end{bmatrix}
$$
$$
r_{wp} = \left\| \begin{bmatrix} x_{p-1} \\ y_{p-1} \end{bmatrix} - \begin{bmatrix} x_p \\ y_p \end{bmatrix} \right\|_2 ,
\tag{6.2}
$$

where x_{p-1} and y_{p-1} are the coordinates of the last waypoint $p-1$; x_p and y_p are the coordinates of the current waypoint p; r_{wp} is the distance between the above two waypoints; ψ_{Sp} is the current predefined heading along the waterway direction; θ is the altering angle, satisfying $\theta > 0°$ for clockwise rotation.

The new reference $\mathbf{v}_{Sn}$ is updated according to the COLREGS Rule 6. This rule suggests a safe speed for every vessel to make sure it can take proper and effective action to avoid collisions. Although Rule 8 points out that altering only the course may be the most effective action to avoid a close-quarters situation with sufficient sea room, this is in the case of a single vessel. For a physical-connected multi-vessel system, a safe speed can guarantee more response time for such a motion-restricted system taking actions of avoidance. Thus, the updated speed profile is defined as:

$$
\mathbf{v}_{\mathrm{n}} = \begin{bmatrix} u_{\mathrm{n}} \\ v_{\mathrm{n}} \\ r_{\mathrm{n}} \end{bmatrix} = \begin{bmatrix} a_u & & \\ & 1 & \\ & & 1 \end{bmatrix} \begin{bmatrix} u_p \\ v_p \\ r_p \end{bmatrix} ,
\tag{6.3}
$$

where u_p, v_p and r_p are the current surge, sway and yaw speed profiles, respectively; a_u is the speed reduction coefficient and $0 < a_u < 1$. From (6.3), the speed profile update is to slow down the surge speed. The value of a_u is determined by the relative position, course, and velocity between the ship and obstacles, which belongs to the research of the risk assessment and is out of the scope in this thesis.

6.2.2 Supervisory and Tug Controller

The supervisory controller is to make the ship follow waypoints, track speed profile, and resolve collision. Since the MPC strategy is adopted here, the core is the optimizer, solving the following optimization problem:

$$
\min_{\boldsymbol{\tau}_S} \quad \sum_{h=1}^{H_{\mathrm{P}}} J_S(k+h|k),
\tag{6.4}
$$

subject to   *i*) Ship dynamics given by (5.8),

ii) Actuator saturation given by (4.13) − (4.14),

iii) Configuration restriction given by (3.11), (4.4), (4.5),

where H_P is the length of the prediction horizon; k is the current time instant; h is the hth time prediction step; $J_S(k+h|k)$ are the prediction made at k about the cost function of the ship at $k+h$. The performance function J_S is designed as:

$$J_S(k) = e_{\eta_S}^T(k)W_{S1}P_S(k)e_{\eta_S}(k) + e_{v_S}^T(k)W_{S2}e_{v_S}(k) + W_{S3} \sum_{j=1}^{n} \left(d_{Sj}(k) - d_{Sj_d}\right)^{-2}, \quad (6.5)$$

where $e_{\eta_S}(k) \in \mathbb{R}^3$ and $e_{v_S}(k) \in \mathbb{R}^3$ are the position and velocity error of the ship; n is the number of obstacles; d_{Sj_d} is the safe distance between the ship and obstacle j ($d_{Sj_d} < d_D$); W_{S1}, W_{S2} and W_{S3} are the weight coefficients, $W_{S1} = \text{diag}(w_{Sx}\ w_{Sy}\ w_{S\psi})$ and $W_{S2} = \text{diag}(w_{Su}\ w_{Sv}\ w_{Sr})$ are the positive diagonal matrices, W_{S3} is the positive scalar; $P_S(k)$ is the ship weight factor.

The performance function (6.5) contains three parts: the position error is minimized to achieve waypoints following, the velocity error is minimized to track the speed profile, the reciprocal distance error is minimized to keep away from the obstacles. In the process of waypoint following, the value of position error at the beginning is maximum, the controller focuses on approaching the waypoint and increases the ship's speed. As the value of position error reduces, the velocity part is gradually dominant in the performance function, the speed profile tracking then starts to perform. Thus, the ship weight factor $P_S(k)$ is designed to normalize the order of magnitude between the position and velocity errors, and to reduce the sensitivity of the controller to the waypoint distance, expressed as a diagonal matrix:

$$P_S(t) = \begin{bmatrix} 1/\left(d_p(t) + d_{\text{non}}\right) & & \\ & 1/\left(d_p(t) + d_{\text{non}}\right) & \\ & & 1 \end{bmatrix} \quad (6.6)$$

$$d_p(t) = \sqrt{\left(x_S(t) - x_p\right)^2 + \left(y_S(t) - y_p\right)^2},$$

where $d_p(t)$ is the distance from current position of the ship $\left(x_S(t), y_S(t)\right)$ to the current position of the waypoint p (x_p, y_p); d_{non} is a small positive real number, which is to prevent the denominator in (6.6) is zero when the current position of the ship is exactly located on the current waypoint ($d_p(t) = 0$).

The tug controller is to make the tugs track their trajectories, track the predicted ship surge speed, and resolve collisions, and the optimization problem is expressed as:

$$\min_{\tau_{T_i}} \sum_{h=1}^{H_P} J_i(k+h|k), \quad (6.7)$$

subject to i) Dynamics of tug i given by (5.9),

$\quad\quad\quad\quad ii$) Actuator saturation of tug i given by (4.18),

$\quad\quad\quad\quad iii$) Configuration restriction given by (3.11), (4.4), (4.5),

where the performance function J_i is designed as:

$$J_i(k) = e_{\eta_i}^T(k)W_{i1}e_{\eta_i}(k) + e_{v_i}^T(k)W_{i2}e_{v_i}(k) + W_{i3} \sum_{j=1}^{n} \left(d_{ij}(k) - d_{ij_d}\right)^{-2} \quad (6.8)$$

where $\boldsymbol{e}_{\eta_i}(k) \in \mathbb{R}^3$ and $\boldsymbol{e}_{v_i}(k) \in \mathbb{R}^3$ are the position and velocity error of the tug i; d_{*j_d} is the safe distance between the tug i and obstacle j; $\boldsymbol{W}_{i1}$, $\boldsymbol{W}_{i2}$ and W_{i3} are the weight coefficients: $\boldsymbol{W}_{i1} = \mathrm{diag}(w_{ix} \ w_{iy} \ w_{i\psi})$ and $\boldsymbol{W}_{i2} = \mathrm{diag}(w_{iu} \ w_{iv} \ w_{ir})$ are the positive diagonal matrices, W_{i3} is the positive scalar.

The vessel dynamics (the first constraint) and actuator saturation (the second constraint) in (6.4) and (6.7) are the same as in Chapter 5, so they are not illustrated in detail here. The configuration restriction (the third constraint) is to make sure two tugboats successfully track the desired trajectories calculated by the supervisory controller. In other words, this constraint is to reach the consensus between the supervisory controller and two tug controllers to achieve the distributed control architecture. This part is illustrated in the next subsection.

6.2.3 Distributed Control Architecture

The distributed control architecture is achieved by satisfying the configuration restriction of the towing system, namely the first part in (6.8):

$$\boldsymbol{e}_{\eta_i}(k) = \boldsymbol{\eta}_{iP}(k) - \boldsymbol{\eta}_{id}(k), \tag{6.9}$$

where $\boldsymbol{\eta}_{iP}(k) \in \mathbb{R}^3$ and $\boldsymbol{\eta}_{id}(k) \in \mathbb{R}^3$ are the predicted and desired position vector of the tug i. The term $\boldsymbol{\eta}_{iP}(k)$ is calculated by tug dynamics, which is a function of $\boldsymbol{\tau}_{Ti}$ ($\boldsymbol{\eta}_{iP}(k) = g_i(\boldsymbol{\tau}_{Ti}(k))$); $\boldsymbol{\eta}_{id}(k)$ is calculated by the predicted ship position $\boldsymbol{\eta}_{SP}$, which is a function of $\boldsymbol{\tau}_S(k)$ ($\boldsymbol{\eta}_{id}(k) = f_i(\boldsymbol{\tau}_S(k))$).

Then, the performance function J_i in (6.8) is decoupled into two components:

$$\begin{aligned}
J_i(k) &= J_{Ti}(k) + J_{Ci}(k) \\
J_{Ti}(k) &= \boldsymbol{e}_{v_i}^{\mathrm{T}}(k)\boldsymbol{W}_{i2}\boldsymbol{e}_{v_i}(k) + W_{i3} \sum_{j=1}^{n} \left(d_{ij}(k) - d_{i\mathrm{safe}}\right)^{-2} \\
J_{Ci}(k) &= \left(g_i(\boldsymbol{\tau}_{Ti}(k)) - f_i(\boldsymbol{\tau}_S(k))\right)^{\mathrm{T}} \boldsymbol{W}_{i1} \left(g_i(\boldsymbol{\tau}_{Ti}(k)) - f_i(\boldsymbol{\tau}_S(k))\right)
\end{aligned} \tag{6.10}$$

where $J_{Ti}(k)$ is the performance function of the tug i without the system configuration, $J_{Ci}(k)$ is the performance function of the tug i with only the system configuration.

Thus, the augmented Lagrangian form for our problem by using ADMM at time instant k can be formulated as:

$$\begin{aligned}
\boldsymbol{\tau}_{Ti}^s(k) := \operatorname*{arg\,min}_{\boldsymbol{\tau}_{Ti}(k)} \bigg(& J_{Ti}(\boldsymbol{\tau}_{Ti}(k)) + \lambda_i^{s-1}(k)^{\mathrm{T}} \left[g_i(\boldsymbol{\tau}_{Ti}(k)) - f_i(\boldsymbol{\tau}_S^{s-1}(k))\right] \\
& + (\rho/2) \left\| g_i(\boldsymbol{\tau}_{Ti}(k)) - f_i(\boldsymbol{\tau}_S^{s-1}(k)) \right\|_2^2 \bigg),
\end{aligned} \tag{6.11}$$

$$\begin{aligned}
\boldsymbol{\tau}_S^s(k) := \operatorname*{arg\,min}_{\boldsymbol{\tau}_S(k)} \bigg(& J_S(\boldsymbol{\tau}_S(k)) + \sum_{i=1}^{2} \Big(-\lambda_i^{s-1}(k)^{\mathrm{T}} f_i(\boldsymbol{\tau}_S(k)) \\
& + (\rho/2) \left\| g_i(\boldsymbol{\tau}_{Ti}^s(k)) - f_i(\boldsymbol{\tau}_S(k)) \right\|_2^2 \Big) \bigg),
\end{aligned} \tag{6.12}$$

$$\lambda_i^s(k) := \lambda_i^{s-1}(k) + \rho_i\Big(g_i\big(\boldsymbol{\tau}_{Ti}^s(k)\big) - f_i\big(\boldsymbol{\tau}_S^s(k)\big)\Big),\tag{6.13}$$

where $\lambda_i(k)$ is the Lagrange multiplier; ρ is the penalty parameter; s is the iteration with $s \in \{1, 2, \cdots S\}$, S is the maximum iteration; $\cdot^s$ stands for the corresponding variable at the sth iteration.

The termination criterion is defined by the primal ($\boldsymbol{R}_{\text{pri},i}^s$) and dual ($\boldsymbol{R}_{\text{dual},i}^s$) residual, which can be referred to in Chapter 5. Since the optimization problem in (6.11) – (6.13) is complex, to increase the speed of convergence, the penalty parameter ρ_i is designed according to the comparison of the primal and dual residuals:

$$\rho_i^s = \begin{cases} \min\{2\rho_i^{s-1}, \rho_{i\max}\} & \text{if}\left\|R_{\text{pri},i}^s(k)\right\|_2 > 10\left\|R_{\text{dual},i}^s(k)\right\|_2 \\[2ex] \max\{\rho_i^{s-1}/2, \rho_{i\min}\} & \text{if}\left\|R_{\text{pri},i}^s(k)\right\|_2 < 10\left\|R_{\text{dual},i}^s(k)\right\|_2 \\[2ex] \rho_i^{s-1} & \text{otherwise} \end{cases}\tag{6.14}$$

where $\rho_{i\max}$ and $\rho_{i\min}$ are the maximum and minimum values of the penalty parameter.

Therefore, the distributed cooperative control scheme for a ship towing system is summarized in the Algorithm 6.1 chart.

Algorithm 6.1 - Distributed Cooperative Control Scheme

Input: Obstacle position $\boldsymbol{\eta}_{\text{ob}}(t)$;

Ship reference position and velocity $\boldsymbol{\eta}_{Sp}(t)$, $\mathbf{v}_{Sp}(t)$;

Current ship position and velocity $\boldsymbol{\eta}_S(t)$, $\mathbf{v}_S(t)$;

Current tug position and velocity $\boldsymbol{\eta}_i(t)$, $\mathbf{v}_i(t)$.

Step 1: Compute the desired position $\boldsymbol{\eta}_{Sd}(t)$ and velocity $\mathbf{v}_{Sd}(t)$ of the ship for collision free by (6.1) - (6.3).

For $s = 1 : S$

Step 2: Calculate the thruster forces and moment of the tug $\boldsymbol{\tau}_{T_i}^s(k)$ in each tug local controller according to (6.11). Then send the results to the supervisory controller.

Step 3: Calculate the manipulation forces and moment for the ship $\boldsymbol{\tau}_S^s(k)$ in the supervisory controller according to (6.12).

Step 4: Update the Lagrange multiplier $\lambda_i^s(k)$ based on the results from **Step 2** and **Step 3** according to (6.13).

Step 5: check the termination criterion by primal $\boldsymbol{R}_{\text{pri},i}^s(k)$ and dual $\boldsymbol{R}_{\text{dual},i}^s(k)$ residuals: if the termination criterion is not satisfied, then updated the penalty parameter ρ_i^s according to (6.14) and return to **Step 2**; otherwise, jump out of the iteration.

End

Output: Thruster forces and moment of the tug $\boldsymbol{\tau}_{Ti}^s(k)$;

Manipulation forces and moment for the ship $\boldsymbol{\tau}_S^s(k)$.

6.3   Key Performance Indicator

Since there are multiple objectives for the designed controllers, it is necessary to define the following key performance indicators (KPIs) for checking to what extent these goals are achieved.

- Ship Waypoints Following.

  This performance is reflected by the minimum error percentage of distance from the position of the ship to each waypoint p ($p \in \{1, 2, ... N\}$, N is the number of waypoints), expressed as:

  $$e_{Pp} = \frac{\min\left\{\sqrt{(x_S(k) - x_p)^2 + (y_S(k) - y_p)^2}\right\}}{\sqrt{(x_{p-1} - x_p)^2 + (y_{p-1} - y_p)^2}}, \tag{6.15}$$

  where (x_{p-1}, y_{p-1}) is the last waypoint coordinates and (x_0, y_0) stands for the origin coordinates (when $p = 1$). The smaller e_{Pp} indicates better following performance between waypoint $p - 1$ and p.

- Ship Heading Adjusting

  At each waypoint, there is the desired heading to guide the ship sailing along the waterway. When encountering obstacles, the tugboats should manipulate the ship taking avoidance operations for safety while the desired heading becomes unimportant. Thus, different from the first indicator, what we are concerned about is the heading of the ship at the destination, so the KPI is expressed as:

  $$e_\psi = |\psi_S(k_D) - \psi_{Sd_N}|, \tag{6.16}$$

  where ψ_{Sd_N} is the desired ship heading at the destination; k_D is the settling time satisfying:

  $$d_{S_D} < 0.25 L_{oaS}; \quad \psi_S < 1°; \quad u_S < 0.01 \text{ m/s};$$
  $$v_S < 0.01 \text{ m/s}; \quad r_S < 0.001 \text{ rad/s}.$$

  where d_{S_D} is the distance between the ship and the destination; L_{oaS} is the length of the ship.

  The smaller value of the e_ψ shows the better performance of the heading adjusting.

- Ship Speed Profile Tracking

  As the speed profile is time-varying, this KPI is calculated by the root-mean-square error (RMSE), which is expressed as:

  $$e_u = \sqrt{\frac{\sum_{k=1}^{k_D} (u_S(k) - u_{Sd}(k))^2}{k_N}}, \tag{6.17}$$

where the smaller value of the e_u illustrates better performance of speed profile tracking.

- Consensus reaching

  The performance of the consensus reaching can be indicated by the maximum error percentage of the towline elongation. If the elongation keeps its desired value, the consensus between the higher layer and lower layer control is well achieved. According to Chapter 5, the maximum error of the towline is expressed as:

  $$e_{l_{\text{tow}i}} = \left| \frac{\max\left\{l_{\text{el}i}(k)\right\} - l_{\text{tow}i}}{l_{\text{tow}i}} \right|, \tag{6.18}$$

  where $l_{\text{el}i}$ is the distance from the towing point of the tug i to the towing point of the ship. The smaller the $e_{l_{\text{tow}i}}$ is, the better this performance of consensus reaching is.

- Ship and Tugs Collision Resolution

  The performance of the collision resolution is mentioned in Chapter 5, which is reflected by the normalized minimum distance between the three vessels and the obstacles, expressed as:

  $$D_{*j} = \min\ d_{*j}/L_{oa*} \tag{6.19}$$

  where L_{oa*} is the length of the vessel. The larger of D_* shows the better performance.

These KPIs will be used in the next section to see the performance of the proposed control scheme.

6.4 Simulations and Results Discussion

Simulation results are presented in this section to show the performance of the proposed control method applied to small scale vessels. Simulation experiments are carried out using Matlab 2018b. The model of the two tugs are represented by the "*TitoNeri*", while the ship is represented by the "*CyberShip II*". The parameters of the vessel model and the towing system can be found in [41], the parameters of the control system are given in Table 6.1, and the simulation settings are shown in Table 6.2.

To highlight the importance of speed control for the towing process, we compare two scenarios, I and II. In scenario I, no speed profile is provided, the control objectives are the ship waypoint following, the ship heading adjusting and the towing system collision resolution. In scenario II, the proposed cooperative control scheme is used to manipulate the ship.

Fig 6.5 and 6.6 show the towing process of the two scenarios. In general, the trajectories in scenario II are smoother than those in scenario I, especially in the steering process (stage $W_{\text{p1}} \rightarrow W_{\text{p2}}$ and stage $W_{\text{p3}} \rightarrow W_{\text{p4}}$). In the first case of collision avoidance (detailed trajectories are shown in the top box), the static obstacle is successfully bypassed by the towing system in both scenarios. In the second case (detailed trajectories are shown in the bottom box), the towing system takes actions of starboard-side steering to avoid the dynamic obstacle in both scenarios, which complies with COLERGS rules. But we can infer from the

Table 6.1: Parameters of the control system.

Altering angle	$\theta = 10°$
Speed reduction coefficient	$a_u = 2/3$
Prediction horizon	$H_P = 3$
Weight coefficients of J_S	$\boldsymbol{W}_{S1} = diag(1\ \ 1\ \ 1)$ $\boldsymbol{W}_{S2} = diag(200\ \ 20\ \ 20)$ $W_{S3} = 1$
Weight coefficient of J_i	$\boldsymbol{W}_{i1} = diag(1\ \ 1\ \ 1)$ $\boldsymbol{W}_{i2} = diag(2\ \ 2\ \ 2)$ $W_{i3} = 0.1$
Maximum towing angles	$\alpha_{i\max} = 45°$
Maximum towing forces	$F_{i\max} = 3\text{N}$
Maximum change rate of towing angle	$\bar{\alpha}_i = 5°/\text{s}$
Maximum change rate of towing forces	$\bar{F}_1 = 0.3\text{N/s}$
Maximum value of tug thruster forces	$\boldsymbol{\tau}_{i\max} = [5\text{N}\ 5\text{N}\ 2.5\text{Nm}]^{\text{T}}$
Absolute tolerance in ADMM	$\varepsilon^{\text{abs}} = 0.001$
Relative tolerance in ADMM	$\varepsilon^{\text{rel}} = 0.001$
Minimum penalty parameter in ADMM	$\rho_{i\min} = 1$
Maximum penalty parameter in ADMM	$\rho_{i\max} = 100$

Table 6.2: Simulation settings.

Initial states of the ship[1]	W_{pO}: $\boldsymbol{\eta}_{S0} = [-15\ \ -30\ \ 0]^{\text{T}}$ $\boldsymbol{v}_{S0} = [0\ \ 0\ \ 0]^{\text{T}}$
Final States of the ship[1]	W_{pD}: $\boldsymbol{\eta}_{St} = [25\ \ 30\ \ 0]^{\text{T}}$ $\boldsymbol{v}_{St} = [0\ \ 0\ \ 0]^{\text{T}}$
Waypoints[1]	W_{p1}: $\boldsymbol{\eta}_{p1} = [-15\ \ -15\ \ 0]^{\text{T}}$ W_{p2}: $\boldsymbol{\eta}_{p2} = [0\ \ 0\ \ 80]^{\text{T}}$ W_{p3}: $\boldsymbol{\eta}_{p3} = [20\ \ 4\ \ 80]^{\text{T}}$ W_{p4}: $\boldsymbol{\eta}_{p4} = [25\ \ 17\ \ 0]^{\text{T}}$
Speed profile[2]	$W_{pO} \rightarrow W_{p2}$: $\boldsymbol{v}_{d1} = [0.15\ \ 0\ \ 0]^{\text{T}}$ $W_{p2} \rightarrow W_{pD}$: $\boldsymbol{v}_{d2} = [0.09\ \ 0\ \ 0]^{\text{T}}$
Static Obstacle	Shape: Circle; Radius: 1.5m; Position: $(0, -4)$
Dynamic Obstacle	Shape: Ellipse; Semi-major axes: 0.6m; semi-minor axes: 0.15m; Initial position: $(57, 20)$; Course: $260°$; Speed: 0.1m/s

[1] The units of the first two elements are the meter, the unit of the last element is the degree.
[2] The units of the first two elements are the meter per second, the unit of the last element is the degree per second.
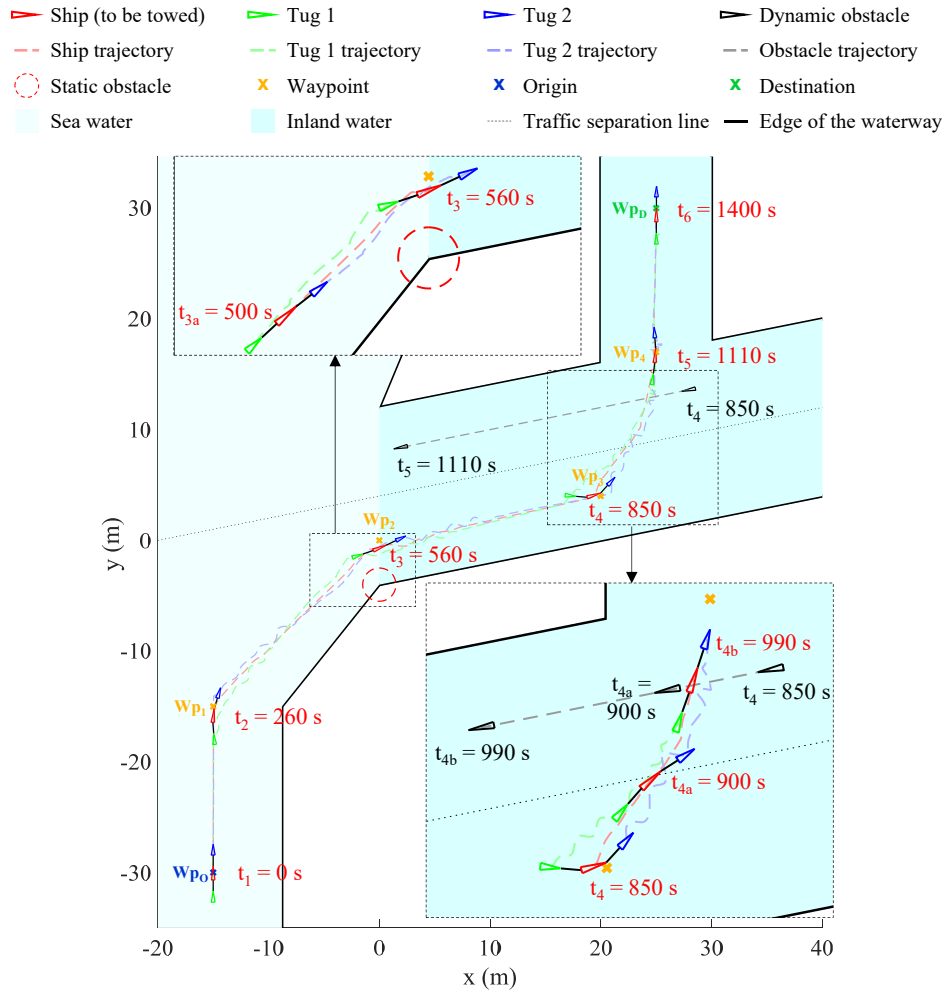
Figure 6.5: Towing process in Scenario I.

trajectories that the towing system in scenario II has fewer fluctuations in the avoidance process. Comparing the time of arriving at each waypoint, scenario II has better efficiency than scenario I. Thus, although the two scenarios succeed to manipulate the ship to the desired states, scenario II (the proposed control scheme) shows better motion quality (smoother trajectories) and time efficiency.

The time-varying error of the ship position and the ship heading are shown in Fig 6.7. In Fig 6.7 (a), there are five curves for each scenario standing for the five times of waypoint following. At the end of each curve, the percentage error closes to zero, especially after the fifth blue dotted curve (the destination-point following task in Scenario II) reaches the red dashed line, its value is stable at zero. Fig 6.7 (b) shows that in both scenarios the ship achieves the desired heading, but the changes in Scenario I have more oscillations than Scenario II.
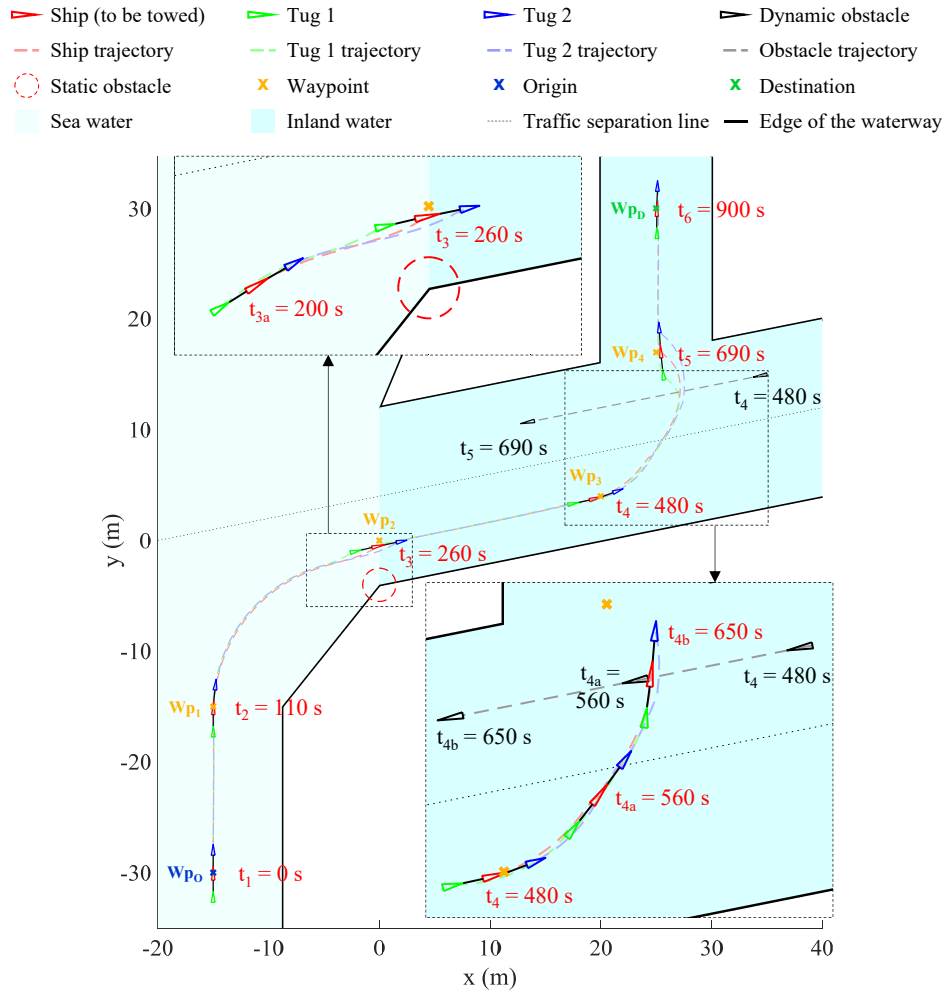
Figure 6.6: Towing process in Scenario II.

The time-varying linear velocities of the ship are shown in Fig 6.8. The ship in Scenario II tracks the predefined surge profile from 0.15 m/s decreasing to 0.09 m/s and finally fixing at 0 m/s (Fig 6.8 (a)). It is noticed that in the second collision avoidance case when the surge speed profile is updated (decreased from 0.09 m/s to 0.06 m/s), the ship still successfully tracks the new desired speed (around 530-620s). However, in Scenario I, the ship surge velocity shows five jagged shape changes. These "jags" come from the decreasing of the position errors in each waypoint following, which motivates the surge speed to vary from the highest to the lowest. When the towing system performs the steering operations, the ship sway velocity adjusts to high values in both scenarios (Fig 6.8 (b)), but the oscillation in Scenario II is much smaller than Scenario I. Thus, there are frequent fluctuations of the trajectories for scenario I in Fig 6.5.

Fig 6.9 shows the time-varying distance from the towing point of the two tugs to the
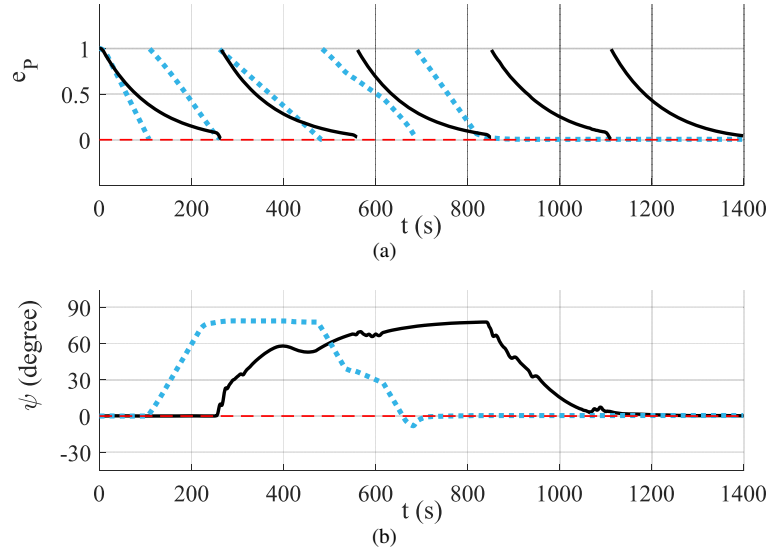
Figure 6.7: Performance of the waypoint following and heading adjusting: (a) Error of the ship position; (b) Temporal evolution of the ship heading. The red dashed line is the desired value, the black solid curve stands for Scenario I, the blue dotted curve stands for Scenario II.
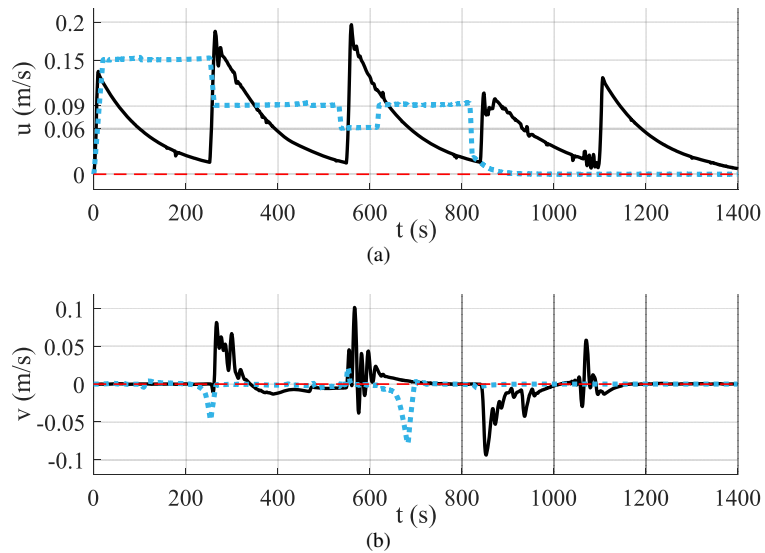
Figure 6.8: Time-varying linear velocities of the ship: (a) Surge velocity; (b) Sway velocity. The red dashed line is the final desired value, the black solid curve stands for Scenario I, the blue dotted curve stands for Scenario II.
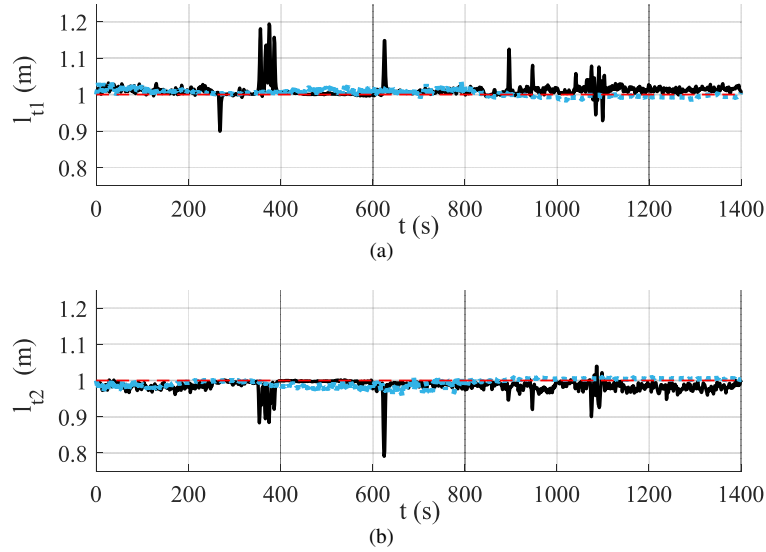
Figure 6.9: *Time-varying distance from the towing point of the tug to the towing point of the ship: (a) Distance from the bow of the tug 1 to the stern of the ship; (b) Distance from the stern of the tug 3 to the bow of the ship. The red dashed line is the desired value, the black solid curve stands for Scenario I, the blue dotted curve stands for Scenario II.*

towing point of the ship. The magnitude of the distance in Scenario I has large fluctuations at each waypoint changing, while in Scenario II, the distance change is always within a small range around the desired towline elongation (1 m).

Table 6.3: *Control performance of the first three KPIs*

Simulation Group	Waypoint Following		Heading Adjusting	Speed Profile Tracking
Scenario I	$e_{P1} = 1.15\%$ $e_{P2} = 3.04\%$ $e_{P3} = 2.69\%$ $e_{P4} = 0.64\%$ $e_{P5} = 0.79\%$		$e_\psi = 0.22°$	—
Scenario II	$e_{P1} = 0.41\%$ $e_{P2} = 2.09\%$ $e_{P3} = 0.31\%$ $e_{P4} = 3.18\%$ $e_{P5} = 0.57\%$		$e_\psi = 0.39°$	$e_u = 0.015$

Fig 6.10 and 6.11 show the normalized distance from the vessels in the towing system to the obstacles. From the static obstacle distance (Fig 6.10), the duration of the close distance between the three vessels and the obstacle in Scenario I is longer; from the dynamic obstacle distance (Fig 6.11), the minimum distance from the ship and tug 1 to the obstacle is larger than Scenario II.

The time varying control inputs of the ship (towing angles and forces) and their change
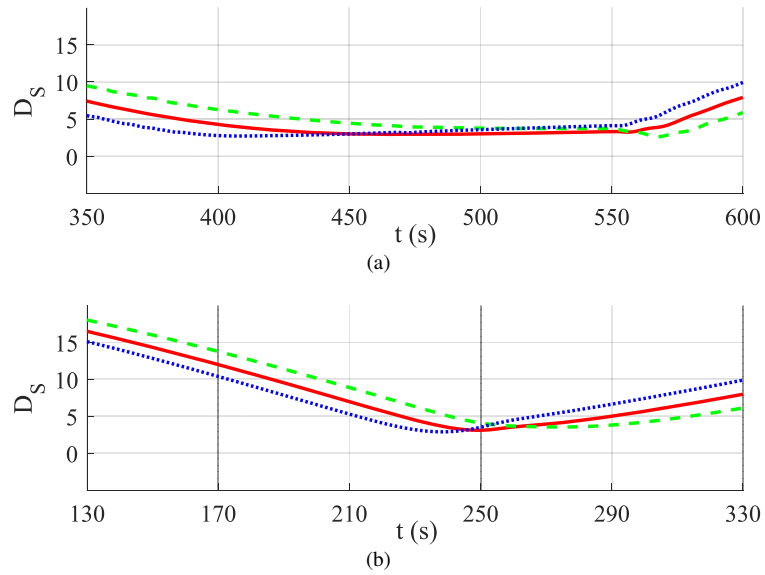
Figure 6.10: Normalized distance from the vessels to the static obstacle: (a) Scenario I; (b) Scenario II. The red solid line is the ship, the green dashed line is the tug 1, the blue dotted line is the tug 2.
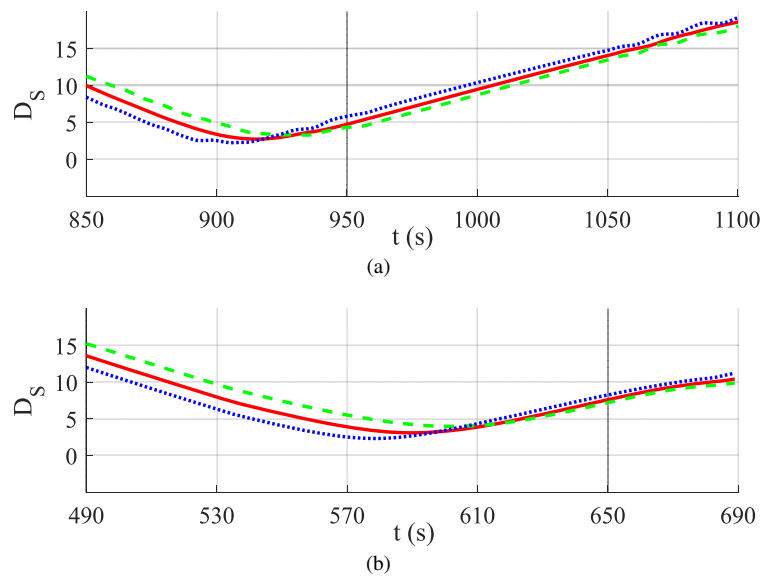
Figure 6.11: Normalized distance from the vessels to the dynamic obstacle: (a) Scenario I; (b) Scenario II. The red solid line is the ship, the green dashed line is the tug 1, the blue dotted line is the tug 2.
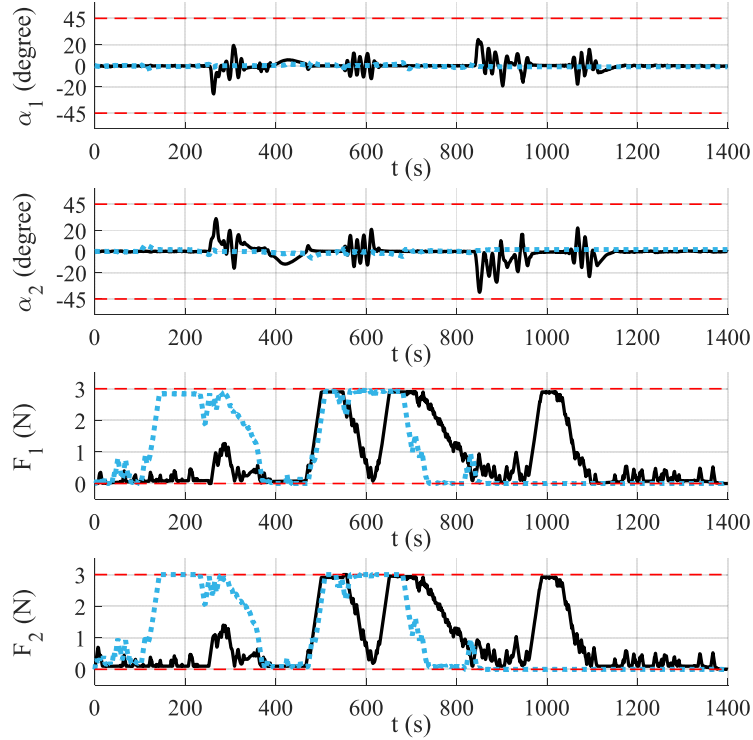
Figure 6.12: Towing angles and forces: the red dashed line is the boundary given in the constraints; the black solid line stands for Scenario I, the blue dotted line stands for Scenario II.

rates are shown in Fig 6.12 and Fig 6.13, respectively. It can be seen that the values of these variables are within the boundary in both scenarios, which satisfies the actuator saturation constraints. For the towing angles, the values of magnitude and the change rates in scenario II are smaller than those in scenario I. For the towing forces, the change rates and the final stage oscillations in scenario II are smaller than those in scenario I.

The control performances quantified judged by the five KPIs defined in subsection 6.3 are shown in Table 6.3 and 6.4, we can infer that:

1. Each distance error in Scenario II is smaller than I, except the e_{P4}. The reason may come from the larger steering areas of avoiding the dynamic obstacle, meaning that the towing system in Scenario II requires more space for navigation safety.

2. The heading error in both scenarios is quite small, so they have good performance in ship heading adjusting.

3. The RMSE of the surge speed in Scenario II is small, indicating the objective of the ship speed profile tracking is well achieved.
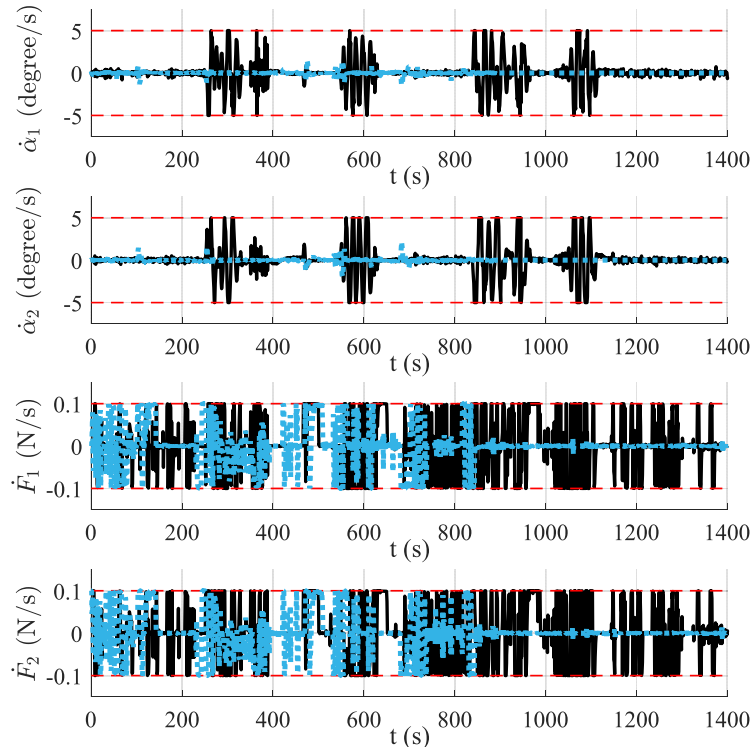
Figure 6.13: Change rate of the towing angles and forces: the red dashed line is the bound-ary given in the constraints; the black solid line stands for Scenario I, the blue dotted line stands for Scenario II.

4. The error of the towline elongation in Scenario II is one-fifth of that in Scenario I, so the performance of consensus reaching in Scenario II is much better.

5. The minimum normalized distances from the three vessels to the obstacles in Scenario II are larger than Scenario I, indicating that the towing process in Scenario II is safer.

Therefore, from the above results, the proposed control scheme succeeds multiple control objectives and shows better motion quality and time efficiency.

6.5 Conclusions

This chapter focuses on the speed regulation-based multi-objective control for a ship towing system. It addresses the fifth research question **Q5**: How to improve the quality of the manipulation process and achieve multiple control objectives as much as possible for a ship-towing system?

An ADMM-based multi-layer MPC approach with speed regulation is proposed to coordinate autonomous tugboats for manipulating a large ship to follow the waypoints, adjust the

Table 6.4: Control performance of the last two KPIs

Simulation Group	Consensus Reaching	Collision Resolution	
		Static Obstacle	Dynamic Obstacle
Scenario I	$e_{l_{\text{tow1}}} = 19.35\%$ $e_{l_{\text{tow2}}} = 20.93\%$	$D_S = 2.36$ $D_1 = 2.64$ $D_2 = 2.72$	$D_S = 2.73$ $D_1 = 4.11$ $D_2 = 2.82$
Scenario II	$e_{l_{\text{tow1}}} = 3.55\%$ $e_{l_{\text{tow2}}} = 4.19\%$	$D_S = 2.48$ $D_1 = 3.55$ $D_2 = 2.90$	$D_S = 3.10$ $D_1 = 4.97$ $D_2 = 2.89$

heading, track the speed profile, and resolve collisions in congested water traffic environments. Such a complex multi-objective control problem is solved by the design of different controllers distributed in two layers. In the higher layer, the supervisory controller calculates the predicted towing forces and angles for the ship objectives of waypoint following, speed profile tracking, and collision resolution. The tug controller in the lower layer computes the thruster forces and moment for the tug system for the tug objectives of trajectory, surge speed tracking and collision resolution. The consensus between the lower-level and higher-level control is achieved by using the ADMM method through the iterations to make the predicted tug position and heading output by the tug controller approach to the desired tug trajectory output by the supervisory controller as much as possible.

To check to what extent these multiple objectives are achieved, we define several KPIs for the tasks of ship waypoint following, ship heading adjusting, ship speed profile tracking, consensus reaching, and ship & tugboats collision avoidance. Simulation experiments indicate that the proposed control scheme coordinates multiple autonomous tugboats to transport a floating object smoothly and effectively and succeeds in multiple control objectives, in the meantime, the avoidance operation complies with COLREGS rules.

In the next chapter, the towing scenario changes to open sea, the floating object becomes an offshore platform, and the research focus transfers to the vessel role. Thus, how to coordinate different roles for multiple tugboats to adaptive different waypoint goals will be investigated in Chapter 7.

Chapter 7

Dynamic Coordination of Multiple Vessels for Platform Transportation under Disturbances

Chapters 4 to 6 focus on the different towing applications of manipulating a large ship by two autonomous tugboats. When the number of tugboats is more than two, the towing manipulation system becomes an over-actuated system, so the role of each tugboat can be flexible and the cooperation between tugboats can be more intelligent. This chapter addresses the sixth research question (**Q6**): "In what way can we increase the flexibility and efficiency of the cooperation of multiple vessels for an offshore platform transportation system of the open sea?"

This chapter is organized as follows. Section 7.1 gives the platform manipulation system model and the control objectives of the problem. Section 7.2 describes the design of the dynamic coordination decision mechanism to adaptively adjust the role of each tugboat according to the current waypoint. Section 7.3 proposes a distributed coordination control scheme based on Section 7.2 for four autonomous tugboats to transport an offshore platform under ocean disturbances. Section 7.4 presents the results of simulation experiments to compare the performance of the proposed control scheme to that of the fixed role control scheme. Section 7.5 concludes the chapter.

Parts of this chapter have been published in [46][1].

---

1. Reach the desired position of the platform.
2. Don't care about the platform's heading.
3. Follow the steering path.
4. Environmental Disturbances:
   (1) Winds;
   (2) Waves;
   (3) Current.
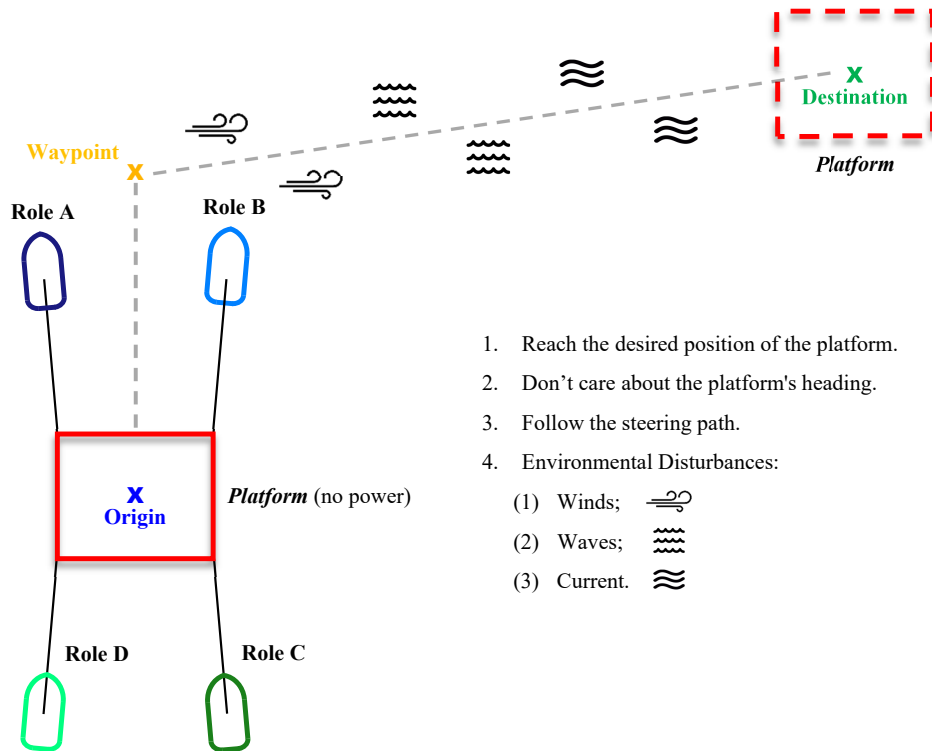
Figure 7.1: *Configurations of the platform-towing system.*

7.1 Problem Statement

7.1.1 Towing System and Control Objective

The towing system in this chapter consists of one unpowered offshore platform and four tugboats as shown in Fig 7.1. In the process of platform transportation, the four tugboats are divided into two identities: role A and B are leading tugboats, whose role is to accelerate the speed and adjust the heading of the platform; role C and D are following tugboats, whose role is to slow down the speed and stabilize the heading of the platform. For convenient switching roles, the towing point on the tugboat is located at the center of gravity.

The control objective is to move the platform from the origin to the destination. Because the cross-section of the maritime platform is usually a rectangle or a circle, its heading is not necessary to care about. In the manipulation process, the four tugboats have to manipulate the platform following a set of waypoints that compose a steering path, meanwhile, the towing system should be against the influence of ocean disturbances, including winds, waves, and currents.
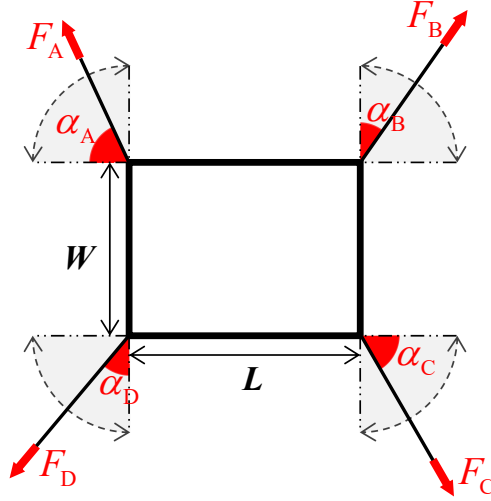
Figure 7.2: Force diagram of the offshore platform.

7.1.2   Dynamics Model of the Platform and Four Tugboats

The motion of the platform and tugboats is formulated by the 3-DoF hydrodynamic model, expressed as

$$
\begin{aligned}
\dot{\boldsymbol{\eta}}_*(t) &= \boldsymbol{R}\big(\psi_*(t)\big)\mathbf{v}_*(t) \\
\boldsymbol{M}_*\dot{\mathbf{v}}_*(t) + \boldsymbol{C}_*\big(\mathbf{v}_*(t)\big)\mathbf{v}_*(t) + \boldsymbol{D}_*\mathbf{v}_*(t) &= \boldsymbol{\tau}_*(t) + \boldsymbol{\tau}_{*\text{wind}}(t) + \boldsymbol{\tau}_{*\text{wave}}(t),
\end{aligned}
\tag{7.1}
$$

where $*$ stands for O (offshore platform) or I (tugboat, $I \in \{\text{A}, \text{B}, \text{C}, \text{D}\}$); $\boldsymbol{\tau}_*(t) \in \mathbb{R}^3$ is the controllable input; $\boldsymbol{\tau}_{*\text{wind}}(t) \in \mathbb{R}^3$ and $\boldsymbol{\tau}_{*\text{wave}}(t) \in \mathbb{R}^3$ are the wind and wave forces.

Fig 7.2 shows the force diagram of the offshore platform. The controllable inputs denoted by $\boldsymbol{\tau}_O(t)$ are the forces from the towing lines applied by four tugs, expressed as:

$$
\begin{aligned}
\boldsymbol{\tau}_O(t) &= \boldsymbol{\tau}_{O_\text{A}}(t) + \boldsymbol{\tau}_{O_\text{B}}(t) + \boldsymbol{\tau}_{O_\text{C}}(t) + \boldsymbol{\tau}_{O_\text{D}}(t) \\
&= \boldsymbol{B}_{O_\text{A}}\big(\alpha_\text{A}(t)\big)F_\text{A}(t) + \boldsymbol{B}_{O_\text{B}}\big(\alpha_\text{B}(t)\big)F_\text{B}(t) + \\
&\quad\ \boldsymbol{B}_{O_\text{C}}\big(\alpha_\text{C}(t)\big)F_\text{C}(t) + \boldsymbol{B}_{O_\text{D}}\big(\alpha_\text{D}(t)\big)F_\text{D}(t),
\end{aligned}
\tag{7.2}
$$

where $F_\text{A}(t), F_\text{B}(t), F_\text{C}(t), F_\text{D}(t)$ are the towing forces; $\alpha_\text{A}(t), \alpha_\text{B}(t), \alpha_\text{C}(t), \alpha_\text{D}(t)$ are the towing angles, whose range is defined clockwise from 0 to 90° (the grey areas in Fig 7.2). This setting restrains the operational range of each tugboat to prevent collisions with each other. The term $\boldsymbol{B}_{O_I} \in \mathbb{R}^3$ is the platform configuration matrix which is a function of $\alpha_I(t)$:

$$
\boldsymbol{B}_{O_\text{A}} = \begin{bmatrix} \sin(\alpha_\text{A}(t)) \\ -\cos(\alpha_\text{A}(t)) \\ 0.5L\sin(\alpha_\text{A}(t)) - 0.5W\cos(\alpha_\text{A}(t)) \end{bmatrix},
\tag{7.3}
$$
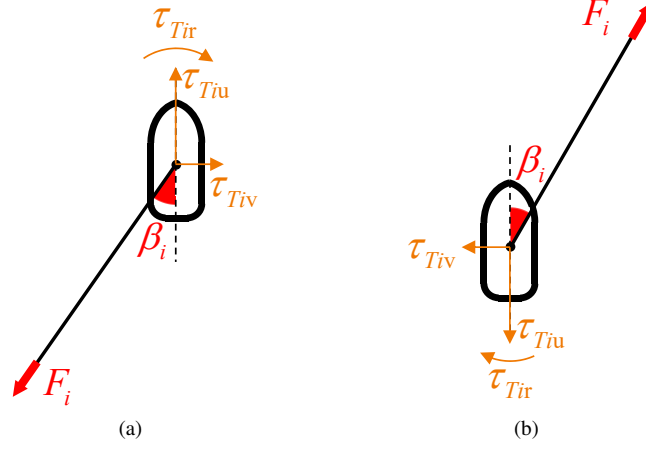
Figure 7.3: Force diagram of the tugs: (a) Type I: Tug A and B; (b) Type II: Tug C and D.

$$\boldsymbol{B}_{O_{\mathrm{B}}} = \begin{bmatrix} \cos(\alpha_{\mathrm{B}}(t)) \\ \sin(\alpha_{\mathrm{B}}(t)) \\ 0.5W\sin(\alpha_{\mathrm{B}}(t)) - 0.5L\cos(\alpha_{\mathrm{B}}(t)) \end{bmatrix}, \tag{7.4}$$

$$\boldsymbol{B}_{O_{\mathrm{C}}} = \begin{bmatrix} -\sin(\alpha_{\mathrm{C}}(t)) \\ \cos(\alpha_{\mathrm{C}}(t)) \\ 0.5L\sin(\alpha_{\mathrm{C}}(t)) - 0.5W\cos(\alpha_{\mathrm{C}}(t)) \end{bmatrix}, \tag{7.5}$$

$$\boldsymbol{B}_{O_{\mathrm{D}}} = \begin{bmatrix} -\cos(\alpha_{\mathrm{D}}(t)) \\ -\sin(\alpha_{\mathrm{D}}(t)) \\ 0.5W\sin(\alpha_{\mathrm{D}}(t)) - 0.5L\cos(\alpha_{\mathrm{D}}(t)) \end{bmatrix}, \tag{7.6}$$

where L and W are the length and width of the platform.

Fig 7.3 shows the force diagram of the tugs. The controllable inputs denoted by $\boldsymbol{\tau}_I(t)$ are the resultant forces by the thruster forces (omnidirectional forces generated by azimuth thrusters) and the towline reaction forces.

For tugboats with role A and B, the effects from the towline are the drag forces (as seen in Fig 7.3 (a)), the controllable inputs are expressed as:

$$\boldsymbol{\tau}_I(t) = \boldsymbol{\tau}_{T_I}(t) - \boldsymbol{B}_T\left(\beta_I(t)\right)F_I(t) \quad (I = \mathrm{A}, \mathrm{B}), \tag{7.7}$$

for tugboats with role C and D, the effects from the towline are the propulsive forces (as seen in Fig 7.3 (b)), the controllable inputs are expressed as:

$$\boldsymbol{\tau}_I(t) = \boldsymbol{\tau}_{T_I}(t) + \boldsymbol{B}_T\left(\beta_I(t)\right)F_I(t) \quad (I = \mathrm{C}, \mathrm{D}), \tag{7.8}$$

where $\boldsymbol{\tau}_{T_I}(t) = [\tau_{T_{I\mathrm{u}}}(t)\ \tau_{T_{I\mathrm{v}}}(t)\ \tau_{T_{I\mathrm{u}}}(t)]^{\mathrm{T}} \in \mathbb{R}^3$ is the thruster forces of the tug I; $\boldsymbol{B}_T \in \mathbb{R}^3$ is

the tug configuration matrix, which is a function of the tug angle $\beta_I(t)$:

$$\boldsymbol{B}_T = \begin{bmatrix} \cos\left(\beta_I(t)\right) \\ \sin\left(\beta_I(t)\right) \\ 0 \end{bmatrix} \quad (I = \mathrm{A,B,C,D}). \tag{7.9}$$

7.1.3 Kinematic Model of the Platform Transportation System

As shown in Fig 7.4, each role corresponds to a specific reference trajectory of the tugboat, which is calculated through the desired kinematics configuration of the towing system.

Figure 7.4: Force diagram of the offshore platform.

For the leading tugs A and B, the key to coupling the motion of the platform and the tugboats are the following angles:

$$\gamma = \arctan\left(\frac{W}{L}\right)$$
$$\delta_A(t) = 90° - \gamma - \psi_O(t) \tag{7.10}$$
$$\delta_B(t) = \gamma - \psi_O(t),$$

where γ is the platform configuration angle; $\delta_A(t)$ and $\delta_B(t)$ are the linking angles of tug A and B; $\psi_O(t)$ is the heading of the platform. The reference position and heading of the tugboats then are expressed as:

$$\psi_{Ad}(t) = \alpha_A(t) + \psi_O(t) - 90°$$
$$x_{Ad}(t) = x_O(t) + L_O \cos\left(\delta_A(t)\right) + L_{tow} \cos\left(\psi_{Ad}(t)\right) \tag{7.11}$$
$$y_{Ad}(t) = y_O(t) - L_O \sin\left(\delta_A(t)\right) + L_{tow} \sin\left(\psi_{Ad}(t)\right),$$

$$\psi_{Bd}(t) = \alpha_B(t) + \psi_O(t)$$
$$x_{Bd}(t) = x_O(t) - L_O \sin\left(\delta_B(t)\right) + L_{tow} \cos\left(\psi_{Bd}(t)\right) \tag{7.12}$$
$$y_{Bd}(t) = y_O(t) + L_O \cos\left(\delta_B(t)\right) + L_{tow} \sin\left(\psi_{Bd}(t)\right),$$

where (x_O, y_O) is the position of the platform; L_{tow} is the desired length of the towline (all the towlines are assumed the same value); L_O is the distance from the centre of gravity of the platform to its towing point, which is calculated by:

$$L_O = \sqrt{(0.5L)^2 + (0.5W)^2}. \tag{7.13}$$

For the following tugs C and D, the key angles are calculated by:

$$\delta_C(t) = 90° - \gamma - \psi_O(t)$$
$$\delta_D(t) = \gamma - \psi_O(t), \tag{7.14}$$

where $\delta_C(t)$ and $\delta_D(t)$ are the linking angles of tug C and D. The reference position and heading of the tugboats then are expressed as:

$$\psi_{Cd}(t) = \alpha_C(t) + \psi_O(t) - 90°$$
$$x_{Cd}(t) = x_O(t) - L_O \cos\left(\delta_C(t)\right) - L_{tow} \cos\left(\psi_{Cd}(t)\right) \tag{7.15}$$
$$y_{Cd}(t) = y_O(t) + L_O \sin\left(\delta_C(t)\right) - L_{tow} \sin\left(\psi_{Cd}(t)\right),$$

$$\psi_{Dd}(t) = \alpha_D(t) + \psi_O(t)$$
$$x_{Dd}(t) = x_O(t) + L_O \sin\left(\delta_D(t)\right) - L_{tow} \cos\left(\psi_{Dd}(t)\right) \tag{7.16}$$
$$y_{Dd}(t) = y_O(t) - L_O \cos\left(\delta_D(t)\right) - L_{tow} \sin\left(\psi_{Dd}(t)\right).$$

Besides, it can be seen in Fig 7.4 that the tug angle $\beta_I(t)$ in (7.9) is solved by the towing

angle, tugboat heading, and platform heading:

$$
\begin{aligned}
\beta_A(t) &= \alpha_A(t) + \psi_O(t) - 90° - \psi_A(t) \\
\beta_B(t) &= \alpha_B(t) + \psi_O(t) - \psi_B(t) \\
\beta_C(t) &= \alpha_C(t) + \psi_O(t) - 90° - \psi_C(t) \\
\beta_D(t) &= \alpha_D(t) + \psi_O(t) - \psi_D(t).
\end{aligned}
\tag{7.17}
$$

7.1.4   Effects of Ocean Disturbances

As mentioned in Chapter 4, the effects of wind are expressed as:

$$
\boldsymbol{\tau}_{*\text{wind}}(t) = \frac{1}{2}\rho_a V_{rw}^2(t)
\begin{bmatrix}
-c_x\cos(\gamma_{\text{rw}}(t))A_{\text{Fw}} \\
c_y\sin(\gamma_{\text{rw}}(t))A_{\text{Lw}} \\
c_n\sin(2\gamma_{\text{rw}}(t))A_{\text{Lw}}L_{oa}
\end{bmatrix},
\tag{7.18}
$$

where ρ_a is the air density; c_x, c_y and c_n are the wind coefficients for horizontal plane motions; A_{Fw} and A_{Lw} are the transverse and lateral projected area of vessel above the water, respectively; L_{oa} is the overall length of vessel; $V_{rw}(t)$ and $\gamma_{rw}(t)$ are the relative wind speed and the wind angle of attack relative to the vessel bow, respectively.

The effects of wave disturbances on a vessel can be modelled by simplifying the wave excitation forces [64, 81, 133]:

$$
\boldsymbol{\tau}_{*\text{wave}}(t) = \sum_{q=1}^{N_w}
\begin{bmatrix}
K_{*qX}(t) & & \\
& K_{*qY}(t) & \\
& & K_{*qN}(t)
\end{bmatrix}
\cdot
\begin{bmatrix}
A_q\cos(\omega_q t + \varepsilon_{qX}) \\
A_q\cos(\omega_q t + \varepsilon_{qY}) \\
A_q\cos(\omega_q t + \varepsilon_{qN})
\end{bmatrix},
\tag{7.19}
$$

where q is the qth wave component; N_w is the total number of harmonic components; A_q is the wave amplitude; ω_q is the wave frequency; ε_{qX}, ε_{qY} and ε_{qN} are the random phase angles; $K_{*qX}(t)$, $K_{*qY}(t)$ and $K_{*qN}(t)$ are the tunable parameters related to the wave encounter angle $\chi_{*q}(t)$ and wave frequency ω_q [92]. To simplify the model, the tunable gains are modelled as follows

$$
\begin{aligned}
K_{*qX}(t) &= k_{*qX}\cdot\cos\left(\chi_{*q}(t)\right) \\
K_{*qY}(t) &= k_{*qY}\cdot\sin\left(\chi_{*q}(t)\right) \\
K_{*qN}(t) &= k_{*qN}\cdot\sin\left(\chi_{*q}(t)\right) \\
\chi_{*q}(t) &= \beta_{qw} - \psi_*(t)
\end{aligned}
\tag{7.20}
$$

where k_{*qX}, k_{*qY} and k_{*qN} are the constant parameters; β_{qw} is the incident wave angle of the qth wave component.

The effects of irrotational current disturbances on a vessel reflect on the vessel kinetics in (7.1) [56]:

$$
\boldsymbol{M}_*\dot{\boldsymbol{v}}_{*r}(t) + \boldsymbol{C}_*\left(\boldsymbol{v}_{*r}(t)\right)\boldsymbol{v}_{*r}(t) + \boldsymbol{D}_*\boldsymbol{v}_{*r}(t) = \boldsymbol{\tau}_*(t) + \boldsymbol{\tau}_{*\text{wind}}(t) + \boldsymbol{\tau}_{*\text{wave}}(t),
\tag{7.21}
$$

where $\mathbf{v}_{*r}(t)$ is the relative velocity, calculated by:

$$\mathbf{v}_{*r}(t) = \mathbf{v}_{*}(t) - \mathbf{v}_c(t), \tag{7.22}$$

where $\mathbf{v}_c(t)$ is the current velocity in the body-fixed frame:

$$\mathbf{v}_c(t) = \begin{bmatrix} u_c(t) \\ v_c(t) \\ 0 \end{bmatrix} = \begin{bmatrix} V_c \cos(\beta_c - \psi_*(t)) \\ V_c \sin(\beta_c - \psi_*(t)) \\ 0 \end{bmatrix}, \tag{7.23}$$

where V_c is the current speed; β_c is the sideslip angle. Thus, the derivative of $\mathbf{v}_{*r}(t)$ in (7.21) is expressed as:

$$\dot{\mathbf{v}}_{*r}(t) = \dot{\mathbf{v}}_{*}(t) - \begin{bmatrix} V_c \sin(\beta_c - \psi(t)) \cdot r(t) \\ -V_c \cos(\beta_c - \psi(t)) \cdot r(t) \\ 0 \end{bmatrix}. \tag{7.24}$$

7.2   Dynamic Coordination Decision Mechanism

The mechanism of the dynamic coordination decision is based on the relative position between the platform and the current waypoint. As shown in Fig 7.5, when the angle θ_O from the heading of the platform to the direction of the current waypoint is within a certain value and the waypoint is at the front of the platform, (Fig 7.5 (a)), the front tugboats ① and ② are assigned as the leading tugs (A and B), the behind tugboats ③ and ④ are assigned as the following tugs (C and D); when the angle θ_O is over the certain value and the waypoint is at the direction of the right side of the platform (Fig 7.5 (b)), the right-side tugboats ② and ③ are appointed as the leader tugs (A and B), the left-side tugboats ④ and ① are appointed as the follower tugs (C and D).

The calculation of the angle from the heading of the platform to the direction of the waypoint is expressed as:

$$\theta_O(t) = \arctan\left(\frac{x_{\text{wp}}(j) - x_O(t)}{y_{\text{wp}}(j) - y_O(t)}\right) - \psi_O(t), \tag{7.25}$$

where $(x_O(t), y_O(t))$ are the coordinates of the platform.

There are four role combinations according to the different relative position angle θ_O, and the range for each combination is $90°$. The different role combinations are shown in Fig 7.6. Therefore, the decision mechanism of the dynamic coordination for four tugboats is provided in Algorithm 7.1.

7.3   Distributed Coordination Control Design

The control diagram is shown in Fig 7.7. Based on dynamic coordination decision mechanism, the waypoint set $\mathcal{W}$, and the current position vector of the platform $\boldsymbol{\eta}_O(t)$, the dynamic coordination & waypoint decision system calculates the desired position of the platform $\boldsymbol{\eta}_{O\text{d}}$ and the role of each tugboat $g(i,t), (i \in \{1,2,3,4\})$. The supervisory controller
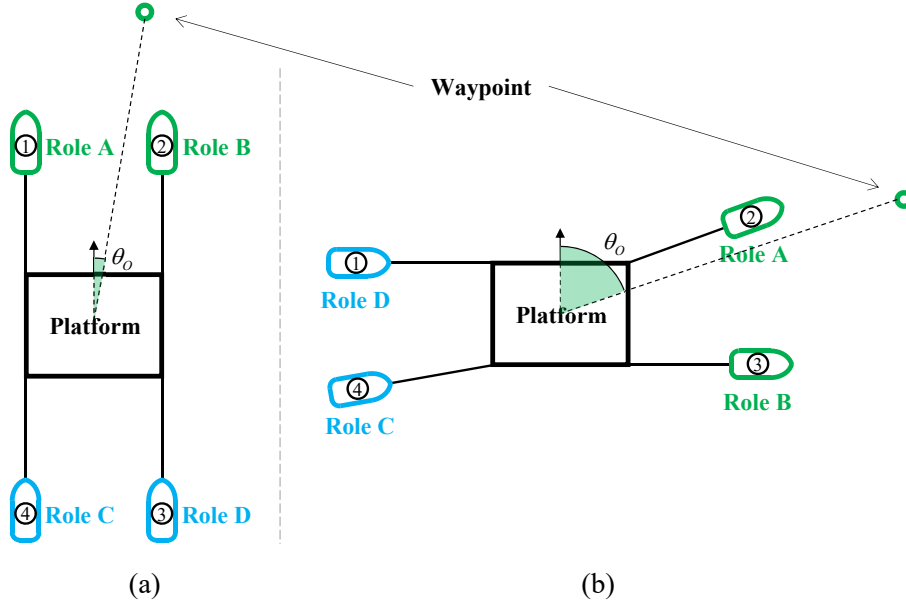
Figure 7.5: Alternating roles between tugboats.

Algorithm 7.1 Dynamic Coordination Decision Mechanism

Acquire coordinates of the current waypoint j $(x_{\mathrm{wp}}(j), y_{\mathrm{wp}}(j))$ and the current position and heading of the platform $x_O(t), y_O(t), \psi_O(t)$;

if $y_{\mathrm{wp}}(j) == y_O(t)$ && $x_{\mathrm{wp}}(j) > x_O(t)$ **then**

    Assign: role B to $g(1,t)$; role C to $g(2,t)$; role D to $g(3,t)$; role A to $g(4,t)$;

else if $y_{\mathrm{wp}}(j) == y_O(t)$ && $x_{\mathrm{wp}}(j) <= x_O(t)$ **then**

    Assign: role D to $g(1,t)$; role A to $g(2,t)$; role B to $g(3,t)$; role C to $g(4,t)$;

else

    Calculate $\theta_O(t)$ according to (7.25)

    if $-45° <= \theta_O(t) < 45°$ **then**

        Assign: role A to $g(1,t)$; role B to $g(2,t)$; role C to $g(3,t)$; role D to $g(4,t)$;

    else if $45° <= \theta_O(t) < 135°$ **then**

        Assign: role B to $g(1,t)$; role C to $g(2,t)$; role D to $g(3,t)$; role A to $g(4,t)$;

    else if $135° <= \theta_O(t) < 180°$ && $-180° <= \theta(t) < -135°$ **then**

        Assign: role C to $g(1,t)$; role D to $g(2,t)$; role A to $g(3,t)$; role B to $g(4,t)$;

    else $-135° <= \theta_O(t) < -45°$

        Assign: role D to $g(1,t)$; role A to $g(2,t)$; role B to $g(3,t)$; role C to $g(4,t)$;

    end if

end if

Send $g(i,t)$ to the Control Allocation System
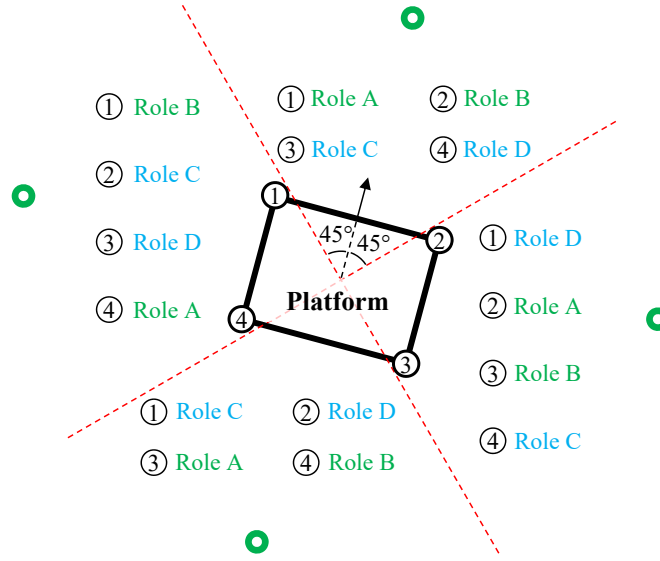
Figure 7.6: Four role combinations of the tugboats. The number within the circle indicates the tugboat with an assigned role (A, B, C or D). The green color indicates the leading tugs and the blue color the following tugs.

uses the calculated $\boldsymbol{\eta}_{Od}$, $g(i,t)$, and the data of the platform $\boldsymbol{\eta}_O(t)$, $\mathbf{v}_O(t)$ to compute the desired position of the tugboats $\boldsymbol{\eta}_{id}(t)$. According to the information of $\boldsymbol{\eta}_{id}(t)$ and the current tug position $\boldsymbol{\eta}_i(t)$ and velocity $\mathbf{v}_i(t)$, the tug controller computes the thruster forces $\boldsymbol{\tau}_{Ti}(t)$ and predicted position $(x_{iP}(t), y_{iP}(t))$ for each tug. The data $(x_{iP}(t), y_{iP}(t))$ is sent back to the supervisory controller to compare with the tug desired position to reach a consensus between the supervisory controller and each tug controller. When the consensus is achieved, the tug controller sends $\boldsymbol{\tau}_{Ti}(t)$ to the tug system under the environmental disturbances $\boldsymbol{\tau}_{i\text{wind}}(t)$, $\boldsymbol{\tau}_{i\text{wave}}(t)$, $\mathbf{v}_{ic}(t)$. Finally, each tugboat outputs the towing forces $\boldsymbol{\tau}_{O_i}(t)$ according to the system configuration to the offshore platform system under the environmental disturbances $\boldsymbol{\tau}_{O\text{wind}}(t)$, $\boldsymbol{\tau}_{O\text{wave}}(t)$, $\mathbf{v}_{Oc}(t)$ for executing transportation missions.

According to the above analysis, there are two types of controllers: the supervisory controller aims to allocate the control inputs of the platform $\boldsymbol{\tau}_O(t)$ to the four tugboats by calculating the corresponding towing angles and forces; the tug controller calculates the thrust forces and moment for the tugboats $\boldsymbol{\tau}_i(t)$ to provide the towing forces and track the tug's reference trajectories. Considering the offshore platform transportation towing system characterized by multiple control inputs, multiple control constraints, and highly heterogeneous, the model predictive control (MPC) method is used to achieve control allocation and trajectory tracking.

For the offshore platform, the MPC-based supervisory controller solves the following optimization problem:

$$\min_{\boldsymbol{\tau}_O} \quad \sum_{h=1}^{H_P} J_O(k+h|k), \tag{7.26}$$
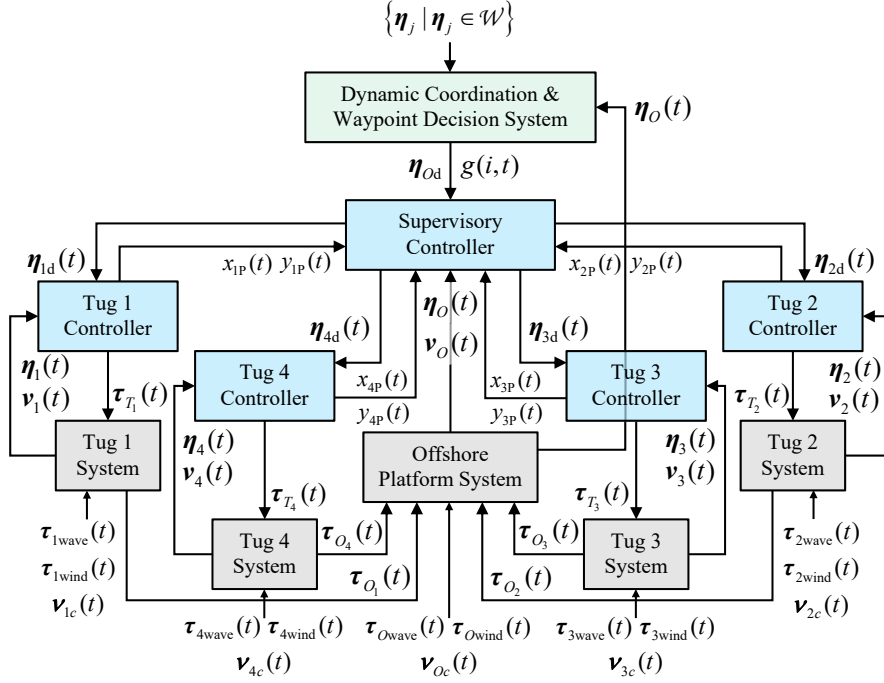
Figure 7.7: Control diagram for the offshore platform towing system.

subject to   *i*) Platform dynamics given by $(7.1) - (7.6)$;

             ii) Actuator saturation given by $(4.13) - (4.14$;

          iii) System configuration restriction given by $(7.10) - (7.16)$;

where H_P is the length of the prediction horizon; k is the current time instant; h is the hth time prediction step; $J_O(k+h|k)$ are the prediction made at k about the cost function of the ship at $k+h$.

The control objectives of the offshore platform are to track the waypoint and steady the heading, so the cost function at time instant k is designed as:

$$J_O(k) = w_P \boldsymbol{e}_P^T(k)\boldsymbol{e}_P(k) + w_H \psi_{Op}^2(k) + w_V \mathbf{v}_{Op}^T(k)\mathbf{v}_{Op}(k), \qquad (7.27)$$

where w_P, w_H and w_V are the weight coefficients of the platform (positive scalar); $\boldsymbol{e}_P(k) \in \mathbb{R}^2$ is the position error expressed as:

$$\boldsymbol{e}_P(k) = [x_{O_P}(k) \ \ y_{O_P}(k)]^T - [x_{wp}(j) \ \ y_{wp}(j)]^T, \qquad (7.28)$$

where $x_{O_P}(k)$, $y_{O_P}(k)$ are the predicted position coordinates; $\psi_{O_P}(k)$ is the predicted heading, which is to prevent the heading of the platform from oscillating frequently during the towing process; $\mathbf{v}_{O_P}(k) \in \mathbb{R}^3$ is the predicted velocity vector.

The predicted states $\mathbf{v}_{Op}(k)$, $x_{Op}(k)$, $y_{Op}(k)$ and $\psi_{Op}(k)$ in (7.27) and (7.28) satisfy the platform dynamics (the first constraint), calculated by the discretization of the equations (7.1) - (7.6). The actuator saturation (the second constraint) stemming from the physical laws and maritime practice [68] are given in (4.13) and (4.14).

For the ith ($i = 1, 2, 3, 4$) tugboat, the MPC-based tug controller is to solve the following optimization problem:

$$\min_{\boldsymbol{\tau}_{T_i}} \quad \sum_{h=1}^{H_P} J_i(k+h|k), \tag{7.29}$$

subject to i) Tugboat dynamics given by (7.1) and (7.7) − (7.9);

ii) Actuator saturation given by (4.18) and (7.32);

iii) System configuration restriction given by (7.10) − (7.16);

where the cost function is designed as:

$$J_i(k) = w_{\mathrm{I}} \boldsymbol{e}_{\eta i}^{\mathrm{T}}(k) \boldsymbol{e}_{\eta i}(k) + w_{\mathrm{II}} \mathbf{v}_{ip}^{\mathrm{T}}(k) \mathbf{v}_{ip}(k), \tag{7.30}$$

where w_{I} and w_{II} are the weight coefficients of the tugboat (positive scalar); $\mathbf{v}_{ip}(k) \in \mathbb{R}^3$ is the predicted velocity vector; $\boldsymbol{e}_{\eta i}(k) \in \mathbb{R}^3$ is the position and heading error of the tugboat i, expressed as:

$$\boldsymbol{e}_{\eta i}(k) = \boldsymbol{\eta}_{ip}(k) - \boldsymbol{\eta}_{id}(k), \tag{7.31}$$

where $\boldsymbol{\eta}_{ip}(k) \in \mathbb{R}^3$ and $\boldsymbol{\eta}_{id}(k) \in \mathbb{R}^3$ are the predicted and desired trajectory of the tugboat i, respectively.

The predicted states $\mathbf{v}_{ip}(k)$, $\boldsymbol{\eta}_{ip}(k)$ in (7.30) and (7.31) satisfy the tugboat dynamics (the first constraint), calculated by the discretization of the equations (7.1) and (7.7) − (7.9). Besides the tug actuator saturation given in (4.18), the change rate of the thruster forces and moment should also be restrained:

$$|\dot{\boldsymbol{\tau}}_{Ti}(k)| \le \bar{\boldsymbol{\tau}}_{Ti}, \tag{7.32}$$

where $\bar{\boldsymbol{\tau}}_{Ti}$ is the maximum change rate of the thruster forces and moment.

The system configuration restriction (the third constraint) in (7.26) and (7.29) are used to reach the consensus between the supervisory controller and the tug controllers for achieving the distributed control architecture by using the Alternating Direction Method of Multipliers (ADMM). For our case, the key is to make the desired tug trajectory ($\boldsymbol{\eta}_{id}(k)$ output by the supervisory controller) and the predicted tug trajectory ($\boldsymbol{\eta}_{ip}(k)$ output by the tug controllers) equal as much as possible.

Because there exists tug angles $\beta_i(t)$, ($i = 1, 2, 3, 4$), the desired tug heading will not be achieved immediately by the tug controller, especially in the process of role changing. Thus, the desired tug position is the key element for reaching a consensus other than the desired tug heading. Based on the above analysis, the tugboat cost function except the position consensus part is revised from (7.30) to:

$$J_{Ti}(k) = w_{\mathrm{IH}} e_{\psi i}^2(k) + w_{\mathrm{II}} \mathbf{v}_{ip}^{\mathrm{T}}(k) \mathbf{v}_{ip}(k), \tag{7.33}$$

where w_{IH} is the weight coefficients for the tugboat heading (positive scalar); $e_{\psi i}(k) = \psi_{ip}(k) - \psi_{id}(k)$ is the heading error of the tugboat i. Then the augmented lagrangian form of the adaptive functional role offshore platform transportation problem at time instant k is formulated as:

$$
\begin{aligned}
L_p\big(\boldsymbol{\tau}_O(k), \boldsymbol{\tau}_{T_i}(k), \lambda_i(k)\big) = J_O\big(\boldsymbol{\tau}_O(k)\big) \; &+ \sum_{i=1}^{4} \Big(J_{Ti}\big(\boldsymbol{\tau}_{T_i}(k)\big) + \\
&\lambda_i^{\mathrm{T}}(k)[\boldsymbol{p}_{ip}(k) - \boldsymbol{p}_{id}(k)] + (\rho_i/2)\big\|\boldsymbol{p}_{ip}(k) - \boldsymbol{p}_{id}(k)\big\|_2^2\Big),
\end{aligned}
\tag{7.34}
$$

where $\lambda_i(k)$ is the Lagrange multiplier or dual variable, and ρ_i is the penalty parameter; $\boldsymbol{p}_{ip}(k) = [x_{ip}(k) \;\; y_{ip}(k)]^{\mathrm{T}}$ and $\boldsymbol{p}_{id}(k) = [x_{id}(k) \;\; y_{id}(k)]^{\mathrm{T}}$ are the predicted and desired tug position. According to (7.11), (7.12), (7.15), (7.16), $\boldsymbol{p}_{id}(k)$ is a function of the towing angle $\alpha_i(k)$ and the predicted platform position vector $\boldsymbol{\eta}_{O_p}(k)$; $\alpha_i(k)$ is a part of the $\boldsymbol{\tau}_O(k)$, $\boldsymbol{\eta}_{O_p}(k)$ can be calculated by $\boldsymbol{\tau}_O(k)$ through the platform dynamics. Thus, $\boldsymbol{p}_{id}(k)$ can be expressed as a function of $\boldsymbol{\tau}_O(k)$: $\boldsymbol{p}_{id}(k) = f_i\big(\boldsymbol{\tau}_O(k)\big)$. Similarly, $\boldsymbol{p}_{ip}(k)$ can be calculated by $\boldsymbol{\tau}_{T_i}(k)$ through the tug dynamics, so $\boldsymbol{p}_{ip}(k) = g_i\big(\boldsymbol{\tau}_{T_i}(k)\big)$.

Therefore, the iteration procedure of the ADMM at time instant k is then formulated as follows:

$$
\begin{aligned}
\boldsymbol{\tau}_{T_i}^s(k) := \operatorname*{arg\,min}_{\boldsymbol{\tau}_{T_i}(k)} \Big(&J_{Ti}\big(\boldsymbol{\tau}_{T_i}(k)\big) + \lambda_i^{s-1}(k)^{\mathrm{T}}\Big[g_i\big(\boldsymbol{\tau}_{T_i}(k)\big) - f_i\big(\boldsymbol{\tau}_O^{s-1}(k)\big)\Big] \\
&+ (\rho_i/2)\Big\|g_i\big(\boldsymbol{\tau}_{T_i}(k)\big) - f_i\big(\boldsymbol{\tau}_O^{s-1}(k)\big)\Big\|_2^2\Big),
\end{aligned}
\tag{7.35}
$$

$$
\begin{aligned}
\boldsymbol{\tau}_O^s(k) := \operatorname*{arg\,min}_{\boldsymbol{\tau}_O(k)} \Big(&J_O\big(\boldsymbol{\tau}_O(k)\big) + \sum_{i=1}^{4}\Big(-\lambda_i^{s-1}(k)^{\mathrm{T}}f_i\big(\boldsymbol{\tau}_O(k)\big) \\
&+ (\rho_i/2)\Big\|g_i\big(\boldsymbol{\tau}_{T_i}^s(k)\big) - f_i\big(\boldsymbol{\tau}_O(k)\big)\Big\|_2^2\Big)\Big),
\end{aligned}
\tag{7.36}
$$

$$
\lambda_i^s(k) := \lambda_i^{s-1}(k) + \rho_i\Big(g_i\big(\boldsymbol{\tau}_{T_i}^s(k)\big) - f_i\big(\boldsymbol{\tau}_O^s(k)\big)\Big),
\tag{7.37}
$$

where s is the iteration, $\cdot^s$ stands for the corresponding variable at the sth iteration.

The termination criterion is provided based on the following residuals:

$$
\begin{aligned}
\Big\|\boldsymbol{R}_{\mathrm{pri},i}^s(k)\Big\|_2 &= \Big\|g_i\big(\boldsymbol{\tau}_{T_i}^s(k)\big) - f_i\big(\boldsymbol{\tau}_O^s(k)\big)\Big\|_2 \le \varepsilon_{\mathrm{pri},i}^s(k), \\
\Big\|\boldsymbol{R}_{\mathrm{dual},i}^s(k)\Big\|_2 &= \Big\|f_i\big(\boldsymbol{\tau}_O^s(k)\big) - f_i\big(\boldsymbol{\tau}_O^{s-1}(k)\big)\Big\|_2 \le \varepsilon_{\mathrm{dual},i}^s(k),
\end{aligned}
\tag{7.38}
$$

where $\boldsymbol{R}_{\mathrm{pri},i}^s$ and $\boldsymbol{R}_{\mathrm{dual},i}^s$ are the primal and dual residual at iteration s; $\varepsilon_{\mathrm{pri},i}^s > 0$ and $\varepsilon_{\mathrm{dual},i}^s > 0$ are the feasibility tolerances, determined by

$$
\begin{aligned}
\varepsilon_{\mathrm{pri},i}^s(k) &= \sqrt{n_s}\varepsilon^{\mathrm{abs}} \; + \\
&\qquad \varepsilon^{\mathrm{rel}}\max\Big\{\big\|g_i\big(\boldsymbol{\tau}_{T_i}^s(k)\big)\big\|_2, \; \big\|f_i\big(\boldsymbol{\tau}_O^s(k)\big)\big\|_2\Big\}, \\
\varepsilon_{\mathrm{dual},i}^s(k) &= \sqrt{n_s}\varepsilon^{\mathrm{abs}} \; + \varepsilon^{\mathrm{rel}}\big\|\lambda_i^s(k)\big\|_2,
\end{aligned}
\tag{7.39}
$$

Algorithm 7.2 - Consensus Iteration for Distributed Control

Input: Current platform position and velocity $\boldsymbol{\eta}_O(k)$, $\mathbf{v}_O(k)$;
Current tug position and velocity $\boldsymbol{\eta}_i(k)$, $\mathbf{v}_i(k)$;
Desired platform position $\boldsymbol{\eta}_{Od}$;
Functional role of the tugs $g(i,t)$.

Step 1: Receive $g(i,t)$ from the Dynamic Coordination Decision System;

for i=1 to 4 **do**

    if $g(i,t)$ is assigned as role A **then**

        $\boldsymbol{p}_{ip}$ and ψ_{id} in (7.34) is calculated using (7.11);

    else if $g(i,t)$ is assigned as role B **then**

        $\boldsymbol{p}_{ip}$ and ψ_{id} in (7.34) is calculated using (7.12);

    else if $g(i,t)$ is assigned as role C **then**

        $\boldsymbol{p}_{ip}$ and ψ_{id} in (7.34) is calculated using (7.15);

    else

        $\boldsymbol{p}_{ip}$ and ψ_{id} in (7.34) is calculated using (7.16);

    end if

end for

for i=1 to S **do**

    Step 2: Calculate the thruster forces and moment of the tug $\boldsymbol{\tau}_{T_i}^s(k)$ in each tug controller according to (7.35), and send the results to the supervisory controller.

    Step 3: Calculate the manipulation forces and moment for the ship $\boldsymbol{\tau}_O^s(k)$ in the supervisory controller according to (7.36).

    Step 4: Update the Lagrange multiplier $\lambda_i^s(k)$ based on the results from **Step 2** and **Step 3** according to (7.37).

    Step 5: Update the primal $\varepsilon_{pri,i}^s(k)$ and dual $\varepsilon_{dual,i}^s(k)$ tolerances according to (7.39), then check the primal $\boldsymbol{R}_{pri,i}^s(k)$ and dual $\boldsymbol{R}_{dual,i}^s(k)$ residuals to see whether they meet the termination criteria according to (7.38);

    Step 6: If (7.38) is not satisfied, then update the penalty parameter ρ_i^s according to (7.40) and return to **Step 2**; otherwise, jump out of the iteration.

    end for

Output: Thruster forces and moment of the tug $\boldsymbol{\tau}_{T_i}^s(k)$;
Manipulation forces and moment for the platform $\boldsymbol{\tau}_O^s(k)$.

where n_s is the size of the variable $\boldsymbol{\tau}_{T_i}$; $\varepsilon^{abs} > 0$ and $\varepsilon^{rel} > 0$ are the absolute and relative tolerance, respectively.

The penalty parameter ρ_i is usually designed to be variable according to the comparison

Table 7.1: Data of the towing system.

Size of the platform	$W = 1.2$ m, $L = 1.6$ m
Size of the tugboat	$w_i = 0.25$ m, $l_i = 0.6$ m
Desired length of the towing line	$L_{\text{tow}i} = 1.5$ m
Maximum towing angle	$\alpha_{i\max} = 90°$
Minimum towing angle	$\alpha_{i\min} = 0°$
Maximum towing force	$F_{i\max} = 0.3$ N
Maximum thruster forces and moment	$\boldsymbol{\tau}_{i\max} = [2\text{N} \ \ 2\text{N} \ \ 1\text{Nm}]^{\text{T}}$
Maximum change rate of the towing angle	$\bar{\alpha}_i = 5°/\text{s}$
Maximum change rate of the towing force	$\bar{F}_i = 0.02$ N/s
Maximum change rate of the thruster forces & moment	$\bar{\boldsymbol{\tau}}_i = [1\text{N/s} \ \ 1\text{N/s} \ \ 0.5\text{Nm/s}]^{\text{T}}$

of the primal and dual residuals to increase the speed of convergence:

$$\rho_i^s = \begin{cases} \min\{2\rho_i^{s-1}, \ \rho_{i\max}\} & \text{if } \left\|R_{\text{pri},i}^s(k)\right\|_2 > 10\left\|R_{\text{dual},i}^s(k)\right\|_2 \\ \max\{\rho_i^{s-1}/2, \ \rho_{i\min}\} & \text{if } \left\|R_{\text{dual},i}^s(k)\right\|_2 > 10\left\|R_{\text{pri},i}^s(k)\right\|_2 \\ \rho_i^{s-1} & \text{otherwise} \end{cases} \tag{7.40}$$

where $\rho_{i\max}$ and $\rho_{i\min}$ are the maximum and minimum values of the penalty parameter.

Therefore, the distributed control scheme is summarized in Algorithm 7.2.

7.4 Simulation Experiments and Results Discussion

Simulation results are presented in this section to show the performance of the proposed dynamic coordination scheme applied to an offshore platform towing system of small-scale lab vessels.

7.4.1 Simulation Setup

The parameters of the towing system in this chapter are set as shown in Table 7.1, where the data of the four tugboats are the same. The dynamic model terms (e.g. hydrodynamic coefficients) of the platform and the tugboats can be found in [67] and [28] respectively. The environmental disturbances are set as shown in Table 7.2, consisting of winds, waves and currents, where the effects of the waves are coupled by two wave components. The

Table 7.2: Data of environmental disturbances.

Wind velocity	$V_w = 0.2$ m/s
Wind direction	$0°$, from the North
Current velocity	$V_c = 0.05$ m/s
Current direction	$180°$, to the South
Number of wave component	$N = 2$
Wave frequency	$\omega_1 = 0.5$ rad/s, $\omega_2 = 0.1$ rad/s
Incident wave angle	$\beta_{1w} = 0°$, $\beta_{2w} = 0°$
Wave amplitude	$A_1 = 0.05$ m, $A_2 = 0.1$ m
Wave phase angle	$\varepsilon_{1X} = \pi/3$, $\varepsilon_{1Y} = \pi/6$, $\varepsilon_{1N} = \pi/9$; $\varepsilon_{2X} = \pi/4$, $\varepsilon_{2Y} = \pi/8$, $\varepsilon_{2N} = \pi/12$
Wave constant gains[1]	$k_{S1X} = 0.1$, $k_{S1Y} = 0.1$, $k_{S1N} = 0$; $k_{T1X} = 0.02$, $k_{T1Y} = 0.02$, $k_{T1N} = 0$; $k_{S2X} = 0.25$, $k_{S2Y} = 0.25$, $k_{S2N} = 0$; $k_{T2X} = 0.05$, $k_{T2Y} = 0.05$, $k_{T2N} = 0$

[1] The values of the wave constant gains are related to the force Response Amplitude Operator (RAO) [56], and different dimensions of the marine craft have different gains. Since the dimension of the platform is much larger than tugboats, the value of the platform gains k_{Sq} is much larger than that of the tugboats k_{Tq} for the qth wave component.

Table 7.3: Parameters of the control system.

Prediction horizon	$H_P = 3$
Weight coefficients of J_O	$w_P = 1$, $w_H = 100$, $w_V = 20$
Weight coefficient of J_{Ti}	$w_{IH} = 0.25$, $w_{II} = 2$
Absolute tolerance	$\varepsilon^{abs} = 0.001$
Relative tolerance	$\varepsilon^{rel} = 0.001$
Minimum penalty parameter	$\rho_{i\min} = 1$
Maximum penalty parameter	$\rho_{i\max} = 100$

information of the control system is shown in Table 7.3, including the parameters of the ADMM strategy.

Two simulation scenarios are defined with the same towing system parameters, environmental disturbances parameters, control system parameters, and control objectives, except for the mechanism of the functional role for tugboats: the tugboats in Scenario I have a fixed functional role control, while in Scenario II the proposed dynamic coordination scheme is applied.

7.4.2 Results and Discussion

Fig 7.8 and Fig 7.9 show the towing process under environmental disturbances, where figures (a) and (b) are the effects of the winds, waves, and currents in two scenarios; figures (c) and (d) are the five time-sampled typical states of the towing system in two scenarios. From $t_1 = 0$ s to $t_2 = 60$ s, the trajectories of the platform and four tugs in two scenarios are the same (straight path), also affected by the same environmental disturbances.

From $t_2 = 60$ s to $t_3 = 120$ s the waypoint changes, the four tugboats keep their previous configurations and slowly move the platform in Scenario I; while in Scenario II, tug 1 changes its role from leading to following, tug 3 changes its role from following to leading, meanwhile the four tugboats dynamically coordinate themselves to move the platform toward to the destination. The process of the functional role changes for the tugs is shown in Fig 7.10.

From $t_3 = 120$ s to $t_4 = 165$ s, the four tugboats in Scenario I still slowly transport the platform with the same configurations, but tug 2 and tug 3 as the tugs of Type I in Scenario II continue adjusting to make an all-out effort toward to the destination. Finally from $t_4 = 165$ s to $t_5 = 400$ s, the platform in Scenario II is successfully transported to the destination, the same mission in Scenario I is not finished yet.

After $t_2 = 60$ s, the effects of environmental disturbances in the two scenarios are also different. For the platform, since its heading has not many changes in Scenario I, the environmental effects mainly work on the x-axis direction in the body-fixed frame; but the platform heading in Scenario II is changed, so there are environmental effects on the y-axis direction. The differences are more explicitly reflected in the four tugs whose environmental influence in Scenario II is much more changed than Scenario I because of the functional role adjustment.

The time-varying position and linear velocity of the platform and four tugs are shown in Fig 7.11. It can be seen that around 200 s, the position of the platform in Scenario II has already achieved the desired value, while the platform in Scenario I has not reached the destination yet even at the 400 s. The value of surge velocity of the platform in both scenarios has a similar varying but as to the tugs, except the phase of the functional role adjustment, the magnitude of the surge velocity changes in Scenario II is smaller than Scenario I. The sway velocities of the platform and tugs are much different in the two scenarios. Due to the functional role adjustment, there are great sway motions for tugs, which makes the sway velocity of the platform have a large increase after $t_2 = 60$ s. This explains the reason for enhanced efficiency of the towing process in Scenario II.

Fig 7.12 shows the time-varying values of the towline elongation. Compared to Scenario I, the changes of the towline elongation in Scenario II are much smaller, reflecting a better consensus achievement between the supervisory and tug controller in Scenario II. The
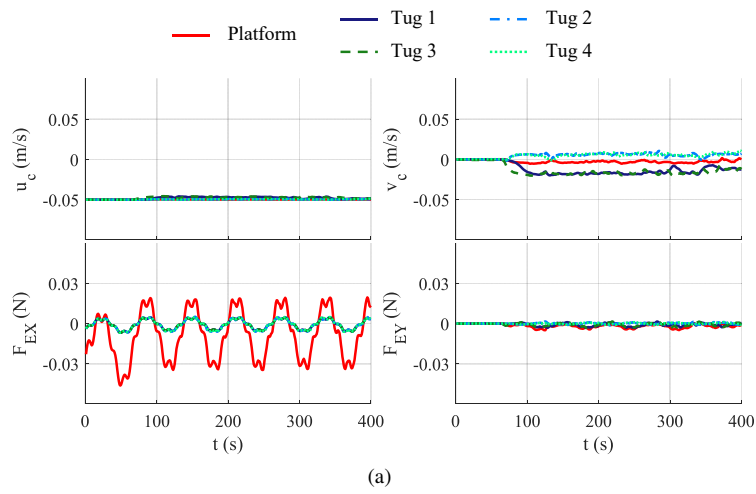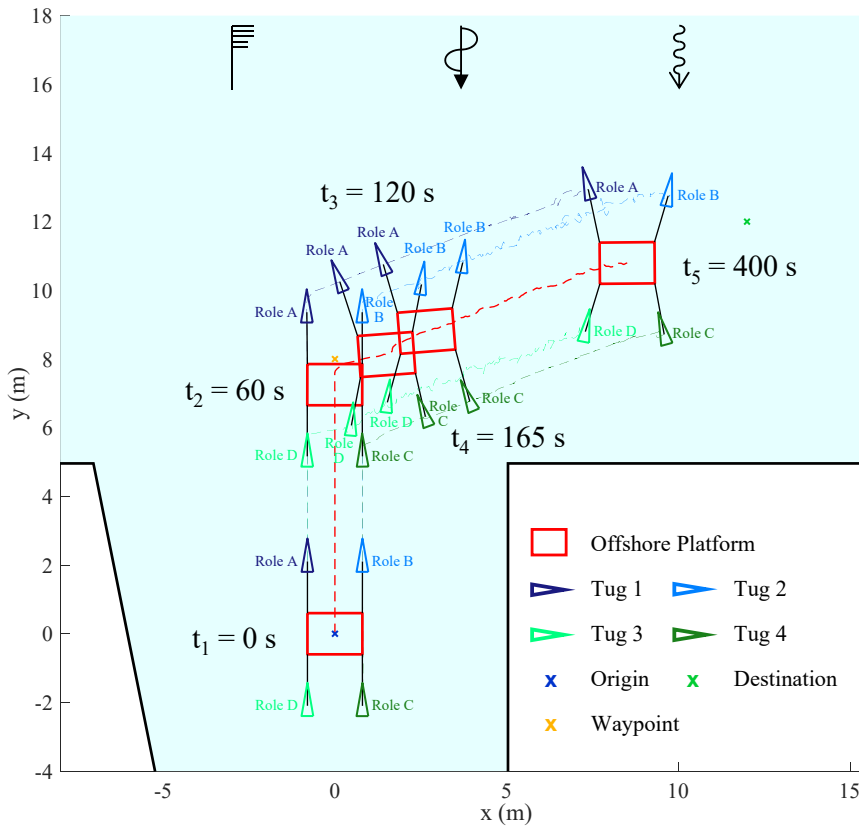
Figure 7.8: Towing processes under environmental disturbances in Scenario I: (a) Current
velocities (u_c, v_c) and wind & wave resultant forces (F_{EX}, F_{EY}) on x and y axis
in the body-fixed frame of Scenario I; (b) Towing process.
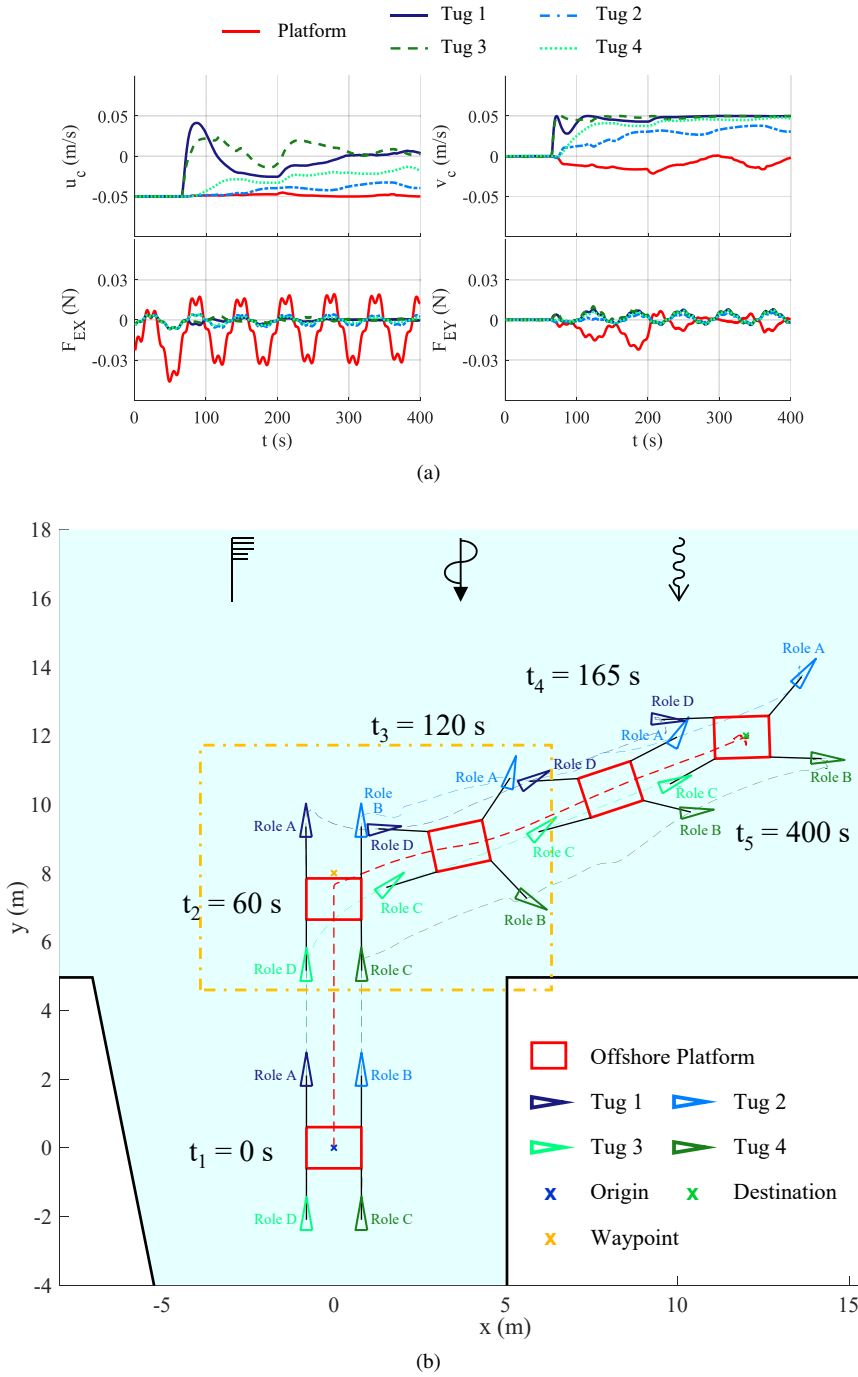
Figure 7.9: Towing processes under environmental disturbances in Scenario II: (a) Current velocities (u_c, v_c) and wind & wave resultant forces (F_{EX}, F_{EY}) on x and y axis in the body-fixed frame of Scenario II; (b) Towing process.
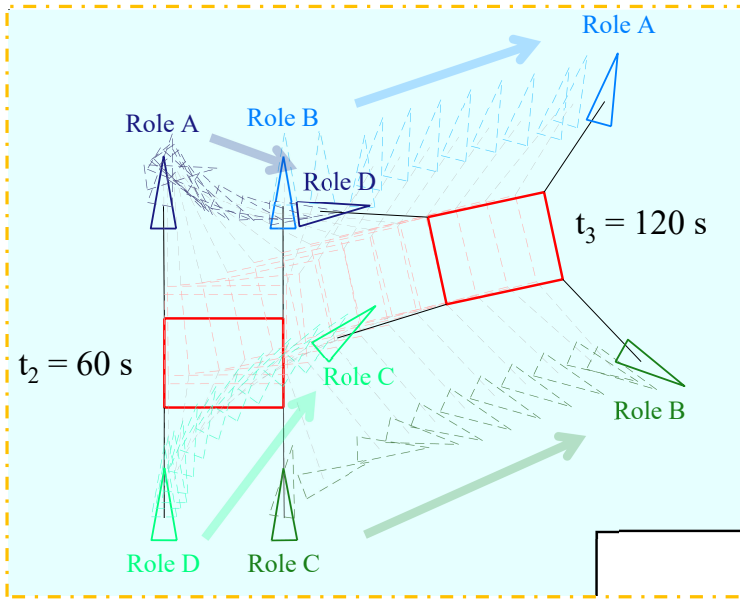
Figure 7.10: Process of the functional role changes for the tugs.

Table 7.4: Control performance of the two scenarios.

Scenario	Settling Time	Towline Elongation Error	
I	> 400 s	$e_{l_{\text{tow1}}} = 11.21\%,$ $e_{l_{\text{tow2}}} = 25.32\%,$	$e_{l_{\text{tow3}}} = 13.94\%,$ $e_{l_{\text{tow4}}} = 16.42\%$
II	212 s	$e_{l_{\text{tow1}}} = 5.99\%,$ $e_{l_{\text{tow2}}} = 5.01\%,$	$e_{l_{\text{tow3}}} = 4.50\%,$ $e_{l_{\text{tow4}}} = 5.83\%$

control performance of the two scenarios, characterized by settling time and maximum tow-line elongation error, is quantified and compared in Table 7.4. The settling time is defined that the states of the ship satisfy the following conditions: *i*) the distance from the current position to the desired position is less than half length of the ship; *ii*) the surge and sway velocities are less than 0.01 m/s. The towline elongation error is calculated by (6.18). From Table 7.4, it is clear that the control performance in Scenario II is better.

The temporal evolution of the towing angles, towing forces, and their change rate in Scenario II are shown in Fig 7.13 and Fig 7.14. In Fig 7.13, the four towing angels and their change rates satisfy the saturation constraints, and because of the tugboat role adjustment, the magnitude of the towing angle change is large. From Fig 7.14, during the time of 0 s to 60 s, since tug 1 & 2 are the leading roles and tug 3 & 4 are the following roles, the values of F_1 and F_2 keep increasing and F_3 and F_4 remain around zero; during the time of 60 s to
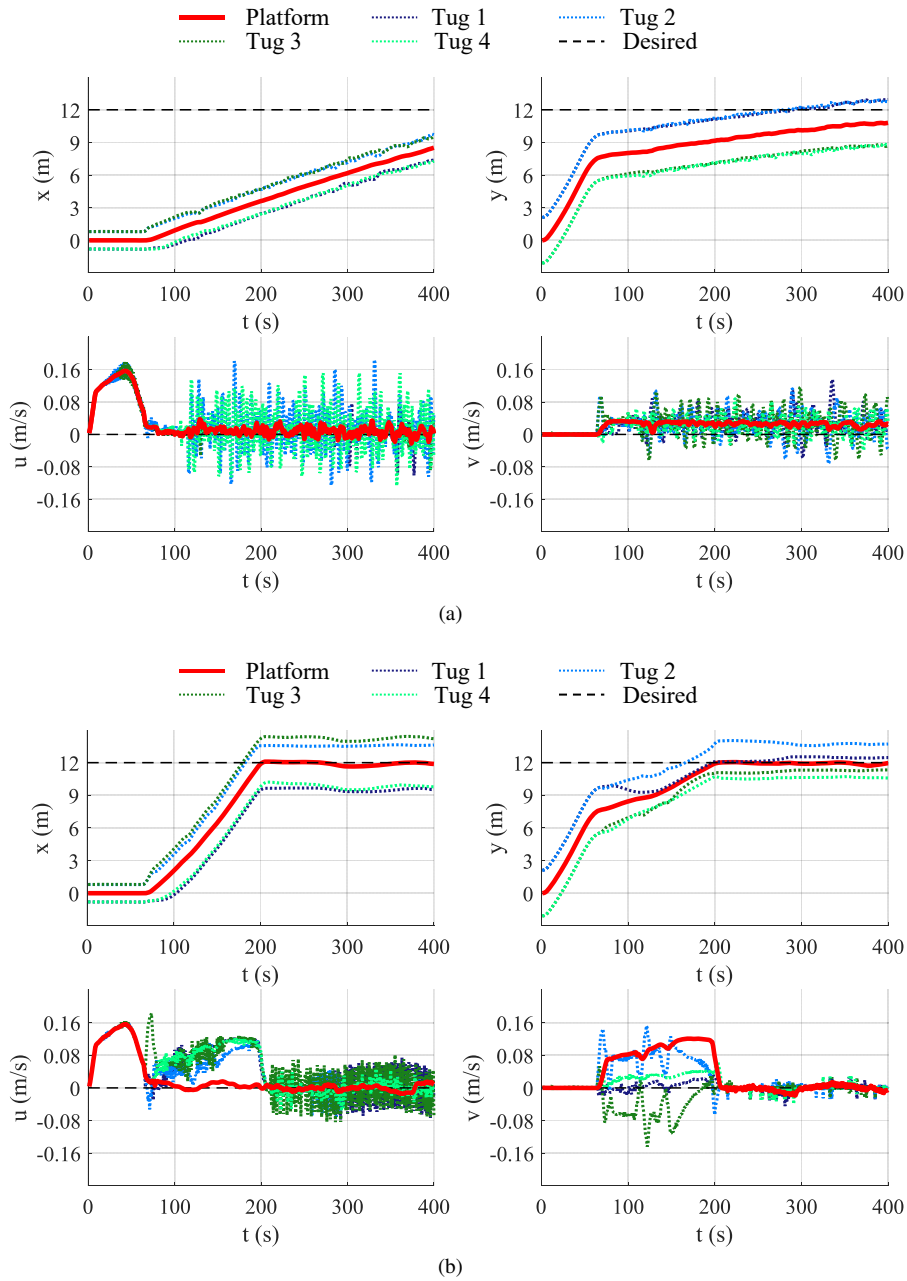
Figure 7.11: Time-varying of the position and linear velocity of the platform and four tugs: (a) Scenario I; (b) Scenario II.
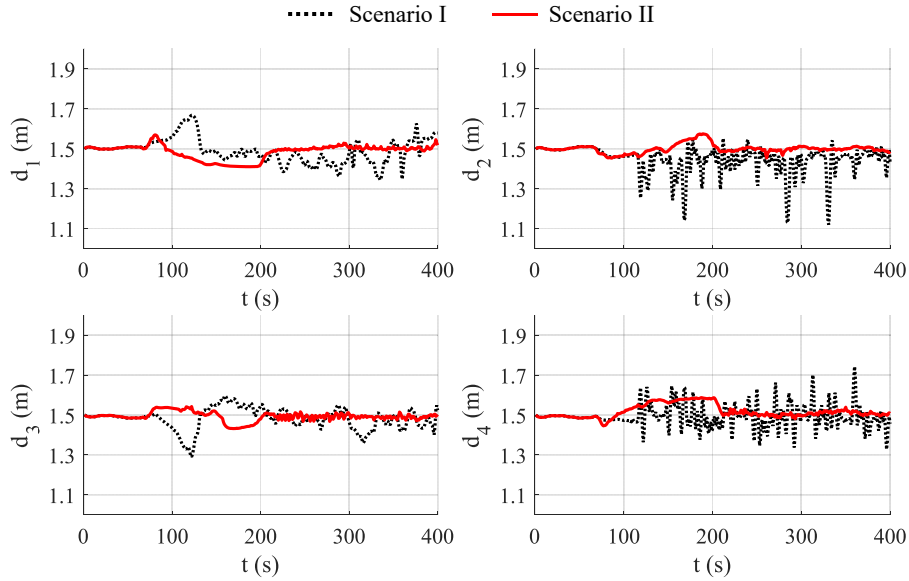
Figure 7.12: Time-varying of the towline elongation.

200 s, the tugboat role adjustment makes tug 2 & 3 be the leading roles and tug 1 & 4 be the following roles, so the values of F_1 and F_4 reduce to zero and F_3 and F_4 increase to their maximum value. After 200 s, since environmental disturbances do not vanish, the towing forces are always existing against environmental forces to reach a dynamic balance for the towing system.

7.5   Conclusions

This chapter focuses on the dynamic coordination control of multiple autonomous tugboats for an offshore platform transportation system. It addresses the sixth research question **Q6**: In what way can we increase the flexibility and efficiency of the cooperation of multiple vessels for an offshore platform transportation system of the open sea?

A distributed coordination control scheme is proposed for a multi-vessel towing system to transport an offshore platform under environmental disturbances. The core of the proposed control scheme includes the dynamic coordination decision mechanism, the controller design, and the distributed control architecture design. The decision mechanism is based on the relative position between the platform and the current waypoint. According to this relative position, there are four sets of role combinations presented to assign the type of each tugboat. The controllers are designed based on the MPC strategy with different cost functions: for the supervisory controller, the cost function consists of the position error, heading, and velocity of the platform; for the tug controller, its cost function components are the heading error and velocity of the tugboats. The distributed control architecture is built based on the ADMM strategy that is to design an augmented Lagrangian function for reach-

Figure 7.13: Temporal evolution of the towing angles and their change rates in Scenario II: (a) Value of the four towing angles; (b) Change rate of the four towing angles.

(a)

(b)
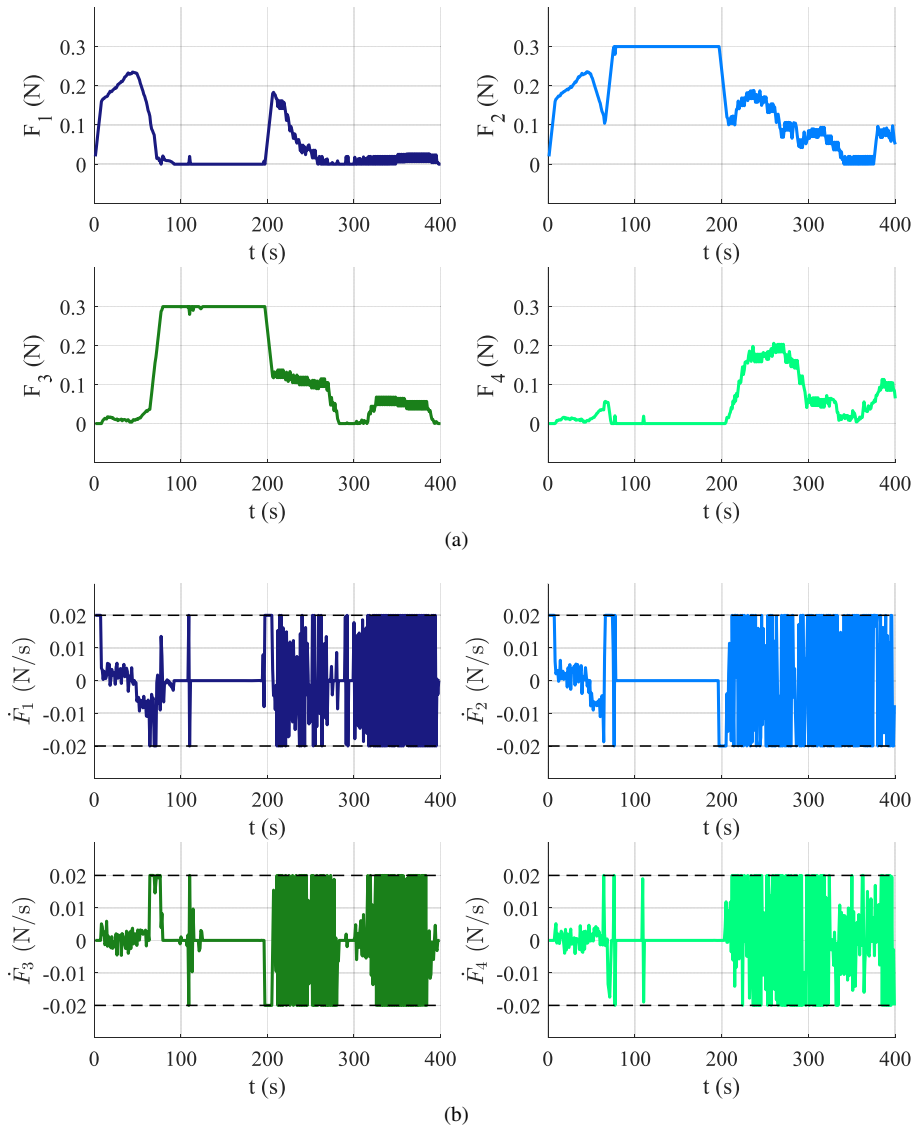
*Figure 7.14: Temporal evolution of the towing forces and their change rates in Scenario II:
(a) Value of the four towing forces; (b) Change rate of the four towing forces.*

ing a consensus between the desired tug position output from the supervisory controller and the predicted tug position output from the tug controller.

Comparison simulation experiments indicate that the proposed control scheme has a better consensus achievement for the distributed control architecture accomplishment and is more efficient for offshore platform transportation under environmental disturbances.

Chapter 8

Conclusions and Future Research

In this thesis, we investigate the cooperative control of an autonomous multi-vessel system for floating object manipulation through physical interconnections. From the summarized four maritime object manipulation ways, towing manipulation is selected as the research foundation to establish the system model and control framework. Various operational application scenarios and control attributes were considered and studied to show the performance of the proposed control scheme.

This last chapter concludes the thesis. Firstly the answers to research questions in Chapter 1 are provided and given in Section 8.1. Subsequently, potential directions for future research are recommended in Section 8.2.

8.1 Conclusions

The six key sub-research questions and the main research question presented in Chapter 1 are answered in this section. These answers conclude the work and contributions of this thesis. Meanwhile, we hope these answers may provide some inspiration for the research community in investigating the floating object manipulation problem by physically connected multi-vessel systems.

8.1.1 Key Sub-Research Questions

1. *What are the characteristics and concrete research gaps of the physically connected multi-vessel system?*

   Chapter 2 reviewed the existing research works on floating object manipulation, whose research object is the physically connected multi-vessel system. Inspired by the three typical manipulations of the object manipulation problem in the field of multi-robot systems, four maritime object manipulation ways are summarized, namely attaching, caging, pushing, and towing. Attaching is a manipulation with tight connections and the capability of fully controlling a floating object, but the design of connection device and planning of the vessel trajectory are the two issues that have to be solved. Caging is a manipulation for coping with the specific problem of oil spill skimming and cleaning. There is no direct contact between the object and vessels, so there is no

147

collision avoidance problem. But the model of the floating boom is required to establish. Pushing is a manipulation that is easy to implement, and gives the object more degrees of freedom. However, the limited maneuverability of the object restrains its application scenarios and increases the manipulation risk under the disturbance environments. Towing is a manipulation for transportation of a large marine structure, such as a container ship or an offshore platform. It requires certain distances between the object and vessels to ensure manipulation safety. The manipulated object has more degrees of freedom than attaching and better maneuverability than caging and pushing. But the model of the towing manipulation system is challenging.

In addition, several important control attributes are analyzed to find the research gaps. Regrading control objectives, the majority of research works emphasize the position and heading control of the floating object, while the control objective of velocity is a lack of concern. With respect to the control architecture, except for the attaching manipulation, more than half of the works in the other three manipulation ways use centralized control. Considering collision avoidance, few papers focus on the avoidance problem of external static and dynamic obstacles. Under disturbances consideration, except for the towing manipulation, the majority of the works in the other three manipulation ways do not address this issue. Taking into account role of each tugboat, the vessels in the manipulation of attaching, caging, and pushing have their specific fixed roles. As to the manipulation of towing, the vessels in the manipulation system have more situations of roles, and the role of the vessel can even be switched.

Overall, towing manipulation has the advantage of better ensuring system safety, floating object maneuverability, and operational scenarios flexibility, which is selected as the preferred manipulation way in this thesis. The research problems in this manipulation are summarized as: (1) rigorous towing system model and design of the distributed control architecture; (2) robustness of the towing manipulation system under environmental disturbances; (3) collision avoidance of the external static and dynamic obstacles; (4) velocity control of the floating object; (5) flexible vessel role strategy of the multi-vessel towing system.

2. *How to establish the dynamics model of the physically connected multi-vessel system, and the control framework?*

Chapter 3 focused on the system modelling and the control framework establishing the foundation of this work. First, the 3 DOF vectorial representation model is used to describe the motion of a vessel, including its kinematics and kinetics. Besides, the physical and hydrodynamic information of three small-scale lab vessels, *CyberShip II*, *TitoNeri*, and *Delfia*, is utilized for simulation experiments of the case study. Then, based on the conclusion of Chapter 2 and several reasonable assumptions related to system modelling, control design, and application scenarios, a generic model of the towing system is built. For the manipulated floating object, the towing angles and forces are the control inputs; for each powerful tugboat, the thruster forces and moment are its control inputs. The interconnections between the floating object and tugboats are the towing angles and forces, where the angles affect the kinematics and the forces affect the kinetics.

Considering that the floating object manipulation system is characterized by multiple

control inputs, multiple control constraints, and limited maneuverability, the model predictive control (MPC) strategy is adopted to achieve the desired objectives. For the control architecture, the advantages of lower computation time, scalable application scenarios, and tolerance to failures motivate the distributed control architecture applied to decouple the large optimization problem. Thus, the distributed MPC is the main approach in this thesis, and it is achieved by using the alternating direction method of multipliers (ADMM) to satisfy the interconnecting constraints between the floating object and each tugboat.

3. *How to increase the robustness of the towing operation to handle the influence of environmental disturbances in port areas?*

   In Chapter 4, a multi-layer multi-agent control scheme is proposed for two autonomous tugboats to manipulate a ship to reach the desired position and heading under environmental disturbances in port areas. The control scheme consists of a supervisory controller in the higher layer and two tug controllers in the lower layer. The supervisory controller computes the desired towing forces and angles by minimizing the cost function of position and heading errors and velocity, where the weight coefficients determine the performance of the control. To guarantee that the towing system functions well under environmental disturbances in port area, an adaptive weight function is designed according to the real-time position error and wind velocity. By applying this weight, the controller shows disturbance robustness, time efficiency, and tracking performance. The calculated towing angles by the supervisory controller are used to compute the online reference trajectories for the autonomous tugs based on the kinematics of the ship towing system. The tug controller, on one hand, provides the towing forces to move the ship; on the other hand, it tracks the reference trajectory to reach the configuration determined by the towing angle.

   Simulation experiments illustrate the outperformance of the proposed control scheme. When there are no disturbances, the proposed method shows much more efficiency with the settling time being reduced by 50%. When the motion of the towing system is affected by environmental disturbances in port, the proposed method shows better robustness especially in guaranteeing the heading of the ship to the desired value. Moreover, in harsh conditions, the proposed method can still manipulate the ship to achieve the control objective.

4. *In what way can the multi-vessel system avoid collisions with static and dynamic obstacles to improve the safety of towage operations in inland waterways?*

   In Chapter 5, a COLREGS compliant (Rules 13-17) ADMM-based MPC approach is proposed to coordinate multiple autonomous tugboats, dealing with obstacle avoidance in the towing process in restricted waters. The main idea of the approach is to design a distributed model predictive control strategy to decouple a large global optimization control problem into three sub-optimization control problems. The coordinator MPC controller uses ship reference determined by the COLREGS-complied (Rules 13-17) waypoint altering system to optimize the towing forces and angles to make the ship follow the waypoints and avoid obstacles, where the cost function consists of position error, heading error, velocity, and distance error to the obstacles. The tug local MPC controller on the tugboat utilizes the computed towing force and the

tug reference calculated by the tug-ship configuration system to optimize the thruster forces and moment for tug online trajectory tracking and obstacle avoidance. The consensus problem between the ship and tugs is solved by using the ADMM algorithm to find the optimal Lagrange multipliers (dual variables) to achieve the distributed control architecture.

Simulation experiments indicate that the proposed distributed control approach can avoid static and dynamic obstacles in restricted waterways for a physically interconnected multi-vessel system in the towing process, making the collision avoidance COLREGS compliant (Rules 13-17). In addition, the control performance of the proposed distributed local optimization resolution is quite close to that of the centralized global optimization resolution, revealing that the proposed distributed control scheme is feasible.

5. *How to improve the quality of the manipulation process and achieve multiple control objectives as much as possible for a ship-towing system?*

   In Chapter 6, an ADMM-based multi-layer MPC approach with speed regulation is proposed to coordinate autonomous tugboats for manipulating a large ship to follow the waypoints, adjust the heading, track the speed profile, and resolve collisions in congested water traffic environments. To improve the quality of the manipulation process and increase the safety of collision avoidance, speed regulation is necessary. So the control problem becomes multi-objective aiming at waypoint following, heading adjusting, speed profile tracking, and collisions resolving. Such a complex multi-objective control problem is solved by the design of different controllers distributed in two layers. In the higher layer, the supervisory controller on the one hand calculates the predicted towing forces and angles for the ship objectives of waypoint following, speed profile tracking, and collision resolution, where a ship weight factor is designed to normalize the order of magnitude between the position and velocity error and reduce the sensitivity of the controller to the waypoint. On the other hand, it outputs the predicted ship surge speed and the desired tug trajectory for the lower controllers. The tug controller in the lower layer computes the thruster forces and moment of the tug system for the tug objectives of trajectory and surge speed tracking and collision resolution. The consensus between the lower-level and higher-level control is achieved by using the ADMM method. Through the iterations, it makes the predicted tug position and heading output by the tug controller approach to the desired tug trajectory output by the supervisory controller as much as possible.

   Simulation experiments indicate that the proposed control scheme coordinates multiple autonomous tugboats to transport a floating object smoothly and effectively. Compared to no speed regulation control, the proposed scheme has a similar performance in waypoint following and heading adjusting, the out-performance in consensus reaching and speed profile tracking. In the meantime, the towing process of the proposed scheme is safer for collision avoidance.

6. *In what way can we increase the flexibility and efficiency of the cooperation of multiple vessels for an offshore platform transportation system of the open sea?*

   In Chapter 7, a distributed coordination control scheme is proposed for a multi-vessel towing system to transport an offshore platform under environmental disturbances.

The main parts of the proposed control scheme are the dynamic coordination decision mechanism, the controller design, and the distributed control architecture design. The decision mechanism is based on the relative position between the platform and the current waypoint. According to this relative position, there are four sets of role combinations presented to assign the type of each tugboat. The controllers are designed based on the MPC strategy with different cost functions: for the supervisory controller, the cost function consists of the position error, heading, and velocity of the platform; for the tug controller, its cost function components are the heading error and velocity of the tugboats. The distributed control architecture is built based on the ADMM strategy that is to design an augmented Lagrangian function for reaching a consensus between the desired tug position output from the supervisory controller and the predicted tug position output from the tug controller. Because the desired tug heading is not achieved immediately, especially in the process of role changing, the tug heading is not selected as the key element for reaching the consensus.

The results from simulation experiments show that compared to the fixed tugboat role control, under environmental disturbances of winds, waves, and currents, the proposed flexible tugboat role scheme is much more efficient with the settling time being reduced by more than 50%. Furthermore, the proposed scheme has a better consensus achievement for the distributed control architecture accomplishment with the towing elongation error reduced to one-half to one-fifth.

The control attributes of the large floating object towing manipulation application that has been addressed in each chapter of this thesis are shown in Table 8.1.

8.1.2 Main research question

The main research question is: ***How to design a scalable and cooperative control scheme for multiple ASVs to manipulate a floating object through physical interconnections?***

To manipulate a large floating object through physical interconnections, the manipulation way, system model, and control framework are required to be determined first. Considering the system safety, object controllability, and application flexibility, towing maneuvrability is selected for the research focus. For system modeling, the towing angles and forces are used as the interconnections between the floating object and tugboats to describe the motion of the system. Based on such a system of multiple control inputs, multiple control constraints, and limited maneuverability, the control framework is established by distributed optimization-based control strategy. Then, considering different scenarios, concrete cooperative control schemes can be proposed. In port areas, a robust control scheme is designed for two autonomous tugboats to manipulate a ship under environmental disturbances. In inland waterways, a COLREGS compliant ADMM-based MPC approach is proposed for autonomous tugboats to avoid obstacles while maneuvering the large ship. To improve the quality of the towing process, a distributed control scheme with speed regulation is proposed to manipulate a ship to achieve multiple control objectives. In offshore waters, a dynamic coordination control scheme is proposed for a multi-vessel towing system to transport an offshore platform under the wind, wave, and current influence.

Table 8.1: Control attributes of the large floating object towing manipulation application that has been addressed in each chapter of this thesis.

Attribute / Chapter	Application Scenario	Control Objectives	Control Architecture	Collision Avoidance	Disturbance Consideration	Role of each Tugboat
Chapter 4	Port areas	Position; Heading.	Distributed	Internal	Winds; Unknown.	Leading role ×1 Following role ×1
Chapter 5	Inland waterways	Position; Heading.	Distributed	Internal; Static Obstacles; Dynamic Obstacles.	-	Leading role ×1 Following role ×1
Chapter 6	Inland waterways	Position; Heading; Velocity.	Distributed	Internal; Static Obstacles; Dynamic Obstacles.	-	Leading role ×1 Following role ×1
Chapter 7	Offshore waters	Position	Distributed	Internal	Winds; Waves; Currents.	Flexible role ×4

8.2   Future research

Since the research on floating object manipulation by autonomous multi-vessel systems has just started, there exist significant challenges for the implementation in real applications. These challenges are also the potential future directions to further the existing research works for better feasibility and applicability.

1. *Precise Manipulation System Model*

   Scholars usually simplify the manipulation system model to make the floating object manipulation problem simple. This simplification is good for finding a control solution quickly and reducing the computation time. But for validating the proposed solution to the real system in practice, it is necessary to establish a relative precise manipulation system model.

   For the towing manipulation way, the key to the system modelling is the interconnection between the tugboat and the floating object, namely, the towline. In most cases, the towline is treated as a massless cable transferring the towing forces from the tugboat to the floating object [5, 40–45, 48, 62, 63, 71, 81, 98, 186]. To simulate the real towing operations, some scholars use the catenary model to calculate the towline tension and resistance in the horizontal direction [76, 161, 182, 183, 192]. In these research works, the simulated manipulation system is usually composed of real tugboats and a floating platform so that the mass of the towline can not be omitted. Thus, for different scales of scenario, the towing manipulation system model should be changed to adjust to different situations.

2. *Multi-DOF Motion Control*

   The majority of the works in floating object manipulation focus on the 3-DOF planar motion control. However, in the real marine environment, the winds, waves, and currents will cause the manipulation system in vertical movement. Therefore, apart from the surge, sway, and yaw, the motion of pitch, roll, and heave should also be concerned.

   The additional DOF that should be considered in towing manipulation way is the pitch and heave, as shown in Fig 8.1. The height difference between the tugboat and the floating object makes the towing force from the tugboat to the object decompose into two components. The component force along the x-axis makes the floating object move in the forward direction (surge motion), and the component force along the z-axis makes the floating object move in the vertical direction (heave motion). In addition, both x-axis and z-axis component forces generate torques with respect to the y-axis (pitch motion). Under the environmental disturbances (especially the waves), the motion of heave and pitch will be more obvious.

3. *Proper Choice of Sampling Rate and Horizon Time*

   For the control method of MPC, the choice of sampling rate and horizon time is crucial for the implementation and the efficiency of the controller.

   In the process of implementation, the continuous-time vessel dynamics formulation has to be discretized and to be solved on a digital computer, the continuous-time constraints should then be replaced with a finite number of equality constraints between
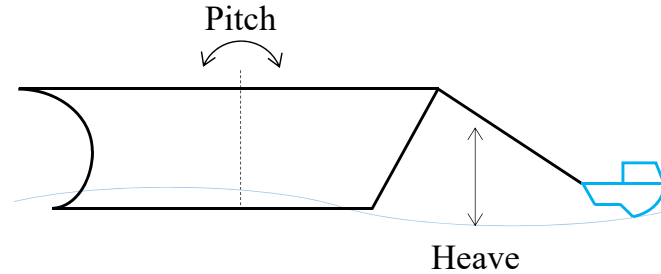
Figure 8.1: Additional DOF that should be considered in towing manipulation ways (the black vessel stands for the floating object, the blue vessel is the tugboat).

the samples. So the original problem becomes a very large numerical optimization problem that impacts the computation time [179]. Thus, the proper choice of sampling rate and horizon time is worthy of research for MPC implementations.

4. *Lower-layer Control for the Tugboats and the Floating Object*

The controller design in this thesis focuses on the higher-layer system, which means the computed control inputs are forces and moments. In practice, the real executable control inputs are the variables related to the lower-layer mechanical system.

For the floating object, the lower-layer control refers to winch control [157] which is to regulate the towing force on the towline. The lower-layer controller should regulate the winch to provide the actual tension on the towline close to the expected towing force as much as possible.

For the tugboats, the lower-layer control refers to propeller control [67]. As mentioned in Section 3.3, most of the applied tugboats are Azimuth Stern Drive (ASD) tugs, which means the real executable control variables are the rotation speed (or revolutions per minute (rpm)) and the angle of the propeller. The lower-layer controller should regulate the above two variables to achieve the desired thruster forces and moments.

5. *Observer Design and Fault Diagnosis*

The state information output from sensors is important for designing the cooperative control strategy for the floating object manipulation system, which involves two aspects of problems.

The first is the observer design. The observer is necessary to estimate this important information. The basic information for the manipulation system is the state of motion containing position, heading, and velocity. Besides, for the towing manipulation system, the other necessary information is the towing angle and force. These two variables are the control inputs of the floating object. The desired states of the floating object are reached by controlling the towing force and angle. Thus, two observers should be designed onboard each tugboat to measure and estimate the towing force by the winch and the towing angle from the tugboat to the floating object.

The second is fault diagnosis. Fault diagnosis consists of fault detection and fault isolation [142]. Fault detection is to judge the presence of faults and estimate their occurrence time, fault isolation deals with finding the location of the fault and determining the type of fault. These two parts are significant to increase the robustness of the control.

6. *Collision Avoidance in Complex Situation*

The number of research works focusing on collision avoidance of external obstacles is limited. However, the research on collision avoidance is important for ensuring the safety of the floating manipulation system, it is also the premise to implement other tasks. Thus, collision avoidance of the manipulation system should be studied in-depth, even for some complex situations.

For a towing system, the research works on collision avoidance of external obstacles is more than other manipulation ways [19, 20, 42, 44, 45]. But due to the restricted maneuverability and the redundant structure of the towline-connected multi-vessel system, the challenge lies in the long response time of the avoiding operation and the limited collision avoidance space, especially in the narrow waterways. Thus, in what way a towing manipulation system can quickly and efficiently take actions to eliminate collision risk is a worthwhile research direction. Besides, in a busy water traffic environment, there is a situation of multiple target vessels (dynamic obstacles). How to avoid multiple dynamic obstacles simultaneously is another challenging but also worthwhile research problem.

7. *Coordination control for tugboat replacement and increment*

In some cases, the floating object may be heavier and larger than expected that the working tugboats are not enough; or in other cases, a part of the tugboats in the manipulation system may be faulty and out of work. If the above situation happens, adding or replacing some tugboats is necessary to make sure the manipulation task carrying on smoothly.

It is rare for a towing manipulation system to replace or increase tugboats. Besides the tugboat fault, a possible situation may come from the sudden bad weather during the towing process. In this case, the original tugboats may have no ability to fully control the floating object with the harsh winds, waves, and currents. Thus, at this moment it is necessary to dispatch additional tugboats to help the manipulation system on the verge of getting out of control.

8. *Hybrid Floating Object Manipulation*

Different floating object manipulation ways can cooperate to take advantage of their strengths. For the way of attaching, the fully controllable characteristic of the manipulation system will not take advantage of other ways to help. For the way of caging, the limited floating object and application scenarios result in that other ways are difficult to join in. Thus, the hybrid manipulation can only happen between pushing and towing ways.

A typical scenario is shown in Fig 8.2. In the operation of berthing near the pier, the towing manipulation can control the floating object to reach the goal position in the
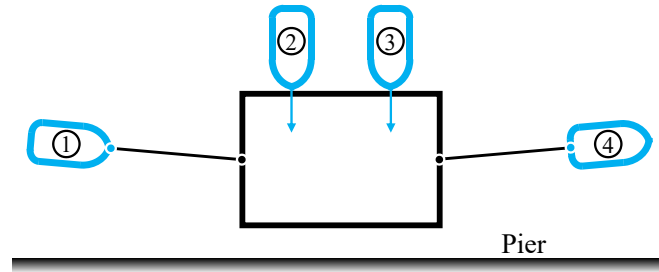
Figure 8.2: Hybrid object manipulation with towing and pushing.

lateral direction. (tugboat 1 and 4 in Fig 8.2). To make the floating object close to the pier in the longitudinal direction, other tugboats are usually required for providing pushing manipulation from the outside to the inside of the pier (tugboat 2 and 3 in Fig 8.2). Meanwhile, the tugboats in the towing manipulation should also control the speed of the floating object for preventing it from colliding with the pier. Thus, the coordination of towing and pushing is required to cooperate tacitly to accomplish the hybrid manipulation task.

Bibliography

[1] A. Aguiary, J. Almeiday, M. Bayaty, B. Cardeiray, R. Cunhay, A. Hauslery, P. Mauryay, A. Oliveiray, A. Pascoaly, A. Pereira, M. Rufinoy, L. Sebastiaoy, C. Silvestrey, and F. Vanniy. Cooperative autonomous marine vehicle motion control in the scope of the EU GREX project: theory and practice. In *Proceedings of the OCEANS 2009-EUROPE*, pages 1–10, Bremen, Germany, 2009.

[2] Y. A. Ahmed and K. Hasegawa. Automatic ship berthing using artificial neural network trained by consistent teaching data using nonlinear programming method. *Engineering Applications of Artificial Intelligence*, 26(10):2287–2304, 2013.

[3] Y. A. Ahmed, M. A. Hannan, M. Y. Oraby, and A. Maimun. COLREGs compliant fuzzy-based collision avoidance system for multiple ship encounters. *Journal of Marine Science and Engineering*, 9(8):790, 2021.

[4] A. Alop. The main challenges and barriers to the successful "Smart Shipping". *TransNav, the International Journal on Marine Navigation and Safety of Sea Transportation*, 13(3):521–528, 2019.

[5] I. Amin, S. Oterkus, M. E. A. Ali, H. Shawky, and E. Oterkus. Experimental investigation on a towing assessment for a floating desalination plant for Egypt. *Ocean Engineering*, 238:109746, 2021.

[6] M. Arnold, R. R. Negenborn, G. Andersson, and B. D. Schutter. Multi-area predictive control for combined electricity and natural gas systems. In *Proceedings of the 2009 European Control Conference (ECC)*, pages 1408–1413, Budapest, Hungary, 2009.

[7] F. Arrichiello, S. Chiaverini, and T. Fossen. Formation control of underactuated surface vessels using the null-space-sased sehavioral control. In *Proceedings of the 2006 IEEE/RSJ International Conference on Intelligent Robots and Systems*, pages 5942–5947, Beijing, China, 2006.

[8] F. Arrichiello, S. Chiaverini, and T. Fossen. Formation control of underactuated surface vessels using the null-space-based behavioral control. In *Proceedings of the 2006 IEEE/RSJ International Conference on Intelligent Robots and Systems*, pages 5942–5947, Beijing, China, 2006.

[9] F. Arrichiello, H. K. Heidarsson, S. Chiaverini, and G. S. Sukhatme. Cooperative caging and transport using autonomous aquatic surface vehicles. *Intelligent Service Robotics*, 5(1):73–87, 2011.

[10] P. I. B. Berntsen, O. M. Aamo, B. J. Leira, and A. J. Sørensen. Structural reliability-based control of moored interconnected structures. *Control Engineering Practice*, 16 (4):495–504, 2008.

[11] V. Bertram. Unmanned surface vehicles-a survey. In *Proceedings of the Skibsteknisk Selskab*, pages 1–14, Copenhagen, Denmark, 2008.

[12] S. Bhattacharya, H. Heidarsson, G. S. Sukhatme, and V. Kumar. Cooperative control of autonomous surface vehicles for oil skimming and cleanup. In *Proceedings of the 2011 IEEE International Conference on Robotics and Automation*, pages 2374–2379, Shanghai, China, 2011.

[13] S. Bhattacharya, H. Heidarsson, G. S. Sukhatme, and V. Kumar. Supplementary report: Cooperative control of autonomous surface vehicles for oil skimming and cleanup. Technical report, The GRASP Laboratory, University of Pennsylvania, 2011. http://www.subhrajit.net/files/Projects-Work/OilBoom_Catenary_2010/icra2011_Supplementary.pdf.

[14] B. Bidikli, E. Tatlicioglu, and E. Zergeroglu. Robust control design for positioning of an unactuated surface vessel. In *Proceedings of the 2015 IEEE/RSJ International Conference on Intelligent Robots and Systems (IROS)*, pages 1071–1076, Hamburg, Germany, 2015.

[15] B. Bidikli, E. Tatlicioglu, and E. Zergeroglu. Robust dynamic positioning of surface vessels via multiple unidirectional tugboats. *Ocean Engineering*, 113:237–245, 2016.

[16] B. E. Bishop. Swarm-based object manipulation using redundant manipulator analogs. In *Proceedings of the 2008 IEEE International Conference on Robotics and Automation*, pages 1495–1500, Pasadena, CA, USA, 2008.

[17] D. Braganza, M. Feemster, and D. Dawson. Positioning of large surface vessels using multiple tugboats. In *Proceedings of the 2007 American Control Conference*, pages 912–917, New York, NY, USA, 2007.

[18] D. J. J. B. Bruggink, Q. C. Cremer, R. R. Groenewegen, and A. G. C. Klokgieters. Differentiation of maneuvering coefficients for scaled model vessels. Technical report, Delft University of Technology, 2018.

[19] G. Bruzzone, M. Bibuli, M. Caccia, and E. Zereik. Cooperative robotic maneuvers for emergency ship towing operations. In *Proceedings of the 2013 MTS/IEEE OCEANS*, pages 1–7, Bergen, Norway, 2013.

[20] G. Bruzzone, M. Bibuli, E. Zereik, A. Ranieri, and M. Caccia. Cooperative adaptive guidance and control paradigm for marine robots in an emergency ship towing scenario. *International Journal of Adaptive Control and Signal Processing*, 31(4): 562–580, 2016.

[21] P. Van Bui and Y. B. Kim. Development of constrained control allocation for ship berthing by using autonomous tugboats. *International Journal of Control, Automation and Systems*, 9(6):1203–1208, 2011.

[22] V. P. Bui, H. Kawai, Y. B. Kim, and K. S. Lee. A ship berthing system design with four tug boats. *Journal of Mechanical Science and Technology*, 25(5):1257–1264, 2011.

[23] V. P. Bui, S. W. Ji, J. S. Jang, and Y. B. Kim. Ship trajectory tracking in harbour area by using autonomous tugboats. *IFAC Proceedings Volumes*, 45(13):740–745, 2012.

[24] S. Campbell, W. Naeem, and G. W. Irwin. A review on improving the autonomy of unmanned surface vehicles through intelligent collision avoidance manoeuvres. *Annual Reviews in Control*, 36(2):267–283, 2012.

[25] L. Cavaleri, B. F. Kemper, and M. Hemer. Wind waves in the coupled climate system. *Bulletin of the American Meteorological Society*, 93(11):1651–1661, 2012.

[26] L. Chen, H. Hopman, and R. R. Negenborn. Distributed model predictive control for vessel train formations of cooperative multi-vessel systems. *Transportation Research Part C: Emerging Technologies*, 92:101–118, 2018.

[27] L. Chen, H. Hopman, and R. R. Negenborn. Distributed model predictive control for cooperative floating object transport with multi-vessel systems. *Ocean Engineering*, 191:106515, 2019.

[28] L. Chen, Y. Huang, H. Zheng, H. Hopman, and R. Negenborn. Cooperative multi-vessel systems in urban waterway networks. *IEEE Transactions on Intelligent Transportation Systems*, 21(8):3294–3307, 2020.

[29] Y. Y. Chen and Y. P. Tian. Formation tracking and attitude synchronization control of underactuated ships along closed orbits. *International Journal of Robust and Nonlinear Control*, 25(16):3023–3044, 2014.

[30] H. T. L. Chiang and L. Tapia. COLREG-RRT: An RRT-based COLREGS-compliant motion planner for surface vehicle navigation. *IEEE Robotics and Automation Letters*, 3(3):2024–2031, 2018.

[31] J. K. Choi. Preliminary study on the docking control of a large ship using tugboats. *Journal of Advanced Marine Engineering and Technology*, 44(4):311–317, 2020.

[32] A. N. Cockcroft and J. N. F. Lameijer. *Guide to the Collision Avoidance Rules*. Elsevier, 2003.

[33] R. Coelho, R. Daltry, V. Dobbin, E. Lachaud, and I. Miller. Design process and validation of an autonomous surface vehicle for the offshore industry. In *Proceedings of the Offshore Technology Conference (OTC) Brasil*, pages 1–14, Rio de Janeiro, Brazil, 2015. Offshore Technology Conference.

[34] A. Devaraju, L. Chen, and R. R. Negenborn. Autonomous surface vessels in ports: Applications, technologies and port infrastructures. In *Proceedings of the International Conference on Computational Logistics 2018*, pages 86–105, Vietri sul Mare, Italy, 2018.

[35] F. Ding, J. Wu, and Y. Wang. Stabilization of an underactuated surface vessel based on adaptive sliding mode and backstepping control. *Mathematical Problems in Engineering*, 2013:1–5, 2013.

[36] dJI FORUM. Tugboat attaching to big ship, 2019. https://forum.dji.com/thread-191617-1-1.html, (Accessed: 16-05-2022).

[37] DMT MARINE EQUIPMENT. Towing Winches, 2016. https://www.dmt-winches.com/towing-winches/, (Accessed: 01-06-2022).

[38] DrillingFormulas. You Can Travel To North Sea's Oil Platform as Tourists, 2016. https://www.drillingformulas.com/you-can-travel-to-north-seas-oil-platform-as-tourists/, (Accessed: 16-05-2022).

[39] DRONE TECH PLANET. Delivery Drones: The Future of Drone Delivery Business, 2018. https://www.dronetechplanet.com/delivery-drones-the-future-of-drone-delivery-business/, (Accessed: 02-16-2022).

[40] Z. Du, V. Reppa, and R. R. Negenborn. Cooperative control of autonomous tugs for ship towing. *IFAC-PapersOnLine*, 53(2):14470–14475, 2020.

[41] Z. Du, R. R. Negenborn, and V. Reppa. Cooperative multi-agent control for autonomous ship towing under environmental disturbances. *IEEE/CAA Journal of Automatica Sinica*, 8(8):1365–1379, 2021.

[42] Z. Du, R. R. Negenborn, and V. Reppa. COLREGS-compliant collision avoidance for physically coupled multi-vessel systems with distributed MPC. *Submitted to a journal*, 2021.

[43] Z. Du, R. R. Negenborn, and V. Reppa. Multi-vessel cooperative speed regulation for ship manipulation in towing scenarios. *IFAC-PapersOnLine*, 54(16):384–389, 2021.

[44] Z. Du, R. R. Negenborn, and V. Reppa. MPC-based COLREGS compliant collision avoidance for a multi-vessel ship-towing system. In *Proceedings of the European Control Conference*, pages 1857–1862, Delft, Netherlands, 2021.

[45] Z. Du, R. R. Negenborn, and V. Reppa. Multi-objective cooperative control for a ship-towing system in congested water traffic environments. *Submitted to a journal*, 2022.

[46] Z. Du, R. R. Negenborn, and V. Reppa. Dynamic coordination of multiple vessels for offshore platform transportation under ocean environmental disturbances. *Submitted to a journal*, 2022.

[47] Z. Du, R. R. Negenborn, and V. Reppa. Review of floating object manipulation by autonomous multi-vessel systems. *Submitted to a journal*, 2022.

[48] Z. Du, R. R. Negenborn, and V. Reppa. Dynamic coordination of multiple vessels for offshore platform transportation. In *Proceedings of the 6th IEEE Conference on Control Technology and Applications*, pages 1–6, Trieste, Italy, 2022.

[49] G. Eoh, J. D. Jeon, J. S. Choi, and B. H. Lee. Multi-robot cooperative formation for overweight object transportation. In *Proceedings of the 2011 IEEE/SICE International Symposium on System Integration (SII)*, pages 726–731, Kyoto, Japan, 2011.

[50] J. Esposito, M. Feemster, and E. Smith. Cooperative manipulation on the water using a swarm of autonomous tugboats. In *Proceedings of the 2008 IEEE International Conference on Robotics and Automation*, pages 1501–1506, Pasadena, CA, USA, 2008.

[51] J. M. Esposito. Distributed grasp synthesis for swarm manipulation with applications to autonomous tugboats. In *Proceedings of the 2008 IEEE International Conference on Robotics and Automation*, pages 1489–1494, Pasadena, CA, USA, 2008.

[52] J. M. Esposito. Decentralized cooperative manipulation with a swarm of mobile robots. In *Proceedings of the 2009 IEEE/RSJ International Conference on Intelligent Robots and Systems*, pages 5333–5338, St. Louis, MO, USA, 2009.

[53] J. M. Esposito. Decentralized cooperative manipulation with a swarm of mobile robots: The approach problem. In *Proceedings of the 2010 American Control Conference*, pages 4762–4767, Baltimore, MD, USA, 2010.

[54] M. Feemster, J. Esposito, and J. Nicholson. Manipulation of large object by swarms of autonomous marine vehicles, part I: Rotational motions. In *Proceedings of the 2006 Thrity-Eighth Southeastern Symposium on System Theory*, pages 205–209, Cookeville, TN, USA, 2006.

[55] M. G. Feemster and J. M. Esposito. Comprehensive framework for tracking control and thrust allocation for a highly overactuated autonomous surface vessel. *Journal of Field Robotics*, 28(1):80–100, 2010.

[56] T. I. Fossen. *Handbook of Marine Craft Hydrodynamics and Motion Control*. John Wiley & Sons, Chichester, West Sussex, UK, 2011.

[57] G. E. Gapingsi, R. Korbas, and M. Santos. Modelling and control of a flexible floating boom: First approach. *IFAC-PapersOnLine*, 50(1):13108–13113, 2017.

[58] B. Gheneti, S. Park, R. Kelly, D. Meyers, P. Leoni, C. Ratti, and D. Rus. Trajectory planning for the shapeshifting of autonomous surface vessels. In *Pordeedings of the 2019 International Symposium on Multi-Robot and Multi-Agent Systems*, pages 76–82, New Brunswick, NJ, USA, 2019.

[59] J. Ghommam, F. Mnif, A. Benali, and N. Derbel. Asymptotic backstepping stabilization of an underactuated surface vessel. *IEEE Transactions on Control Systems Technology*, 14(6):1150–1157, 2006.

[60] E. F. P. González, G. R. Torres, and G. T. Pulido. Motion planning for cooperative multi-robot box-pushing problem. In *Proceedings of the Advances in Artificial Intelligence*, pages 382–391, Berlin, Heidelberg, 2008. Springer Berlin Heidelberg.

[61] I. B. Hagen, D. K. M. Kufoalor, E. F. Brekke, and T. A. Johansen. MPC-based collision avoidance strategy for existing marine vessel guidance systems. In *2018 IEEE International Conference on Robotics and Automation (ICRA)*, Brisbane, QLD, Australia, 2018.

[62] H. Hajieghrary, D. Kularatne, and M. A. Hsieh. Cooperative transport of a buoyant load: A differential geometric approach. In *Proceedings of the 2017 IEEE/RSJ International Conference on Intelligent Robots and Systems (IROS)*, pages 2158–2163, Vancouver, BC, Canada, 2017.

[63] H. Hajieghrary, D. Kularatne, and M. A. Hsieh. Differential geometric approach to trajectory planning: Cooperative transport by a team of autonomous marine vehicles. In *Proceedings of the 2018 Annual American Control Conference (ACC)*, pages 858–863, Milwaukee, WI, USA, 2018.

[64] S. H. Ham, M. Roh, H. Lee, J. W. Hong, and H. R. Lee. Development and validation of a simulation-based safety evaluation program for a mega floating crane. *Advances in Engineering Software*, 112:101–116, 2017.

[65] R. H. Hansen. DNV Towing Recommendations. techreport, Det Norske Veritas, 2014.

[66] I. O. Hara, J. Paulos, J. Davey, N. Eckenstein, N. Doshi, T. Tosun, J. Greco, J. Seo, M. Turpin, V. Kumar, and M. Yim. Self-assembly of a swarm of autonomous boats into floating structures. In *Proceedings of the 2014 IEEE International Conference on Robotics and Automation (ICRA)*, pages 1234–1240, Hong Kong, China, 2014.

[67] A. Haseltalab and R. R. Negenborn. Model predictive maneuvering control and energy management for all-electric autonomous ships. *Applied Energy*, 251(113308): 1–27, 2019.

[68] Henk Hensen. *Tug Use in Port: A Practical Guide*. Nautical Institute, London, UK, 2003.

[69] M. Hepworth. Collision avoidance for autonomous inland vessels using stereovision. Master's thesis, Delft University of Technology, Delft, Netherlands, 2021.

[70] M. A. Hinostroza, H. Xu, and C. G. Soares. Cooperative operation of autonomous surface vehicles for maintaining formation in complex marine environment. *Ocean Engineering*, 183:132–154, 2019.

[71] M. Hoffmann, S. Roy, A. Berger, W. Bergmann, K. Chan, M. Shubbak, J. Langhorst, T. Schnauder, O. Struss, and C. Buskens. Wind affected maneuverability of tugboat-controlled ships. *IFAC-PapersOnLine*, 54(16):70–75, 2021.

[72] Y. Hu, L. Wang, J. Liang, and T. Wang. Underwater box-pushing with multiple vision-based autonomous robotic fish. In *Proceedings of the 2010 IEEE/RSJ International Conference on Intelligent Robots and Systems*, pages 4219–4224, Taipei, Taiwan, 2010.

[73] Y. Hu, T. Wang, L. Wang, and J. Liang. Cooperative box-pushing with multiple autonomous robotic fish in underwater environment. *IET Control Theory & Applications*, 5(17):2015–2022, 2011.

[74] Y. Huang, L. Chen, and P. H. A. J. M. van Gelder. Generalized velocity obstacle algorithm for preventing ship collisions at sea. *Ocean Engineering*, 173:142–156, 2019.

[75] Y. Huang, L. Chen, P. Chen, R. R. Negenborn, and P. H. A. J. M. van Gelder. Ship collision avoidance methods: State-of-the-art. *Safety Science*, 121:451–473, 2020.

[76] A. S. S. Ianagui and E. A. Tannuri. Automatic load maneuvering and hold-back with multiple coordinated DP vessels. *Ocean Engineering*, 178:357–374, 2019.

[77] I. A. F. Ihle, J. Jouffroy, and T. I. Fossen. Robust formation control of marine craft using lagrange multipliers. In *Group Coordination and Cooperative Control*, pages 113–129. Springer-Verlag, 2006.

[78] International Maritime Organization. COLREGS - International Regulations for Preventing Collisions at Sea. *Convention on the International Regulations for Preventing Collisions at Sea, 1972*, pages 1–74, 1972.

[79] International Maritime Organization. Maritime Safety Committee (MSC), 98th session, 2017. https://www.imo.org/en/MediaCentre/MeetingSummaries/Pages/MSC-98th-session.aspx, (Accessed: 02-01-2022).

[80] International Maritime Organization. IMO takes first steps to address autonomous ships, 2018. https://www.imo.org/en/MediaCentre/PressBriefings/Pages/08-MSC-99-MASS-scoping.aspx, (Accessed: 02-01-2022).

[81] M. M. Ismail, N. G. Chalhoub, and V. Pilipchuk. Dynamics and control of a two-ship ensemble connected by a massless towline. *Ocean Engineering*, 234:109295, 2021.

[82] iStock. Aerial view of inland freight ships in canal in Friesland, the Netherlands, 2020. https://www.istockphoto.com/nl/foto/luchtmening-van-binnenlandse-vrachtschepen-gm1280718891-378957154, (Accessed: 13-05-2022).

[83] S. W. Ji, K. H. Choi, and Y. B. Kim. Nonlinear observer and sliding mode control design for dynamic positioning of a surface vessel. In *Proceedings of the 2012 12th International Conference on Control, Automation and Systems*, pages 1900–1904, JeJu Island, South Korea, 2012.

[84] J. Jimenez and J. M. G. Sierra. Modelling the automatic deployment of oil-spill booms: A simulation scenario for sea cleaning. In *Proceedings of the 2018 Winter Simulation Conference (WSC)*, pages 1192–1203, Gothenburg, Sweden, 2018.

[85] J. F. Jimenez and J. M. G. Sierra. USV based automatic deployment of booms along quayside mooring ships: Scaled experiments and simulations. *Ocean Engineering*, 207:107438, 2020.

[86] T. A. Johansen and T. I. Fossen. Control allocation: A survey. *Automatica*, 49(5): 1087–1103, 2013.

[87] T. A. Johansen and T. I. Fossen. Control allocation—A survey. *Automatica*, 49(5): 1087–1103, 2013.

[88] T. A. Johansen, T. Perez, and A. Cristofaro. Ship collision avoidance and COLREGS compliance using simulation-based control behavior selection with predictive hazard assessment. *IEEE Transactions on Intelligent Transportation Systems*, 17(12):3407–3422, 2016.

[89] E. Kayacan, S. Park, C. Ratti, and D. Rus. Learning-based nonlinear model predictive control of reconfigurable autonomous robotic boats: Roboats. In *Proceedings of the 2019 IEEE/RSJ International Conference on Intelligent Robots and Systems*, pages 8230–8237, Macau, China, 2019.

[90] kenstevenson. Skycity au roadtrain, 2007. https://www.flickr.com/photos/19568729@N08/3222317200/, (Accessed: 02-16-2022).

[91] K. Kepaptsoglou, G. Fountas, and M. G. Karlaftis. Weather impact on containership routing in closed seas: A chance-constraint optimization approach. *Transportation Research Part C: Emerging Technologies*, 55:139–155, 2015.

[92] N. Khaled and N. G. Chalhoub. A dynamic model and a robust controller for a fully-actuated marine surface vessel. *Journal of Vibration and Control*, 17(6):801–812, 2010.

[93] W. B. Klinger, I. R. Bertaska, K. D. von Ellenrieder, and M. R. Dhanak. Control of an unmanned surface vehicle with uncertain displacement and drag. *IEEE Journal of Oceanic Engineering*, 42(2):458–476, 2017.

[94] KOTUG. OFFSHORE & TERMINAL TOWAGE, 2018. https://www.kotug.com/towage/offshore-and-terminal-towage/, (Accessed: 13-05-2022).

[95] KOTUG Canada. KOTUG and SEABULK awarded contact at BAHAMAS, 2017. https://www.kotugcanada.ca/newsmedia/kotug-seabulk-maritime-starts-bahamas, (Accessed: 02-16-2022).

[96] S. Kragelund, V. Dobrokhodov, A. Monarrez, M. Hurban, and C. Khol. Adaptive speed control for autonomous surface vessels. In *Proceedings of the MTS/IEEE OCEANS 2013*, pages 1–10, San Diego, CA, USA, 2013.

[97] V. J. Kurian, C. Y. Ng, and M. S. Liew. Numerical investigation on dynamic responses of classic spar platforms: Long crested waves vs. short crested waves. In *Proceedings of the 2012 IEEE Colloquium on Humanities, Science and Engineering*, pages 724–728, Kota Kinabalu, Malaysia, 2012.

[98] D. H. Lee, S. Chakir, Y. B. Kim, and D. Q. Tran. Control system design for vessel towing system by activating rudders of the towed vessel. *International Journal of Naval Architecture and Ocean Engineering*, 12:943–956, 2020.

[99] S. M. Lee, J. H. Lee, M. Roh, K. S. Kim, S. H. Ham, and H. W. Lee. An optimization model of tugboat operation for conveying a large surface vessel. *Journal of Computational Design and Engineering*, 8(2):654–675, 2021.

[100] J. H. Li, P. M. Lee, B. H. Jun, and Y. K. Lim. Point-to-point navigation of underactuated ships. *Automatica*, 44(12):3201–3205, 2008.

[101] Y. Li, A. C. Landsburg, R. A. Barr, and S. M. Calisal. Improving ship maneuverability standards as a means for increasing ship controllability and safety. In *Proceedings of the IEEE/MTS/ OCEANS 2005*, pages 1972–1981, Washington, DC, USA, 2005.

[102] Z. Li and J. Sun. Disturbance compensating model predictive control with application to ship heading control. *IEEE Transactions on Control Systems Technology*, 20(1): 257–265, 2011.

[103] Y. Liu and R. Bucknall. A survey of formation control and motion planning of multiple unmanned vehicles. *Robotica*, 36(7):1019–1047, 2018.

[104] Y. Liu, C. Guo, and R. Zhou. Asymptotic stabilization control of an underactuated surface vessel with optimization based on genetic algorithm. In *Proceedings of the 2008 Second International Symposium on Intelligent Information Technology Application*, volume 3, pages 622–626, Shanghai, China, 2008.

[105] Z. Liu, Y. Zhang, X. Yu, and C. Yuan. Unmanned surface vehicles: An overview of developments and challenges. *Annual Reviews in Control*, 41:71–93, 2016.

[106] C. Lv, H. Yu, Z. Hua, L. Li, and J. Chi. Speed and heading control of an unmanned surface vehicle based on state error PCH principle. *Mathematical Problems in Engineering*, 2018:1–9, 2018.

[107] C. Lv, H. Yu, J. Chi, T. Xu, H. Zang, H. l. Jiang, and Z. Zhang. A hybrid coordination controller for speed and heading control of underactuated unmanned surface vehicles system. *Ocean Engineering*, 176:222–230, 2019.

[108] H. Lyu and Y. Yin. COLREGS-constrained real-time path planning for autonomous ships using modified artificial potential fields. *Journal of Navigation*, 72(3):588–608, 2018.

[109] Marine Insight. Rolls-Royce Demonstrates World's First Remotely Operated Commercial Vessel, 2017. https://www.marineinsight.com/shipping-news/rolls-royce-demonstrates-worlds-first-remotely-operated-commercial-vessel/, (Accessed: 02-01-2022).

[110] Marine Insight. Wartsila's Autonomous Harbour Tug Takes A Big Leap Towards Reality, 2019. https://www.marineinsight.com/shipping-news/wartsilas-autonomous-harbour-tug-takes-a-big-leap-towards-reality/, (Accessed: 02-01-2022).

[111] Marine Insight. Abu Dhabi Ports To Develop World's First Unmanned Autonomous Commercial Tugboats, 2020. https://www.marineinsight.com/shipping-news/abu-dhabi-ports-to-develop-worlds-first-unmanned-autonomous-commercial-tugboats/, (Accessed: 02-01-2022).

[112] Marine Insight. ABB To Power First Fully Electric US Tugboat For Zero-Emission Operations, 2021. https://www.marineinsight.com/shipping-news/abb-to-power-first-fully-electric-us-tugboat-for-zero-emission-operations/, (Accessed: 02-01-2022).

[113] Marine Oil Gobbler. Environmentally acceptable oil spill dispersant for the effective treatment of marine oil spills, 2018. https://www.ecozyme.co.za/marine-oil-spill-dispersant.pdf, (Accessed: 02-14-2022).

[114] I. Mas and C. Kitts. Object manipulation using cooperative mobile multi-robot systems. In *Proceedings of the World Congress on Engineering and Computer Science*, volume 1, pages 1–6, San Francisco, USA, 2012.

[115] I. Mas and C. Kitts. Cooperative tasks using teams of mobile robots. In *Lecture Notes in Electrical Engineering*, pages 83–99. Springer Netherlands, 2013.

[116] L. A. Mateos. Bio-inspired adaptive latching system for towing and guiding power-less floating platforms with autonomous robotic boats. *arXiv preprint arXiv:2001.04293*, pages 1–7, 2020.

[117] L. A. Mateos, W. Wang, B. Gheneti, F. Duarte, C. Ratti, and D. Rus. Autonomous latching system for robotic boats. In *Proceedings of the 2019 International Conference on Robotics and Automation*, pages 7933–7939, Montreal, QC, Canada, 2019.

[118] S. Misik, A. Cela, and Z. Bradac. Optimal predictive control - A brief review of theory and practice. *IFAC-PapersOnLine*, 49(25):324–329, 2016.

[119] N. Mizuno, Y. Uchida, and T. Okazaki. Quasi real-time optimal control scheme for automatic berthing. *IFAC-PapersOnLine*, 48(16):305–312, 2015.

[120] L. Moreira, T. I. Fossen, and C. G. Soares. Path following control system for a tanker ship model. *Ocean Engineering*, 34(14-15):2074–2085, 2007.

[121] R. R. Negenborn and J. M. Maestre. On 35 approaches for distributed MPC made easy. In *Distributed Model Predictive Control Made Easy*, pages 1–37. Springer Netherlands, 2013.

[122] L. Nesi, G. Pepe, M. Bibuli, E. Zereik, A. Carcaterra, and M. Caccia. A new tow maneuver of a damaged boat through a swarm of autonomous sea drones. *IFAC-PapersOnLine*, 52(21):360–366, 2019.

[123] C. Z. Pan, X. Z. Lai, S. X. Yang, and M. Wu. An efficient neural network approach to tracking control of an autonomous surface vehicle with unknown dynamics. *Expert Systems with Applications*, 40(5):1629–1635, 2013.

[124] S. Park, E. Kayacan, C. Ratti, and D. Rus. Coordinated control of a reconfigurable multi-vessel platform: Robust control approach. In *Proceedings of the 2019 International Conference on Robotics and Automation (ICRA)*, pages 4633–4639, Montreal, QC, Canada, 2019.

[125] V. Paulauskas and D. Paulauskas. Research on work methods for tugs in ports. *Transport*, 26(3):310–314, 2011.

[126] J. Paulos, N. Eckenstein, T. Tosun, J. Seo, J. Davey, J. Greco, V. Kumar, and M. Yim. Automated self-assembly of large maritime structures by a team of robotic boats. *IEEE Transactions on Automation Science and Engineering*, 12(3):958–968, 2015.

[127] Z. Peng, D. Wang, Z. Chen, X. Hu, and W. Lan. Adaptive dynamic surface control for formations of autonomous surface vehicles with uncertain dynamics. *IEEE Transactions on Control Systems Technology*, 21(2):513–520, 2013.

[128] Z. Peng, C. Meng, L. Liu, D. Wang, and T. Li. PWM-driven model predictive speed control for an unmanned surface vehicle with unknown propeller dynamics based on parameter identification and neural prediction. *Neurocomputing*, 432:1–9, 2021.

[129] Z. Peng, J. Wang, D. Wang, and Q. L. Han. An overview of recent advances in coordinated control of multiple autonomous surface vehicles. *IEEE Transactions on Industrial Informatics*, 17(2):732–745, 2021.

[130] F. J. Pereda, H. G. de Marina, J. M. G. Sierra, and J. Jimenez. Towards automatic oil spill confinement with autonomous marine surface vehicles. In *Proceedings of the IEEE/MTS OCEANS 2011*, pages 1–6, Santander, Spain, 2011.

[131] A. Pereira, J. Das, and G. S. Sukhatme. An experimental study of station keeping on an underactuated ASV. In *Proceedings of the 2008 IEEE/RSJ International Conference on Intelligent Robots and Systems*, pages 3164–3171, Nice, France, 2008.

[132] G. A. S. Pereira, M. F. M. Campos, and V. Kumar. Decentralized algorithms for multi-robot manipulation via caging. *The International Journal of Robotics Research*, 23(7-8):783–795, 2004.

[133] Tristan Perez. *Ship Motion Control: Course Keeping and Roll Stabilisation Using Rudder and Fins*. Springer Science & Business Media, London, UK, 2006.

[134] Port Technology. Kotug Shows How Remotely Operated Tugs Can Work, 2018. https://www.porttechnology.org/news/kotug_shows_how_remotely_operated_tugs_can_work/, (Accessed: 02-01-2022).

[135] Port Technology International Team. Autonomous Tugs: A Feature of the Future?, 2017. https://www.porttechnology.org/news/autonomous_tugs_a_feature_of_the_future/, (Accessed: 02-01-2022).

[136] H. Pourbabak, T. Chen, and W. Su. *Centralized, decentralized, and distributed control for energy internet*, pages 3–19. Elsevier, 2019.

[137] Z. Qin, Z. Lin, D. Yang, and P. Li. A task-based hierarchical control strategy for autonomous motion of an unmanned surface vehicle swarm. *Applied Ocean Research*, 65:251–261, 2017.

[138] T. D. Quan, J. H. Suh, and Y. B. Kim. Leader-following control system design for a towed vessel by tugboat. *Journal of Ocean Engineering and Technology*, 33(5): 462–469, 2019.

[139] E. Raboin, Petr Švec, D. S. Nau, and S. K. Gupta. Model-predictive asset guarding by team of autonomous surface vehicles in environment with civilian boats. *Autonomous Robots*, 38(3):261–282, 2014.

[140] M. S. Rana, H. R. Pota, and I. R. Petersen. Model predictive control of atomic force microscope for fast image scanning. In *Proceedings of the 2012 51st IEEE Conference on Decision and Control*, pages 2477–2482, Maui, HI, USA, 2012.

[141] W. Ren, R. W. Beard, and E. M. Atkins. A survey of consensus problems in multi-agent coordination. In *Proceedings of the 2005 American Control Conference*, pages 1859–1864, Portland, OR, USA, 2005.

[142] V. Reppa, M. M. Polycarpou, and C. G. Panayiotou. Sensor fault diagnosis. *Foundations and Trends in Systems and Control*, 3(1-2):1–248, 2016.

[143] Riviera Maritime Media. Dutch tug owner takes autonomous command punt, 2020. https://www.rivieramm.com/news-content-hub/dutch-tug-owner-takes-an-autonomous-command-punt-61988, (Accessed: 02-01-2022).

[144] R. V. C. Rosario, J. P. V. S. Cunha, and P. B. G. Rosa. Stabilizing control of an unmanned surface vehicle pushing a floating load. *International Journal of Control, Automation and Systems*, 18(12):3194–3203, 2020.

[145] Rotterdam Port Authority. Port Information Guide. techreport, Port of Rotterdam, Rotterdam, the Netherlands, 2019.

[146] G. Sartoretti, S. Shaw, and M. A. Hsieh. Distributed planar manipulation in fluidic environments. In *Proceedings of the 2016 IEEE International Conference on Robotics and Automation*, pages 5322–5327, Stockholm, Sweden, 2016.

[147] K. Shojaei. Leader–follower formation control of underactuated autonomous marine surface vehicles with limited torque. *Ocean Engineering*, 105:196–205, 2015.

[148] Y. Shuai, G. Li, X. Cheng, R. Skulstad, J. Xu, H. Liu, and H. Zhang. An efficient neural-network based approach to automatic ship docking. *Ocean Engineering*, 191:106514, 2019.

[149] J. M. G. Sierra and J. F. Jimenez. Using an USV for automatic deployment of a boom around a ship: Simulation and scale experiment. In *Proceedings of the IEEE/MTS OCEANS 2018*, pages 1–10, Charleston, SC, USA, 2018.

[150] J. M. G. Sierra, A. T. Gheorghita, G. Angulo, and J. F. Jimenez. Towing a boom with two USVs for oil spill recovery: Scaled experimental development. In *Proceedings of the 2014 13th International Conference on Control Automation Robotics & Vision (ICARCV)*, pages 1729–1734, Singapore, Singapore, 2014.

[151] J. M. G. Sierra, A. T. Gheorghita, G. Angulo, and J. F. Jimenez. Preparing the automatic spill recovery by two unmanned boats towing a boom: Development with scale experiments. *Ocean Engineering*, 95:23–33, 2015.

[152] J. M. G. Sierra, A. T. Gheorghita, and J. F. Jimenez. Fully automatic boom towing by unmanned ships: Experimental study. In *Proceedings of the IEEE/MTS OCEANS 2015*, pages 1–10, Washington, DC, USA, 2015.

[153] M. Simon. Assumptions, limitations and delimitations. Dissertation and scholarly research: Recipes for success, 2011. https://5y1.org/download/068c4e1d10288d2e822303d352ff3a09.pdf, (Accessed: 03-03-2022).

[154] R. Skjetne, S. Moi, and T. I. Fossen. Nonlinear formation control of marine craft. In *Proceedings of the 41st IEEE Conference on Decision and Control*, pages 1699–1704, Las Vegas, NV, USA, 2002.

[155] R. Skjetne, Ø. Smogeli, and T. I. Fossen. Modeling, identification, and adaptive maneuvering of Cybership II: A complete design with experiments. *IFAC Proceedings Volumes*, 37(10):203–208, 2004.

[156] S. Skjong and E. Pedersen. Modeling hydraulic winch system. In *Proceedings of the 2014 International Conference on Bond Graph Modeling and Simulation*, volume 46, pages 181–187, 2014.

[157] S. Skjong and E. Pedersen. Model-based control designs for offshore hydraulic winch systems. *Ocean Engineering*, 121:224–238, 2016.

[158] E. T. Smith, M. G. Feemster, and J. M. Esposito. Swarm manipulation of an unactuated surface vessel. In *Proceedings of the 2007 39th Southeastern Symposium on System Theory*, pages 16–20, Macon, GA, USA, 2007.

[159] M. E. N. Sorensen, M. Breivik, and B. O. H. Eriksen. A ship heading and speed control concept inherently satisfying actuator constraints. In *Proceedings of the 2017 IEEE Conference on Control Technology and Applications (CCTA)*, pages 323–330, Maui, HI, USA, 2017.

[160] B. Stephen, P. Neal, C. Eric, P. Borja, and E. Jonathan. Distributed optimization and statistical learning via the alternating direction method of multipliers. *Foundations and Trends in Machine Learning*, 3(1):1–122, 2010.

[161] J. Tao, L. Du, M. Dehmer, Y. Wen, G. Xie, and Q. Zhou. Path following control for towing system of cylindrical drilling platform in presence of disturbances and uncertainties. *ISA Transactions*, 95:185–193, 2019.

[162] K. P. Tee and S. S. Ge. Control of fully actuated ocean surface vessels using a class of feedforward approximators. *IEEE Transactions on Control Systems Technology*, 14(4):750–756, 2006.

[163] Texas Boom Company. Oil Spill Containment Booms, 2018. https://texasboom.com, (Accessed: 02-14-2022).

[164] The Maritime Executive. PMI Teams With Robert Allan on Autonomous Tug, 2016. https://maritime-executive.com/corporate/pmi-teams-with-robert-allan-on-autonomous-tug, (Accessed: 02-01-2022).

[165] The Maritime Executive. Developing World's First Fully Remotely Controlled Commercial Tug, 2017. https://www.maritime-executive.com/article/developing-world-s-first-fully-remotely-controlled-commercial-tug, (Accessed: 02-01-2022).

[166] The Maritime Executive. Japan Prepares for Autonomous Tugboat Test, 2018. https://www.maritime-executive.com/article/japan-prepares-for-autonomous-tugboat-test, (Accessed: 02-01-2022).

[167] The Maritime Executive. Initial Sea Trials for Autonomous Tug Project, 2020. https://maritime-executive.com/corporate/initial-sea-trials-for-autonomous-tug-project, (Accessed: 02-01-2022).

[168] The Maritime Executive. Testing Autonomous Remote Control of Ships in Singapore, 2021. https://www.maritime-executive.com/article/testing-autonomous-remote-control-of-ships-in-singapore, (Accessed: 02-01-2022).

[169] The Maritime Executive. Sea Machines Sets Out to Prove AI Potential with Tugboat Voyage, 2021. https://www.maritime-executive.com/article/sea-machines-to-prove-autonomous-tech-potential-with-tugboat-voyage, (Accessed: 02-01-2022).

[170] The Maritime Executive. OSV Operator Vallianz Joins the All-Electric Tugboat Trend, 2021. https://www.maritime-executive.com/article/osv-operator-vallianz-joins-the-all-electric-tugboat-trend, (Accessed: 02-01-2022).

[171] The Maritime Executive. Port of Tianjin Signs Up for Semi-Autonomous Tugs, 2021. https://www.maritime-executive.com/article/port-of-tianjin-signs-up-for-semi-autonomous-tugs, (Accessed: 02-01-2022).

[172] The Maritime Executive. Foss Builds First U.S. Tug With Autonomous Capabilities, 2021. https://www.maritime-executive.com/article/foss-builds-first-u-s-tug-with-autonomous-capabilities, (Accessed: 02-01-2022).

[173] The Shipowners' Club. Tugs and Tows - A Practical Safety and Operational Guide. London, UK, 2015.

[174] C. F. L. Thorvaldsen and R. Skjetne. Formation control of fully-actuated marine vessels using group agreement protocols. In *Proceedings of the IEEE Conference on Decision and Control and European Control Conference*, pages 4132–4139, Orlando, FL, USA, 2011.

[175] T. S. Tiang and M. N. Mahyuddin. Cooperative formation control algorithm of a generic multi-agent system applicable for multi-autonomous surface vehicles. In *Proceedings of the 2016 IEEE International Conference on Underwater System Technology: Theory and Applications (USYS)*, pages 133–138, Penang, Malaysia, 2016.

[176] T. Trym, E. F. Brekke, and T. A. Johansen. On collision risk assessment for autonomous ships using scenario-based MPC. *IFAC-PapersOnLine*, 53(2):14509–14516, 2020.

[177] E. Tuci, M. H. M. Alkilabi, and O. Akanyeti. Cooperative object transport in multi-robot systems: A review of the state-of-the-art. *Frontiers in Robotics and AI*, 5:59, 2018.

[178] UC San Diego News Center. Economists Price BP Oil Spill Damage to Natural Resources at \$17.2 Billion, 2017. https://ucsdnews.ucsd.edu/pressrelease/economists_price_bp_oil_spill_damage_to_natural_resources_at_17.2_billion, (Accessed: 16-05-2022).

[179] A. Veksler, T. A. Johansen, F. Borrelli, and B. Realfsen. Dynamic positioning with model predictive control. *IEEE Transactions on Control Systems Technology*, 24(4): 1340–1353, 2016.

[180] W. Wang, Z. Wang, L. Mateos, K. W. Huang, M. Schwager, C. Ratti, and D. Rus. Distributed motion control for multiple connected surface vessels. In *Proceedings of the 2020 IEEE/RSJ International Conference on Intelligent Robots and Systems*, pages 11658–11665, Las Vegas, NV, USA, 2020.

[181] Z. Wang and V. Kumar. Object closure and manipulation by multiple cooperating mobile robots. In *Proceedings of the 2002 IEEE International Conference on Robotics and Automation*, pages 394–399, Washington, DC, USA, 2002.

[182] G. Wu, X. Zhao, Y. Sun, and L. Wang. Cooperative maneuvering mathematical modeling for multi-tugs towing a ship in the port environment. *Journal of Marine Science and Engineering*, 9(4):384, 2021.

[183] G. Xia, C. Sun, B. Zhao, Xi. Sun, and X. Xia. Robust cooperative trajectory tracking control for an unactuated floating object with multiple vessels system. *ISA Transactions*, pages 1–9, 2021.

[184] J. Xie, J. Luo, Y. Peng, S. Xie, H. Pu, X. Li, Z. Su, Y. Liu, and R. Zhou. Data driven hybrid edge computing-based hierarchical task guidance for efficient maritime escorting with multiple unmanned surface vehicles. *Peer-to-Peer Networking and Applications*, pages 1–11, 2020.

[185] Y. Yang, J. Du, H. Liu, C. Guo, and A. Abraham. A trajectory tracking robust controller of surface vessels with disturbance uncertainties. *IEEE Transactions on Control Systems Technology*, 22(4):1511–1518, 2014.

[186] L. Yun and Z. Jian. Design and implementation of cooperative turning control for the towing system of unpowered facilities. *IEEE Access*, 6:18713–18722, 2018.

[187] R. Zaccone. COLREG-compliant optimal path planning for real-time guidance and control of autonomous ships. *Journal of Marine Science and Engineering*, 9(4):405, 2021.

[188] D. Zhang, L. Wang, J. Yu, and M. Tan. Coordinated transport by multiple biomimetic robotic fish in underwater environment. *IEEE Transactions on Control Systems Technology*, 15(4):658–671, 2007.

[189] L. J. Zhang, H. M. Jia, and X. Qi. NNFFC-adaptive output feedback trajectory tracking control for a surface ship at high speed. *Ocean Engineering*, 38(13):1430–1438, 2011.

[190] P. Zhang, Y. Peng, H. Ding, R. Hu, and J. Shi. Numerical analysis of offshore integrated meteorological mast for wind farms during wet towing transportation. *Ocean Engineering*, 188:106271, 2019.

[191] Q. Zhang, W. Pan, and V. Reppa. Model-reference reinforcement learning for collision-free tracking control of autonomous surface vehicles. *IEEE Transactions on Intelligent Transportation Systems*, pages 1–12, 2021.

[192] Y. Zheng, J. Tao, Q. Sun, H. Sun, M. Sun, and Z. Chen. An intelligent course keeping active disturbance rejection controller based on double deep Q-network for towing system of unpowered cylindrical drilling platform. *International Journal of Robust and Nonlinear Control*, 31(17):8463–8480, 2021.

[193] X. Zhou, Y. Ge, W. Li, and G. Ye. Time-constrained multiple unmanned surface vehicles cooperation for sea surface oil pollution cleanup. In *Proceedings of the 2021 6th International Conference on Robotics and Automation Engineering*, pages 40–45, Guangzhou, China, 2021.

Glossary

Conventions

The following conventions are used in this thesis for notation and symbols:

- A character typeset in boldface, e.g., **M**, represents a matrix or a column vector.

- A capital case character typeset in calligraphics , e.g., $\mathcal{W}$ represents a set.

- A subscript case character represents a particular element in a set, e.g., F_i represents the i-th element from set **F**.

- A superscript T e.g., x^T represents that a transpose is taking place.

- A bar over a variable, e.g., $\bar{F}$ represents the change rate of F.

- Subscripts max and min of a variable, e.g., $F_{\max}$ and $F_{\min}$ represent the maximum and minimum value of F, respectively.

- A superscript s of a variable, e.g., x^s represents the variable at the iteration s.

- A variable followed by $(k+l|k)$, i.e., $\lambda(k+l|k)$ indicates the prediction of the variable at time step $k+l$ made at time step k.

List of symbols and notations

Below follows a list of the most frequently used symbols and notations in this thesis.

a^{incr}	parameter of penalty for increasing
a^{decr}	parameter of penalty for decreasing
a_j	length of the long axis of the ellipse obstacle j
a_u	speed reduction coefficient
a_X, a_Y, a_N	disturbance constants in the unknown disturbances
A	cross-sectional area of the stream
A_{FW}, A_{LW}	transverse and lateral projected area of vessel above the water, respectively
A_{FD}, A_{LD}	transverse and lateral projected area of vessel under the water, respectively

A_q	wave amplitude of the qth wave component
$\boldsymbol{B}_{\mathrm{fo}i}$	configuration matrix of the floating object with respect to tugboat i
$\boldsymbol{B}_{Oi}$ or $\boldsymbol{B}_{OI}$	configuration matrix of the offshore platform with respect to tugboat i, $(i = 1, 2, 3, ...)$ or tug role I, $(I = A, B, C, ...)$
$\boldsymbol{B}_{Si}$	configuration matrix of the manipulated ship with respect to tugboat i
$\boldsymbol{B}_T$	configuration matrix of the tugboats in the offshore platform towing system
$\boldsymbol{B}_{Ti}$	configuration matrix of the tugboat i
c_x, c_y, c_n	wind coefficients for horizontal plane motion
$\boldsymbol{C}$	Coriolis-Centripetal matrix
$\boldsymbol{C}_{RB}$	rigid-body part of the Coriolis-Centripetal matrix
$\boldsymbol{C}_A$	added-mass part of the Coriolis-Centripetal matrix
d_{*j}	distance between the vessel and obstacle j
$d_{*j_{\mathrm{d}}}$	safe distance between the vessel and obstacle j
d_0	distance from the origin to the destination
d_1	distance between two waypoints
d_2	distance from the predefined path to the edge of the spatial boundaries
d_{D}	detection distance
d_{non}	small positive value for preventing the denominator from zero
d_{ob}	obstacle distance
d_p	distance from current position of the vessel to the current waypoint p
d_{S0}	surplus distance (buffer) of the obstacles
d_{S_D}	distance between the ship and the destination
D_{*j}	normalized minimum distance to the obstacle j
$\boldsymbol{D}$	damping matrix
$\boldsymbol{D}_l$	linear part of the damping matrix
$\boldsymbol{D}_n$	non-linear part of the damping matrix
$\boldsymbol{e}_{\eta i}$	position error of the tug i
$\boldsymbol{e}_{\mathrm{v}i}$	velocity error of the tug i
$e_{l_{\mathrm{tow}i}}$	towline elongation error of the tug i
e_p	position distance error
e_{Pp}	position distance error to the waypoint p
e_u	(surge) speed error
e_ψ	heading error
$\boldsymbol{e}_{\mathrm{P}}$	position vector (without heading) error
$\boldsymbol{e}_{\eta S}$	position vector (with heading) error vector of the manipulated ship
$\boldsymbol{e}_{\mathrm{v}S}$	velocity vector error of the manipulated ship

E	Young's modulus of the towline
$\boldsymbol{E}_i$	angle vector of tug i related to the object's heading and the towing angle
f_i	function of dynamics for the tug i
f_{FO}	function of dynamics for the floating object
F_i or F_I	towing force through the towline from the tugboat $i, (i = 1, 2, ...)$ or tug role $I, (I = \text{A}, \text{B}, \text{C}, ...)$
$\bar{F}_i$	maximum change rate of towing force for the towline from the tugboat i
$F_{i\min}, F_{i\max}$	minimum and maximum value of towing force for the towline from the tugboat i
F_i'	force applied through a controlled winch onboard the tugboat i to the towline
$\boldsymbol{F}_i$	angle vector of tugboat i related to the object's heading and configuration center angle
g_i	function of the towing system kinematics with respect to tug i
$g(i, t)$	index function of the role of tugboat i
h	time prediction step
H_D	horizontal distance between the two ends of the towline
H_{P}	length of the prediction horizon
J_{Central}	cost function in the centralized control architecture
J_{FO}	cost function of the floating object
J_{Ci}	cost function of the tug i with only the system configuration
J_i	cost function of the tug i
J_O	cost function of the manipulated platform
J_S	cost function of the manipulated ship
J_{Ti}	cost function of the tug i without the system configuration
k	discrete time step
k_D	settling time
k_F	scaling factor of length
k_X, k_Y, k_N	unknown disturbance gain
k_0, k_1, k_2, k_t	positive parameters in weight coefficient
k_{qX}, k_{qY}, k_{qN}	constant parameters of the qth wave component
$K_{qX}(t), K_{qY}(t), K_{qN}(t)$	tunable parameters of the qth wave component
$l_{\text{el}i}$	actual towline elongation of the tug i
l_i	distance from the center of gravity of the floating object to the towing point
$l_{\text{tow}i}$	desired length of the towline that guarantees the action of the

	restoring force and the collision avoidance between the object and tugboat i
l_{Ti}	distance from the center of gravity of the tugboat to the tugboat i towing point
L	length of the manipulated platform
L_O	distance from the centre of gravity of the platform to its towing point
L_{oa}	overall length of the vessel
L_p	Lagrangian form of the problem
L_R	length of the towline
$\boldsymbol{M}$	mass (inertia) matrix
$\boldsymbol{M}_{RB}$	rigid-body part of the mass (inertia) matrix
$\boldsymbol{M}_A$	added-mass part of the mass (inertia) matrix
n	number of tugs
n_s	size of the variable
N	number of waypoints
N_w	total number of harmonic components
$\boldsymbol{P}_S$	weight factor of the manipulated ship
$\boldsymbol{p}_{i\mathrm{d}}$	desired position vector (without heading) of the tugboat i
$\boldsymbol{p}_{i\mathrm{p}}$	predicted position vector (without heading) of the tugboat i
r	yaw velocity
r_{wp}	distance between the above two waypoints
$\boldsymbol{R}$	rotation matrix from the body frame to the world frame
R_j	radius of the circle obstacle j
$R_{mathrmpri,i}$	primal residual of the control agent i
$R_{mathrmdual,i}$	dual residual of the control agent i
s	iteration
S	maximum iteration
T	component of the towline tension in the horizontal plane
T_s	sampling time
u	surge velocity
u_w	component of wind speed in the x direction (in world NED frame)
u_{rw}	relative wind speed in the x direction (in body frame)
$\boldsymbol{U}$	control input vector of the manipulation system
$\boldsymbol{U}_{\mathrm{FO}}$	control input vector of the floating object
$\boldsymbol{U}_i$	control input vector of the tug i
$\mathbb{U}_{\mathrm{FO}}$	constraints of the control input saturation for the floating object
$\mathbb{U}_i$	constraints of the control input saturation for the tug i

v	sway velocity
v_w	component of wind speed in the y direction (in world NED frame)
v_{rw}	relative wind speed in the y direction (in body frame)
V_c	water current speed
V_w	wind speed
V_{rw}	relative wind speed
w_{i1}, w_{i2}, w_{i3}	weight coefficient elements for the tug i
$w_{\mathrm{I}}, w_{\mathrm{II}}$	weight coefficients of the tugboats in the offshore platform towing system
w_{IH}	weight coefficients for the tugboat heading in the offshore platform towing system
w_{S1}, w_{S2}, w_{S3}	weight coefficients for the manipulated ship
$w_{\mathrm{P}}, w_{\mathrm{H}}, w_{\mathrm{V}}$	weight coefficients of the platform
W	width of the manipulated platform
$\boldsymbol{W}_{i1}, \boldsymbol{W}_{i2}, \boldsymbol{W}_{i3}$	weight matrices for the tug i
$\boldsymbol{W}_{S1}, \boldsymbol{W}_{S2}, \boldsymbol{W}_{S3}$	weight matrices for the manipulated ship
(x, y)	position coordinates
(x_*, y_*)	position coordinates of the own vessel
$(x_{i\mathrm{d}}, y_{i\mathrm{d}})$ or $(x_{I\mathrm{d}}, y_{I\mathrm{d}})$	desired position coordinates of the tugboat $i, (i = 1, 2, 3, ...)$ or tug role $I, (I = \mathrm{A}, \mathrm{B}, \mathrm{C}, ...)$
$(x_{Fj1}, y_{Fj1}), (x_{Fj2}, y_{Fj2})$	coordinates of the two focuses for dynamic obstacle
$(x_{\mathrm{n}}, y_{\mathrm{n}})$	position coordinates of the new waypoint
(x_O, y_O)	position coordinates of the platform
$(x_{O_{\mathrm{P}}}, y_{O_{\mathrm{P}}})$	predicted position coordinates of the platform
(x_{Oj}, y_{Oj})	position coordinates of the static obstacle
$(x_{\mathrm{Sd}}, y_{\mathrm{Sd}})$	desired position coordinates of the manipulated ship
$(x_{\mathrm{So}}, y_{\mathrm{So}})$	initial position coordinates of the manipulated ship
(x_p, y_p)	position coordinates of the waypoint p
$\boldsymbol{X}_{\mathrm{FO}}$	state vector of the floating object
$\boldsymbol{X}_i$	state vector of the tug i
$\mathbb{X}_{\mathrm{FO}}$	constraints of the floating object dynamics
$\mathbb{X}_i$	constraints of the tug i dynamics
α_i or α_I	towing angle through the towline from the tugboat $i, (i = 1, 2, ...)$ or tug role $I, (I = \mathrm{A}, \mathrm{B}, \mathrm{C}, ...)$
$\bar{\alpha}_i$	maximum change rate of towing angle for the towline from the tugboat i
$\alpha_{i\min}, \alpha_{i\max}$	minimum and maximum value of towing angle for the towline from the tugboat i
β_c	sideslip angle with respect to the water current

β_i or β_I	tug angle of the tugboat i, $(i = 1, 2, ...)$ or tug role I, $(I = A, B, C, ...)$
β_{qw}	incident wave angle of the qth wave component
β_w	wind direction
γ	platform configuration angle
γ_i	angle between the heading of the object and the direction from the center of gravity of the object to the towing point
γ_{rw}	wind angle of attack
δ_I	linking angles of tug role I, $(I = A, B, C, ...)$
ε^{abs}	absolute tolerance
ε^{rel}	relative tolerance
ε_{pri}	primal feasibility tolerance
ε_{dual}	dual feasibility tolerance
ε_{qX}, ε_{qY}, ε_{qN}	random phase angles of the qth wave component
$\boldsymbol{\eta}$	position vector in the world frame (North-East-Down)
$\boldsymbol{\eta}_{FO}$	position vector of the floating object
$\boldsymbol{\eta}_i$	position vector of the tug i
$\boldsymbol{\eta}_{iC}$	calculated position vector of the tug i
$\boldsymbol{\eta}_{id}$	desired position vector of the tug i
$\boldsymbol{\eta}_{iP}$	predicted position vector of the tug i
$\boldsymbol{\eta}_{ob}$	position vector of the obstacle
$\boldsymbol{\eta}_O$	position vector of the manipulated platform
$\boldsymbol{\eta}_{Od}$	desired position vector of the manipulated platform
$\boldsymbol{\eta}_S$	position vector of the manipulated ship
$\boldsymbol{\eta}_{SC}$	calculated position vector of the manipulated ship
$\boldsymbol{\eta}_{Sd}$	desired position vector of the manipulated ship
$\boldsymbol{\eta}_{Sn}$	new position vector of the manipulated ship
$\boldsymbol{\eta}_{SP}$	predicted position vector of the manipulated ship
$\boldsymbol{\eta}_{W_p}$	position vector of the predefined waypoint
θ	altering angle
θ_{max}	maximum altering angle
θ_O	angle from the heading of the platform to the direction of the waypoint
λ_i	Lagrange multiplier with respect to tug i
μ	parameter of penalty for determining whether to update
$\boldsymbol{\nu}$	velocity vector in the body-fixed frame
$\boldsymbol{\nu}_c$	water current velocity vector in the body-fixed frame

$\mathbf{v}_{FO}$	velocity vector of the floating object
$\mathbf{v}_i$	velocity vector of the tug i
$\mathbf{v}_{iC}$	calculated velocity vector of the tug i
$\mathbf{v}_{id}$	desired velocity vector of the tug i
$\mathbf{v}_{iP}$	predicted velocity vector of the tug i
$\mathbf{v}_O$	velocity vector of the manipulated platform
$\mathbf{v}_{O_P}$	predicted velocity vector of the manipulated platform
$\mathbf{v}_r$	relative velocity vector in the water current environment
$\mathbf{v}_S$	velocity vector of the manipulated ship
$\mathbf{v}_{SC}$	calculated velocity vector of the manipulated ship
$\mathbf{v}_{Sd}$	desired velocity vector of the manipulated ship
$\mathbf{v}_{Sn}$	new velocity vector of the manipulated ship
$\mathbf{v}_{SP}$	predicted velocity vector of the manipulated ship
ρ_i	penalty parameter with respect to tug i
ρ_a	air density
$\boldsymbol{\tau}$	controllable input vector
$\boldsymbol{\tau}_{drag}$	drag forces vector
$\boldsymbol{\tau}_E$	environmental disturbances vector
$\boldsymbol{\tau}_{Fi}$	forces and moment to compensate for the reaction of towing force by the tugboat i
$\boldsymbol{\tau}_{FO}$	controllable input of the floating object
$\boldsymbol{\tau}_{foi}$	towing forces and moment by tug i
$\boldsymbol{\tau}_i$ or $\boldsymbol{\tau}_I$	controllable input of the tugboat $i, (i = 1, 2, ...)$ or tug role I, $(I = A, B, C, ...)$
$\boldsymbol{\tau}_{i\,max}$	maximum value of the controllable input of the tugboat i
$\boldsymbol{\tau}_O$	controllable input of the manipulated offshore platform
$\boldsymbol{\tau}_S$	controllable input of the manipulated ship
$\boldsymbol{\tau}_{Ti}$ or $\boldsymbol{\tau}_{TI}$	forces and moment provided by the actuator of the tugboat i, $(i = 1, 2, ...)$ or tug role $I, (I = A, B, C, ...)$
$\bar{\boldsymbol{\tau}}_{Ti}$	maximum change rate of the thruster forces and moment of the tugboat i
$\boldsymbol{\tau}_{unknown}$	unknown effect of the environmental disturbances
$\boldsymbol{\tau}_{wave}$	wave effect of the environmental disturbances
$\boldsymbol{\tau}_{wind}$	wind effect of the environmental disturbances
$\boldsymbol{\chi}(t)$	state vector of the manipulation system
$\chi_{*q}(t)$	wave encounter angle of the qth wave component
$\psi(t)$	heading of a vessel
ψ_{id} or ψ_{Id}	desired heading of the tugboat $i, (i = 1, 2, ...)$ or tug role I, $(I = A, B, C, ...)$
ψ_O	heading of the manipulated platform
ψ_{O_P}	predicted heading of the manipulated platform

ψ_S	heading of the manipulated ship
ψ_{Sd}	desired heading of the manipulated ship
ψ_n	course of the new waypoint
ψ_p	course of the waypoint p
ψ_{Sd_N}	desired ship heading at the destination
ψ_{So}	initial heading of the manipulated ship
ω	weight of the towline per unit length
ω_q	wave frequency of the qth wave component

List of abbreviations

The following abbreviations are used in this thesis:

ADMM	Alternating Direction Method of Multipliers
APF	Artificial Potential Fields
ASD	Azimuth Stern Drive
ASV	Autonomous Surface Vessel (Vehicle)
CA	Collision Avoidance
COLREGS	Convention on the International Regulations for Preventing Collisions at Sea
DOF	Degrees Of Freedom
GNC	Guidance, Navigation, Control
GPS	Global Positioning System
IMO	International Maritime Organization
IMU	Inertial Measurement Unit
KPI	Key Performance Indicator
MASS	Maritime Autonomous Surface Ship
MPC	Model Predictive Control
MRS	Multi-Robot System
MSC	Maritime Safety Committee
PID	Proportional-Integral-Derivative
RAO	Response Amplitude Operators
RRT	Rapidly-exploring Random Tree
VO	Velocity Obstacle

TRAIL Thesis Series

The following list contains the most recent dissertations in the TRAIL Thesis Series. For a complete overview of more than 275 titles see the TRAIL website: www.rsTRAIL.nl.

The TRAIL Thesis Series is a series of the Netherlands TRAIL Research School on transport, infrastructure and logistics.

Du, Z., *Cooperative Control of Autonomous Multi-Vessel Systems for Floating Object Manipulation*, T2022/10, September 2022, TRAIL Thesis Series, the Netherlands

Larsen, R.B., *Real-time Co-planning in Synchromodal Transport Networks using Model Predictive Control*, T2022/9, September 2022, TRAIL Thesis Series, the Netherlands

Zeinaly, Y., *Model-based Control of Large-scale Baggage Handling Systems: Leveraging the theory of linear positive systems for robust scalable control design*, T2022/8, June 2022, TRAIL Thesis Series, the Netherlands

Fahim, P.B.M., *The Future of Ports in the Physical Internet*, T2022/7, May 2022, TRAIL Thesis Series, the Netherlands

Huang, B., *Assessing Reference Dependence in Travel Choice Behaviour*, T2022/6, May 2022, TRAIL Thesis Series, the Netherlands

Reggiani, G., *A Multiscale View on Bikeability of Urban Networks*, T2022/5, May 2022, TRAIL Thesis Series, the Netherlands

Paul, J., *Online Grocery Operations in Omni-channel Retailing: opportunities and challenges*, T2022/4, March 2022, TRAIL Thesis Series, the Netherlands

Liu, M., *Cooperative Urban Driving Strategies at Signalized Intersections*, T2022/3, January 2022, TRAIL Thesis Series, the Netherlands

Feng, Y., *Pedestrian Wayfinding and Evacuation in Virtual Reality*, T2022/2, January 2022, TRAIL Thesis Series, the Netherlands

Scheepmaker, G.M., *Energy-efficient Train Timetabling*, T2022/1, January 2022, TRAIL Thesis Series, the Netherlands

Bhoopalam, A., *Truck Platooning: planning and behaviour*, T2021/32, December 2021, TRAIL Thesis Series, the Netherlands

Hartleb, J., *Public Transport and Passengers: optimization models that consider travel de-*

mand, T2021/31, TRAIL Thesis Series, the Netherlands

Azadeh, K., *Robotized Warehouses: design and performance analysis*, T2021/30, TRAIL Thesis Series, the Netherlands

Chen, N., *Coordination Strategies of Connected and Automated Vehicles near On-ramp Bottlenecks on Motorways*, T2021/29, December 2021, TRAIL Thesis Series, the Netherlands

Onstein, A.T.C., *Factors influencing Physical Distribution Structure Design*, T2021/28, December 2021, TRAIL Thesis Series, the Netherlands

Olde Kalter, M.-J. T., *Dynamics in Mode Choice Behaviour*, T2021/27, November 2021, TRAIL Thesis Series, the Netherlands

Los, J., *Solving Large-Scale Dynamic Collaborative Vehicle Routing Problems: an Auction-Based Multi-Agent Approach*, T2021/26, November 2021, TRAIL Thesis Series, the Netherlands

Khakdaman, M., *On the Demand for Flexible and Responsive Freight Transportation Services*, T2021/25, September 2021, TRAIL Thesis Series, the Netherlands

Wierbos, M.J., *Macroscopic Characteristics of Bicycle Traffic Flow: a bird?s-eye view of cycling*, T2021/24, September 2021, TRAIL Thesis Series, the Netherlands

Qu, W., *Synchronization Control of Perturbed Passenger and Freight Operations*, T2021/23, July 2021, TRAIL Thesis Series, the Netherlands

Nguyen, T.T., *Highway Traffic Congestion Patterns: Feature Extraction and Pattern Retrieval*, T2021/22, July 2021, TRAIL Thesis Series, the Netherlands

Pud?ne, B., *Time Use and Travel Behaviour with Automated Vehicles*, T2021/21, July 2021, TRAIL Thesis Series, the Netherlands

Gent, P. van, *Your Car Knows Best*, T2021/20, July 2021, TRAIL Thesis Series, the Netherlands

Wang, Y., *Modeling Human Spatial Behavior through Big Mobility Data*, T2021/19, June 2021, TRAIL Thesis Series, the Netherlands

Coevering, P. van de, *The Interplay between Land Use, Travel Behaviour and Attitudes: a quest for causality*, T2021/18, June 2021, TRAIL Thesis Series, the Netherlands

Landman, R., *Operational Control Solutions for Traffic Management on a Network Level*, T2021/17, June 2021, TRAIL Thesis Series, the Netherlands

Zomer, L.-B., *Unravelling Urban Wayfinding: Studies on the development of spatial knowledge, activity patterns, and route dynamics of cyclists*, T2021/16, May 2021, TRAIL Thesis Series, the Netherlands

Núñez Velasco, J.P., *Should I Stop or Should I Cross? Interactions between vulnerable road users and automated vehicles*, T2021/15, May 2021, TRAIL Thesis Series, the Netherlands

Duivenvoorden, K., *Speed Up to Safe Interactions: The effects of intersection design and road users' behaviour on the interaction between cyclists and car drivers*, T2021/14, April 2021, TRAIL Thesis Series, the Netherlands

Samenvatting

Dit proefschrift biedt een reeks coöperatieve controleschema's voor autonome systemen met meerdere vaartuigen om een drijvend object te manipuleren via fysieke verbindingen in onshore (binnenwateren en havens) en offshore-gebieden.

Dankzij de volwassenheid en populariteit van de voortschrijdende technologieën op het gebied van informatie, communicatie, sensoren, automatische besturing en computationele intelligentie, hebben we gezien dat de toepassingsscenario's van de autonome schepen geleidelijk zijn uitgebreid van fundamenteel onderzoek naar civiel en commercieel gebruik. Om ervoor te zorgen dat het regelgevingskader voor autonome schepen gelijke tred houdt met de technologische ontwikkelingen, is de Internationale Maritieme Organisatie (IMO) de afgelopen jaren begonnen om de kwestie van autonome schepen op te nemen in haar sessies.

Maritieme operaties zijn complexer geworden en hun schaal wordt groter, waardoor de inzet van systemen met meerdere vaartuigen nodig is. In de afgelopen decennia is de formatiecontrole van meerdere schepen onderzocht en er zijn verschillende volwassen controlemethoden voorgesteld om verschillende typische missies het hoofd te bieden. Er is echter een gebrek aan onderzoek gericht op manipulatie van drijvende objecten door meerdere autonome schepen via fysieke onderlinge verbindingen. De onderzoeksvraag van dit proefschrift is dus: *Hoe ontwerp je een schaalbaar besturingsschema voor meerdere ASV's om een zwevend object te manipuleren via fysieke onderlinge verbindingen?*

Door de analyse van vier typische manipulatiemethoden op maritiem gebied, is in dit proefschrift de sleepweg geselecteerd als het fysieke basismanipulatiemodel, dat voordelen heeft in een goede manoeuvreerbaarheid van het drijvende object, een betere veiligheid van het manipulatiesysteem en meer flexibiliteit van de operationele scenario's. Het dynamische model van het sleepsysteem is gebouwd met behulp van de 3 DOF vectoriële representatie, waarbij de sleepkrachten en sleephoeken de kinetische en kinematische verbindingen zijn tussen respectievelijk het drijvende object en de sleepboten. Rekening houdend met de meervoudige controle-ingangen, meervoudige controlebeperkingen en beperkte manoeuvreerbaarheid van het sleepsysteem, is de model voorspellende controle (MPC) strategie de onderzoeksbenadering in dit proefschrift. Om de gedistribueerde besturingsarchitectuur te bereiken, wordt bovendien de alternerende richtingsmethode van vermenigvuldigers (ADMM) gebruikt.

In dit proefschrift wordt de voorgestelde methode gebruikt in drie verschillende operationele omgevingen, havengebieden, binnenwateren en open zee voor het manipuleren van drijvende objecten.

Coöperatieve controle voor scheepsmanipulatie in havengebieden

In havengebieden wordt een meerlagig controleschema met meerdere agenten voorgesteld om een schip te manipuleren om een gewenste positie met de gewenste koers te bereiken. Het besturingsschema bestaat uit een toezichthoudende controller en twee sleepbootcontrollers in twee verschillende lagen. De toezichthoudende controller berekent de controle-ingangen door het optimalisatieprobleem van positie, koers en snelheid op te lossen. Om te garanderen dat het treksysteem goed functioneert onder omgevingsinvloeden (voornamelijk wind), is een adaptieve gewichtsfunctie ontworpen. De sleepbootcontroller zorgt enerzijds voor de sleepkrachten om het schip te verplaatsen; aan de andere kant volgt het het referentietraject van de sleepboot berekend door de toezichthoudende controller. De resultaten illustreren dat, voor het geval er geen verstoringen zijn, de voorgestelde methode meer efficiëntie vertoont, waarbij de insteltijd met 50% wordt verminderd; voor onder de wind (voornamelijk) en onbekende verstoringen, toont de voorgestelde methode een betere robuustheid bij het bereiken van de gewenste koers van het schip, zelfs in barre omstandigheden.

Coöperatieve controle voor scheepsmanipulatie op de binnenwateren

In de binnenwateren wordt een COLREGS (Regels 13-17) conforme ADMM-gebaseerde MPC-benadering voorgesteld om het vermijden van obstakels voor een scheepssleepsysteem aan te pakken. De voorgestelde regelaanpak is gebaseerd op het ontkoppelen van een groot globaal optimalisatieprobleem in drie kleine optimalisatieproblemen. De problemen van het volgen van waypoints van het schip en het vermijden van obstakels worden aangepakt door de coördinerende MPC-controller en het COLREGS-conforme waypoint-wijzigingssysteem. De problemen van het volgen van het traject van de sleepboot en het vermijden van obstakels worden aangepakt door de lokale MPC-controller van de sleepboot. Het probleem van het bereiken van gedistribueerde architectuur wordt opgelost door het ADMM-algoritme te gebruiken om de optimale Lagrange-multipliers te vinden. De resultaten geven aan dat de voorgestelde aanpak statische en dynamische obstakels in beperkte waterwegen kan vermijden voor een sleepsysteem voor schepen, waardoor het vermijden van aanvaringen COLREGS in overeenstemming is (Regels 13-17). De voorgestelde gedistribueerde besturingsarchitectuur is haalbaar waarvan de optimalisatieoplossingen vrij dicht bij die van de globale optimalisatie liggen.

Om de kwaliteit van het manipulatieproces te verbeteren en de veiligheid van het vermijden van botsingen te vergroten, wordt bovendien een op ADMM gebaseerde meerlaagse MPC-benadering met snelheidsregeling voorgesteld. Het controleprobleem wordt dan multi-objectief, gericht op het volgen van waypoints, het aanpassen van de koers, het volgen van snelheidsprofielen en het oplossen van botsingen. Om de orde van grootte tussen de positie- en snelheidsfout te normaliseren en de gevoeligheid van de controller voor het waypoint te verminderen, is een scheepsgewichtsfactor ontworpen in de toezichthoudende controller voor het schip. Overeenkomstig wordt in de sleepbootcontroller de voorspelde scheepssnelheid toegevoegd als een ander controledoel voor de sleepboot. Om te controleren in hoeverre deze meerdere doelstellingen zijn bereikt, zijn vijf KPI's gedefinieerd voor het volgen van waypoints, het aanpassen van de koers, het volgen van snelheidsprofielen, het bereiken van consensus en het vermijden van botsingen. De resultaten geven aan dat in vergelijking met geen snelheidsregeling, het voorgestelde controleschema beter presteert

voor het bereiken van consensus, het volgen van snelheidsprofielen en het vermijden van botsingen.

Coöperatieve controle voor offshore platformmanipulatie in open zee

Op open zee wordt een gedistribueerd coördinatiecontroleschema voorgesteld voor een sleepsysteem met meerdere schepen om een offshore-platform te vervoeren onder omgevingsverstoringen. De kern van het voorgestelde besturingsschema is het dynamische coördinatiebeslissingsmechanisme, het controllerontwerp en het ontwerp van de gedistribueerde besturingsarchitectuur. Het beslissingsmechanisme is gebaseerd op de relatieve positie tussen het platform en het huidige waypoint. De controllers zijn ontworpen op basis van de MPC-strategie met verschillende kostenfuncties voor het offshore platform en vier sleepboten. De gedistribueerde besturingsarchitectuur is gebouwd op basis van de ADMM-strategie. Aangezien de gewenste koers van de sleepboot niet onmiddellijk wordt bereikt, vooral in het proces van rolwisseling, is het belangrijkste element voor het bereiken van de consensus de gewenste en voorspelde positie van de sleepboot. De resultaten laten zien dat het voorgestelde schema efficiënter is (de insteltijd is met meer dan 50% verminderd) en een betere consensus heeft (de sleeprekfout is teruggebracht tot de helft tot een vijfde).

Over het algemeen maken de voorgestelde controleschema's in dit proefschrift de samenwerking mogelijk van meerdere autonome sleepboten om een groot drijvend object in havengebieden, binnenwateren en open zee te manipuleren. Tijdens het slepen kan het manipulatiesysteem omgaan met omgevingsstoringen, botsingen voorkomen, de objectsnelheid regelen en de rollen van sleepboten dynamisch coördineren. Daarom verbetert dit onderzoek de veiligheid en efficiëntie van de sleepmanipulatie en is het een belangrijke stap in de richting van "smart shipping".

Summary

This thesis provides a set of cooperative control schemes for autonomous multi-vessel systems to manipulate a floating object through physical interconnections in onshore (inland waterways and ports) and offshore areas.

Thanks to the maturity and popularity of the advancing technologies in information, communication, sensors, automatic control, and computational intelligence, we have seen the application scenarios of the autonomous vessels being gradually extended from fundamental research to civil and commercial uses. In recent years, to ensure that the regulatory framework for autonomous vessels keeps pace with technological developments, the International Maritime Organization (IMO) has started to include the autonomous vessels issue in its sessions.

Maritime operations have become more complex and their scale is getting larger, requiring the involvement of multi-vessel systems. In recent decades, the formation control of multiple vessels has been investigated and several mature control methods are proposed to cope with different typical missions. However, there is a lack of research focusing on floating object manipulation by multiple autonomous vessels through physical interconnections. Thus, the research question of this thesis is *How to design a scalable control scheme for multiple ASVs to manipulate a floating object through physical interconnections?*

Through the analysis of four typical manipulation ways in the maritime field, the towing way is selected in this thesis as the basic physical manipulation model, which has advantages in good maneuverability of the floating object, better safety of the manipulation system, and more flexibility of the operational scenarios. The dynamic model of the towing system is built by using the 3 DOF vectorial representation, where the towing forces and towing angles are the kinetic and kinematic interconnections between the floating object and tugboats, respectively. Considering the multiple control inputs, multiple control constraints, and limited maneuverability of the towing system, the model predictive control (MPC) strategy is the research approach in this thesis. Furthermore, to achieve the distributed control architecture, the alternating direction method of multipliers (ADMM) is used.

In this thesis, the proposed method is used in three different operational environments, port areas, inland waterways, and open sea for floating object manipulation.

Cooperative control for ship manipulation in port areas

In port areas, a multi-layer multi-agent control scheme is proposed to manipulate a ship to reach a desired position with desired heading. The control scheme consists of a supervisory controller and two tug controllers in two different layers. The supervisory controller computes the control inputs by solving the optimization problem of position, heading, and

velocity. To guarantee that the towing system functions well under environmental distur-
bances (mainly wind), an adaptive weight function is designed. The tug controller, on the
one hand, provides the towing forces to move the ship; on the other hand, it tracks the re-
ference trajectory of the tugboat computed by the supervisory controller. Results illustrate
that, for the case of no disturbances, the proposed method shows more efficiency with the
settling time being reduced by 50%; for the case of under the wind (mainly) and unknown
disturbances, the proposed method shows better robustness in achieving the desired heading
of the ship, even in harsh conditions.

Cooperative control for ship manipulation in inland waterways

In inland waterways, a COLREGS (Rules 13-17) compliant ADMM-based MPC appro-
ach is proposed to deal with obstacle avoidance for a ship towing system. The proposed
control approach is based on decoupling a large global optimization problem into three
small optimization problems. The problems of the ship waypoint following and obstacle
avoidance are addressed by the coordination MPC controller and the COLREGS compliant
waypoint altering system. The problems of the tug trajectory tracking and obstacle avoi-
dance are addressed by the tug local MPC controller. The problem of distributed architecture
achieving is solved by using the ADMM algorithm to find the optimal Lagrange multipliers.
Results indicate that the proposed approach can avoid static and dynamic obstacles in re-
stricted waterways for a ship-towing system, making the collision avoidance COLREGS
compliant (Rules 13-17). The proposed distributed control architecture is feasible whose
optimization solutions are quite close to that of the global optimization.

Moreover, to improve the quality of the manipulation process and increase the safety
of collision avoidance, an ADMM-based multi-layer MPC approach with speed regulation
is proposed. The control problem then becomes multi-objective aiming at waypoint follo-
wing, heading adjusting, speed profile tracking, and collisions resolving. To normalize the
order of magnitude between the position and velocity error and reduce the sensitivity of
the controller to the waypoint, a ship weight factor is designed in the supervisory control-
ler for the ship. Corresponding, in the tug controller, the predicted ship speed is added as
another control objective for the tugboat. To check the extent of these multiple objectives
achieved, five KPIs are defined for waypoint following, heading adjusting, speed profile
tracking, consensus reaching, and collision avoidance. Results indicate that compared to no
speed regulation control, the proposed control scheme outperforms for consensus reaching,
speed profile tracking, and collision avoidance distance.

Cooperative control for offshore platform manipulation at open sea

In open sea, a distributed coordination control scheme is proposed for a multi-vessel to-
wing system to transport an offshore platform under environmental disturbances. The core
of the proposed control scheme is the dynamic coordination decision mechanism, the con-
troller design, and the distributed control architecture design. The decision mechanism is
based on the relative position between the platform and the current waypoint. The control-
lers are designed based on the MPC strategy with different cost functions for the offshore
platform and four tugboats. The distributed control architecture is built based on the ADMM
strategy. Considering the desired tug heading is not achieved immediately, especially in the
process of role changing, the key element for reaching the consensus is the desired and the
predicted tug position. The results show that the proposed scheme is more efficient (the

settling time is reduced by more than 50%) and has a better consensus achievement (the towing elongation error is reduced to one-half to one-fifth).

Overall, the proposed control schemes in this thesis enable the cooperation of multiple autonomous tugboats to manipulate a large floating object in port areas, inland waterways, and open sea. In the process of towing, the manipulation system can deal with environmental disturbances, avoid collisions, regulate object speed, and dynamically coordinate the roles of tugboats. Therefore, this research improves the safety and efficiency of the towing manipulation and is a significant step toward "smart shipping".

Curriculum vitae

Zhe Du was born on February 4, 1992 in Wuhan, China. He obtained his B.Sc. degree in Maritime Administration at Wuhan University of Technology, Wuhan, China in 2015; in the same year, he got his second B.Sc. degree in Computer Science at Huazhong University of Science and Technology, Wuhan, China. After this, Zhe Du obtained the M.Sc. degree in Traffic Information Engineering and Control at Wuhan University of Technology, Wuhan China, in 2018.

Starting from November 2018, Zhe Du is sponsored by China Scholarship Council as a PhD candidate supervised by Prof. Dr. Rudy R. Negenborn and Dr. Vasso Reppa at the Department of Maritime Technology and Transport, Delft University of Technology, Delft, the Netherlands. In his PhD project, Zhe focused on cooperative control of physically connected autonomous multi-vessel systems for floating object manipulation. His research interests include autonomous vessels, multi-vessel systems, cooperative control, distributed control, and floating object manipulation.

Publications

1. Z. Du, R. R. Negenborn, and V. Reppa. Cooperative control of autonomous tugs for ship towing. *IFAC-PapersOnLine*, 53(2):14470-14475, 2020.

2. Z. Du, R. R. Negenborn, and V. Reppa. Cooperative multi-agent control for autonomous ship towing under environmental disturbances. *IEEE/CAA Journal of Automatica Sinica*, 8(8):1365-1379, 2021.

3. Z. Du, R. R. Negenborn, and V. Reppa. MPC-based COLREGS compliant collision avoidance for a multi-vessel ship-towing system. In *Proceedings of the European Control Conference*, pages 1857-1862, Delft, Netherlands, 2021.

4. Z. Du, R. R. Negenborn, and V. Reppa. Multi-vessel cooperative speed regulation for ship manipulation in towing scenarios. *IFAC-PapersOnLine*, 54(16):384-389, 2021.

5. Z. Du, R. R. Negenborn, and V. Reppa. COLREGS-compliant collision avoidance for physically coupled multi-vessel systems with distributed MPC. *Ocean Engineering*, 260:111917, 2022.

6. Z. Du, R. R. Negenborn, and V. Reppa. Multi-objective cooperative control for a ship-towing system in congested water traffic environments. *under review in IEEE Transactions on Intelligent Transportation Systems*, 2022.

7. Z. Du, R. R. Negenborn, and V. Reppa. Dynamic coordination of multiple vessels for offshore platform transportation. In *Proceedings of the 6th IEEE Conference on Control Technology and Applications*, pages 1-6, Trieste, Italy, 2022.

8. Z. Du, R. R. Negenborn, and V. Reppa. Dynamic coordination of multiple vessels for offshore platform transportation under ocean environmental disturbances. *Submitted to a journal*, 2022.

9. Z. Du, R. R. Negenborn, and V. Reppa. Review of floating object manipulation by autonomous multi-vessel systems. *Submitted to a journal*, 2022.